**Universidade de Évora - Instituto de Investigação e Formação Avançada**

Programa de Doutoramento em Engenharia Mecatrónica e Energia

Área de especialização | Energia

Tese de Doutoramento

# Integration, control and optimization of the solar photovoltaic-battery system in microgrids

Ana Catarina das Neves Foles

Orientador(es) | Luís Fialho

Manuel Collares-Pereira

Évora 2023

**Universidade de Évora - Instituto de Investigação e Formação Avançada**

Programa de Doutoramento em Engenharia Mecatrónica e Energia

Área de especialização | Energia

Tese de Doutoramento

# Integration, control and optimization of the solar photovoltaic-battery system in microgrids

Ana Catarina das Neves Foles

Orientador(es) | Luís Fialho

Manuel Collares-Pereira

Évora 2023

A tese de doutoramento foi objeto de apreciação e discussão pública pelo seguinte júri nomeado pelo Diretor do Instituto de Investigação e Formação Avançada:

| | | |
|---|---|---|
| Presidente | \| | João Manuel Figueiredo (Universidade de Évora) |
| Vogais | \| | Eduardo López González ()<br>Luis Narvarte Fernandez ()<br>Luís Fialho (Universidade de Évora) (Orientador)<br>Miguel Ángel Ridao Carlini (Universidad de Sevilla)<br>Rui Amaral Lopes () |

Évora 2023

# Acknowledgements

This thesis comprises the work developed throughout the years of the doctoral program and that was impossible to achieve without vital elements of a team with an aligned vision for the future.

I want to express my gratitude to my supervisors, Dr Luís Fialho and Professor Dr Manuel Collares-Pereira, for believing in this work, providing me with the opportunity to develop it and for their guidance and encouragement during these years. Also, I would like to acknowledge their support at the beginning of this PhD, with the provided scholarships from the Renewable Energies Chair of the University of Évora projects. A dedicated acknowledgement should I give to the supervisor Dr Luís Fialho, who made me a better engineer in the real sense of the word and taught me more things than I could ever list.

I would like to thank the current chairman of the Renewable Energies Chair of the University of Évora, Dr Pedro Horta, for the opportunity provided to continue pursuing these PhD objectives and for the support given throughout the process and the hosting of this thesis.

I would like to acknowledge the support of the FCT (Fundação para a Ciência e a Tecnologia) – through grant no. SFRH/BD/147087/2019 – for the last half of the period of this thesis. In that context, I would like to acknowledge the support of the ICT – Institute of Earth Sciences – by hosting this thesis during the earned scholarship.

I would like to thank all the R&D project partners I have worked with during the development of this thesis, who shared their knowledge and experience, which made me a better professional.

I would like to thank the support and contribution of my colleagues from the Renewable Energies Chair of the University of Évora, with a unique companionship, inside and outside the offices/ laboratories, and whose discussions have contributed to these results and whose friendliness helped to release the spirit in less inspirational days.

Finally, I want to express my gratitude to my family, friends, and life partner, Dorin, for their unconditional support during this journey.

Obrigada!

# Integration, control and optimization of the solar photovoltaic-battery system in microgrids

## Abstract

This document composes the work realised and the research results developed within the scope of electric energy storage at the Renewable Energy Chair of the University of Évora. The current legal and technological framework of electrochemical energy storage technologies is reported, and its framework is demonstrated in the Portuguese and European contexts. Next, the experimental microgrid that comprises several electric energy storage technologies is described. The lithium-ion and vanadium redox flow technologies were tested and characterized for later validation of the electrical models that describe their performance. A state-of-the-art review allowed the experimentation of energy management strategies that fit the technologies studied, allowing smarter management in residential and services sectors. In this thesis, management algorithms, battery models, and an indication of technical, economic and energy parameters were combined in a tool to study the simulation of the operation of these technologies, allowing to define different operating objectives, fine-tune parameters and even join the operation of different technologies. This work was accompanied by national and international projects, attempting to respond to existing problems in the operation of real systems and gaps identified in the design phase, such as a robust dimensioning tool, with the integration of different battery managing methods.

**Keywords:** Solar photovoltaic energy, Electric energy storage, Energy management strategies, Competitiveness, Sustainability

# Integração, controlo e otimização do sistema solar fotovoltaico-bateria em microrredes

## Resumo

Este documento compõe o trabalho realizado e respetivos resultados da investigação desenvolvida no âmbito do armazenamento de energia elétrica na Cátedra Energias Renováveis da Universidade de Évora. Os atuais enquadramentos legais e tecnológicos das tecnologias eletroquímicas de armazenamento de energia são relatados, nos contextos português e europeu. Seguidamente, uma microrrede experimental que inclui diversas tecnologias de armazenamento de energia elétrica é descrita. As tecnologias de fluxo redox de vanádio e de iões de lítio foram objeto de ensaio e caracterização, para posterior validação dos correspondentes modelos que descrevem a sua performance elétrica. A revisão do estado da arte permitiu a experimentação de estratégias de gestão de energia que se adequam às tecnologias estudadas, que permitam a sua gestão inteligente, no contexto residencial e de serviços. Nesta tese, os algoritmos de gestão, os modelos das baterias, a indicação de parâmetros técnicos, económicos e energéticos foram combinados numa ferramenta para estudo da simulação da operação destas tecnologias permitindo definir diferente objetivos, afinar parâmetros e até operar conjuntamente diferentes tecnologias. Este trabalho foi acompanhado pelo paralelismo de projetos nacionais e internacionais, tentado dar resposta a problemas existentes na operação de sistemas reais, e lacunas identificadas na fase de projeto, tal como uma ferramenta de dimensionamento robusto, com a integração de diferentes formas de gerir baterias.

**Palavras-chave:** Energia Solar Fotovoltaica, Armazenamento de Energia Elétrica, Estratégias de Gestão de Energia, Competitividade, Sustentabilidade

# List of Publications

This thesis includes the following papers:

Foles, A.; Fialho, L.; Horta, P.; Collares-Pereira, M. “Economic and energetic assessment of a hybrid vanadium redox flow and lithium-ion batteries, considering power sharing strategies impact”, Journal of Energy Storage, vol. 71, 2023, DOI: 10.1016/j.est.2023.108167.

Foles, A.; Fialho, L.; Horta, P.; Collares-Pereira, M. “Validation of a lithium-ion commercial battery pack model using experimental data for stationary energy management application”, Open Research Europe, 2022, 2:15, DOI: 10.12688/openreseurope.14301.2.

Foles, A.; Fialho, L.; Collares-Pereira, M.; Horta, P. “An approach to implement photovoltaic self-consumption and ramp-rate control algorithm with a vanadium redox flow battery day-to-day forecast charging”, Sustainable Energy, Grids and Networks Journal, vol. 30, 2022, DOI: 10.1016/j.segan.2022.100626.

Foles, A.; Fialho, L.; Collares-Pereira, M. “Microgrid energy management control with a vanadium redox flow and a lithium-ion hybrid battery system for pv integration,” in 38th European Photovoltaic Solar Energy Conference and Exhibition, p. 1464–1469, 2021, DOI: 10.4229/EUPVSEC20212021-6BV.5.17.

Foles, A.; Fialho, L.; Collares-Pereira, M. “Techno-economic evaluation of the portuguese pv and energy storage residential applications,” Sustainable Energy, Technologies and Assessments, vol. 39, p. 100686, 2020, DOI: 10.1016/j.seta.2020.100686.

Foles, A.; Fialho, L.; Collares-Pereira, M.; Horta, P. “Vanadium Redox Flow Battery Modelling and PV Self-Consumption Management Strategy Optimization,” in 39th

European Photovoltaic Solar Energy Conference and Exhibition, 2020, DOI: 10.4229/EUPVSEC20202020-5EO.2.1.

López, E.; Fialho, L.; Vásquez, L. V.; Foles, A.; Cuesta, J. S.; Collares-Pereira, M. "Testing and evaluation of batteries for commercial and residential applications in AGERAR project," in *Mission 10 000: BATTERIES*, 2019.

Other publications related to the subject of the present thesis, but not included, are:

Foles, A.; Fialho, L.; Winzer, J.; González-García, N.; Horta, P.; Collares-Pereira, M. "Upcycling lithium-ion batteries: A case study", in 8th World Conference on Photovoltaic Energy Conversion (WCPEC-8) Conference, 2022, DOI: 10.4229/WCPEC-82022-5CO.10.4.

López González, E.; Fialho, L.; Vargas Vázquez, L.; Foles, A.; Saénz Cuesta, J. "Testing and evaluation of batteries for commercial and residential applications", in VII Symposium on Hydrogen, Fuel Cells and Advanced Batteries, HYCELTEC 2019.

# Contents

# List of Figures

Note: The figures of the scientific papers included in the chapters of this thesis are not included in this list to preserve their formatting and numbering. In that sense, their figures are presented as the published version.

# List of Tables



Note: The tables of the scientific papers included in the chapters of this thesis are not included in this list to preserve their formatting and numbering. In that sense, their tables are presented as the published version.

# List of Acronyms

| | |
|---|---|
| ADENE | *Agência Nacional de Energia* |
| AFC | Alkaline Fuel Cell |
| ASCII | American Standard Code for Information Interchange |
| BEPA | Batteries European Partnership Association |
| BESS | Battery Energy Storage System |
| BMS | Battery Management System |
| BMU | Building maintenance unit |
| CAES | Compressed Air Energy Storage |
| CAPEX | Capital expenditure (€) |
| CEC | California Energy Commission |
| CEP | (European) Clean Energy Package |
| DL | Decree-Law |
| DMFC | Direct Methanol Fuel Cell |
| DOD | Depth of Discharge (%) |
| EBA | European Battery Alliance |
| EC | European Commission |
| EES | Electrochemical Energy Storage |
| EMS | Energy Management Strategy |
| EOL | End Of Life |
| ERSE | *Entidade Reguladora dos Serviços Energéticos* |
| ESS | Energy Storage System |
| EU | European Union |
| EV | Electric Vehicle |
| FC | Fuel Cell |
| FES | Flywheel Energy Storage |
| GHG | Greenhouse gas(es) |
| HESS | Hybrid Energy Storage System |
| HFB | Hybrid Flow Battery |
| INIESC | Infraestrutura Nacional de Investigação para Energia Solar de Concentração |
| IPCEI | Important Project of Common European Interest |
| IU | Utilization installation |
| KPI | Key-performance Indicator |
| LabVIEW | Laboratory Virtual Instrument Engineering Workbench |
| LCA | Life Cycle Assessment |
| LCOE | Levelized cost of electricity (€/kWh) |
| LFP | Lithium Iron Phosphate |
| LIB | Lithium-ion Battery |
| Li-ion | Lithium-ion |

| | |
|---|---|
| Lithium-S | Lithium Sulphur |
| LMO | Lithium Manganese Oxide |
| LTO | Lithium Titanate Oxide |
| LXI | LAN eXtensions for Instrumentation |
| MATLAB | MATrix LABoratory |
| Na-ion | Sodium-ion |
| $NaMeCl_2$ | Sodium-Metal Chloride |
| $NaNiCl_2$ | Sodium-Nickel chloride |
| NaS | Sodium-sulphur |
| NCA | Nickel Cobalt Aluminium Oxide |
| NI | National Instruments |
| Ni-Cd | Nickel-cadmium |
| Ni-MH | Nickel-metal hydride |
| NMC | Nickel Manganese Cobalt |
| O&M | Operating and Maintenance Costs (€) |
| OPEP | Organization of the Petroleum Exporting Countries |
| Pb-A / LA | Lead-acid |
| PECS | *Plataforma de Ensaios de Coletores Solares* |
| PEMFC | Proton-exchange Membrane Fuel Cell |
| PHS | Pumped Hydroelectric Storage |
| PNEC | *Plano Nacional de Energia e Clima* |
| PSB | Polysulfide Bromine Flow Battery |
| PV | Photovoltaic |
| R&D | Research and Development |
| RE | Renewable Energy |
| REC | Renewable Energy Community |
| RES | Renewable Energy Sources |
| RFB | Redox Flow Battery |
| RNC | *Roteiro Nacional para a Neutralidade Carbónica* |
| RS | Recommended Standard |
| RTD | Resistance Temperature Detector |
| RTIEBT | *Regras Técnicas das Instalações Elétricas de Baixa Tensão* |
| RTU | Remote Terminal Unit |
| SAT | Storage As a Transmission asset |
| SCES | Supercapacitor Energy Storage |
| SLIB | Second Life Lithium-ion Battery |
| SMES | Super Magnetic Energy Storage |
| SOC | State Of Charge (%) |
| SOFC | Solid Oxide Fuel Cell |
| TCP/IP | Transmission Control Protocol/ Internet Protocol |
| TES | Thermal Energy Storage |
| TRL | Total Readiness Level |

| | |
|---|---|
| UÉvora | University of Évora |
| UPAC | *Unidade de Produção para Autoconsumo* |
| UPP | *Unidade de Pequena Produção* |
| UPS | Uninterruptible Power Supply |
| USB | Universal Serial Bus |
| VI | Virtual Instrument |
| VRE | Variable Renewable Energy |
| VRFB / VRB | Vanadium Redox Flow Battery |
| VRLA | Valve-regulated Lead-Acid |
| ZEBRA | Zero Emissions Batteries Research Activity |
| Zn-air | Zinc-air |
| ZnBr / ZBFB | Zinc Bromine Flow Battery |

# CHAPTER 1

# Introduction

## 1.1. Framework

The decarbonisation of the energy sector has been defined in national and international agreements, regulations, and energy policies worldwide. In 2015, at COP 21 of the United Nations Framework Convention on Climate Change (UNFCCC), held in Paris, 195 countries supported a global legally binding target for climate action. The agreement intended to control climate change by holding the global average temperature below 2°C above pre-industrial levels and pursuing efforts to keep it up to 1.5°C [1]. This significant landmark was effective as of November 2016.

The European Commission's (EC) Green Deal policy has set a greenhouse gas (GHG) emission reduction target of at least 55% compared with 1990 by 2030 [2]. In July 2021, the EC adopted a package of proposals to achieve these targets and to have at least a 32% share of renewable energy (RE) technologies deployment (currently at 29%) [3]. The European Union aims to reach carbon neutrality in 2050, a long-term strategy to reduce GHG emissions with an updated target of 80-90% by 2050 [4].

The availability of energy resources and their associated emissions must be considered and compared amongst them in order to achieve sustainable energy production and consumption. The transition from fossil fuels to energy sources with less impact on the environment and human health is currently central to policymaking, emphasising renewable energy sources (RES), such as hydropower, solar, wind and biomass. In what concerns other energy sources or carriers, hydrogen is considered a promising energy carrier, nuclear fusion is at its early stages (laboratory level), and the controversial nuclear fission has prominence in the energy generation sector of some European countries, such as France, Ukraine or the United Kingdom [5].

As the energy transition to cleaner generation sources occurs, changes in the oil market are felt [6]. The OPEP+ plan - Organisation of the Petroleum Exporting Countries, where the “+” includes a number of countries that voluntary supply cuts - foreseen a drastic oil supply reduction within the next years, with the consequences of increased

prices and volatility of the market [6]. The decommissioning of coal-fired power plants is central to the energy and climate policy debates, and natural gas (considered the cleanest among the fossil-fuelled sources) is showing a rapid growth in generation, transport and use. Although the energy sources transition is underway, the global energy supply is still largely supplied by fossil fuels, associated with high carbon dioxide emissions, as illustrated in Figure 1 (a, b).

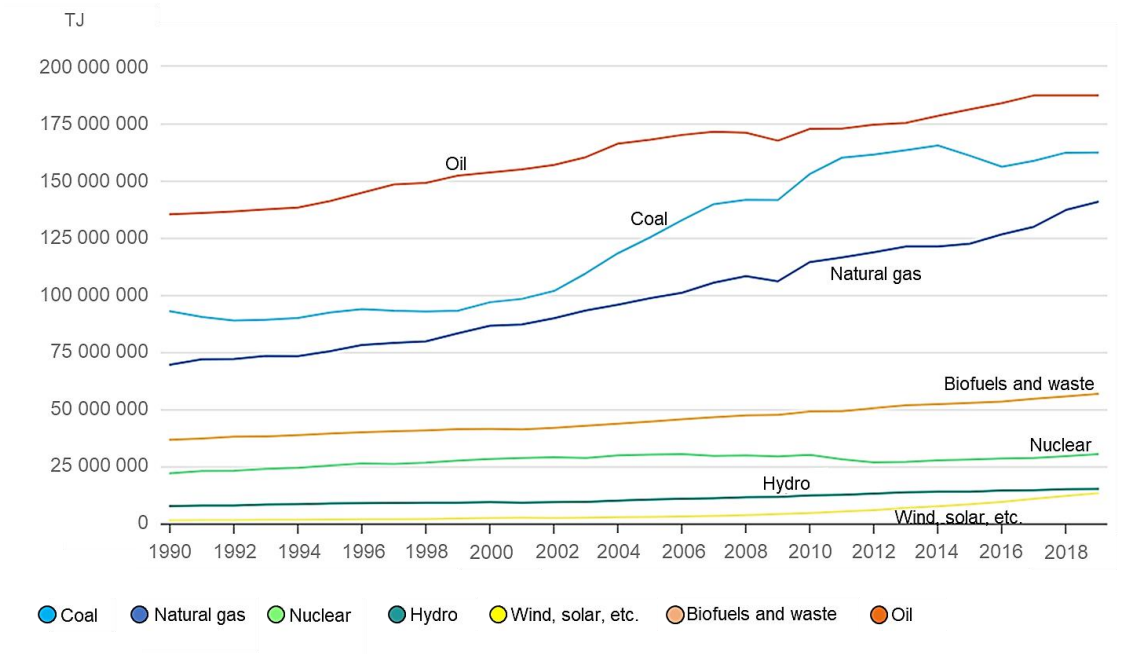


(a)

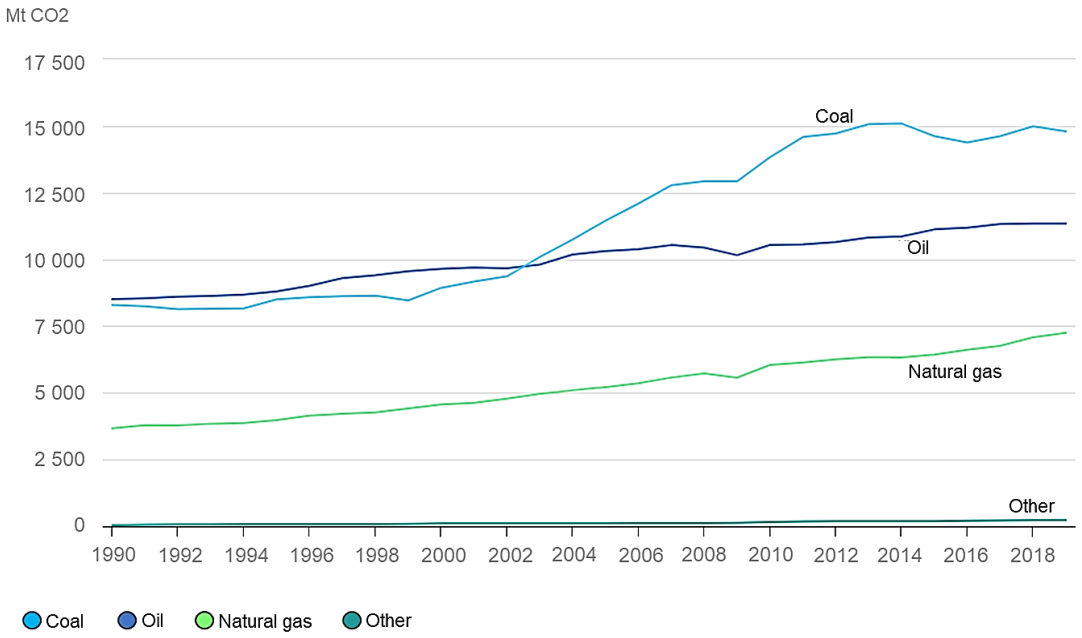


(b)

Figure 1. (a) Worldwide total energy supply (TES) by source and (b) Carbon dioxide ($CO_2$) emissions by energy source, World 1990-2019. Adapted from International Energy Agency (IEA) [7].

In November 2019, the European Parliament declared a global climate and environmental emergency, urging their member states to comply with the previously mentioned targets [8]. The EC's Long-Term Strategy includes decisive points to reach 80-100% decarbonisation levels predominantly related to the energy sector. When it comes to the use of electricity as a final energy source, its availability depends largely on the ability to produce it "on demand" by means of "dispatchable" technologies (e.g., coal, natural gas, nuclear or hydropower plants) or to store it in large quantities (mainly dependent on hydroelectric reverse pumping).

Electricity can be closer to a net zero emission provider at the use point, being generated by RES [9]. The significant deployment of RES is forecasted to be linked to direct or indirect electrification of different sectors. The decarbonisation of industry and transport sectors is planned to rely on power-to-gas (P2G) technologies producing renewable gases or fuels, such as hydrogen or methane. BloombergNEF (BNEF) predicts that in 2022 the worldwide global solar photovoltaic (PV) power capacity will surpass the 200 GW milestone [8], as shown in Figure 2.

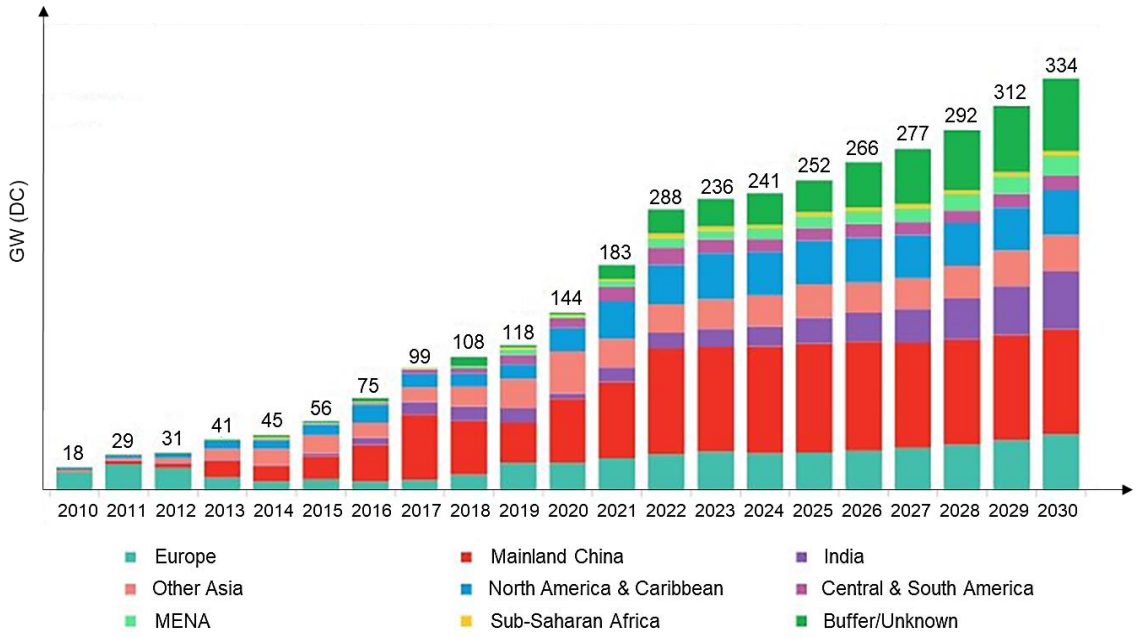


Figure 2. Global solar PV installed and forecasted capacity estimation as of January 2022. Adapted from [10].

Figure 2 presents the estimation and forecast of the continuously growing global solar PV installed capacity, where the European continent is placed in the third position from 2022 to 2030. BNEF estimates that solar PV modules will improve their efficiency,

increase the wafer size, and reduce module prices by 11 to 15 % in the second half of 2022. China's reliance on the beginning of the life cycle of these materials is expected to be reduced by the announcement of solar module manufacturing plants outside that country [10]. Solar PV and wind energy sources are described as variable renewable energies (VRE) due to their availability throughout the day, month, and seasons. In order to accommodate the intermittency of the generated energy from those technologies while servicing the power grid, dispatchable technologies currently provided by utilities and behind-the-meter batteries enable the global integration of VRE.

As of May 2019, the EC introduced long-term storage support through the European Clean Energy Package (CEP) [11] with updated targets on RES shares, although with a lack of definitions concerning storage operation. On recognising the potential role of batteries, European countries such as Germany and France plan to deploy storage on the grid as a transmission (SAT) asset (inject or absorb electricity to facilitate power flows on transmission lines over a certain period). China has been deploying energy storage to reduce VRE curtailment, and the United States is supporting research to clarify better the role of storage in the US networks. Australian grid operators are allowed to have their storage facilities, and in Chile, storage permits for emergency transmission amplification are stipulated by law [12].

In 2020, the COVID-19 pandemic presented social challenges across the energy, economy, and social sectors' coexistence and resilience. Post-COVID-19 Europe is built on a "recovery plan" that offers financial support for a more environmentally friendly, digital, and resilient society. More than 50% of the funding foreseen in this plan is dedicated to modernisation, research and innovation, climate fairness and digital transition. It is also focused on the modernisation of traditional policies, biodiversity protection and gender equality, and supporting the fight against climate change [13]. Portuguese green and digital transition correspond to a total of €13.9 billion in grants and €2.7 billion in loans, where 38% of the plan supports climate change objectives and 22% is focused on digital transition [14].

The Conference of the Parties 26 (COP26) [15] was held in Glasgow in November 2021. It yielded a commitment by the participating countries in climate change fighting efforts (such as ending and reversing deforestation by 2030) and reducing greenhouse gas emissions (40 countries committed to decommissioning coal-fired power plants). Moreover, a total of 137 countries have agreed on a "series of decisions", including commitments to reduce GHG emissions, and 40 countries mentioned their plans to

deploy affordable and clean technologies (including zero-emission vehicles) by 2030 (to reduce emissions by 2050). Despite the mentioned agreements, the definition of the following steps towards their realisation remained vague [16].

The energy transition to cleaner energy generation sources relies on the power system's flexibility, the grid integration improvement, the optimisation of the VRE generation and use, and the ensuring of stability and reliability of the energy sector. In the current scenario, the identified leading flexibility providers are dispatchable and flexible power generation technologies, demand-response and energy storage. The different coupling of energy sectors provides flexibility to power markets [12], including flexible energy generation and strong distribution and transmission systems, increasing storage integration and more flexible demand [17]. Energy storage can tackle the intermittency of VRE and facilitate energy availability at any period.

Energy storage encompasses different technologies and is generally classified after their energy conversion mode and divided into five major categories, as presented in Figure 3.

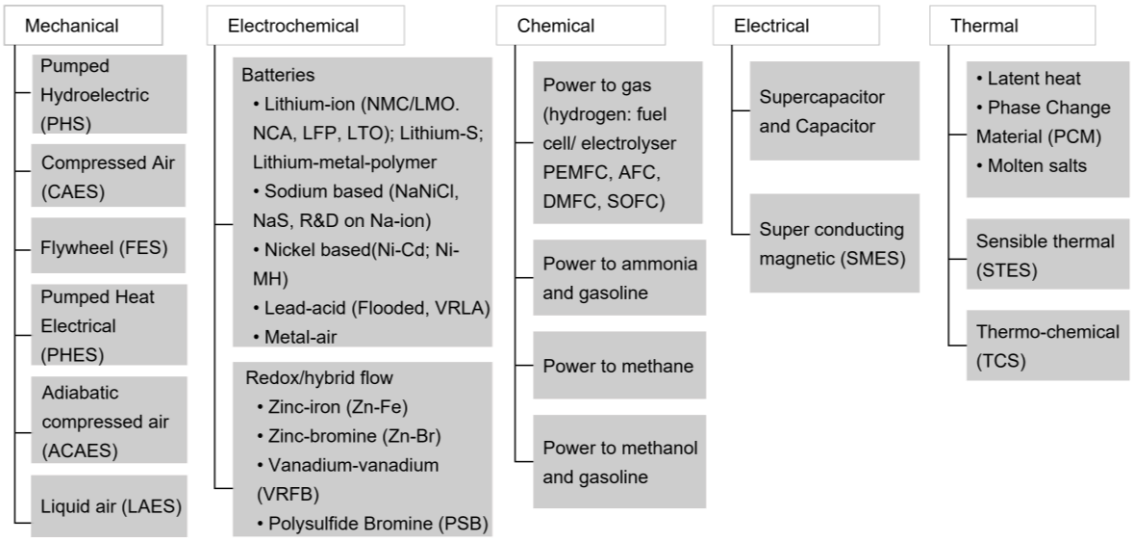


Figure 3. Classification of energy storage technologies by the form of the energy stored [18] [19] [20]. Legend: NMC – Nickel manganese cobalt; LMO – lithium manganese oxide; NCA – nickel cobalt aluminium oxide; LFP – lithium iron phosphate; LTO – lithium titanate oxide; Lithium-S – lithium sulphur; NaNiCl – Nickel sodium chloride; NaS – Sodium-sulphur; R&D – Research and development; Na-ion – Sodium ion; Ni-Cd – Nickel-cadmium; Ni-MH – Nickel-metal hydride; VRLA – Valve regulated lead-acid; VRFB – Vanadium redox flow battery; PEMFC – Proton-exchange membrane fuel cell; AFC – Alkaline fuel cell; DMFC – Direct methanol fuel cell; SOFC – solid oxide fuel cell.

The suitability of electrochemical energy storage (EES) technologies for different applications is dependent on their power and energy density characteristics, as presented in Figure 4.

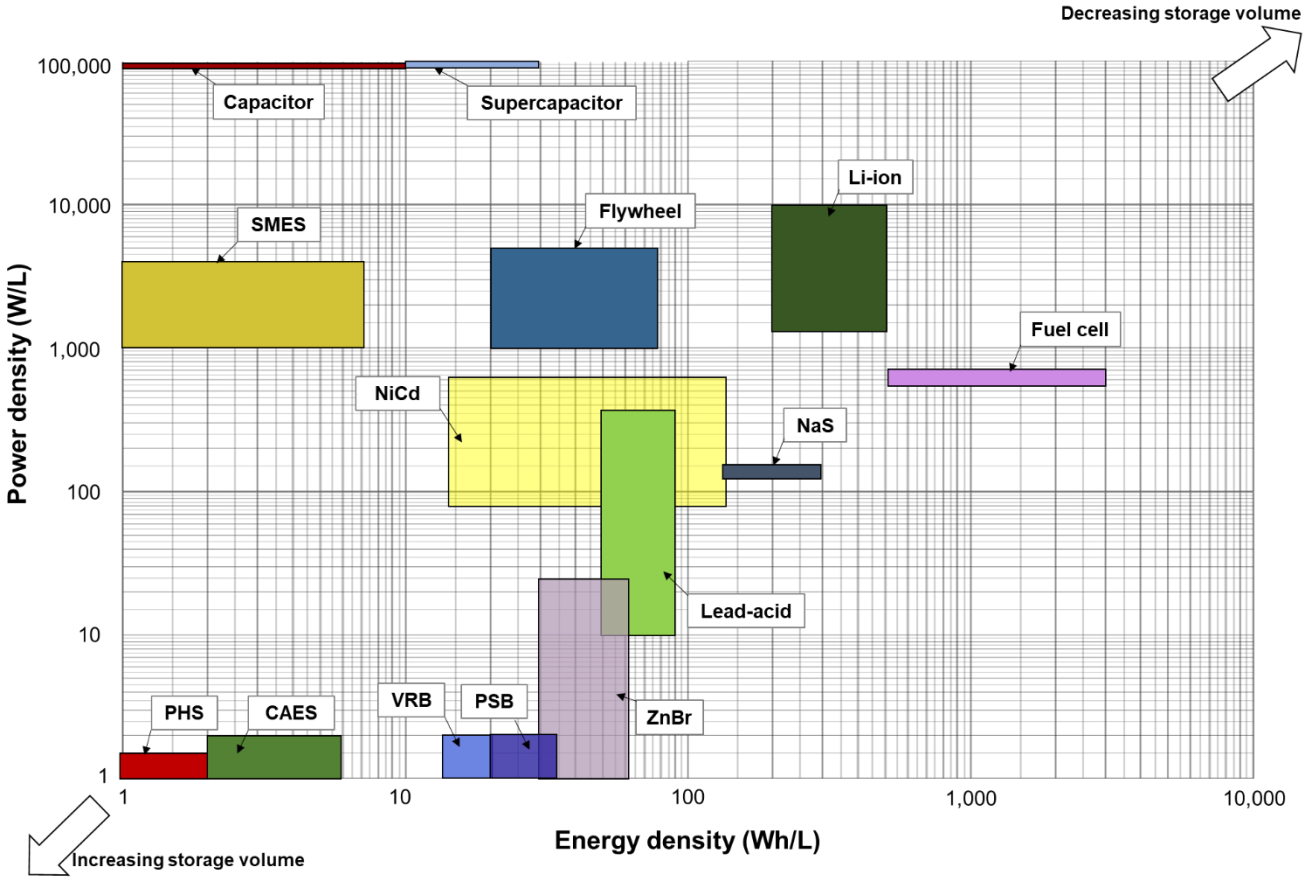


Figure 4. Energy and power densities comparison of the electrochemical and electrical energy storage commercially available technologies. Adapted from [18]. Legend: PHS – Pumped Hydroelectric Storage; CAES – Compressed Air Energy Storage; SMES – Super Magnetic Energy Storage; Ni-Cd – Nickel-cadmium; VRB – Vanadium Redox flow Battery; PSB – Polysulfide Bromine flow Battery; ZnBr – Zinc Bromine flow battery; NaS – Sodium-sulphur; Li-ion – Lithium-ion battery.

Most batteries, fuel cells, and flywheels have moderate power and energy densities, while capacitors and supercapacitors have higher power densities despite their low energy densities. PHS and CAES have low power and energy density (mainly used on-site), and flow batteries (redox or hybrid) exhibit low but moderate energy density. The range of energy storage technologies varies with typical discharge times [18], and the suitability of each energy storage unit for each application/service depends on their characteristics. The energy storage technologies services and applications are presented in Figure 5.

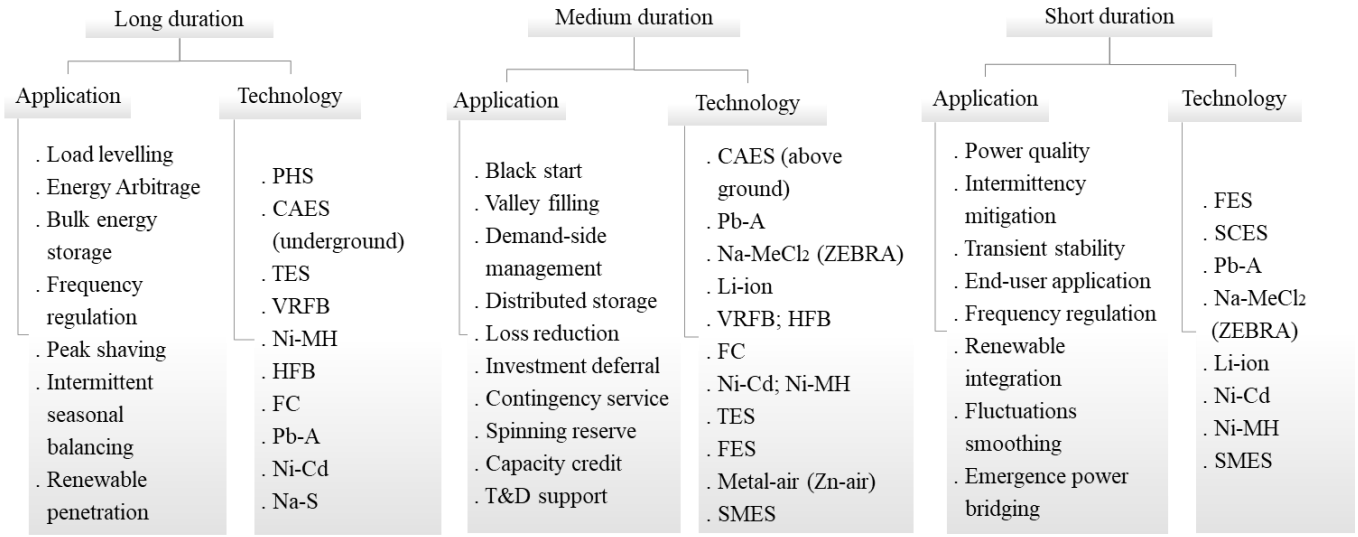


Figure 5. Energy storage applications [21]. Legend: PHS – Pumped hydroelectric storage; CAES – Compressed air energy storage; TES – thermal energy storage; VRFB – Vanadium redox flow battery; Ni-MH – Nickel-metal hydride; HFB – hybrid flow battery; FC – fuel cell; T&D – Transmission and Distribution; Pb-A – Lead-acid; Ni-Cd – Nickel-cadmium; Na-S – sodium sulphur; NaMeCl2 – Sodium metal chloride; Li-ion – lithium-ion; FES – flywheel energy storage; Zn-air – Zinc-air; SMES – superconducting energy storage; SCES – Supercapacitor energy storage.

Among the many services and applications of energy storage technologies revealed in

Figure 5, one can observe that short and medium-duration storage technologies are the most suited to apply to the buildings sector (residential, commercial, and public buildings). Given the additional 1 billion new households from 2018 to 2050 [22], IRENA forecasts an increase of VRE of about 89% share of the final consumption for 2050 for that sector [22], in their "World Energy Transitions Outlook" report. There, RES complements the scenario with distributed energy storage, aiming at reaching 99 GW of the installed power capacity in 2030 and 2200 GW in 2050. According to this study, the deployment of solar and storage technologies is based on several key aspects, such as fostering distributed energy sources and improvement of regulations by prosumers or increasing smartness and digitalisation in homes to improve their management.

In the report, IRENA developed a 1.5ºC scenario [22] – to comply with the COP21 target of keeping the global temperature rise up to 1.5°C –, where buildings could incorporate an array of solutions such as heat pumps, smart meters and energy storage, representing an 8% of the total energy sector investment during 2021-2030. An objective energy transition to cleaner energy sources should tackle concrete measures:

the acceleration of the adoption of electric vehicles, the decarbonisation of the railway sector, the wider adoption of renewable fuels (sustainable biofuels, green hydrogen, synthetic fuels), the adoption of new transportation models or the introduction of green hydrogen and electric (or hybrid) novel aircraft by 2035.

Inexpensive mass-produced batteries enable the competitive decarbonisation of the road transport sector and buildings sectors, allow the storing of VRE and promote the management of electricity within the network as frequency response, reserve capacity, and black-start capability [22]. They enhance renewable energy communities, empower prosumers, and allow the creation of virtual power plants: current research topics and strong candidates to contribute to shaping the future electricity sector.

The commercial battery costs declined by around 90% in the last decade. The 2030 forecasted reduction of the installation costs (in USD/kWh) of the currently commercialised batteries [23] is shown in Figure 6.

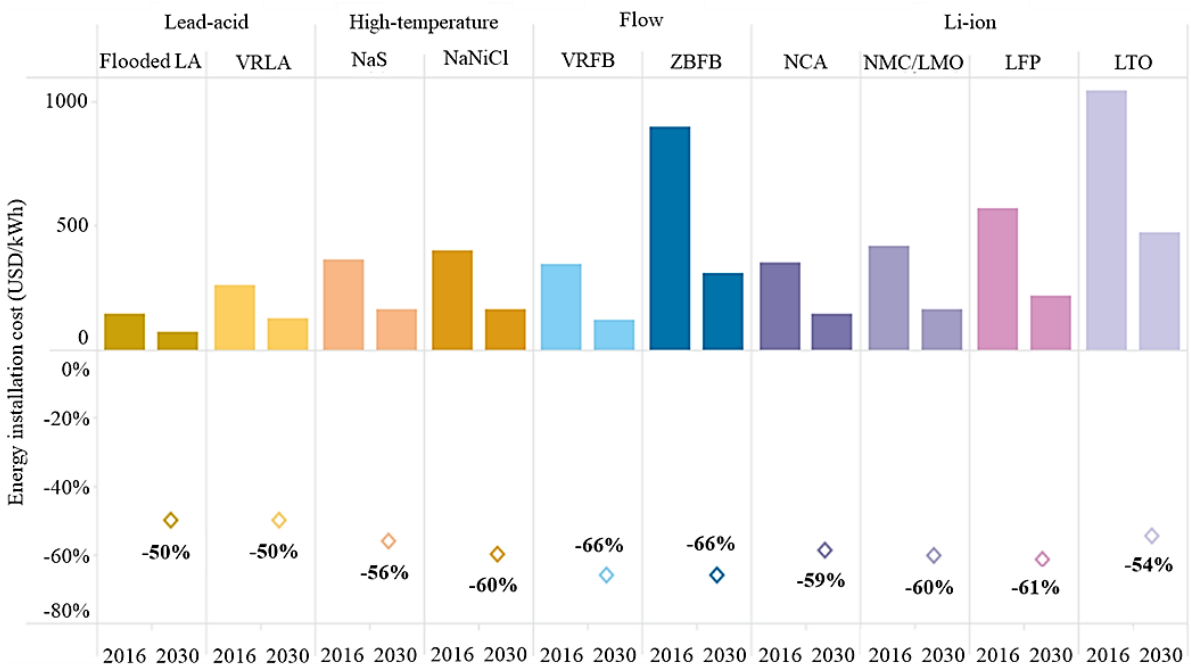


Figure 6. Total installed cost reduction potential of the EES, from 2016-2030 [23]. Legend: LA: lead-acid; VRLA: valve-regulated lead-acid; NaS: sodium-sulphur; NaNiCl: sodium nickel chloride; VRFB: vanadium redox flow battery; ZBFB: zinc-bromine flow battery; NCA: nickel cobalt aluminium; NMC/LMO: nickel manganese cobalt oxide/lithium manganese oxide; LFP: lithium iron phosphate; LTO: lithium titanate.

The study of Figure 6 estimates high reductions (50-66 %) from the 2016-2030 for the generality of battery technologies, considering the economies of scale, technology

improvements, material cost reductions and higher competition in the supply chain. Despite this cost reduction scenario, significant uncertainty is tied to these projections. The economic viability of an investment considering BESS could be a combination of the use/application, capital cost reduction and increased lifetime [23]. The cost-effectiveness determines whether to consider a particular technology for an application. In this sense, research developed on this topic is deemed relevant to the market characterisation and identification of potential improvements. Newly developed projects of batteries foster their price decrease [12].

Research and development (R&D) focus on finding energy storage solutions that are scalable, flexible and inexpensive and that could balance the energy efficiency, the social/environmental aspects, and the economic prosperity of a project. The current investigation has been focusing on abundant and inexpensive materials, such as battery chemistries of aluminium, sulphur [24], salt/ sodium [25], zinc [26], or iron [27]. The new materials that will compose the batteries should follow the guidelines described by the Battery2030+ roadmap in [28][29], ensuring recyclability and repurposing, addressing battery manufacturing through ethical sources, among other relevant measures.

The distributed energy sources allow for decentralised energy production, as implementing local system optimisation avoids costly flexibility measures. On the demand side, energy storage enables the electrification of end-use sectors through load management and grid congestion relief, increasing flexibility if batteries are supplied with VRE. Usually, residential solar PV systems that maximise self-consumption integrate batteries into their configuration [30].

Global battery production is increasing primarily with the introduction of electric vehicles - lithium-ion technology -, while other energy storage technologies are becoming commercially mature to enable decarbonisation. Each energy storage application needs to be optimised for each specific need. Further R&D is required to expand batteries' role in energy conversion and maximise their potential for decarbonisation [22]. Characterisation and modelling of batteries provide crucial insights regarding the performance output and help clarify their possible roles in the applications. The simulation of the batteries allows the research of their operation and management. Research can contribute to the overall improvement of the batteries' application in finding optimised ways of managing their energy flows following the evaluated needs.

### 1.1.1. Portuguese context

The World Energy Council defines energy sustainability in three dimensions: energy equity, energy security, and environmental sustainability of energy systems. Portugal is placed in the 14th position in the 2021 world energy ranking [31]. Due to the low use of fossil fuels as primary energy sources and the consequent reduction in carbon dioxide emissions associated with the COVID-19 pandemic, electricity generation from RES accounted in Portugal stood for 61% of total electricity production in 2021 (approximately 51 TWh) [32]. Figure 7 shows the installed RE power generation capacity by source in Portugal for the period 2000 to 2020.

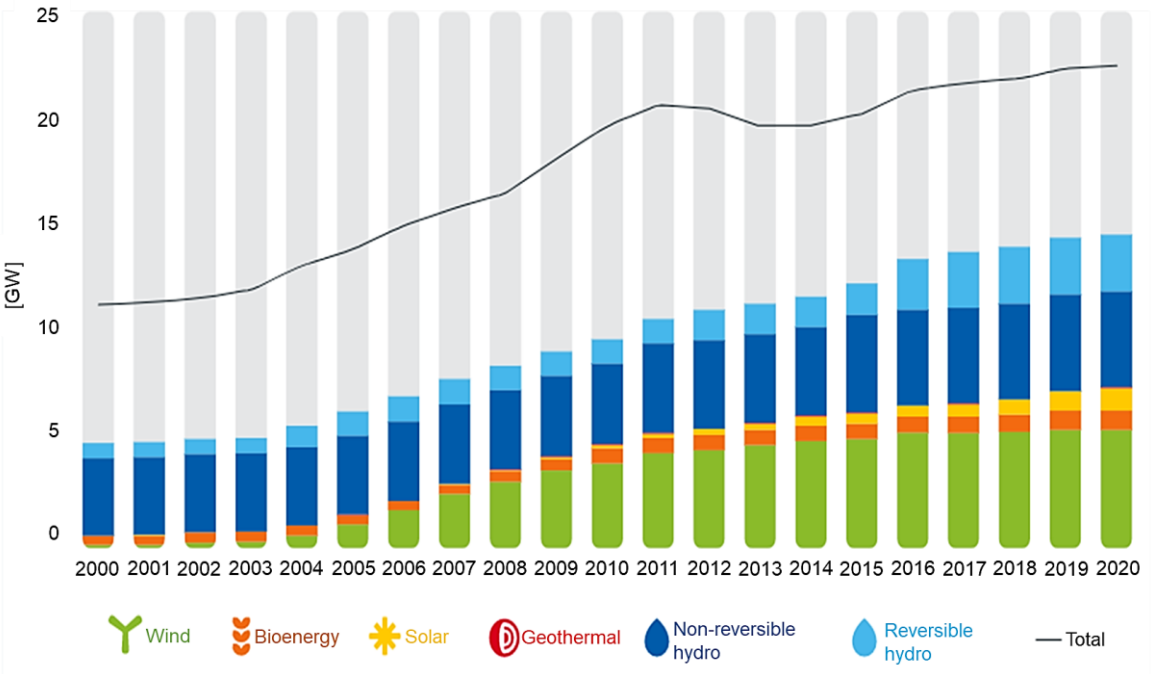


Figure 7. Installed capacity of the different electricity generation sources in Portugal [32].

Portugal has set four national goals to support the climate transition through its national energy and climate plan, the PNEC 2021-2030 (*Plano Nacional de Energia e Clima)* [33]:

- Reduce GHG emissions from 45% to 55% by 2030 compared to 2005.
- Account for 47% share of RES in gross final energy consumption in 2030.
- Reduce primary energy consumption by 35% in order to achieve better energy efficiency.
- Achieve 15% electricity interconnections [33].

The PNEC 2030 includes 58 topics and 206 policies to achieve the targets mentioned above, in conjunction with the RNC [34] - *Roteiro para a Neutralidade Carbónica* - where Portugal has committed to achieving carbon neutrality by 2050. The agreements include reducing greenhouse gas emissions, integrating renewable energy technologies, increasing energy efficiency, and promoting society's decarbonisation and energy transition. The plan includes green hydrogen production and solar PV capacity auctions, fostering electric mobility, and the end of electricity generation from coal power plants, already achieved with the decommission of Sines (January 2021) and Pego (November 2021) power plants. This decommissioning anticipated the earlier estimations of full decommissioning for 2023 [35] (Portugal was the third country to anticipate the decommission of a coal plant in Europe that year, after Austria and Sweden). The cause is linked to coal market prices, costs associated with the emissions related to the energy generation from coal (carbon costs) and the competitiveness of alternative sources [36], such as solar PV [37][38].

The most recent Portuguese legislation regulating the power generation system is the Decree-Law (DL) 15/2022 [39] (as the earlier DLs on the topic are revoked) aiming at the implementation of the EU legislation (Directive 2019/944 and Directive 2018/2001). DL 15/2022 describes the regulatory framework for the generation, transmission, distribution, storage, and commercialisation of electricity and the electricity markets organisation, covered by a single framework of prior control (depending on the size of the system (e.g., PV installation) and nature of activity). It includes the definitions of power ranges where the RES and storage regimes are applied. The self-consumers are obliged to prior communication procedure to *Direção Geral de Energia e Geologia* (DGEG) – Portuguese authority - for their installation. The tariffs for their connection to the electricity grid, usage of the grid, and location of the production unit for self-consumption - UPAC (*Unidade de Produção para Autoconsumo)* - should be as close as possible to the consumption location, contributing to reducing grid constraints.

Self-consumers have the right to: install one or more UPACs; establish direct lines and internal networks when there is no access to the public grid; consume the electricity produced in UPACs in the utilisation installation (IU); operate storage facilities; and trade surplus energy from production for self-consumption through electricity markets, bilateral contracts, or peer trading regimes, directly or through third parties. It is mandatory to meter the total electricity production, the electricity injected and extracted from energy storage facilities connected to the national electricity grid and in a collective UPAC named REC – renewable energy community – when the installed

power is higher than 4 kW. Electric vehicles (EVs) as energy storage units are not defined in this DL, only referred to in the previous Decree-Law 162/2019 [40]. Its definition of storage energy includes storage in vehicles when the user's installation has a bi-directional charging point.

The installed storage power capacity currently available in Portugal reaches more than 3.3 GW, dominated by mechanical storage (reverse pumping) with 3345 MW, but including also electrochemical storage (in operation and at the project phase) of about 6 MW; and chemical energy storage of 1 MW [12]. Closer to 2030, the increase in energy storage capacity will be mainly in the reversible pumping of hydroelectric power. Daivões and Alto Tâmega are the places of new hydroelectric powerplants with storage and reverse pumping capabilities that will be operational from 2026. Portugal and The Netherlands have signed a green hydrogen agreement to advance the strategic value chain of production and transport of hydrogen, where the ports of Sines and Rotterdam are strategic [41]. The role of batteries will be mainly linked to the deployment of additional wind and solar energy capacity. In addition, the PNEC highlights the importance of behind-the-meter energy management and smart charging for electric vehicles.

The Portuguese needs for energy storage have been addressed in a recent publication that joined Portuguese authorities (ADENE and DGEG) and Universities (the University of Lisbon and Técnico de Lisboa) through the use of a modelling tool, the EnergyPLAN, that helped to build future scenarios for 2030 and 2040 [42]. These scenarios took into account the PNEC and RNC-defined targets. They discussed different energy storage technologies, although offering a technical analysis only. A technical-economic approach would be more realistic in such scenarios, promoting discussion and further adoption.

The promotion of energy storage systems should rely on the following framework [12] [42]:

- Creation of a legal framework that fosters the implementation of energy storage through direct or indirect political incentives (e.g., promoting self-consumption maximisation).
- Promotion of a roadmap for energy storage in Portugal.
- Rule definitions on the energy storage units' possession, ensuring their only utilisation through markets and not by grid operations to operate or manage systems.

- Promotion of storage and renewable energy projects related to electricity generation centres.
- Foster R&D projects that can implement pilot technologies, validate them in real applications, and serve as demonstrators.
- Foster the implementation of storage in islands.

For an efficient energy transition, the Portuguese low-voltage (BTN) network must integrate smart grids, energy management devices, energy storage, local energy generation, energy communities, and electric transportation. In order to include this new equipment, the adequacy of the current network must be adapted [12]. The decarbonisation of the power generation system should be accompanied by public politics that promotes the effective interaction among all the elements and allow its optimized management.

### 1.1.2. Towards a sustainable battery value chain?

As well as other goods and products, the batteries' lifecycle impacts the environment at different stages: raw material extraction, processing, manufacturing, use, recycling, and disposal. The materials that compose batteries are geographically distributed along three major regions, often politically and economically unstable [43] [44]. The European Battery Alliance (EBA) [45] has established in 2017 the support of innovative battery solutions and the expansion of European manufacturing capacity. In December 2020, a proposed regulation on batteries and waste batteries was adopted to ensure the sustainability and competitiveness of the European battery value chain. This regulation implies that raw materials mining must be dissociated from environmental pollution and human rights violations. The carbon footprint depends on the energy source and, as a result, the country where the production occurs. In addition to EBA, other organisations and projects such as IPCEI Batteries [46], BEPA/ batt4EU [47] or Battery 2030 [48] are contributing to the sustainability of the battery value chain (mainly in the initial phase of the battery life cycle: raw materials and manufacturing phases). According to sustainable and controlled plans, these associations are bringing these phases to Europe so that battery manufacturing could be more regulated to comply better with standardisation.

The transition to cleaner energy sources described in the European Green Deal requires electrification efforts and diversification of the supply sources, demanding an increase

in raw materials. The EC developed a list of critical raw materials with supply chain dependencies, whose schematic is presented in Figure 8.

The case of batteries presents moderate, low, and very low supply risk. Nevertheless, some battery elements are rare such as lithium and cerium, or expensive, such as mercury and indium [50]. At the end of life, 90-100% of lead from lead-acid batteries is recovered. However, lithium-ion battery recycling is technologically challenging and costly and focused on more economically valuable materials, such as cobalt, nickel or copper. Graphite is not recovered [50]. The proposal for a "New EU regulatory framework for batteries" suggests, among other relevant measures: having a declaration requirement with minimum recyclability levels, an obligation of battery replaceability, minimum electrochemical performance and durability requirements for portable batteries of general use, or safety requirements for stationary battery energy storage systems [50].

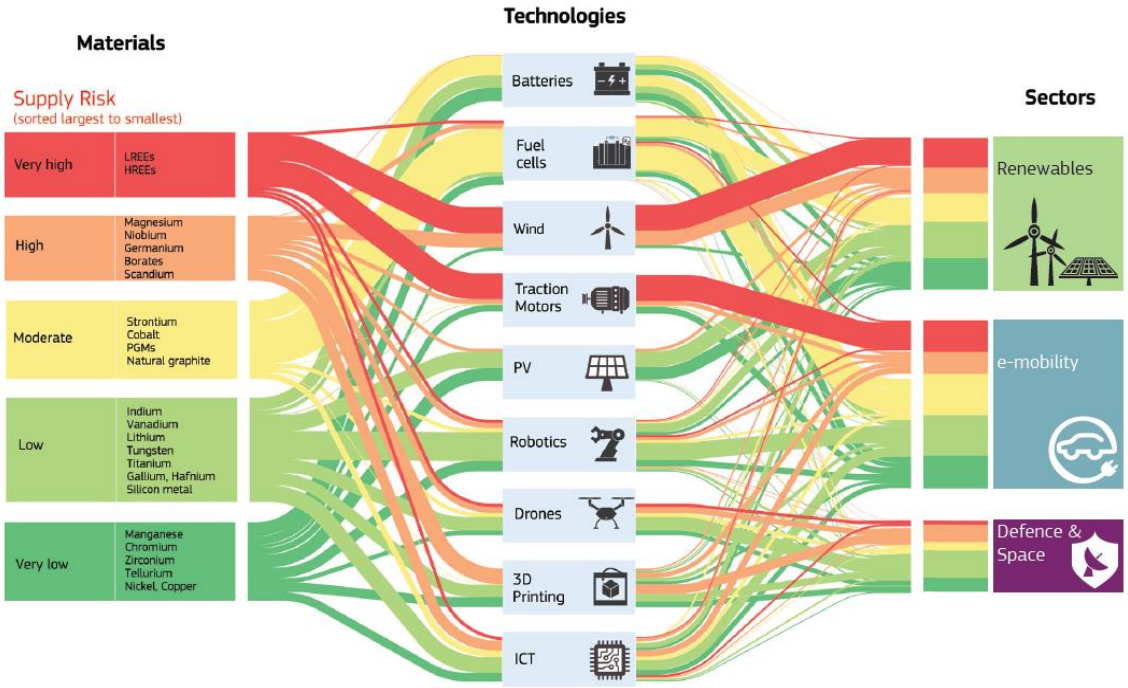


Figure 8. European Commission critical raw materials list of technologies identified by sector [51].

The World Energy Council has developed a 2021 global map that outlines the key challenges, risks, and opportunities worldwide countries face to achieve the energy transition based on national regulations and testimonies. Energy industry leaders indicated the priority setting as challenging and shared concerns about economic

growth. Except for North America, commodity prices are considered a global uncertainty, with record natural gas prices in Europe and the United Kingdom. Countries are increasing their share of RES, though energy-related geopolitics remains uncertain. Equity-related aspects such as commodity prices, affordability, quality energy access (safety, reliability, adequate supply) and market design are highlighted. For Europe, cybersecurity risks, electrical energy storage innovation, system decentralisation, and innovative transportation are discussed as challenges [16].

The need for an overall effort is recognised to avoid rising global temperatures, support energy transition to cleaner energy sources, successfully execute waste management, and promote environmental awareness. Citizens' conscience on energy generation and use is highly relevant and currently present in any of the developed national political programmes. The communication of science should be fostered to avoid misinformation and lead to the accountable direct involvement of the citizens so that political decisions are better understood. Low carbon emissions are to be embraced if based on sustained plans and focused on the primary pillar: to maintain or improve the well-being of the human quotidian with the lowest possible impact on the environment.

## 1.2. Objectives

As of the state-of-the-art, it is currently challenging to identify or determine the application of battery storage from its different perspectives: technical, energetic, and economical. Choosing the appropriate battery, as of technology, size, or type of operation, for a particular application is challenging as it also depends on the intended objectives, implementation restrictions, and possible management options.

The motivation of this work is to create tools to develop and assess battery inclusion in projects and investigate options to optimise their operation and control within that context, promoting the increasing penetration of renewable energy and their better integration with the broad energy mix. In this sense, this thesis proposes the overall characterisation, objective evaluation and proposing of solutions to optimise the operation of battery technologies – mainly focused on lithium-ion and vanadium redox flow. In this context, this thesis aims to answer the following questions:

- How to evaluate the battery application in a project, considering technical, energetic, and economic dimensions?
- How to experimentally characterise the different battery technologies?

- How to simulate and model battery technologies?
- How to develop an optimised energy management strategy combined with self-consumption maximisation of solar PV? How to validate it at a real scale?
- How to design a microgrid with different and innovative energy storage and solar PV technologies? How to install and commission such technology systems?
- How are different battery storage technologies properly combined or hybridised?

The work developed in this thesis appealed to the defined methodologies to answer the above questions. This work can be seen as a contribution to the finding path for those answers.

## 1.3. Main contributions

As a recent research topic, the batteries' characterisation and role assessment need to be clarified, and in Portugal, only a few initiatives exist for efficiently operating, controlling and characterising batteries. One of the key topics that motivated the development of this thesis is the battery potential to be coupled with solar photovoltaic technologies for decentralising energy generation and use and their flexibility to be managed efficiently and smartly.

As a first-problem approach, this thesis focused on framing and characterising the solar PV and battery systems in the Portuguese context to assess their economic and energetic impact on a project, considering the energy management strategy of maximising self-consumption. In this context, the development of a tool that could offer this analysis type was initiated in MATLAB programming. The tool aimed at facilitating the inclusion of batteries under the project's evaluation. This assessment is necessary to estimate the viability of such investments, providing the realisation of informed decisions, and bringing reliability to their framework integration.

In order to improve the tool reproducibility of the real-world systems, electrical models of the existing batteries in the Renewable Energies Chair experimental microgrid were developed and included on the tool. These models presuppose the communication establishment with different brands of inverters. They would allow real-time control of the batteries, developed through LabVIEW programming, and validate the developed

electrical models. The entire test and control programming of inverters and batteries was a disruptive work developed throughout this thesis. Relevant data on battery operation were obtained, which can feed different battery electrical modelling approaches and be an object of testing energy management strategies based on the existing technologies.

The validation of the electrical battery models with their response in a real environment allowed their extended simulation. It validated the previously described tool, increasing its similarity with the real world. With the battery models improved, it was possible to develop energy management strategies that could solve real-world issues and be tested in simulation, which is the case for the work developed with the solar PV ramp rate strategy. The algorithm of this strategy was programmed in the tool and later tested in real-time using the microgrid equipment (LabVIEW), demonstrating its reliability and innovation.

As the future electrical system will be composed of several technologies that need to be controlled and integrated into a single set system (both for centralised and decentralised electrical generation applications), the challenge of finding complementarity in different electrochemical battery technologies was initiated. Considering this concept, the two battery technologies – based on lithium and vanadium – were simulated with different models but jointly controlled in their management and sizing, which is considered a current research challenge. Simulating and implementing hybrid battery operation complemented the developed work of economic and energy assessment and can be seen as disruptive work in this field of research.

## 1.4. Outline of the thesis

This thesis consists of six chapters. Chapter 1 outlines the theme and the framework concerning the conditions, possible uses, and global perspectives of the battery market. Chapter 1 also defines the author's main contributions, the targeted research questions and the general thesis outline.

Chapter 2 presents an overview of the experimental research work developed through the elaboration of this thesis. It includes building and commissioning a complete experimental microgrid consisting of different electrical energy storage technologies, solar PV installations, one electric vehicle charging station, and sensible measurement devices.

Chapter 3 introduces the Portuguese battery storage framework in compliance with Decree-law 153/2014 and further addresses the testing experiments developed to characterise the lithium-ion and vanadium redox flow batteries within the microgrid described in Chapter 2. Chapter 3 describes the electrical modelling of the mentioned batteries with the help of MATLAB software. These models are experimentally validated with LabVIEW programming. Section 3.3.2. includes unpublished work developed on the second-life lithium-ion battery, namely the characterisation testing results and main contributions to the prototype.

Chapter 4 addresses the PV+battery energy management strategies, where evaluation is carried out through key performance indicators. This chapter investigates the hybridisation of the two batteries through simulation, proposing new energy management strategies. In addition to the published work, Section 4.5. presents the contributions to a hybrid battery modelling tool and real-scale prototype.

The List of Papers enunciates the scientific articles presented in Chapter 3 and Chapter 4, published in international peer-reviewed journals and international peer-reviewed conference proceedings. Chapter 5 describes the general conclusions of this thesis. Finally, Chapter 6 points out interesting future research paths.

This work contains two chapters - Chapter 3 and Chapter 4 - that stand for articles published in peer-reviewed journals and are presented to prioritise the maintenance of the published format (including references). The remaining chapters (1, 2, 5 and 6) are formatted sequentially (independent of Chapters 3 and 4). Their references are presented at the end of each chapter.

## 1.5. References

[1] United Nations, “Paris Agreement,” Paris, 2015.

[2] European Commission, “European Green Deal,” *A European Green Deal Striving to be the first climate-neutral continent*, 2020. [Online]. Available: https://ec.europa.eu/info/strategy/priorities-2019-2024/european-green-deal_en.

[3] European Commission, “2030 Climate & Energy Framework,” 2021. [Online]. Available: https://ec.europa.eu/clima/policies/strategies/2030_en.

[4] European Commission, “2050 Long-Term Strategy,” 2020. [Online]. Available: https://ec.europa.eu/clima/policies/strategies/2050_en.

[5] European Nuclear Society, “Nuclear Power Plants in Europe.” 2015.

[6] IEA, “Oil Market Report,” 2022.

[7] IEA, “Data and Statistics,” 2020. [Online]. Available: https://www.iea.org/data-and-statistics/data-browser?country=WORLD&fuel=Energy supply&indicator=TESbySource.

[8] T. Haahr, “European Parliament,” *The European Parliament declares climate emergency*, 2019. [Online]. Available: https://www.europarl.europa.eu/news/en/press-room/20191121IPR67110/the-european-parliament-declares-climate-emergency. [Accessed: 29-Nov-2019].

[9] IEA, “Innovation in batteries and electricity storage,” 2020.

[10] BNEF, “Solar – 10 Predictions for 2022,” 2022. [Online]. Available: https://about.bnef.com/blog/solar-10-predictions-for-2022/.

[11] European Commission, “The EU Clean Energy Package,” 2019.

[12] C. Andrey *et al.*, “Study on energy storage - Contribution to the security of the electricity supply in Europe,” 2020.

[13] European Commission, “Recovery plan for Europe,” 2021. [Online]. Available: https://ec.europa.eu/info/strategy/recovery-plan-europe_en.

[14] European Commission, “Portugal’s recovery and resilience plan.” [Online]. Available: https://ec.europa.eu/info/business-economy-euro/recovery-coronavirus/recovery-and-resilience-facility/portugals-recovery-and-resilience-plan_en.

[15] European Commission, “EU at COP26 Climate Change Conference | European Commission,” 2021. [Online]. Available: https://ec.europa.eu/info/strategy/priorities-2019-2024/european-green-deal/climate-action-and-green-deal/eu-cop26-climate-change-conference_en. [Accessed: 14-Sep-2022].

[16] World Energy Council, “2022 World energy issues monitor,” London.

[17] IRENA, “Power System Flexibility for the Energy Transition - Part 1: Overview for policy makers,” Abu Dhabi, 2018.

[18] X. Luo, J. Wang, M. Dooner, and J. Clarke, “Overview of current development in electrical energy storage technologies and the application potential in power system operation,” *Appl. Energy*, vol. 137, pp. 511–536, 2015.

[19] J. Liu, C. Hu, A. Kimber, and Z. Wang, "Uses, Cost-Benefit Analysis, and Markets of Energy Storage Systems for Electric Grid Applications," *J. Energy Storage*, vol. 32, no. February, p. 101731, 2020.

[20] Directorate-General for Energy, "data.europa.eu," *Database of european technologies and installations of energy storage*, 2021. [Online]. Available: https://data.europa.eu/data/datasets/database-of-the-european-energy-storage-technologies-and-facilities?locale=pt.

[21] F. Nadeem, S. M. S. Hussain, P. K. Tiwari, A. K. Goswami, and T. S. Ustun, "Comparative review of energy storage systems, their roles, and impacts on future power systems," *IEEE Access*, vol. 7, pp. 4555–4585, 2019.

[22] IRENA, "World Energy Transitions Outlook: 1.5°C Pathway," Abu Dhabi, 2021.

[23] IRENA, "Electricity Storage and Renewables: Costs and Markets to 2030," Abu Dhabi, 2017.

[24] "MIT develops new battery made of inexpensive, abundant materials | Electronics360." [Online]. Available: https://electronics360.globalspec.com/article/18561/mit-develops-new-battery-made-of-inexpensive-abundant-materials. [Accessed: 08-Nov-2022].

[25] "Batteries without critical raw materials: Operando observations show what might work -- ScienceDaily." [Online]. Available: https://www.sciencedaily.com/releases/2022/10/221027124050.htm. [Accessed: 08-Nov-2022].

[26] U. Ali, "Beyond lithium: alternative materials for the battery boom," *Power Technology*, 2019. [Online]. Available: https://www.power-technology.com/analysis/lithium-battery-alternatives/. [Accessed: 08-Nov-2022].

[27] Form Energy, "Battery Technology | Form Energy." [Online]. Available: https://formenergy.com/technology/battery-technology/. [Accessed: 13-Dec-2022].

[28] J. Amici *et al.*, "A Roadmap for Transforming Research to Invent the Batteries of the Future Designed within the European Large Scale Research Initiative BATTERY 2030+," *Adv. Energy Mater.*, vol. 12, no. 17, 2022.

[29] K. Edstrom *et al.*, "Battery 2030 Roadmap - Inventing the Sustainable Batteries of the future: Research Needs and Future Actions," 2020.

[30] A. Anisie *et al.*, “Innovation landscape for a renewable-powered future: Solutions to integrate variable renewables,” Abu Dhabi, 2019.

[31] World Energy Council and Olivier Wyman, “World Energy Trilema Index 2021,” London, 2021.

[32] APREN, Ed., *APREN 2021 Yearbook*. Lisbon, 2021.

[33] República Portuguesa, “Plano Nacional Integrado Energia e Clima 2021-2030,” 2018.

[34] República Portuguesa; Fundo Ambiental; APA, *Roteiro para a Neutralidade Carbónica 2050 - XXI Governo - República Portuguesa*. 2019.

[35] “Sines plant closes ahead of schedule due to market developments – ECO News.” [Online]. Available: https://econews.pt/2021/01/15/sines-plant-closes-ahead-of-schedule-due-to-market-developments/. [Accessed: 16-Sep-2022].

[36] “End of Sines power plant means biggest emissions reduction ever - The Portugal News.” [Online]. Available: https://www.theportugalnews.com/news/2021-01-16/end-of-sines-power-plant-means-biggest-emissions-reduction-ever/57743. [Accessed: 16-Sep-2022].

[37] “Winners, projects, prices of Portugal’s record PV auction – pv magazine International.” [Online]. Available: https://www.pv-magazine.com/2019/08/09/winners-projects-prices-of-portugals-record-pv-auction/. [Accessed: 16-Sep-2022].

[38] “Winners, prices of Portugal’s record-breaking auction for floating PV – pv magazine International.” [Online]. Available: https://www.pv-magazine.com/2022/04/08/winners-prices-of-portugals-record-breaking-auction-for-floating-pv/. [Accessed: 16-Sep-2022].

[39] República Portuguesa, *Decreto-Lei n.º 15/2022 | DRE*. Portugal, 2022, pp. 3–185.

[40] República Portuguesa, *Decreto-Lei n.º 162/2019 de 25 de outubro*. Portugal, 2019, pp. 45–62.

[41] “Portugal and the Netherlands green hydrogen agreement – Policies - IEA.” [Online]. Available: https://www.iea.org/policies/13541-portugal-and-the-netherlands-green-hydrogen-agreement. [Accessed: 16-Sep-2022].

[42] P. Ferrão *et al.*, “Armazenamento de Energia em Portugal,” 2021.

[43] A. R. Dehghani-Sanij, E. Tharumalingam, M. B. Dusseault, and R. Fraser, "Study of energy storage systems and environmental challenges of batteries," *Renew. Sustain. Energy Rev.*, vol. 104, no. January, pp. 192–208, 2019.

[44] P. Meshram, A. Mishra, Abhilash, and R. Sahu, "Environmental impact of spent lithium ion batteries and green recycling perspectives by organic acids – A review," *Chemosphere*, vol. 242, p. 125291, 2020.

[45] "Building a European battery industry - European Battery Alliance." [Online]. Available: https://www.eba250.com/. [Accessed: 16-Sep-2022].

[46] "IPCEI Batteries: IPCEI Batteries." [Online]. Available: https://www.ipcei-batteries.eu/. [Accessed: 16-Sep-2022].

[47] "BEPA – BATT4EU." [Online]. Available: https://bepassociation.eu/about/bepa/. [Accessed: 16-Sep-2022].

[48] "Battery2030+ - Battery 2030+." [Online]. Available: https://battery2030.eu/. [Accessed: 16-Sep-2022].

[49] European Commission, "Raw Materials Information System," 2020.

[50] European Parliament, "New EU regulatory framework for batteries," *Proposal for a Regulation of the European Parliament and the Council concerning batteries and waste batteries, repealing Directive 2006/66/EC and amending Regulation (EU) No 2019/1020*, 2022. [Online]. Available: https://www.europarl.europa.eu/RegData/etudes/BRIE/2021/689337/EPRS_BRI(2021)689337_EN.pdf. [Accessed: 07-Apr-2022].

# CHAPTER 2

# Installation and Commissioning of the Microgrid

---

## 2.1. Introduction

Chapter 2 presents the implementation of a microgrid supporting the experimental work developed in the thesis. This experimental research infrastructure contributes to the validation and demonstration of novel EES technologies. This chapter also describes the activities related to the infrastructure build-up: it describes each battery technology commissioning, related power electronics and dedicated sensors, design and installation of electric switchboards and monitoring equipment, diagnosis and solving technical issues and communication tests.

In view of enabling a flexible "plug-in" of different EES technologies to the infrastructure, customised software was developed to control and communicate with the different microgrid assets. This chapter presents to the reader all the inherent experimental efforts related to the existing full-scale experimental microgrid and ongoing projects which contributed to this thesis's goals.

## 2.2. The microgrid infrastructure design and related integrated equipment

The experimental infrastructures of the Renewable Energies Chair of the University of Évora (pole of INIESC) [8] are located at Herdade da Mitra, near *Plataforma de Ensaios de Coletores Solares* (PECS) [9]. The existing microgrid stem from the merge of pre-existing assets into a single, more flexible infrastructure, Figure 9 (a, b)).

The new microgrid integrates assets such as PV generation (several new technologies), energy storage, grid connection, EVs charging, allowing it to become a new and improved R&D infrastructure. This will enable the existence of future-proof research infrastructure, allowing for easily integrate and test new PV, EES, EVs charging,

vehicle-to-grid (V2G), green hydrogen or other technologies in an isolated or integrated manner.

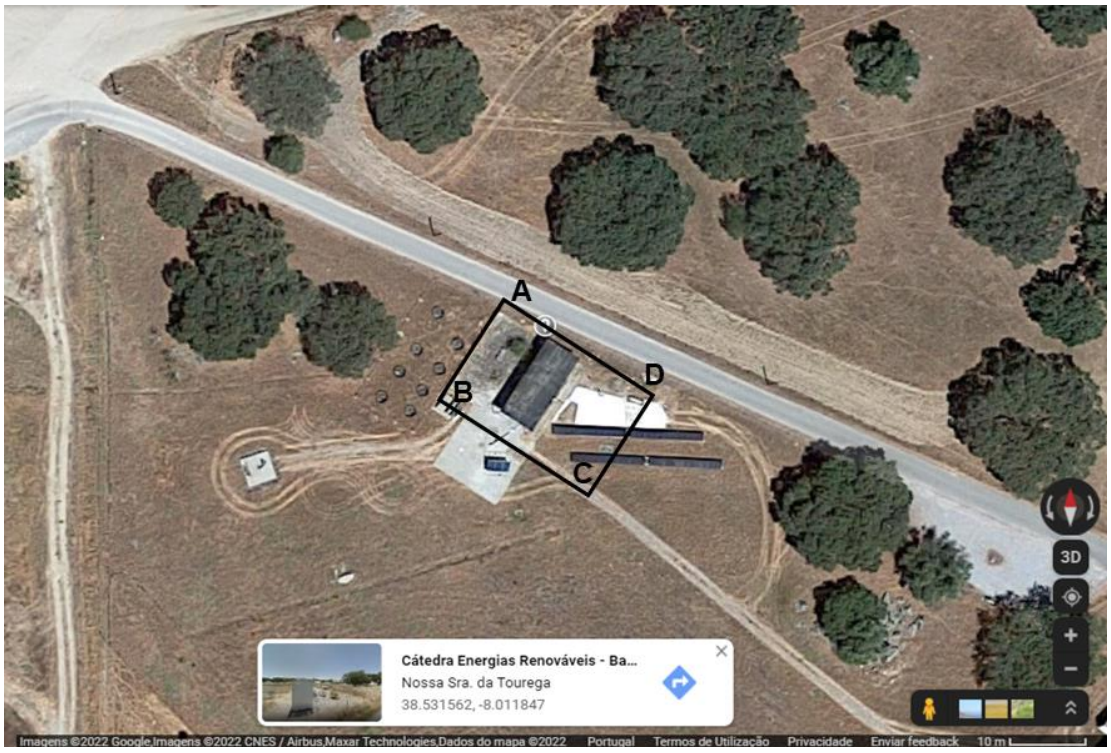


(a)

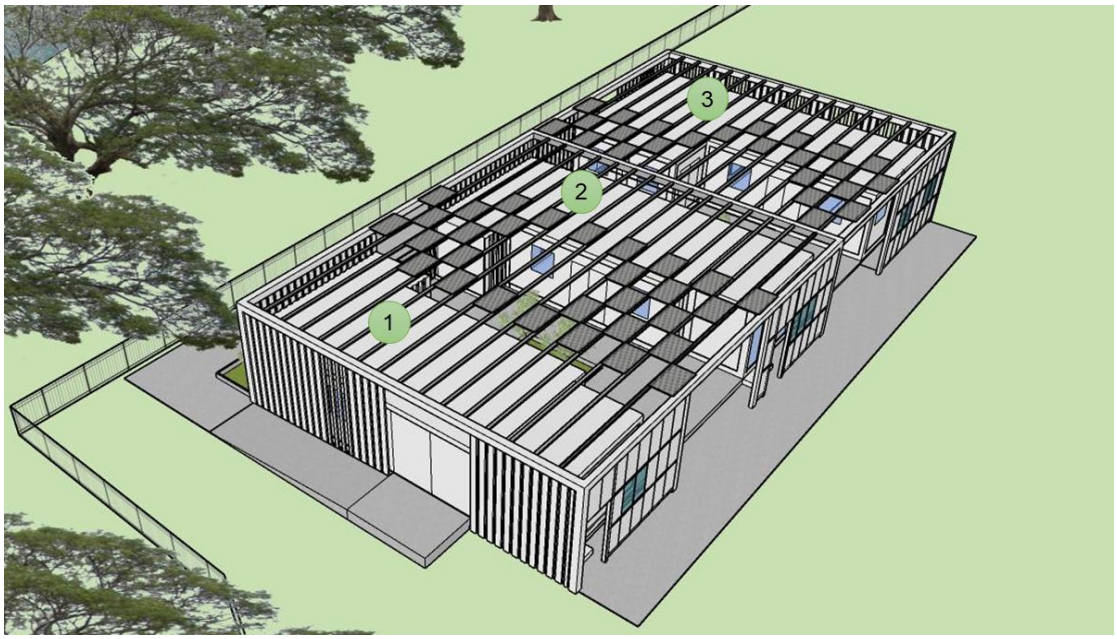


(b)

Figure 9. Location of the newly built infrastructure of the Renewable Energies Chair: (a) older infrastructures [10], with the new infrastructure A-D, correspondent to (b) with the new infrastructures, with general EES microgrid, the SolGrid in (1), the SoLab laboratory infrastructure (2), and the new infrastructure of VRFB (3). Image (b) was kindly provided by the colleague architect Cláudia Petronila.

In Figure 9 (b), the nº1 building is the local of the new microgrid, the SolGrid, designed and installed from scratch to integrate diversified equipment: batteries and power electronics, solar PV installations, internet and communication connection, humidity and temperature sensors, power cables, controller unit with integrated software, electric boards (current protection and grounding). The microgrid comprises electrochemical energy storage, solar PV systems, an electric charging station and sensible measurement devices. A general scheme is shown in Figure 10, where the equipment is connected to the general Switchboard Q8, a 230/400 VAC three-phase bus.

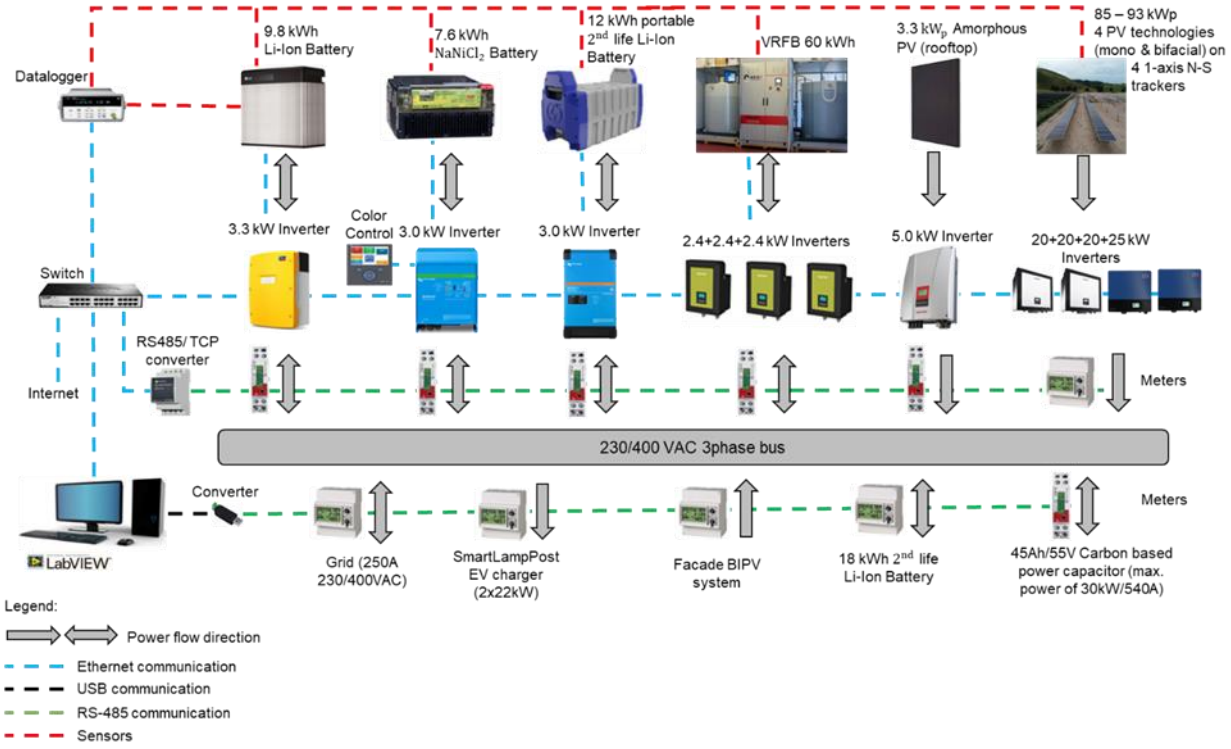


Figure 10. General scheme of the new microgrid, including the connection of PV, EES technologies, EV charger station and related meters, to the 230/400 VAC three-phase bus (Switchboard Q8).

The microgrid provides a complete range for scientific studies' current and future deployment. It provides scientific data on the operation of the technologies, allowing the diagnosis and solving of issues with grid and off-grid integration, the real-time implementation of power/energy management strategies, contributing to EES regulations, and the development of models. The microgrid infrastructure enabled the connection of different EES technologies, which enables the experimental testing of these ESS assets under different operating conditions. The monitoring of these experiments enables the development of new performance models, which are validated

with experimental data. This microgrid will continue to evolve with the addition of new technologies, and grid flexibility projects are one of the future paths for this infrastructure.

The installation progress of the equipment in the SolGrid site is shown in Figure 11. The equipment, the supports for the PV inverters, communications and monitoring, and data logging, were executed and developed by the Renewable Energies Chair team in compliance with the regulations in force in Portugal (e.g., RTIEBT - *Regras Técnicas das Instalações Eléctricas de Baixa Tensão, Dec.-Lei nº153/2014*).

(a)

(b)

(c)

Figure 11. Microgrid ongoing installation: (a) Ethernet, energy and communication cables' organisation in aluminium rails; (b) Microgrid Switchboard Q8 (ongoing installation and commissioning), using a flexible bus system from Rittal [11], (c) The selected building shows some of the installed EES technologies.

The microgrid is equipped with monophasic and triphasic systems connected to Switchboard Q8 with devoted current protections and AC monitoring equipment (providing measurements of RMS current, RMS voltage, active power, power factor, frequency, reactive power, etc.). The communication network was established on the site, including the installation of local switches connected to the University's internal network and the related TCP/RS485 and RS485/USB converters. The Renewable Energies Chair team had the following responsibilities in the commissioning and operation of this microgrid:

- ✓ Perform the engineering, procurement and track the acquisition processes of the following materials: electric switchboards; communication and sensors cabling, related adaptors; current protections; power quality measurement devices; workbenches.
- ✓ Installation of all the equipment in the SolGrid. Integration of the equipment with the dedicated power electronics and dedicated sensors.
- ✓ Establish communication with the power conditioners and related communication equipment (e.g. Color Control GX device - Victron's

communication centre for some models [12] - and internal management and communication devices of other inverters).

- ✓ Establish a local ethernet network in the microgrid and connect and configure the devices with this communication network. Ensure its daily operating functioning (provide solutions when the ethernet network connectivity fails due to, for example, power failures).
- ✓ Development of real-time execution tests programming using LabVIEW. Ensure the data acquisition registering of the sensors and equipment in real-time.
- ✓ Ensure the planned execution of batteries' commissioning: execute constant monitoring of the ongoing testing; optimise the previously developed testing program to better respond to the most needed variables and decrease the time of response; monitor the inverter alarms related to the grid conditions, such as overvoltage or temperatures; and ensure the goal, for example, the uninterrupted control of the power ramp rate within the predefined boundaries throughout the testing protocol.
- ✓ Execute the firmware updates as mandatory by the equipment manufacturer and correct the operational specification of the devices when needed.
- ✓ Develop testing protocols for the execution of outside of the microgrid tests for the second-life lithium-ion battery technology and inside of the microgrid tests for the other technologies of batteries.
- ✓ Analyse, select and organise the output results.

The single and flexible new microgrid integrated much equipment related to this thesis, and in that sense, the following sections are devoted to their description.

In addition to the operational ESS technologies described in the following, two other EES technologies are under procurement: a 9 kW/ 18 kWh second-life lithium-ion battery [6] and a 45 Ah / 2.61 kWh hybrid supercapacitor [5], supported by the SOLAR TECH project, ALT20-03-0246-FEDER-000053 [4]. The integration of those batteries will not be depicted in this thesis since their acquisition process and commissioning is not concluded at the present date.

### 2.2.1. Lithium-ion battery

The AGERAR project (0076_AGERAR_6_E) [2] allowed the development of tasks related to a lithium-ion battery pack from LG, model RESU 10 [13]. Its cathode chemistry type is from NMC (nickel, manganese, and cobalt) and the anode is graphite

($LiNiMnCoO_2$). The battery was installed in the dedicated microgrid. Compared to other cobalt-based battery technologies, the NMC cathode performs a more extended lifespan at a lower cost [14]. The characteristics of the battery are summarised in Table 1, after the manufacturer datasheet and installation manuals [15].

Table 1. Characteristics of the LG lithium-ion battery, model RESU 10.

| Parameter | Units | Value |
|---|---|---|
| Energy capacity (nominal/ usable) | kWh | 9.8 / 8.8 |
| Energy capacity | Ah | 189 |
| Operating voltage range | V | 42 - 58.8 |
| Maximum operating current | A | 119 (at 42 V) |
| Maximum power (nominal/ peak) | kW | 5 / 7 (3s) |
| Weight | kg | 75 |
| Operating temperature range | °C | -10 to 45 |
| Communication port | - | Ethernet |
| Integrated inverter power (nominal/ peak) | kW | 3.3 / 5 (2s) |

The battery contains an internal battery management system (BMS) to monitor its state and prevent its operation outside the safety boundaries (e.g., pre-defined SOC ranges, charge and discharge rates, and operating temperature ranges). The installation was done in compliance with the location requirements, and the energy and internet connections were installed. The battery, Figure 12 (a), is electrically connected to a power inverter from SMA, model Sunny Island 4.4 M [16], Figure 12 (b). The Modbus protocol feature of the inverter allows communication with this inverter, allowing data reading and acquisition in real time, and the deployment of external control.

The DC auxiliary switchboard, shown in Figure 13 (a), is located between the lithium-ion battery and the inverter. It includes a DC precision shunt resistor to provide the calculation of DC current, and extra cabling was included for DC voltage measurement. These DC measurements are achieved by a 20-channel multiplexer module [18], shown in Figure 13 (b). The multiplexer module is compatible with the 34970A LXI data acquisition/logger switch unit [19], as presented in Figure 13 (c), whose device the controller communicates with. In turn, the Keysight 34970A device has a built-in 6 ½ digit digital multimeter, with built-in signal conditioning measures thermocouples, RTDs and thermistors; AC and DC voltage and current; resistance, frequency and period.


(a) (b)

Figure 12. (a) 9.8 kWh LG RESU 10 [17] lithium-ion battery, and (b) 3.3 kVA SMA Sunny Island 4.4.M [16] battery inverter.

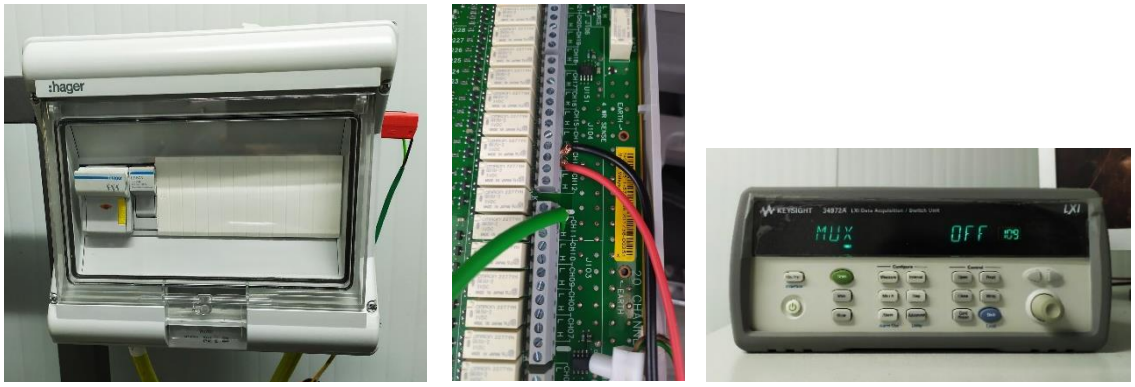


(a) (b) (c)

Figure 13. (a) DC auxiliary switchboard 3: current measurement device, current protections, and voltage measurement points; (b) the 20-channel multiplexer module [18]; and (c) the LXI data acquisition/ switch unit Keysight 34972A [19].

### 2.2.2. Sodium nickel chloride battery

The AGERAR project (0076_AGERAR_6_E) [2] also allowed the acquisition of a sodium-nickel chloride battery ($NaNiCl_2$), often referred to as the ZEBRA battery (Zero Emissions Batteries Research Activity [20]). This battery is a commercial product from FIAMM, model FZSoNick 48TL160 [21]. The most relevant manufacturer-available data are presented in Table 2.

Table 2. Characteristics of the FIAMM nickel-sodium chloride battery, model 48TL160.

| Parameter | Units | Value |
|---|---|---|
| Nominal energy capacity | kWh | 7600 Wh at C4 to 42V |
| Nominal energy capacity | Ah | 160 Ah at C4 to 42V |
| Operating voltage range | V | 54 to 59 V |
| Continuous operating current | A | 120 |
| Maximum power | kW | 7 |
| Weight | kg | 75 |
| Power consumption (standby) | W | 380 in warm-up; 110 for the regular operation |
| Operating temperature range | °C | -20 to +60 |
| Communication port | - | USB / RS 485 / CanBus or Ethernet |
| Integrated inverter power (nominal/ peak) | kW | 3.0 / 5 (2s) |

Regarding the internal structure of this battery, the cathode is composed of $NiCl_2/FeCl_2$, the anode is sodium metal, and the ceramic Na-B''-$Al_2O_3$ is the electrolyte. The battery operates with an internal temperature near 300ºC, so the solid cathode reactants benefit from higher diffusivity and the solid electrolyte benefits from higher conductivity. The integrated BMS allows monitoring, diagnosis, and data logging and ensures a controlled battery operation. Although the high-temperature regular operation, the battery does not require cooling. The materials in its constitution are 100% recyclable, and there is no self-discharge at any state of charge, no memory effect, and no ageing in floating or storage conditions [21].

Sodium-nickel chloride batteries are considered safe in transport, storage, and operation conditions [22]. Its performance characteristics put this technology at a similar performance level as lithium-ion technology batteries. Figure 14 (a) presents the referred $NaNiCl_2$ battery [21], connected to an inverter/charger from Victron, model Multigrid 48/3000/35 [23], Figure 14 (b).

The sodium-nickel chloride battery is connected to an auxiliar switchboard, connected to the inverter. AC metering and current protections are installed in Switchboard Q8. The AC data measurement (voltage, current, active and reactive power, etc.) is achieved through a meter from Circutor, model CVM-1D [24] and an RS485 to TCP/IP adapter.


(a)


(b)

Figure 14. (a) Nickel sodium chloride battery [21], and (b) inverter/charger integrated with the nickel sodium chloride from Victron, Multigrid 48/3000/35 [23].

Concerning the additional installed equipment, the DC auxiliary switchboard includes current protection and measurement devices, including a DC precision shunt resistor and surface temperature sensors. The sensors data acquisition is made with the LXI data acquisition/ switch unit Keysight 34972A [19] presented previously in Figure 13 (c). The battery inverter communicates with the Victron communication controller device (Color Control GX [12]), as shown in Figure 15 (a). At the forefront of the battery (prior to the DC contacts), a built-in DC-DC converter manages the voltage level of the battery. To avoid voltage peaks from the inverter that could affect the DC-DC converter under battery discharge operation, the manufacturer advised the installation of a 0.1F 100V capacitor [22], shown in Figure 15 (b).

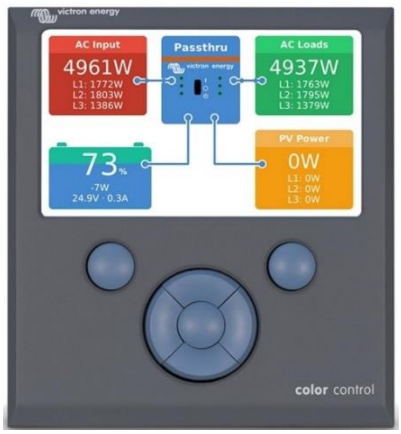


(a)


(b)

Figure 15. (a) Victron Color Control GX [12] as the communication interface with the Victron Multigrid inverter/charger; and (b) Capacitor installed to stabilise voltage to the battery pack.

### 2.2.3. Second-life lithium-ion battery

Through the European Union's Horizon 2020 funded project POCITYF, GA 846600 [3], it was possible to develop R&D activities regarding the operation, characterisation, and evaluation of second-life lithium-ion batteries technology.

The German company *betteries AMPS GmbH* built a second-life lithium-ion battery prototype [25], sourced from end-of-life EV batteries with lithium iron phosphate (LiFePO4) as cathode and graphite as the anode (LFP). This solution is shown in Figure 16 (a) and provide a second life after EVs usage, having the potential to be used in lower energy density applications, such as off-grid stationary or residential systems. These second-life batteries present an indicative power and energy capacity of 2.0 kW/2.3 kWh, respectively, a voltage operating range of 45-64 V, and an approximate weight of 35 kg per pack. With an advisable depth of discharge of 80%, the expected lifetime is estimated at 7-10 years [25].

The *betteries AMPS GmbH* solution aims to be applied to off-grid solar photovoltaic (PV) installations. In contrast to other technological approaches, *betteries AMPS GmbH* solution has a modular design: the modules can be stacked on each other, increasing the usable power/energy capacity output up to 5 kW/9.2 kWh (with the stacking of 4 modules). The second-life lithium-ion battery is connected to the microgrid through a commercial inverter from Victron, model Multiplus II GX [26], with a nominal power of 3.0 kVA, shown in Figure 16 (b).

(a) (b)

Figure 16. (a) 2.0 kW/ 2.3 kWh second-life lithium-ion battery from betteries AMPS GmbH, and (b) the inverter and the battery.

The 2nd life lithium-ion battery prototype was connected to the microgrid to execute its characterisation testing, as shown in Figure 17.

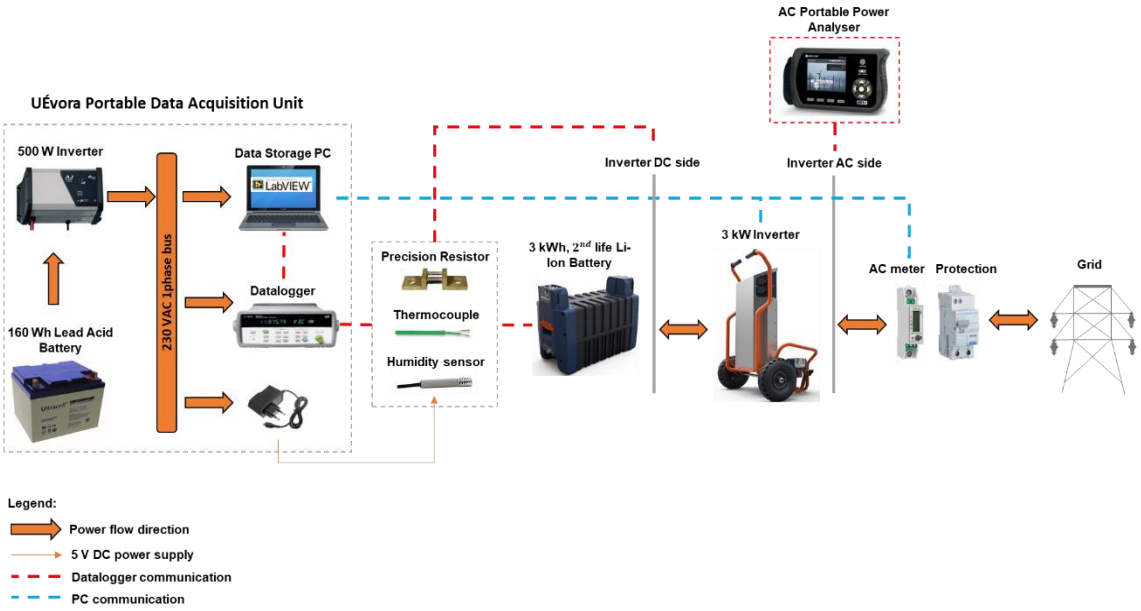


Figure 17. Second-life lithium-ion battery and inverter integration into the Renewable Energies Chair microgrid.

The characterisation tests setup and further off-grid use-cases application required the building of a portable measurement and data acquisition unit. This unit comprises the LXI data acquisition/ switch unit Keysight 34972A [19] to execute temperature and DC voltage measurements, a DC precision shunt resistance and the DC protections. It also includes a computer equipped with the LabVIEW software [27] as the testing controller unit. The AC monitoring is achieved with an AC portable power quality measurement device, the AR6 [28], to better detail the current and voltage measurements and to study the application's energy and power quality, including transients and harmonics. It was possible to install a humidity sensor inside the housing of one of the battery modules, as shown in Figure 18.

The 2nd lithium-ion battery performance and suitability for off-grid applications were tested through the development of a UPS-type housing and a measurement and control unit setup, presented in Figure 19, allowing the tests to occur in off-grid scenarios or outside the microgrid installations.

.

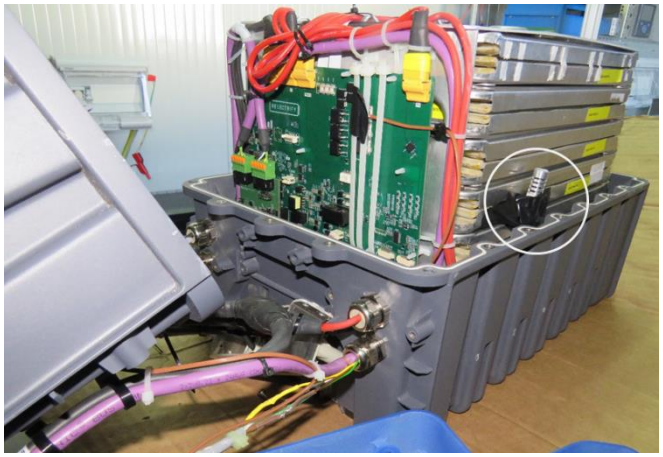

Figure 18. A humidity sensor was installed next to the battery cells and inside the housing of one of the second-life lithium-ion batteries (marked with a white circle to facilitate reading).

(a)

(b)

(c)

Figure 19. Testing of the off-grid use cases with (a) The inclusion of the inverter, the UPS-type housing, the measurement and control unit with one 2nd life lithium-ion battery; (b) Detail of the measurement and control unit, including the computer, the LXI data acquisition unit, sensors, current protections, and the portable AC monitoring equipment; (c) The UPS-type housing, composed by the lead-acid battery, inverter, charger and AC current protection equipment.

The UPS housing supplies energy to the measurement devices and the control unit and is composed of a 12V Rolls S12 31 lead-acid battery [29] with an energy capacity of 80Ah, and a 500 W Studer AJ pure sine wave inverter [30]. A 12V Victron Blue smart charger [31] is part of the UPS-type housing, aiming to charge the lead-acid battery before the test execution. The measurement and control unit gathers the measurement devices and sensors, performs the data acquisition and executes the testing control through LabVIEW [27].

The methodology and the results of the characterisation tests of the 2$^{nd}$ life lithium-ion battery packs and related inverters and the off-grid use case scenarios are detailed in Section 3.2.1.

### 2.2.4. Vanadium redox flow battery

2012 marked the beginning of the Renewable Energies Chair R&D activity on solar PV and electrochemical storage systems (EES) under the framework of the European project PVCROPS, GA 308468 [1], allowing the building and commission of a Vanadium Redox Flow battery (VRFB).

The nominal power of the VRFB stack is 5kW, and the size of the electrolyte tanks totalises an energy capacity of 60 kWh. A previously developed thesis detailed the VRFB integration and microgrid monitoring can be consulted in [32]. The VRFB is connected to three monophasic inverters, with nominal power of 2.4 kW each, resulting in a three-phase integration. The Ingeteam inverters, model EMS Home 2.4 [33], operate at a voltage range from 48 to 330 V. The battery voltage range lies between 45 to 60 V, which restricts the lower battery operation limits, given the left energy capacity at 48 V (limit the DOD of 100 %).

An external computer controls operation parameters: temperatures, flow pressure, DC voltages and currents. Moreover, the battery is equipped with a hydraulically connected reference cell, allowing voltage measurements and obtaining real-time battery SOC measurements, an unique characteristic of this EES type. The top empty space of the tanks is filled with inert gas to avoid unwanted reactions with oxygen. In the case of this battery, argon gas with high purity is used. The stack can be seen in Figure 20 (a) and one of the tanks in (b).

(a)

(b)


(c)

Figure 20. (a) Stack of VRFB, (b) electrolyte tank, and (c) 7.2 kW Ingeteam inverters.

The VRFB, related inverters and advanced monitoring and control equipment will be part of the single microgrid presented in Figure 9 (b) (3) and connected to Switchboard Q8. Since this battery is currently installed in a different building, and in the near future, it will be disassembled, transported and reassembled at the new microgrid site.

### 2.2.5. Solar PV systems

Four solar PV installations, previously associated with the existing infrastructures, will be installed and connected to the microgrid (Figure 21) in novel configurations. The characteristics of the PV installations are described in the following:

- 85-93 kWp PV installation on four 1-axis horizontal North-South trackers, including monofacial and bifacial PV modules, with monocrystalline type *n*

full cell and type *p* half-cell (Figure 21 (a)). Their general efficiencies range from 20.5 to 22.4 % and maximum power degradation rates of 0.33-0.45 %/year. The power range of this installation depends on the "bifaciality" factor, e.g., the albedo.

- 3.2 kWp amorphous PV fixed-mounting installation, approximately of seven years old. This PV installation will compose the rooftop of the new building infrastructure (Figure 21 (b)).
- On ongoing outdoor long-term testing, four PV modules monitor PV repairing techniques, composing nearly 1 kW (Figure 21 (c)).
- A BIPV facade, composed of novel white PV modules, is still pending a final engineering definition (Figure 21 (d)).

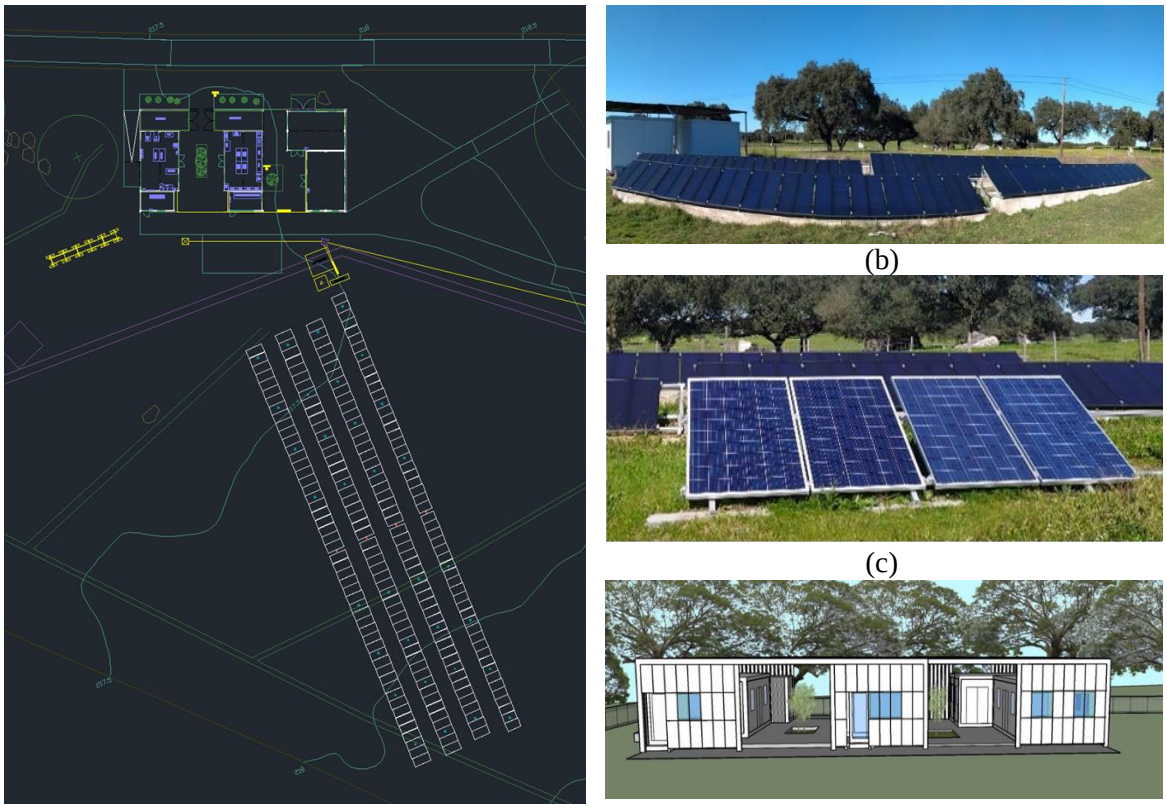

(a) (b) (c) (d)

Figure 21. (a) Future configuration of the 85-93 kW PV trackers plant section; and current configuration of the following: (b) 3.2 kW fixed-mounted amorphous PV system; and (c) 1 kW repaired PV modules; (d) Future microgrid's solar photovoltaic façade – image kindly provided by the colleague architect Cláudia Petronila.

The 85-93 kWp PV system will be connected to 2 Ingeteam Sun 3play 20TL inverters [34], 1 SMA Sunny Tripower (STP) 20000TL-30 and 1 SMA STP 25000TL-30 inverter [35]. This equipment was already installed in the microgrid and is presented in Figure 22 (a). The 3.2 kW installation (Figure 21 (b)) is equipped with an Ingeteam Ingecon Sun Lite 5 TL inverter [37]. The repaired modules of Figure 21 (c) are connected to APS YC250-EU microinverters of 250 W each [36] to be independently monitored. Figure 22 presents the previously described equipment.

(a) (b)

Figure 22. (a) Inverters of the solar PV trackers. The two above inverters are SMA Sunny Tripower (STP) 20000TL-30 and STP 25000TL-30 [35] inverters, and the two below are Ingeteam Sun 3play 20TL inverters [34]. (b) Repaired modules' microinverters from APsystems YC250-EU [36].

The power generation of the grid-connected PV systems is monitored through a dedicated LabVIEW programme at a high resolution (2-3 seconds). The program registers each module's power and energy-related variables that characterise the energy sent and received to and from the grid. The Renewable Energies Chair team is responsible for monitoring and maintaining this database, which is crucial to serving as input (after dedicated analysis) of ongoing scientific tasks, such as the energy management strategies presented throughout this thesis.

## 2.3. Communication and control programming

Performance testing is carried out to properly evaluate the previously described ESS assets enabling the validation of their corresponding performance models. Due to the

inexistence of a controller unit with proper processing capabilities to test, measure and control the microgrid under real-time conditions, the Renewable Energies Chair team developed an in-house centred control within the LabVIEW software (Laboratory Virtual Instrumentation Engineering Workbench, NI). This software is executed at a controlled time step and enables the timely diagnostic of experimental errors, such as communication device errors or processing errors related to the programmed algorithm's data format or cycle efficiency.

The compatibility of the LabVIEW drivers with much of the existing equipment is a valuable feature. The designed user interface in this programme allows input controls within the execution of the general code. It displays real-time control variables, allowing control execution (in virtual instruments - VIs). According to the displayed alarms in the interactive interface, it is possible to visually control the ongoing test loop and perform start/stop commands of all devices as needed and control the alarms. The critical variables are associated with specific alarms, e.g., overvoltage or low battery status. The programming approach used for the developed control is modular, allowing a flexible introduction of additional tasks, namely in the testing of different EMSs, with the ability to control distinct parameters along the execution of the test loop.

The LabVIEW software control relies on the previous establishment of communication to all devices achieved through Modbus protocol over TCP/IP. This protocol is commonly used in power generation and industrial applications and can easily integrate devices from different manufacturers. Each device that communicates through this protocol is given a unique address, for which the master/server and the slave/client share messages (send requests and read responses).

The master targets a function code (to read or write) to the slave/client, which outputs an error checking field; the slave confirms the receiving of the request from the master and verifies the data to be returned, and finally outputs an error-checking. In the case of the occurrence of an error, the slave gives feedback on the error; otherwise, the message is successfully received by the slave, responding to the master. This relation is illustrated in Figure 23.

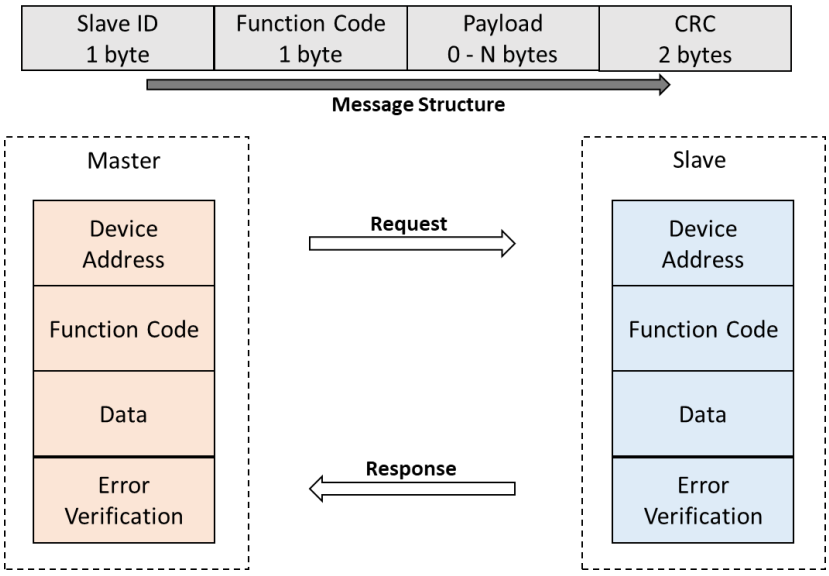


Figure 23. Modbus protocol communication basis. Adapted from [38].

The most common ethernet Modbus protocol is RTU, ASCII, TCP or Plus, communicating over RS-232, RS-485, RS-422 and ethernet. These physical media which differ in speed, effectively communicating at different distances or different aggregating devices in a single network. In the case of this microgrid, an ethernet TCP/IP communication was established with the existing devices enabling the control of their operations.

Each equipment task (reading or writing) is created and saved in an independent block, effectively building an internal customised block library. This standard procedure allows it to be saved and re-used. In regular operation, the software loop is constructed using those blocks, generally organised through the following three main phases:

- Initialisation of VI: Open and establish communication with the equipment and initiate the loop.
- Loop: After initialising the variables, an ongoing loop is initiated. In a defined timeframe, the blocks are sequentially executed (send requests to the equipment (communication), translate in writing commands to the equipment, and receive information from them). Figure 24 (a) presents an example of one block where the communication of reading an information in a specific address is occurring.
  The information is acquired, registered and analysed, and the algorithms are executed. Figure 24 (b) shows the final modular execution of the different blocks. At the end of each iteration of the loop, the data is saved in a predefined file format (either .txt, .csv or .xlsx)

- Finalisation of VI: The loop is ended due to alarms, noticed errors associated with experimentation, or the end of the experimental test.

An example of the developed user interface is shown in Figure 25.

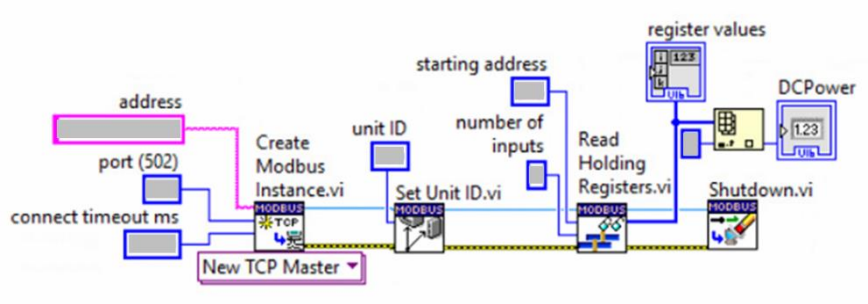


(a)

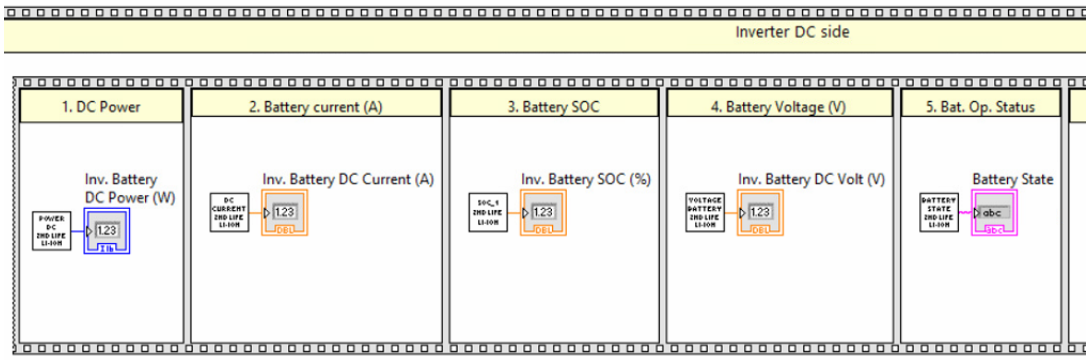


(b)

Figure 24. VIs developed in LabVIEW considering the programming steps: (a) example of a communication block of reading in specific address; (b) execution of the loop in a sequence, composed of several blocks.

The establishment of communication and development of the control aims at providing a solid basis for the development of the testing operation, allowing the characterisation of technologies and validation of models. The validated models are based on the test outcomes of these demonstrators: on the one hand, the characterisation testing results are the input for simulation modelling of the batteries, contributing to the modelling validation; on the other hand, the modelled battery performance allows the energy management strategies development and uses cases optimisation through simulation, whose algorithms are then validated in the real operating environment.

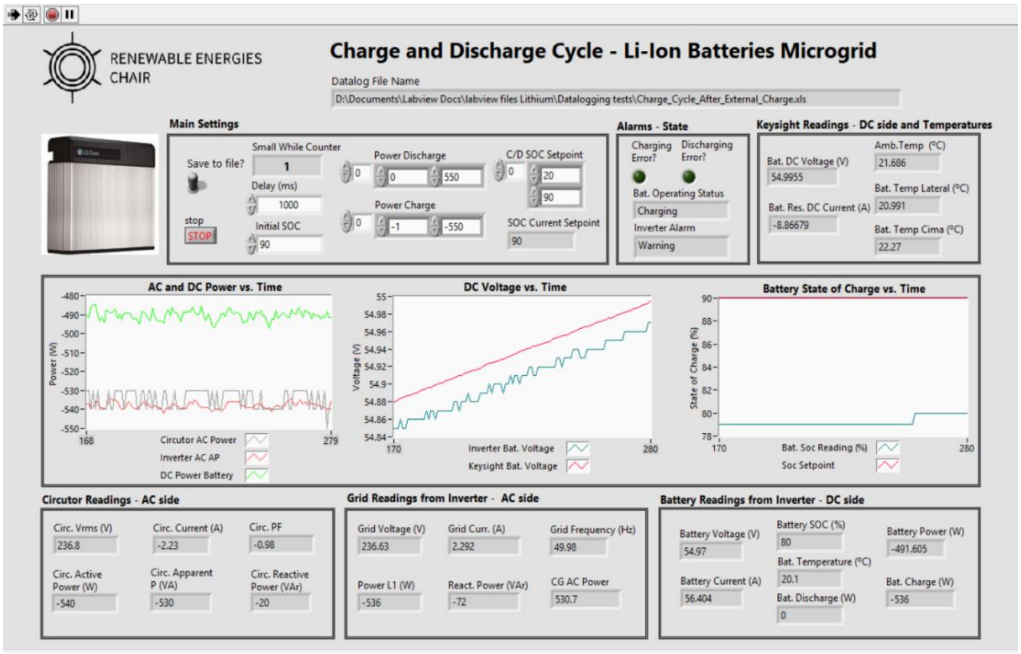


Figure 25. Developed user interface in a LabVIEW framework for the case of LIB characterisation testing.

## 2.4. Implementation outcomes and relevance

The existing demonstrators of the Renewable Energies Chair microgrid allow, along with the many options, to contribute to the electrical energy storage technology state of the art. The infrastructure enables the realisation of experimental works providing real operation data used to develop performance models – validated with the measured operation data. The characterisation tests of the studied technologies provide relevant parameters to fine-tune and improve battery modelling and reduce operational uncertainty, providing experimental data regarding emerging battery technologies. With the data, it is possible to calculate key performance indicators (KPIs) and to place the performance in a real-operational environment under stress conditions. This enables the further fine-tuning and validation of prototyping products reaching a higher total readiness level (TRL). In the case of commercial products, it allows the manufacturer data analysis and detaining available data to build electric models and check their fitting for each application, or even build novel scenarios in which they could fit in and optimise their operation.

The battery prototypes are tested to identify characteristics or develop potential commercial outcomes. Direct contact with the companies or manufacturers allows the improvement of the products, namely relating to: the temperature influence, depth of

discharge (DOD) setpoints, systems alarms and reset issues, transport, communication issues, self-discharging, electrical and environmental protections, regular operation in real-time, control options and limitations, integration with power electronics and related instruments, suitability to application, performance outputs, among others. The results include final usable energy capacity, ageing assessment, availability of power-SOC and other relevant indicators such as IP protection level. Output test data enables further model development and validation or improved state of health estimation.

In the case of the applications, the experimental battery demonstrators are tested within the creation of new controls built upon the existing (if existing) BMSs and the realisation of energy management strategies (EMSs) within each control application goal. This field allows the optimisation of the battery operation to fit a specific application better, increasing its durability and reducing costs.

The operation and integration of the prototyping or commercial battery products allowed the identification of some of the existing market barriers, reflecting on possible problem-solving issues in the near electrified future. It was possible to identify a general lack of technical-expert support by most battery inverter brands. In some cases, it is much more challenging to opt for customised solutions or ask for technical support in the advertised product functionalities. Also, a barrier was identified in the disclosed information and technical documentation provided by the brands. Manufacturers and providers should offer complete technical documentation and operating manuals of the solutions, allowing the providers and installers to develop the needed skills to better respond to the client's and operator’s doubts.

The pair battery-inverter still lacks market competitiveness, with the market monopoly of some suppliers and the inexistence of standard protocols and communication cables. The creation of standardised protocols should help in the dissemination of the solutions. Moreover, Portuguese legislation on technical rules is inexistent and supervising authorities and registering residential and building energy storage systems should foster integration, control and operation of energy storage systems.

The continuous growth of the number of assets connected to the microgrid follows the evolution of the battery market, allowing it to be identified as a real-scale demonstrator of great relevance in Portugal, actively contributing to quality research.

## 2.5. References

[1] University of Évora - Renewable Energies Chair, “INIESC.” [Online]. Available: https://www.en.catedraer.uevora.pt/sobre/iniesc. [Accessed: 04-Oct-2022].

[2] University of Évora - Renewable Energies Chair, “PECS - Solar Concentrators Testing Platform.” [Online]. Available: https://www.en.catedraer.uevora.pt/infraestruturas/pecs. [Accessed: 04-Oct-2022].

[3] Google maps, “Cátedra Energias Renováveis - Bateria de Iões de Litio, Nossa Sra. da Tourega.” [Online]. Available: https://goo.gl/maps/HbXUtnxsm7v9PWCWA.

[4] RITTAL, “Busbar systems RiLine.” [Online]. Available: https://www.rittal.com/com-en/products/PG0229STV1/PG0300STV1/PG0313STV1. [Accessed: 04-Oct-2022].

[5] V. Energy, “Color Control GX.” [Online]. Available: https://www.victronenergy.com/panel-systems-remote-monitoring/color-control. [Accessed: 04-Oct-2022].

[6] Watt4Ever, “The energy storage solution for companies - Watt4Ever.” [Online]. Available: https://watt4ever.be. [Accessed: 04-Oct-2022].

[7] Kurt.Energy, “Kurt.Energy | The next generation battery.” [Online]. Available: https://kurt.energy/. [Accessed: 04-Oct-2022].

[8] University of Évora, “SOLAR TECH - Transferência de Tecnologia e Conhecimento em Energia Solar e Armazenamento de Energia.” [Online]. Available: https://www.uevora.pt/investigar/projetos?id=4195.

[9] Interreg España-Portugal, “AGERAR - Almacenamiento Y Gestión De Energías Renovables En Aplicaciones Comerciales Y Residenciales.” [Online]. Available: https://www.poctep.eu/es/2014-2020/almacenamiento-y-gestión-de-energías-renovables-en-aplicaciones-comerciales-y.

[10] EUROPE - SOLAR STORE.COM, “LG Chem RESU 10 - 48V lithium-ion storage battery.” [Online]. Available: https://www.europe-solarstore.com/lg-chem-resu-10-48v-lithium-ion-storage-battery.html.

[11] G. Saldaña, J. I. S. Martín, I. Zamora, F. J. Asensio, and O. Oñederra, “Analysis of the Current Electric Battery Models for Electric Vehicle Simulation,” *Energies*, vol. 12, no. 2750, 2019.

[12] LG Chem, “Residential Energy Storage Unit for Photovoltaic Systems,” Seoul, Korea, 2016.

[13] EUROPE - SOLAR STORE.COM, “SMA Sunny Island 4.4M.” [Online]. Available: https://www.europe-solarstore.com/solar-inverters/sma/sunny-island/sma-sunny-island-4-4m.html.

[14] LG, “RESU10 | LG Home Battery.” [Online]. Available: https://www.lghomebattery.com.au/resu10. [Accessed: 04-Oct-2022].

[15] Keysight, “34901A 20-Channel Multiplexer (2/4-Wire) Module for 34970A/34972A.” [Online]. Available: https://www.keysight.com/us/en/product/34901A/20-channel-multiplexer-2-4-wire-module.html. [Accessed: 04-Oct-2022].

[16] Keysight, “34972A LXI Data Acquisition / Data Logger Switch Unit [Discontinued].” [Online]. Available: https://www.keysight.com/us/en/product/34972A/lxi-data-acquisition-data-logger-switch-unit.html. [Accessed: 04-Oct-2022].

[17] H. Sakaebe, “ZEBRA Batteries,” *Encycl. Appl. Electrochem.*, pp. 2165–2169, 2014.

[18] FIAMM, “48TL Battery,” *THE SALT BATTERY - Residential Energy Storage*. [Online]. Available: https://www.fzsonick.com/applications/residential-energy-storage. [Accessed: 14-Dec-2022].

[19] R. Manzoni, “Sodium Nickel Chloride Batteries in transportation applications,” in *2015 International Conference on Electrical Systems for Aircraft, Railway, Ship Propulsion and Road Vehicles (ESARS)*, 2015, pp. 1–6.

[20] Victron Energy, “MultiGrid 3000VA.” [Online]. Available: https://www.victronenergy.com/upload/documents/Datasheet-MultiGrid-3000VA-EN.pdf.

[21] Circutor, “CVM-1D Series.” [Online]. Available: http://circutor.com/en/products/measurement-and-control/fixed-power-analyzers/power-analyzers/cvm-1d-series-detail. [Accessed: 14-Dec-2020].

[22] Kemet, “Screw Terminal Aluminum Electrolytic Capacitors.” [Online]. Available: https://connect.kemet.com:7667/gateway/IntelliData-ComponentDocumentation/1.0/download/datasheet/ALS41C104QT100.pdf.

[23] Pocityf, “Leading the smart evolution of historical cities,” 2022. [Online]. Available: https://pocityf.eu.

[24] betteries AMPS GmbH, “betteries. Upcycle batteries. Avert climate change.,” 2022. [Online]. Available: https://betteries.com.

[25] Victron Energy, “MultiPlus-II GX.” [Online]. Available: https://www.victronenergy.pt/inverters-chargers/multiplus-ii-gx. [Accessed: 05-Oct-2022].

[26] National Instruments, “LabVIEW.” [Online]. Available: https://www.ni.com/pt-pt/support/downloads/software-products/download.labview.html#443274.

[27] Circutor, “Kit-AR6: Analisador de redes portátil com display gráfico.” [Online]. Available: https://circutor.com/pt-pt/produtos/analisadores-de-red-portateis/analisador-de-redes-portatil-com-display-grafico/analisador-de-redes-portatil-com-display-grafico/product/m82511/. [Accessed: 05-Oct-2022].

[28] Rolls Battery Engineering, “S12 31 | Rolls Battery.” [Online]. Available: https://www.rollsbattery.com/battery/s12-31/. [Accessed: 05-Oct-2022].

[29] Studer, “AJ 500-12.” [Online]. Available: https://studer-innotec.com/aj500-700/. [Accessed: 05-Oct-2022].

[30] Victron Energy, “Carregador Blue Smart IP65.” [Online]. Available: https://www.victronenergy.pt/chargers/blue-smart-ip65-charger. [Accessed: 05-Oct-2022].

[31] European Commission, “PhotoVoltaic Cost r€duction, Reliability, Operational performance, Prediction and Simulation,” *Final Report Summary - PVCROPS (PhotoVoltaic Cost r€duction, Reliability, Operational performance, Prediction and Simulation)*. [Online]. Available: https://cordis.europa.eu/project/id/308468/reporting/es.

[32] L. Fialho, “Photovoltaic generation with energy storage integrated into the electric grid: Modelling, simulation and experimentation,” University of Évora, 2019.

[33] Ingeteam, “Ingecon EMS,” *Single-phase battery inverter with transformer for energy storage management*. [Online]. Available: https://www.ingeteam.com/Portals/0/Catalogo/Producto/Documento/PRD_1075_Archivo_ingecon-ems-home.pdf.

[34] Ingeteam, “SUN 3Play Série TL M 20TL M / 33TL M / 40TL M480.” [Online]. Available: www.ingeteam.com. [Accessed: 05-Oct-2022].

[35] SMA AG Solar Technology, “SUNNY TRIPOWER 15000TL / 20000TL / 25000TL,” *The versatile specialist for large-scale commercial plants and solar power plants*.

[36] APS, “YC250 Microinverter.” [Online]. Available: http://www.apsmicroinverter.nl/lay/media/downloads/aps-datasheet-yc250eu.jpg. [Accessed: 05-Oct-2022].

[37] Suministros del Sol, “Ingecon Sun 1Play 5TL M Ingeteam Inverter.” [Online]. Available: https://suministrosdelsol.com/en/ingeteam-inverters/276-ingecon-sun-lite-5tl-inverter.html. [Accessed: 11-Jan-2022].

[38] C. R. Steffens *et al.*, “Welding Turns Digital: Electronics and FPGA-based Design to Actuate a Linear Welding Work Cell,” in *ICCEEg*, 2016, pp. 1–14.

# CHAPTER 3

# Characterisation and Modelling of the Batteries

## 3.1. Introduction

Chapter 3 introduces the topic of solar photovoltaic energy generation and its inclusion with electrical energy storage under the Portuguese framework Decree-Law (DL) 153/2014, with a scientific published paper. The mentioned work focused on the batteries' energy fluxes without including a battery model. In the following step, the existing batteries of the Renewable Energies Chair of the University of Évora were subjected to performance testing, allowing their characterisation. The tests precede each battery-specific key-performance indicators calculation, which further allows its real-time operation optimisation. Chapter 3 presents the work developed mainly with the vanadium redox flow and lithium-ion batteries, given their different performance characteristics such as response time, power and energy densities, distinct ageing, and degradation effects, which leads to attractive complementary potential on output results and applications. Following the characterisation testing, battery models were developed based on the existing literature research and integrated microgrid technologies. The battery-measured extracted data allowed the validation of the battery's models.

## 3.2. Techno-Economic Evaluation of the Portuguese PV and Energy Storage Residential Applications

Ana Foles[1,2], Luís Fialho[1,2], Manuel Collares-Pereira[1,2]

*In Journal Sustainable Energy Technologies and Assessments, Vol. 39, 100686, 2020,* https://doi.org/10.1016/j.seta.2020.100686

*Open access version in ArXiv:* https://doi.org/10.48550/arXiv.1909.00657

**Abstract**

In the residential sector, energy micro-generation and its intelligent management have been creating novel energy market models, considering new concepts of energy usage and distribution, in which the prosumer has an active role in the energy generation and its self-consumption. The configuration of a solar photovoltaic system integrating energy storage in Portugal is yet unclear in the technical, energetic and economic point of view. The energy management jointly with the battery operation have great influence in the system configuration's profitability value. The present work evaluates different photovoltaic system configurations with and without batteries for the normal low voltage Portuguese consumer profile with 3.45 kVA contracted power. This study presents the systems' cost-effectiveness, within the Portuguese legislation, which promotes and enables policies for self-generation and self-consumption. The analysis is done in three different representative locations of the country, considering distinct electric tariffs. This work shows that despite the solar photovoltaic system without electricity storage is already economically viable, its integration with storage is not in most of the assessed configurations. However, it is shown that it is already possible to find profitable PV + battery configurations, even potentially improving these positive scenarios if a good energy management strategy is considered.

**Keywords:** Solar Photovoltaic Electricity; Battery Energy Storage; Residential Self-Consumption; Economic Assessment

[1] Renewable Energies Chair, University of Évora, 7000-651, Évora, Portugal
[2] Institute of Earth and Sciences, University of Évora, Rua Romão Ramalho, 7000-671, Évora, Portugal

**Nomenclature**

| | |
|---|---|
| $\Delta S_n$ | The sum value of the annual cash flows net annual costs (€) |
| $C_{bill}$ | Electricity bill of one year for each location and electricity tariff (€) |
| $C_{savings}$ | Electricity bill savings with the studied configuration (€) |
| $E_{Battery\ sent}$ | Energy sent to the battery (kWh) |
| $E_{Load}$ | Sum of the energy load profile for one year (kWh) |
| $E_{supplied,m}$ | Supplied energy in kWh, in month m |
| $F_n$ | Net cash flow in year n |
| $OMIE_m$ | Average Iberian electricity gross market closing price (OMIE) for Portugal in €/kWh, in month m |
| $PV_{consumption}$ | Energy generated through the PV system which is self-consumed (kWh) |
| $PV_{generation}$ | Total generated energy from the PV system (kWh) |
| $Q_n$ | Energy output or saved, in year n |
| $R_{UPAC,m}$ | Sold energy price in €, in month m |
| $\Delta I_n$ | Nondiscounted incremental investment costs (€) |
| Analysis Period, N | The amount of time or the period an analysis covers |
| B/C | Benefit-to-Cost Ratio |
| BAPV | Building Applied Photovoltaics |
| Base Year | Year to which all cash flows are converted to |
| BU | Battery use – quantifies the use of the battery in comparison with the sum of the energy load profile in one year |
| CAPEX | Capital expenditure (€) |
| Cash Flow, F | Net income plus the amount charged off for depreciation, depletion, amortization, and extraordinary charges to reserves |
| CE | Certificate of Exploitation, needed in some of the PV configurations, defined in the Portuguese energy legislation |
| Contracted Power | One of the defined parameters in the electricity contract which defines the maximum power number of household appliances which are generally used simultaneously in the domestic sector |
| DGEG | Director General of Energy and Geology |
| Discount rate, d | Measure of the time value, which is the price put on the time that an investor waits for a return on investment. In other words, it is the rate used for computing the present values, which reflects the fact that the value of a cash flow depends on the time in which the flow occurs |
| DL | Decree-Law |
| DSO | Distributor System Operator |
| Electricity Tariff | The price paid by the consumer for the electricity consumed from the electricity company, generally expressed in €/kWh |
| ERSE | Regulatory Entity of Energy Services |
| Inflation Rate, a | The rise in price levels caused by an increase in available currency and credit without a proportionate increase in available goods and services of equal quality. Inflation does not include real escalation. Inflation is usually expressed in terms of an annual percentage change |
| Investment, I | An expenditure for which returns are expected to extend beyond 1 year |

| | |
|---|---|
| IRR | Internal Rate of Return (%) |
| LCOE | Levelized cost of electricity (€/kWh) |
| LCOES | Levelized cost of energy storage (€/kWh) |
| Life-Cycle Cost, LCC | The present value over the analysis period of the resultant costs of the system |
| MiBEL | Iberian Market for Electricity |
| NPV | Net Present Value (€) |
| OMiP / OMiE | Portuguese/Spanish branch of MIBEL |
| REN | *National Electric Grid* |
| RES | Renewable Energy Sources |
| SCR | Self-consumption Rate |
| SLR | Supplier of Last Resort |
| SMR | Saved Money Rate |
| SSR | Self-supply Rate / Self-sufficiency ratio |
| TLCC | Total Life Cycle Cost (€) |
| TSO | Transmission System Operator |
| UPAC | Self-consumption Production Unit |
| UPP | Small Production Unit. |
| O&M | Operating and maintenance costs, OPEX (€) |

## 1. Introduction

In contrast to the fossil fuelled energy generation, renewable energy (RE) is characterized by an abundance of resources and lower pollution emissions. Developed countries are evolving towards diversifying their renewable energy sources, integrating micro-generation in their low voltage (LV) networks, shaping micro-grids (MG). Micro-grids could be designed for RE to fully meet the local consumption loads, considering the use of storage to balance supply and demand and managing energy flows. Those can require e.g. energy generation, energy shifting or load management in the residential scheme. Electricity generation from RE sources can be described as dispatchable or non-dispatchable, regarding the energy source ability to provide a controlled response to system requirements, such as consumer loads in the residential sector. RE integrated in the existing power grid could require improvements, allowing bidirectional flows of electricity, ensuring grid stability; having efficient grid management to increase grid flexibility, response and security; improvements in the interconnections (increasing capability, reliability and stability), introducing devices and methods of operation to ensure stability and control (voltage, frequency, power balance); and introduction of energy storage (ES) aiming the system flexibility and security of supply [1]. residential sector allows the energy efficiency achievement, increase of local reliability, reduction of energy losses, and easy architecture integration. Cost-competitiveness of solar PV and reduction of support schemes had made possible

new business models to emerge, mostly in northern Europe. PV electricity generates revenues through the injection into the grid or by optimization of self-consumption, allowing the reduction of the electric bill and the growing of new energy flow models for the householder/businessman. Energy consumers are currently interested to play an active role not only in the use of RE sources, but also in the generation/storage of RE. This new consumer is known as prosumer and is mainly driven by the energy bill reduction, higher electricity independency from the main grid suppliers and the environment sustainability.

The energy storage operations also create flexible markets, data access and management, cooperation between the Transmission System Operator (TSO) and the Distribution System Operator (DSO) [2].

Electric battery technologies will play a significant role in Europe's Energy Union framework. Regarding the ten key actions designated in the SET-Plan, it is established to "become competitive in the global battery sector to drive e-mobility and ES forward" [3]. Electricity storage involves the conversion of electricity in another form of energy and is currently executed through technologies which differ in performance, characteristics and operation. ES can be conducted by pumped-hydro storage, compressed-air ES, electric batteries, superconducting magnets, flywheels, super-capacitors, chemical storage and thermal storage, or can be obtained through end-use technologies, such as plugin electric vehicles [1]. New and cost-effective storage technologies are being developed. Apart from mitigating power fluctuations, ES systems can play other roles with PV technologies, such as load-shifting (storing energy during low demand periods and discharging in high demand periods). Compared to other storage options, mentioned above, batteries have become popular in residential appliances due to general simplicity, materials availability, technology maturity and relatively low cost. According to BNEF, the average price of lithium-ion battery technology was 1160 $/kWh in 2010, 176 $/kWh in 2018, and for 2030 the expected value is 62 $/kWh [4].

China is the leader in PV solar energy installations, followed by USA, Japan, Germany and Italy. As market leader, China has in force exclusively photovoltaic policies as the "13th Solar Energy Development Five Year Plan (2016‑2020)" implemented in 8$^{th}$ December 2016, in which committed to reach to at least 105 GW of solar photovoltaic capacity. Since 2011, the non-tendered PV projects could benefit from a solar PV feed-in tariff [5]. the Royal Decree Law 244/2019 is in force, and accounts with different self-consumption schemes, defines communal self-consumption, simplifies the remuneration related with surplus energy for PV installed power no larger than 100 kW

(monthly net-metering) [6]. Spain's "National Renewable Energy Action Plan 2011-2020" defined a 20.8% share of generated renewable energy sources in gross final energy consumption [5]. France works almost exclusively with feed-in tariffs, and it does not have a selfconsumption scheme, although a community power scheme has been studied. The photovoltaic feed-in tariff is in force since 2006, last updated in 2016, and has two main variants: building installations no bigger than 100 kW, and it is adjusted every semester; and tenders for buildings installations larger than 100 kW and ground-mounted plants. On July 2015 France targeted for 2030 a 32% of RES in gross final energy consumption in its "Law on Energy Transition for Green Growth". Italy has made a storage system regulation in 2015 identifying technical specifications to include storage into the national electricity. Its "Integrated national plan for energy and climate 2030" last updated in 2019 aim the primary energy consumption reduction target at 125 Mtep. The solar photovoltaic financial incentives which started in 10$^{th}$ July 2012 were cut in 25th June 2014. MiSE has presented provisions which will grant financial incentives to purchase electric or hybrid vehicles, or low carbon emission ones, up to the end of 2021 [7].

In 1$^{st}$ March of 2016, Germany has started a subsidy for solar photovoltaic installations with battery storage for residential installations: the scheme offers soft loans up to 2000 €/kW for solar photovoltaic systems and capital grant covering up to 25 % of the eligible solar panel. These values are updated (downwards) every six months. The National Energy Action Plan in force in Germany was implemented in 2010 and has the 2020 targets for 18 % of energy generated from RE, through 37 % of electricity and 13 % for transports coming from RES. With the "Renewables Obligation", in force since 2010, United Kingdom has a small-scale (less than 5 MW) feed-in tariff scheme for renewable electricity**.** Targets in 2020 are that RES represent 15 % in gross final energy source, 31 % of electricity and 10 % of energy demand [5].

In India, the "Uttar Pradesh net-metering regulation for rooftop solar" defined net-metering regulations for rooftop solar photovoltaic, running for 25 years. The tariff is set to 7.06 INR/kWh and has entered in force on 20$^{th}$ of March 2015. The Uttar Pradesh Solar Policy support both on-grid and off-grid PV applications and projects, aiming the achievement of 10.7 GW by 2020, from which 4.3 GW from rooftop solar, and 6.4 GW from utility scale PV projects [5].

The Department of the Environment and Energy of Australia 2016 provides funds for the Solar Communities Program, to support community groups in regions across the country to install rooftop solar photovoltaic, solar hot water heaters and solar-connected

battery systems. The Renewable Energy Target aims to deliver a 23.5 % share of renewable energy in Australia's electricity mix by the year of 2020 [5].

### 1.1. State of the art

Several techno-economic studies have been presented in the recent years. The reference [8] presents a techno-economic study based in future price scenario which considers the application of PV and battery energy storage in the Azores Island, with three battery capacities for each battery technology, the lithium-ion and vanadium redox flow. The aim is the minimization of the cost of electricity generation, and the used economic indicators are the NPV and ROI. In [9] an economic analysis is made considering lithium-ion and lead-acid battery technologies with different RE sources applied in India with net-metering. The study addresses the advantages of integrating energy storage in the networks and considering real load and resource profiles data and component prices. It concludes that lithium-ion batteries are more viable to apply in that scenario. In [10] an analysis is made for Almeria (Spain) and Lindenberg (Germany) assessing impacts of orientation and tilt angles in the self-consumption with energy storage. Higher load profiles showed better results for self-consumption, trade-off in self-consumption increase and cost reduction of investment, in the residential sector, and framework regulations. Applied in Australia, the authors of [11] study the PV+battery configuration using NPV, IRR and LCOE economic indicators. The authors conclude that PV-only systems are profitable, unlike the PV+battery setup, reporting that the economic losses of adding a battery can only be balanced with the benefits that it brings to the grid side. In [12] a residential analysis is made for three USA locations, with the configuration PV+lithium-ion battery, concluding that it is possible to be competitive with grid electricity prices through an adequate sizing in those locations, using the LCOE economic indicator. The authors of [13] studied the application of mono-crystalline PV systems and three lead-acid batteries which differ in size, to be installed in Italy, without subsidies. Relevance of the discounted cash-flows (DCF) is highlighted, jointly with NPV economic indicator, giving relevance to the variables of PV and electricity, associated costs, profiles and batteries. In [14] five different cases of storage with net-metering are studied. The study is made for three locations in Italy, considering PV and battery sizing and installation costs. In this study it is concluded that this configuration is not economic feasible, and losses generated by the energy storage are a disadvantage.

Regarding the Portuguese context some relevant approaches have been made considering DL 153/2014, such as the work of [15] which carries a complete economic

analysis using the NPV, LCOE, BCR and IRR as economic indicators to evaluate four configurations of PV and OPzV gel batteries (lead-acid), on a 25-year lifetime analysis. It uses PV kits and concludes that most of the configurations were not economically interesting. In the work [16] economic indicators DPB and IRR are used, and the legislation in Portugal is clarified. An analysis is conducted for different sectors and three different locations (Lisbon, Porto and Faro), with PV systems with different azimuth and tilt angles, evaluating self-consumption. Remarks are made regarding the importance of the tariff, load profile and PV surplus generation. In [17] PV+battery impact is studied, considering two storage control strategies and tariff fee charges, showing that all the configurations are profitable with a payback below 10 years.

Various studies have been also presented to estimate optimum PV+battery configurations, based in the most common economic indicators, for application in the Portuguese context, for the residential case. Recognising the important work done, the present work stands out in the way of evaluating the PV configurations in three different locations in Portugal, for two electric energy tariffs, with current justified market prices, giving support to the decision-making process, in a way is has not been done before. Detailed Portuguese electricity sector remarks are given and legislation for renewable energy micro-generation is clarified, to contribute to a smoother integration of PV-only and PV+battery configurations in the Portuguese residential sector.

### 1.2. Portuguese electricity market and policies overview

The number of RE applications in Portugal is increasing according to the permits request numbers. In March 2018 the electricity generation from RE was higher than the effective consumption of electricity in the Portuguese continent. The Portugal's first PV dedicated auction for 1.4 GW happened in July 2019. The second one will be in the year of 2020 to procure 700 MW. Regarding storage, the aim is to procure 50-100 MW. Two specific PV auctions promote the integration of PV technology from 572 MW in 2018 to 1.6 GW by 2021 and 8.1 GW to 9.9 GW by 2030 [18].

The main supplier and distributor of electricity in Portugal, EDP, has presented plans to install the first PV plant (3.8 MW) coupled with lead-acid batteries storage, focused on self-consumption, in Castanheira do Ribatejo and Azambuja [19].

The Portuguese electric market is divided in three main activities: electricity generation, transmission of electricity through very high and high voltage networks, distribution of electricity through high, medium and low voltage grids and the electricity supply to consumers [20]. The transmission is carried out under an exclusive public service

concession contract made with REN - "Redes Energéticas Nacionais, SGPS, S.A. TSO must connect all the entities to its network if the connection is technically and economically feasible, and if the applicant satisfies the requirements for connection. Regarding supply, there are two regimes:

1. Free market supply to eligible consumers – the supply is made by free market companies using freely negotiated conditions (except some Regulation terms defined by ERSE - Regulatory Entity of Energy Services);
2. Supplier of last resort (SLR) – This supplier must ensure specific consumers with regulated tariffs (yearly defined by ERSE). He must buy all the special regime generation at fixed and regulated prices depending of the generation technology (under feed-in tariffs scheme). This doesn't prevent the SLR generators to sell their energy to other suppliers.

In a free market regime, the participants involved in the production can sell the produced electricity and the ones who need electricity can buy it, whatever the finality.

Portugal and Spain have been integrating their electricity markets into one, the Iberian Electricity Market (MIBEL), based in a group of contracting modalities. They share a spot market operator, the OMIE, which operates since July 2007, and a forward market operator, the OMIP, since July 2006. ERSE defines regulations: commercial relations, tariffs, service quality, network access, interconnections and networks operation. DGEG and independent regulatory entities are responsible by the regulation enforcement. REN owns and maintains on an exclusive basis the electricity transmission system in the Portuguese continent. The DSO of the high and medium voltage is EDP – Distribution SA and has the concession of most LV municipal distribution systems. In Azores the distribution operator is "Eletricidade dos Açores" (EDA), and in Madeira is "Empresa de Electricidade da Madeira" (EEM). Supply is carried out by several companies, the main supplier of last resort is EDP Serviço Universal in the continent, and in Azores and Madeira are the same as mentioned for distribution.

The electricity produced by Portugal is enough to meet the consumption needs, but for commercial reasons Portugal imports electricity from Spain. In 2017 Portugal imported 3,072 GWh, and the surplus production was exported to Spain. Natural gas and coal are the main fossil sources of energy generation in Portugal, nuclear does not exist and the RE production has increased in the last few years [20]. Currently there are no support mechanisms for RE technologies, except for offshore wind and wave energy (new technologies) and small cogeneration.

On 30th November 2016, the European Commission published a proposal for a revised RE Directive with at least 27 % renewables in the final energy consumption in the EU by 2030 is met. Recently, the European Union (EU) has settled at a 32 % share of final energy consumption in 2030 as global leader.

In 2015 Portugal has presented a strategic plan, the "Green Growth Commitment 2030", which identifies the targets for 2030, namely 31 % of RES in gross final energy consumption by 2020 and 40 % by 2030. Portugal energy plan is currently set by PNAER 2020 (National Plan of Action for Renewable Energies 2013-2020), approved by Ministers' Council Resolution No. 20/2013 of April 10. Portuguese Government has committed internationally to reduce its greenhouse gases emissions to achieve carbon neutrality by 2050. This has risen as a form of a report "Roteiro para a Neutralidade Carbónica" – Carbon Neutrality Road Map.

### 1.3. Portuguese legislation framework

The current legislation in force regarding RE decentralized production is the Decree-Law 162/2019, which is in force since January 2020 [21]. This work is based on the previous regulation in force focused on self-consumption, the Decree-Law 153/2014 [22], given the current DL does not changed any of the obtained results on those regimes.

The law establishes the legal regimes of the RE self-consumption, considering two types – the UPP (Small Production Unit) – which includes the former micro and mini generation systems up to 250 kWp, and where the electricity production is exclusively sold to the grid operator, and the installation energy consumption is exclusively supplied by the public grid - and the UPAC (Self-Consumption Production Unit) – which considers the self-consumption based on renewable technologies, but making possible to sell to the grid the surplus energy generation. This law defines the licensing scheme, installation audits and paying regimes of the electricity sold to the grid. DL 153/2014 has established a distribution generation model, which promotes the decentralization – energy generation close to the consumption point -, the generation of energy by RE, the increase of the competition and the security in the supply, the reduction in peak power requirements, the encouragement of the PV industry growing as well as the communities. Given that this legal regime contextualizes the object of study in this work, the general regulation for the UPAC will be presented:

- Connection maximum power must be ≤100 % of the contracted power of the consumer installation.

- The generated electricity from the UPAC should be near to the consumption point in the installation.
- If it is connected to the electric grid, the instantaneous generation surplus can be sold to SLR.
- The consumer can install an UPAC for each electric installation, consume the generated energy or export its surplus to the grid. The Production Unit (UP) is installed in the same site of consumption. The consumer could have multiple registered UPs, although each installation is associated with a single UP.
- If a ≥1.5 kW UPAC is connected to the electric grid, the consumer is obliged to have a dedicated electricity metering equipment, to account the injected electricity.

If the UPAC installed power is higher than 1.5 kW and is connected to RESP, the consumer has a monthly fixed compensation for the first 10 years after receiving the certificate of exploitation (CE). The licensing process is made through electronic register in the SERUP site (UPs register), managed by the DGEG authority, and its summary is showed in Fig. 1. Table 1 presents the related fee charges.

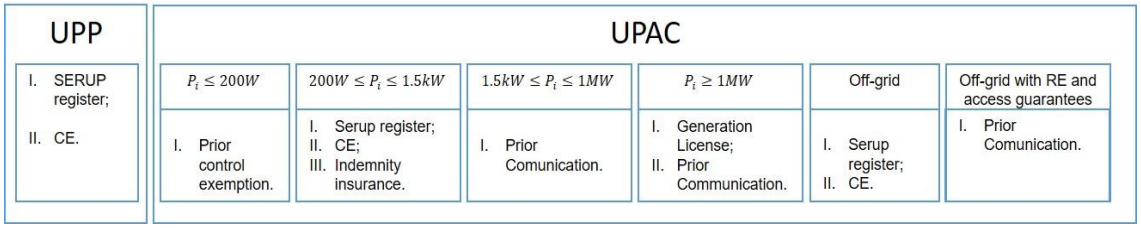


Fig. 1. Resume of DL 153/2015 regimes, the UPP and the UPAC.

Table 1. Fee charges applicable to UPAC regime with and without grid injection, regarding the installed power in kW – DGEG (Portaria 14/2015) remuneration*.

| **Installed Power Capacity** | **UPAC charges with grid injection** | **UPAC charges without grid injection** |
|---|---|---|
| < 1.5 kW | 30 € | N/A |
| 1.5 kW – 5.0 kW | 100 € | 70 € |
| 5 kW – 100 kW | 250 € | 175 € |
| 100 kW – 250 kW | 500 € | 300 € |
| 250 kW – 1000 kW | 750 € | 500 € |

*These fees are not charged; its end or great reduction is expected in future versions of the Portuguese legislation given the approved European Union Directive (RED II)[1], providing the exemption of fees and charges for small self-consumption facilities (up to 30 kW) and the possibility for communities to generate, store and sell the surplus generation.

[1]Directive (EU) 2018/2001 of the European Parliament and of the Council of 11 December 2018 on the promotion of the use of energy from renewable sources

### 1.4. Portuguese market energy prices and tariffs

For the case in which the generated energy by the UPAC is not fully self-consumed and is injected into the public grid (RESP), according to [22], the price of the electricity

injected to the RESP is given by 90 % of the average Iberian electricity market closing price, and can be expressed through Eq. (1),

$$R_{UPAC,m} = E_{supplied,m} \times OMIE_m \times 0.9 \quad (1)$$

where $R_{UPAC,m}$ is the sold energy price in €, in month m; the $E_{supplied,m}$ is the supplied energy in kWh, in month $m$; and the $OMIE_m$ is the average Iberian electricity gross market closing price (OMIE) for Portugal in €/kWh, in month $m$. The average monthly wholesale electricity prices for the year of 2018 are presented next, in Fig. 2, data made available by OMIE [23].

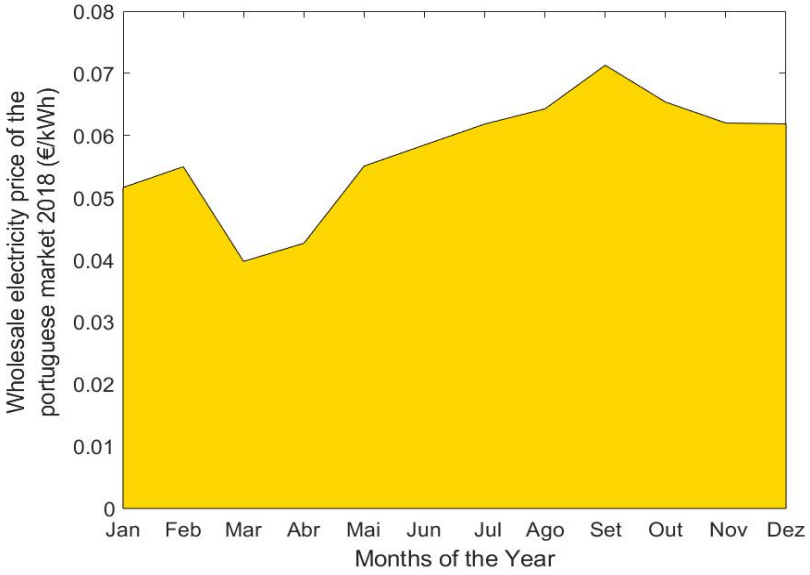


Fig. 2. Average monthly wholesale electricity prices of the year of 2018 for Portugal.

The grid electricity price in Portugal is structured with three tariff regimes, namely the flat, bi-hourly and tri-hourly tariffs. The flat tariff has a constant energy price throughout the day/week. Bi-hourly and tri-hourly tariffs distinguishes, respectively, two and three periods with different electricity price, attributing two or three electric tariffs, for off-peak and peak hours. For the bi-hourly and tri-hourly tariffs, two main variants exist, the daily cycles (Fig. 3) and the weekly cycles. The scheduling of these two tariffs is also different in daylight saving and wintertime, not just reflecting the legal time change adjustment.

The Portuguese continent has different electricity and contracted power prices than the island located installations. Reference prices can be obtained in [24][25], respectively, as shown in Table 2.

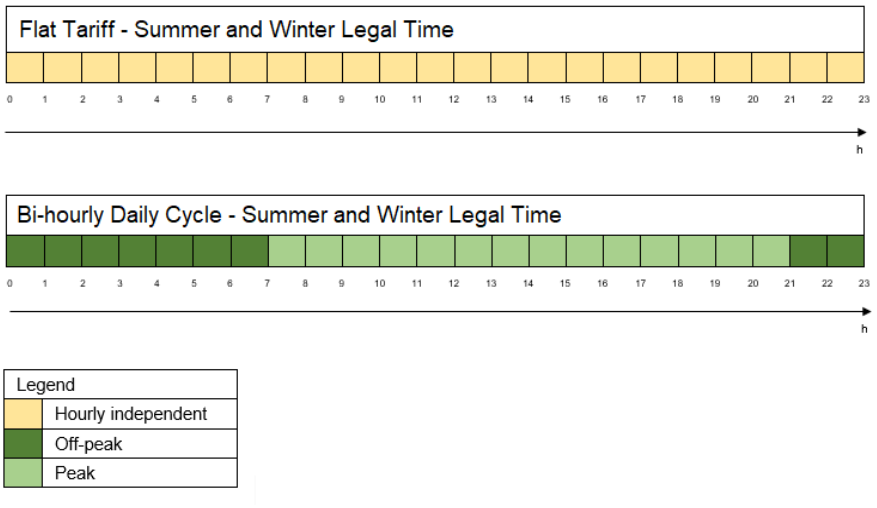


Fig. 3. Peak and off-peak periods of the daily cycles, indifferently for summer and winter legal times [24].

Table 2. Flat and bi-hourly tariffs of EDP Comercial of the Portuguese continent and from EDA in the Azores, for the year of 2019.

| *Tariff* | *Flat* | | *Bi-hourly* | | | |
|---|---|---|---|---|---|---|
| *Location* | *Évora/Porto* | *Azores* | *Évora/Porto* | | *Azores* | |
| *Regime* | Normal | Normal | Peak | Off-peak | Peak | Off-peak |
| *Contracted Power (€/day)* | 0.2187 | 0.1648 | 0.2282 | 0.2282 | 0.1694 | 0.1694 |
| *Energy (€/kWh)* | 0.1493 | 0.1607 | 0.1867 | 0.1098 | 0.1908 | 0.1000 |

### 1.5. Portuguese residential average electricity load profiles

This study was performed using the average electricity load profiles for LV consumers provided by EDP Distribuição [26]. This DSO collects energy data from its clients at 15 minutes intervals, which made possible the estimation of the electric load for 2019, based on historical data from recent years. The Portuguese residential sector is supplied with low voltage (230/400V AC); contracted power ≤13.8 kVA and annual electricity consumption (≤7140 kWh). The EDP Distribuição load profiles for this sector are plotted in Fig. 4.

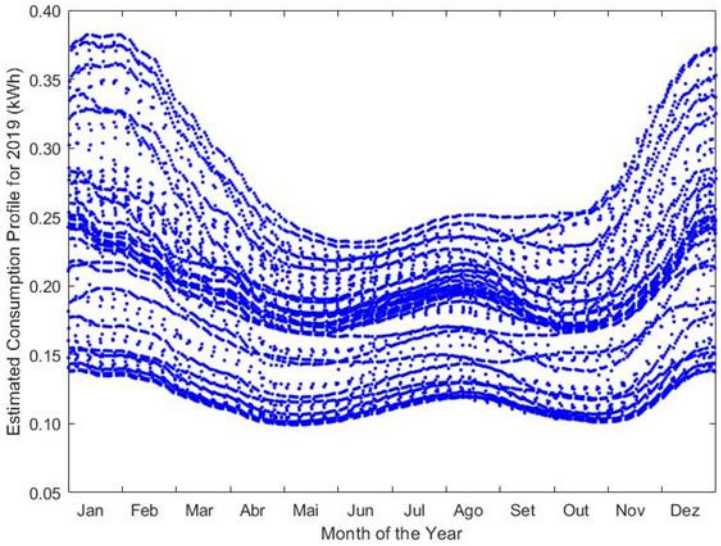


Fig. 4. Estimated electric domestic consumption profile of BTN C for 2019, made available by EDP Distribuição [26].

### 1.6. Portuguese self-consumption PV installed capacity

As explained, the licensing scheme of most installations includes the production unit registry in the SERUP database [27], which has made available some data about the concluded and rejected RE installations. Regarding PV installations in the UPAC and prior communication (MCP) regimes, the data made available is from March to December of 2015, January to December of 2016 and from January to July of 2017. The correspondent data comprises 1843 UPAC installations with 95,995 MW and 12,363 MCP installations with 10,845 kW, comprising a total of 106,8 MW of installed power in Portugal, and can be observed in Fig. 5 and Fig. 6.

A domestic costumer with a suitable sized photovoltaic system in the UPAC regime produces energy and can use it to exclusively supply his loads, generally called exclusive self-consumption. Since the produced energy by the PV system is variable through the day, seasons, and years, usually for the household consumption the electricity generated by the photovoltaic system has a surplus or is not enough to totally satisfy the domestic loads. In the first case, the energy surplus can be curtailed, injected into the grid, or stored in batteries for later consumption. If the generated electricity is not enough to totally supply the loads, the resultant consumption needs must be supplied from the electric grid or from other energy source.

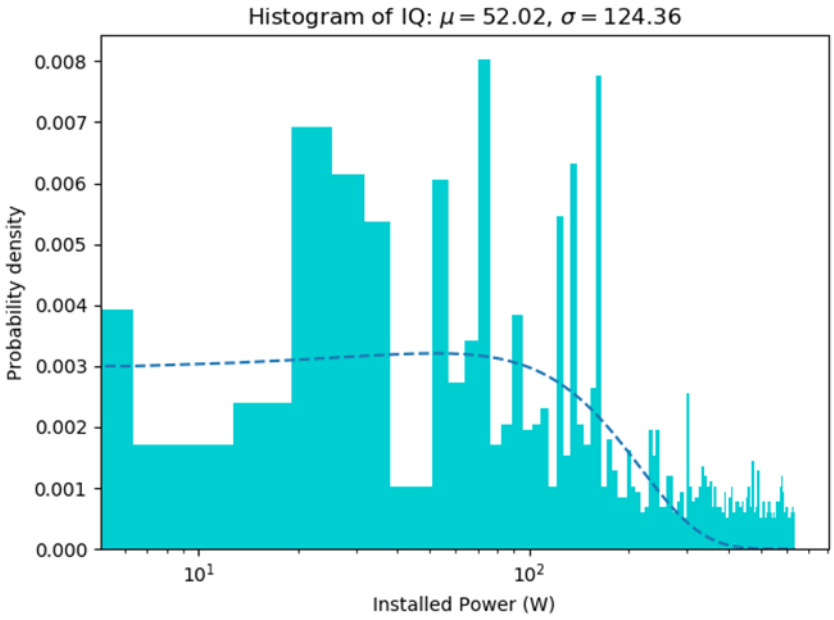


Fig. 5. Installed power distribution of the Portuguese UPAC registered installations from the available data of the SERUP database [27], with 100 bins.

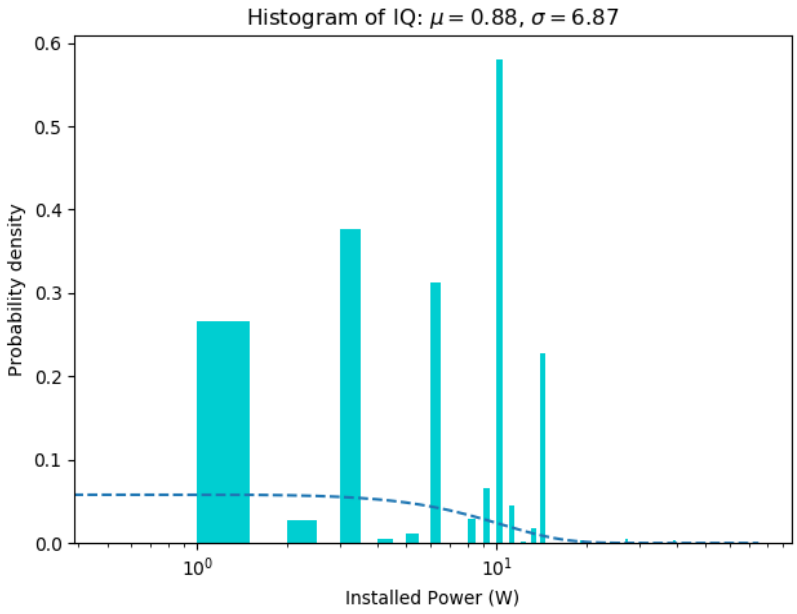


Fig. 6. Probability density of the logarithm MCP installed power (W), made available from the SERUP database [27], with 150 bins.

### 1.7. Portuguese solar radiation average annual availability

Three representative locations were chosen for this study: Évora, Porto and Azores Island, which are showed in Fig. 7. Évora is in a region in the centre-south of Portugal,

a city characterized by an average annual sum value of global horizontal irradiation (GHI) of 1846 kWh/$m^2$ [28], defined as one of the best locations regarding solar irradiation availability in the South of Europe. Porto is the second biggest city of the Portuguese continent, located in a northern coastal region of Portugal, with an average annual GHI of 1706 kWh/$m^2$ [28]. Azores is a Portuguese archipelago with nine islands and has an annual GHI of 1307 kWh/$m^2$ [28], and has different electricity tariffs from the continent.

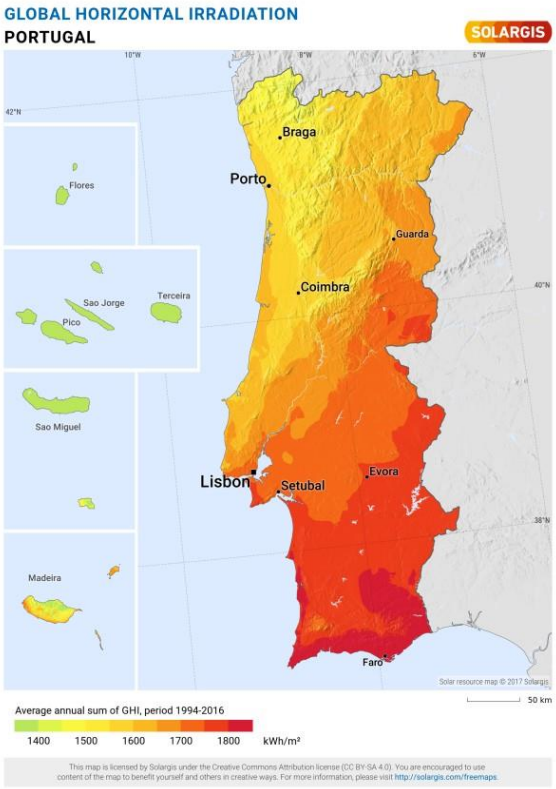


Fig. 7. Solar global horizontal irradiation (GHI) map of Portugal [29].

## 2. Methodology

A technology project investment assessment is an annual investment analysis, considering all the relevant costs, revenues, taxes and rates. The objective of making a techno-economic analysis is the provision of relevant information to make a judgement or a decision [30]. Thus, this analysis aims, in the end, to find whether an investment in solar photovoltaic systems, with or without electricity storage, is profitable for the domestic end user in Portugal.

The analysis defines a lifetime of 25 years for the full system. The indicators [30] considered in this analysis are the Net Present Value (NPV), the Total Life Cycle Cost

(TLCC), the Levelized Cost of Energy (LCOE), the Simple Payback Period (SPB), the Internal Rate of Return (IRR) and the Benefit-to-Cost Ratio (B/C ratio). These indicators are presented in detail in the next section. Due to the importance of the techno-economic assessment in the decision-making process, the use of key indicators provides market accepted values recognized by the user.

This study intends to be a simplified analysis but taking into account sound and consistent data and consistent economic assumptions. An in-depth approach would require sensitivity analysis for some economic parameters, site-specific maintenance costs or energy losses (e.g., soiling) but requiring additional data is not currently available.

For each of the sites, a simulation in SISIFO [31] online simulator was carried out, considering south orientation and optimum inclination for each region, and the hourly irradiation for each month of the year was extracted. The average values were considered and used in the simulation tasks. The SISIFO software uses the PVGIS solar radiation and temperature database [28] for its simulations, as well as all the technical specifications for the selected PV modules (temperature constants, short-circuit current, open voltage, *etc*.) and inverter (efficiency curve for example) on each case.

The economic and energy analysis were made using the interactive computational software MATLAB.

### 2.1. Key indicators

The NPV examines the cash flows associated with a project, over its duration. It is the value in the base year (usually the present), and can be expressed as follows in Eq. (2),

$$NPV = \sum_{n=0}^{N} F_n /(1+d)^n \tag{2}$$

where $F_n$ is the net cash flow, in year $n$; $N$ is the period of the project; $d$ is the annual discount rate. This parameter is generally recommended to evaluate the characteristics and decisions of the investment, and social costs. The NPV value can have some variations, as the calculus includes or not the after-taxes values and being in current or constant euros. If the NPV value is positive the project is considered economical and can be accepted; in contrast, if the NPV value is negative, the project is not economical, meaning that returns are worth less than the initial investment, being an indicator of a no-good decision. In theory, if the NPV value is null, the investor should be indifferent

whether to accept the project or not. The applicability of this indicator should be carefully analysed, since these considerations are not valid for all applications.

The TLCC evaluates differences in costs and the timing of costs, between alternative projects. These costs are referred to the asset acquisition, costs in its life cycle or in the period of interest to the investor. Only the relevant costs are considered, and are discounted to a base year, recurring to the present value analysis. TLCC has three variations, considering no taxes, after tax deductions or before-tax revenue required. In this work, the more suitable form is the no taxes formula, adequate to residential/non-profit/government application, expressed in Eq. (3),

$$TLCC = I + PVOM \tag{3}$$

where $I$ is the initial investment, and $PVOM$ is the present value of all O&M costs, as can be seen in Eq. (4).

$$PVOM = \sum_{n=1}^{N} O\&M_n /(1+d)^n \tag{4}$$

The LCOE is the cost of each unit of energy produced or saved by the system, over the period of the analysis, which will equal the TLCC, discounted back to the base year. In other words, it could be explained as the cost of one unit of energy, which is kept constant in the analysis period, that provide the same net present revenue as the NPV cost of the system. The levelized cost of energy is very useful to compare different scales of operation, investments and/or operating periods. There are many ways of calculating this parameter and the Eq. (5) will be used,

$$LCOE = TLCC/\left\{\sum_{n=1}^{N}[Q_n/(1+d)^n]\right\} \tag{5}$$

where $Q_n$ is the energy output or saved in year $n$. In the case of PV+battery configurations, the analysis was carried out considering the $Q_n$ value as the PV generation (energy output) plus the energy sent to the storage unit and effectively used (saved), in the year $n$.

The Internal Rate of Return (IRR) the rate at which the NPV of the future cash flow is set to zero. When applied, this rate brings the expenses values to the present, and make them equal to the return of the investment values. IRR obtained value is generally compared with a “hurdle rate”. It allows the comparison between many different investment activities. The rate is given by Eq. (6).

$$IRR = \sum_{n=0}^{N} [F_n/(1+d)^n] = 0 = NPV \quad (6)$$

The SPB is a fast and simple way to compare investments. It is defined as the time (number of years) required for the net revenues associated with an investment of a certain project to be recovered, without accounting the time value of money. It could be described as Eq. (7) explicit.

$$\sum_n \Delta I_n \leq \sum_n \Delta S_n \quad (7)$$

Where $\Delta I_n$ are the nondiscounted incremental investment costs (including incremental finance charges), and $\Delta S_n$ is the sum value of the annual cash flows net annual costs. One of the main disadvantages of using this parameter is the fact that it ignores the value of the money over the period, which implies that the investor doesn't have opportunity cost. It also ignores the returns after the payback year. On the other way, it is simple of calculate, implement and explain.

The Benefit-to-Cost Ratio (B/C ratio) ratio of the SUM of all discounted benefits accrued from an investment to the sum of dl associated discounted costs. It is used to discover at which level the benefits of a project exceed the costs. This indicator is generally used from a social perspective. It can be described in Eq. (8).

$$B/C = [PV(All\ benefits)]/\ [PV(All\ costs)] \quad (8)$$

Where $[PV(All\ benefits)]$ is the present value of all positive cash flows, and the $[PV(All\ costs)]$ is the present value of all negative cash flows.

Energy indicators are studied for one complete year. The self-consumption rate (SCR) is a way of quantifying how much energy is generated and self-consumed locally. The SCR is generally given through the formula given by Eq. (9),

$$SCR = PV_{consumption}/PV_{generation} \quad (9)$$

where, $PV_{consumption}$ is the energy generated through the PV system, which is self-consumed, and $PV_{generation}$ is the total generated energy from the PV system. The generated solar photovoltaic energy which is consumed is obtained through the subtraction of the "curtailment" losses or injected into the grid.

The self-supply rate (SSR) is an energetic indicator which quantifies the degree of autonomy from the grid, and is given by the following formula, given by Eq. (10),

$$SSR = PV_{consumption}/E_{Load} \quad (10)$$

where, $E_{Load}$ is the energy load profile.

The battery use (BU) can be described as a way of quantifying the usage of the battery, comparing the energy charged to the battery, and the energy load. This indicator can be given by the following expression, presented by Eq. (11),

$$BU = E_{Battery\ sent}/E_{Load} \tag{11}$$

where, $E_{Battery\ sent}$ is the energy sent to the battery, in kWh.

The saved money rate (SMR) quantifies the degree of autonomy from the grid in €. This indicator only makes sense to be calculated after the payback time break-even is achieved. The energy that was satisfied by the grid before the PV installation and now isn't – through self-consumption, charging/discharging the battery and injection into the grid – is quantified as money saved, as the Eq. (12) shows,

$$SMR = C_{savings}/C_{bill} \tag{12}$$

where $c_{savings}$, in €, is the money payed with the studied configuration, comparing with the $C_{bill}$, in €, which is the current electricity bill (only grid consumption), for each location and electricity tariff, for one year.

## 3. Studied scenarios

This work has the aim of comparing different photovoltaic system configurations (with/without storage), evaluating its economic feasibility in a variety of options. The analysis is made for the Portuguese residential figure characterized through the load profiles presented in section 1.5 and for a contracted power of 3.45 kVA. Four PV power installations are studied, namely 0.50 kWp, 0.75 kWp, 1.50 kWp and 3.45 kWp, either off-grid or grid-connected, for three different Portuguese locations – Évora, Porto and the Azores archipelago. The two chosen continental sites represent Portuguese regions with different solar resource potential and the Azores, a site with different characteristics (solar radiation, tariffs, etc.), located 1600 km West of Portugal, in the Atlantic Ocean. The chosen installed PV power (PV1 = 0.50 kW; PV2 = 0.75 kW; PV3 = 1.50 kW and PV4 = 3.45 kW) for the studied cases was considered the most relevant regarding the current legislation in Portugal (DL 153/2014). For each of these PV power chosen, two electricity tariffs were addressed - the flat tariff and the bi-hourly tariff, but only daily cycle was considered. Given that this work is focused in the residential sector, three different capacities for the batteries were selected: B1 = 3.3 kWh, B2 = 6.6 kWh and B3 = 9.9 kWh (specific battery parameters can be consulted in Table A1).

The present work has studied four main scenarios (Case I, II, III, IV), summarized in Table 3. All the different configurations (site location, tariff schedule, energy/power prices, PV power, battery capacity) are simulated for each case, when applicable.

Table 3. Summary of the studied scenarios.

| Case | *Photovoltaic System* | | *Grid Consumption* | | *Storage* | | *Surplus Electricity (Priority)* | | |
|---|---|---|---|---|---|---|---|---|---|
| | *Off-grid* | *Grid-connected* | *Yes* | *No* | *Yes* | *No* | *Battery* | *Grid* | *Waste* |
| I | x | | | x | | x | | | x |
| II | | x | x | | | x | | x | |
| III | x | | | x | x | | x | | |
| IV | | x | x | | x | | x | | |

- Case I – The domestic prosumer has a photovoltaic system used to perform exclusive self-consumption without energy storage. The surplus of the solar photovoltaic generated electricity is wasted. For the periods in which the photovoltaic generation is not enough to supply the consumer's load needs, being off grid, the consumer will be without power supply (at night) and should do a careful load management.
- Case II – In this scenario, the prosumer's solar photovoltaic system is grid-connected, and self-consumption is used, without energy storage. The surplus of the generated electricity is sold to the grid. In the periods when the solar power is not enough to supply the loads, the prosumer consumes electricity from the grid.
- Case III – The domestic consumer has a photovoltaic system which performs self-consumption, being off-grid. The solar power surplus is stored in the battery. If the battery reaches its maximum state of charge, the surplus electricity is curtailed. For periods without enough solar radiation and with a depleted battery, being an off-grid system, energy/power constraints are similar to case I.
- Case IV – The prosumer has a grid-connected photovoltaic system and self-consumption is made. The surplus electricity is sent to the battery storage, which has priority over the injection into the grid. If the battery achieves the maximum state of charge, the surplus electricity is sold to the grid. In

periods where the solar power is not enough to supply the loads and the battery is depleted, the prosumer uses electricity from the public grid.

The energy flow possibilities for the studied cases are presented in Fig. 8.

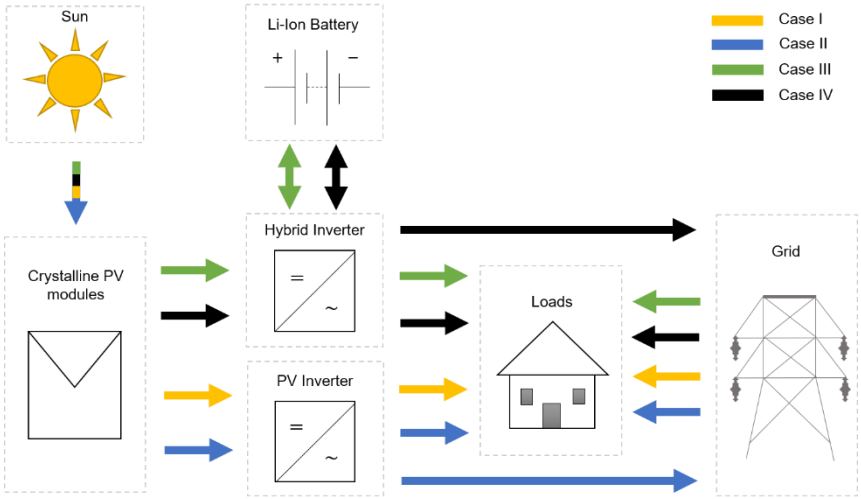


Fig. 8. Energy flows of the proposed scenarios.

Cases III and IV simulate the use of a PV+battery setup. A simple demonstration of the solar photovoltaic energy flows in these scenarios for the 1.50 kW PV power installation in Évora is given in Fig. 9.

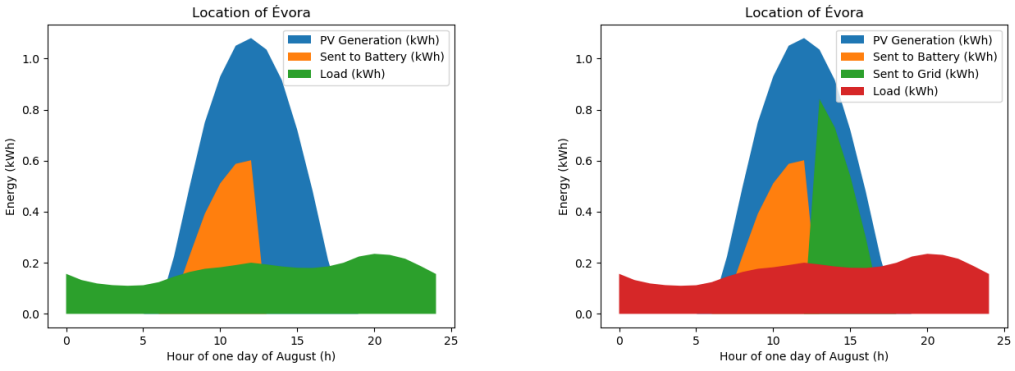


Fig. 9. Example of the Évora 1.50 kW PV installed power with the (a) Case III, energy stored with a 3.3 kWh battery, and (b) Case IV, energy stored to the 3.3 kWh battery and/or exchanged with the grid.

For these cases (III and IV) the energy management strategy used was the maximization of the self-consumption rate (SCR).

### 3.1. Economic parameters and assumptions

For each configuration, an investment assessment was carried out. Cases II and IV, the grid-connected photovoltaic configurations also consider the contracted power cost. The assessment is made considering general assumptions to all the cases, such as Capex, or macroeconomic parameters (inflation rate, etc.) which are given in Table 4. The system initial costs used are shown in Table 5.

Table 4. General assumptions of the case study.

| *Variable* | *Value* |
|---|---|
| *Photovoltaic unit Power (Wp)* | 250 |
| *Photovoltaic Module (€/Wp)* | 0.35 |
| *Power of the Module in year 25 (%)* | 80 |
| *Battery Degradation Capacity (%/year)* | 2.0 |
| *Discount Rate (%)* | 3.0 |
| *Inflation Rate (%)* | 2.5 |

Table 5. Components prices and considered rates, for the year of 2019.

| | *Case I* | | | | *Case II* | | | | *Case III* | | | | *Case IV* | | | |
|---|---|---|---|---|---|---|---|---|---|---|---|---|---|---|---|---|
| *Identification* | *PV1* | *PV2* | *PV3* | *PV4* | *PV1* | *PV2* | *PV3* | *PV4* | *PV1* | *PV2* | *PV3* | *PV4* | *PV1* | *PV2* | *PV3* | *PV4* |
| *Structures (€)* | 50 | 50 | 200 | 300 | 50 | 50 | 200 | 300 | 50 | 50 | 200 | 300 | 50 | 50 | 200 | 300 |
| *Micro-Inverter or Inverter (€)* | 199 | 324 | 597 | 1393 | 199 | 324 | 597 | 1393 | 1833 | 1833 | 1833 | 1833 | 1833 | 1833 | 1833 | 1833 |
| *Cables and Others (€)* | 50 | 50 | 100 | 100 | 50 | 50 | 100 | 100 | 50 | 50 | 100 | 100 | 50 | 50 | 100 | 100 |
| *Installation (€)* | 100 | 150 | 200 | 300 | 100 | 150 | 200 | 300 | 100 | 150 | 200 | 300 | 100 | 150 | 200 | 300 |
| *Battery (€)* | N/A | | | | N/A | | | | B1 – 1625€; B2 – 4060€; B3 – 5370€. | | | | B1 – 1625€; B2 – 4060€; B3 – 5370€. | | | |
| *Obligations fees by DL-153/2014 (€)* | 0 | 0 | 0 | 0 | 30 | 30 | 30 | 100 | 0 | 0 | 0 | 0 | 30 | 30 | 30 | 170 |

Table legend: Installed PV power (PV1 = 0.50 kW; PV2 = 0.75 kW; PV3 = 1.50 kW and PV4 = 3.45 kW); installed battery capacity (B1 = 3.3 kWh, B2 = 6.6 kWh and B3 = 9.9 kWh).

All the component prices were obtained from two main Portuguese suppliers and reflect the current real Portuguese market prices [32] [33] for domestic systems, verified with a market price survey. Potential discounts associated with the purchase of multiple

equipment, e.g., several microinverters, were not considered due to the high subjectivity associated with these commercial discounts. An average value for installation cost was also considered, which may have a substantial variability associated with the selected installer but will tend to be more homogeneous (and possibly lower) with the growth and increased competitiveness of the market. The photovoltaic module prices evolved rapidly in the last years, which justifies the use of the PV spot market prices, with small approximations reflecting the real costs in Portugal [34]. A remark must be made regarding the bidirectional wattmeter. EDP Distribuição is currently replacing the previous analogue wattmeter and deploying new digital versions with bidirectional metering capabilities, in all Portuguese territory, ensuring a 80 % replacement rate until 2020 (European Union directive from 2009). In this way, present analysis ignored the bidirectional counter acquisition costs, obliged by DL 153/2014 whenever its applicable.

Lithium-ion batteries were the selected battery technology, mainly to its efficiency, lowering costs and high energy density, becoming appropriate to domestic applications. The three battery capacity sizes have the same peak power of 3 kW.

Regarding the battery specifications, special attention must be given to its capacity lifetime degradation, depth of discharge and lifetime. To calculate the energy that is stored in the battery storage system and is then effectively used by the prosumer, some aspects were also considered, as the power electronics efficiency, the battery efficiency (charge-discharge) the yearly battery capacity degradation and, finally, the depth of discharge.

The photovoltaic micro-inverters were chosen for some cases: the APS YC 500 micro-inverter (0.5 kW) and the APS 250 (0.25 kW nominal power). The selected hybrid inverter is the Solax SK-SU3000E X-HYBRID SERIES G2.

As a simplification and in order to be able to assign a value to the electricity in off-grid systems, it was considered for these installations the same energy cost and tariff structure as those connected to the grid.

As regards energy and power prices used, the grid electric energy and contracted power prices are from EDP Comercial company [35] (continent) and for the Azores island are used the EDA prices [25], as depicted in Table 2. The surplus energy, injected into the public grid, is valuated accordingly to the Equation (1) and the average monthly wholesale electricity prices for 2018 (Fig. 2).

Regarding the stored energy, it is valuated at the price on the moment of its usage, depending on the selected tariff schedule.

Generally, tariff peak periods are associated with higher prices, so that when sizing the batteries, special care must be given to the number of charge and discharge cycles over the lifetime of the battery and its discharged energy prices, lowering the Levelized Cost of Energy Stored (LCOES).

## 4. Results

In the following tables, the results are shown, with the best results highlighted with a blue coloured cell. Regarding these figures, the initial letter "F" corresponds to the flat tariff, and the letter "B" represents the bi-hourly tariff. In the payback presentation tables, "nan" values correspond to payback periods higher than 25 years (the considered project lifetime) and are interpreted as uninteresting results for the analysis.

### 4.2. Economic Analysis

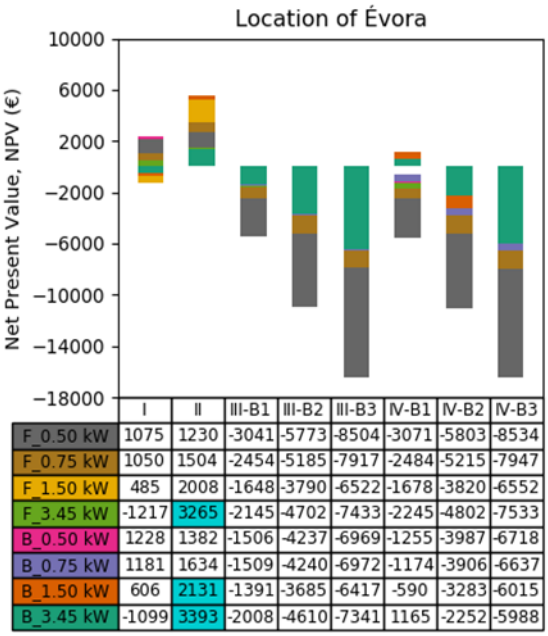


| | I | II | III-B1 | III-B2 | III-B3 | IV-B1 | IV-B2 | IV-B3 |
|---|---|---|---|---|---|---|---|---|
| F_0.50 kW | 1075 | 1230 | -3041 | -5773 | -8504 | -3071 | -5803 | -8534 |
| F_0.75 kW | 1050 | 1504 | -2454 | -5185 | -7917 | -2484 | -5215 | -7947 |
| F_1.50 kW | 485 | 2008 | -1648 | -3790 | -6522 | -1678 | -3820 | -6552 |
| F_3.45 kW | -1217 | 3265 | -2145 | -4702 | -7433 | -2245 | -4802 | -7533 |
| B_0.50 kW | 1228 | 1382 | -1506 | -4237 | -6969 | -1255 | -3987 | -6718 |
| B_0.75 kW | 1181 | 1634 | -1509 | -4240 | -6972 | -1174 | -3906 | -6637 |
| B_1.50 kW | 606 | 2131 | -1391 | -3685 | -6417 | -590 | -3283 | -6015 |
| B_3.45 kW | -1099 | 3393 | -2008 | -4610 | -7341 | 1165 | -2252 | -5988 |

Fig. 10. Results of the NPV economic indicator for the 8th studied configurations, for the location of Évora.

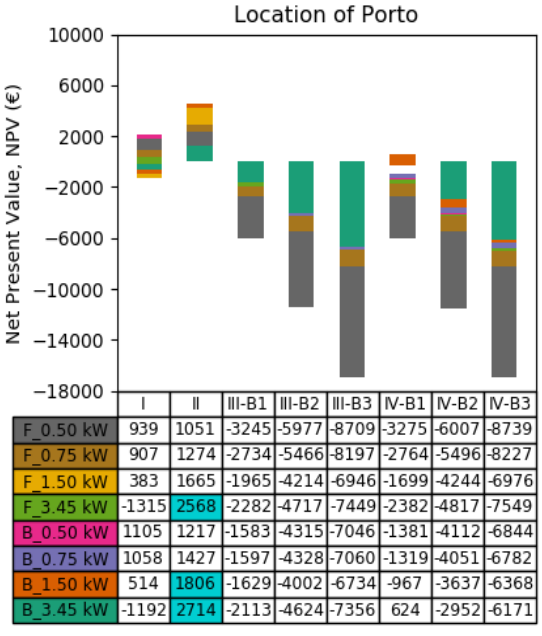


| | I | II | III-B1 | III-B2 | III-B3 | IV-B1 | IV-B2 | IV-B3 |
|---|---|---|---|---|---|---|---|---|
| F_0.50 kW | 939 | 1051 | -3245 | -5977 | -8709 | -3275 | -6007 | -8739 |
| F_0.75 kW | 907 | 1274 | -2734 | -5466 | -8197 | -2764 | -5496 | -8227 |
| F_1.50 kW | 383 | 1665 | -1965 | -4214 | -6946 | -1699 | -4244 | -6976 |
| F_3.45 kW | -1315 | 2568 | -2282 | -4717 | -7449 | -2382 | -4817 | -7549 |
| B_0.50 kW | 1105 | 1217 | -1583 | -4315 | -7046 | -1381 | -4112 | -6844 |
| B_0.75 kW | 1058 | 1427 | -1597 | -4328 | -7060 | -1319 | -4051 | -6782 |
| B_1.50 kW | 514 | 1806 | -1629 | -4002 | -6734 | -967 | -3637 | -6368 |
| B_3.45 kW | -1192 | 2714 | -2113 | -4624 | -7356 | 624 | -2952 | -6171 |

Fig. 11. Economic indicator NPV for the location of Porto, for all the studied configurations.

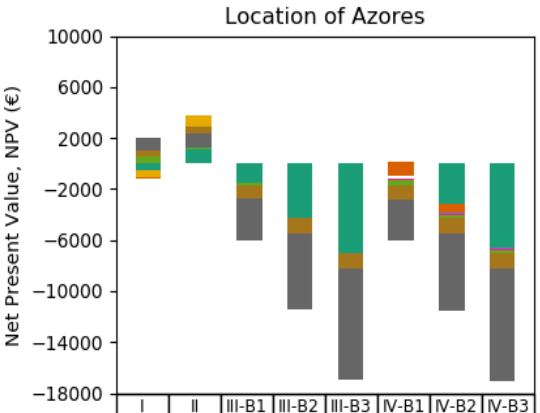


| | I | II | III-B1 | III-B2 | III-B3 | IV-B1 | IV-B2 | IV-B3 |
|---|---|---|---|---|---|---|---|---|
| F_0.50 kW | 1012 | 1063 | -3263 | -5994 | -8726 | -3293 | -6024 | -8756 |
| F_0.75 kW | 1017 | 1277 | -2760 | -5492 | -8223 | -2790 | -5522 | -8253 |
| F_1.50 kW | 552 | 1591 | -1719 | -4288 | -7019 | -1749 | -4318 | -7049 |
| F_3.45 kW | -1063 | 2224 | -1803 | -4255 | -6986 | -1903 | -4355 | -7086 |
| B_0.50 kW | 1047 | 1096 | -1536 | -4268 | -6999 | -1304 | -4036 | -6767 |
| B_0.75 kW | 1010 | 1268 | -1554 | -4285 | -7017 | -1230 | -3962 | -6694 |
| B_1.50 kW | 481 | 1519 | -1676 | -4306 | -7038 | -1132 | -3858 | -6590 |
| B_3.45 kW | -1159 | 2127 | -2090 | -4647 | -7379 | 176 | -3151 | -6697 |

Fig. 12. Location of Azores NPV results, for each of the studied configurations.

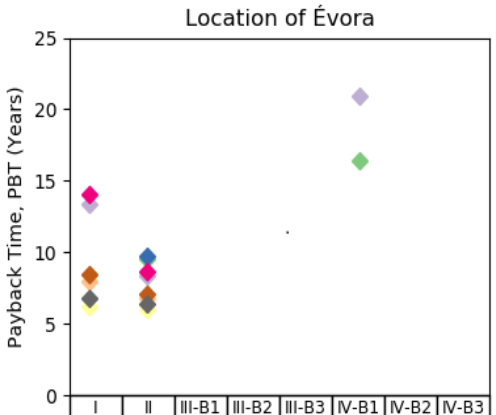


| | I | II | III-B1 | III-B2 | III-B3 | IV-B1 | IV-B2 | IV-B3 |
|---|---|---|---|---|---|---|---|---|
| F_0.50 kW | 6.8 | 6.4 | nan | nan | nan | nan | nan | nan |
| F_0.75 kW | 8.5 | 7.1 | nan | nan | nan | nan | nan | nan |
| F_1.50 kW | 14.1 | 8.6 | nan | nan | nan | nan | nan | nan |
| F_3.45 kW | nan | 9.7 | nan | nan | nan | nan | nan | nan |
| B_0.50 kW | 6.2 | 6.0 | nan | nan | nan | nan | nan | nan |
| B_0.75 kW | 8.0 | 6.7 | nan | nan | nan | nan | nan | nan |
| B_1.50 kW | 13.4 | 8.4 | nan | nan | nan | 21.0 | nan | nan |
| B_3.45 kW | nan | 9.5 | nan | nan | nan | 16.5 | nan | nan |

Fig. 13. Results of the PBT, for the location of Évora, for the configurations studied.

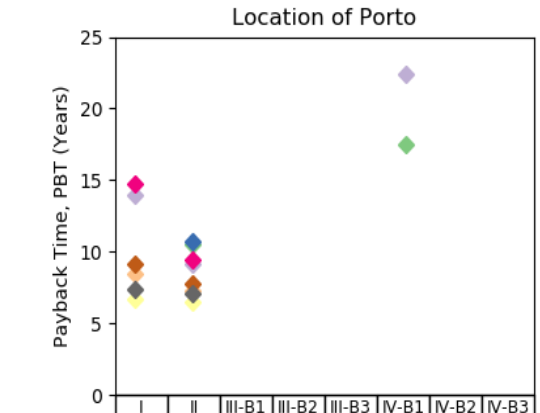


| | I | II | III-B1 | III-B2 | III-B3 | IV-B1 | IV-B2 | IV-B3 |
|---|---|---|---|---|---|---|---|---|
| F_0.50 kW | 7.3 | 7.1 | nan | nan | nan | nan | nan | nan |
| F_0.75 kW | 9.2 | 7.8 | nan | nan | nan | nan | nan | nan |
| F_1.50 kW | 14.7 | 9.5 | nan | nan | nan | nan | nan | nan |
| F_3.45 kW | nan | 10.8 | nan | nan | nan | nan | nan | nan |
| B_0.50 kW | 6.7 | 6.5 | nan | nan | nan | nan | nan | nan |
| B_0.75 kW | 8.5 | 7.3 | nan | nan | nan | nan | nan | nan |
| B_1.50 kW | 13.9 | 9.1 | nan | nan | nan | 22.4 | nan | nan |
| B_3.45 kW | nan | 10.5 | nan | nan | nan | 17.5 | nan | nan |

Fig. 14. Results of the PBT for all the configurations studied, for the location of Porto.

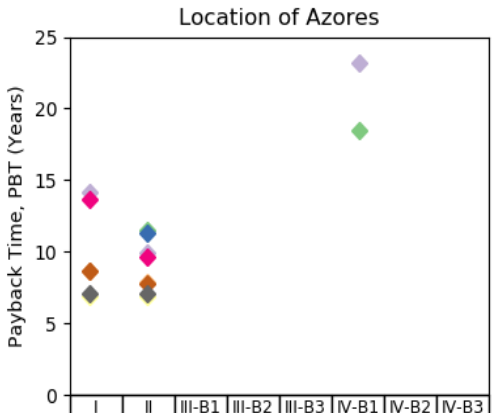


| | I | II | III-B1 | III-B2 | III-B3 | IV-B1 | IV-B2 | IV-B3 |
|---|---|---|---|---|---|---|---|---|
| F_0.50 kW | 7.0 | 7.0 | nan | nan | nan | nan | nan | nan |
| F_0.75 kW | 8.6 | 7.8 | nan | nan | nan | nan | nan | nan |
| F_1.50 kW | 13.7 | 9.7 | nan | nan | nan | nan | nan | nan |
| F_3.45 kW | nan | 11.3 | nan | nan | nan | nan | nan | nan |
| B_0.50 kW | 6.9 | 6.9 | nan | nan | nan | nan | nan | nan |
| B_0.75 kW | 8.7 | 7.8 | nan | nan | nan | nan | nan | nan |
| B_1.50 kW | 14.1 | 9.9 | nan | nan | nan | 23.2 | nan | nan |
| B_3.45 kW | nan | 11.5 | nan | nan | nan | 18.4 | nan | nan |

Fig. 15. Obtained results of the PBT economic indicator for all the studied configurations, for the region of Azores.

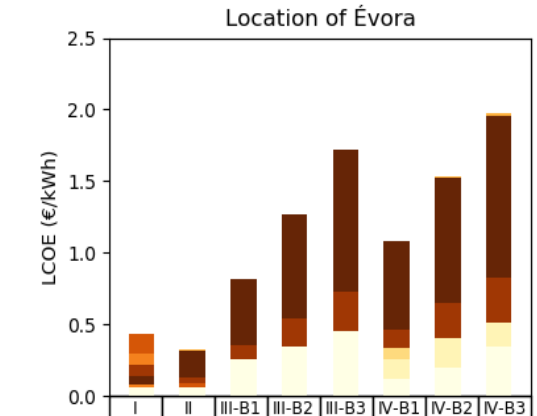


| | I | II | III-B1 | III-B2 | III-B3 | IV-B1 | IV-B2 | IV-B3 |
|---|---|---|---|---|---|---|---|---|
| F_0.50 kW | 0.06 | 0.18 | 0.47 | 0.73 | 0.99 | 0.62 | 0.87 | 1.13 |
| F_0.75 kW | 0.08 | 0.13 | 0.35 | 0.54 | 0.73 | 0.46 | 0.65 | 0.83 |
| F_1.50 kW | 0.14 | 0.09 | 0.26 | 0.34 | 0.45 | 0.33 | 0.40 | 0.51 |
| F_3.45 kW | 0.29 | 0.06 | 0.27 | 0.37 | 0.48 | 0.34 | 0.43 | 0.54 |
| B_0.50 kW | 0.06 | 0.18 | 0.47 | 0.73 | 0.99 | 0.62 | 0.88 | 1.14 |
| B_0.75 kW | 0.08 | 0.14 | 0.35 | 0.54 | 0.73 | 0.46 | 0.65 | 0.84 |
| B_1.50 kW | 0.14 | 0.09 | 0.26 | 0.34 | 0.45 | 0.26 | 0.40 | 0.51 |
| B_3.45 kW | 0.29 | 0.06 | 0.27 | 0.37 | 0.48 | 0.12 | 0.20 | 0.34 |

Fig. 16. Results of the LCOE for the location of Évora, for the studied configurations.

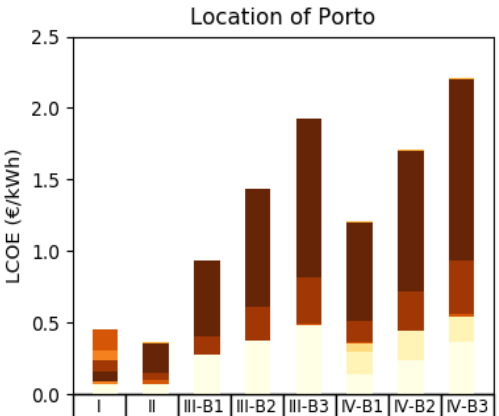


| | I | II | III-B1 | III-B2 | III-B3 | IV-B1 | IV-B2 | IV-B3 |
|---|---|---|---|---|---|---|---|---|
| F_0.50 kW | 0.07 | 0.20 | 0.53 | 0.82 | 1.11 | 0.69 | 0.98 | 1.27 |
| F_0.75 kW | 0.09 | 0.15 | 0.40 | 0.61 | 0.82 | 0.51 | 0.72 | 0.93 |
| F_1.50 kW | 0.15 | 0.10 | 0.28 | 0.37 | 0.49 | 0.36 | 0.44 | 0.56 |
| F_3.45 kW | 0.30 | 0.07 | 0.28 | 0.37 | 0.48 | 0.35 | 0.44 | 0.54 |
| B_0.50 kW | 0.07 | 0.21 | 0.53 | 0.82 | 1.11 | 0.69 | 0.98 | 1.27 |
| B_0.75 kW | 0.09 | 0.15 | 0.40 | 0.61 | 0.82 | 0.52 | 0.73 | 0.94 |
| B_1.50 kW | 0.15 | 0.10 | 0.28 | 0.37 | 0.49 | 0.29 | 0.44 | 0.56 |
| B_3.45 kW | 0.30 | 0.07 | 0.28 | 0.37 | 0.48 | 0.14 | 0.24 | 0.36 |

Fig. 17. Results of the LCOE for the location of Porto, for the studied configurations.

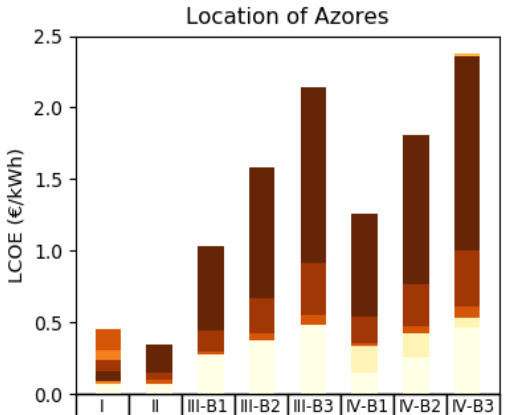


| | I | II | III-B1 | III-B2 | III-B3 | IV-B1 | IV-B2 | IV-B3 |
|---|---|---|---|---|---|---|---|---|
| F_0.50 kW | 0.07 | 0.19 | 0.59 | 0.91 | 1.23 | 0.72 | 1.04 | 1.36 |
| F_0.75 kW | 0.09 | 0.15 | 0.44 | 0.67 | 0.91 | 0.54 | 0.77 | 1.00 |
| F_1.50 kW | 0.15 | 0.10 | 0.29 | 0.42 | 0.55 | 0.35 | 0.47 | 0.61 |
| F_3.45 kW | 0.30 | 0.07 | 0.28 | 0.37 | 0.48 | 0.33 | 0.42 | 0.53 |
| B_0.50 kW | 0.07 | 0.19 | 0.59 | 0.91 | 1.23 | 0.72 | 1.04 | 1.37 |
| B_0.75 kW | 0.09 | 0.15 | 0.44 | 0.67 | 0.91 | 0.54 | 0.77 | 1.01 |
| B_1.50 kW | 0.15 | 0.10 | 0.29 | 0.42 | 0.55 | 0.33 | 0.47 | 0.61 |
| B_3.45 kW | 0.30 | 0.07 | 0.28 | 0.37 | 0.48 | 0.15 | 0.26 | 0.46 |

Fig. 18. Obtained LCOE results for the location of Azores, for all the studied configurations.

In order to improve the readability of this study, the results for the remaining key indicators are presented in the appendix section.

### 4.2. Energy Analysis

The following tables present the energy analysis results. Regarding the SMR (Saved Money Rate) indicator the comparison case was the grid-connected (without battery or PV system), for all the four considered configurations (I to IV).

Table 6. Energetic analysis for the Évora site.

| **Installed PV Power (kW) / Parameters** | **SCR (Self-consumption Ratio)** | **SSR (Self-supply Ratio** | **BU (Battery Use)** | **SMR (Saved Money Rate)** | | | |
|---|---|---|---|---|---|---|---|
| | **Case I and Case II** | | | **Case I** | | **Case II** | |
| | *Tariff independent* | | | **Flat** | **Bi-hourly** | **Flat** | **Bi-hourly** |
| 0.50 | 0.7601 | 0.3230 | N/A | 0.2439 | 0.2529 | 0.2713 | 0.2787 |
| 0.75 | 0.5797 | 0.3695 | N/A | 0.2790 | 0.2831 | 0.3506 | 0.3510 |
| 1.50 | 0.3238 | 0.4128 | N/A | 0.3117 | 0.3126 | 0.5413 | 0.5309 |
| 3.45 | 0.1450 | 0.4253 | N/A | 0.3211 | 0.3213 | 0.9884 | 0.9559 |
| **Installed PV Power (kW) / Parameters** | **SCR (Self-consumption Ratio)** | **SSR (Self-supply Ratio** | **BU (Battery Use)** | **Saved Money Rate (SMR) (€)** | | | |
| | | | | **Flat** | **Bi-hourly** | **Flat** | **Bi-hourly** |
| | **Case III, Case IV** | **Case III** | **Case III, Case IV** | **Case III** | | **Case IV** | |
| 0.50 B1 | 0.7601 | 0.3230 | 0.0697 | 0.2965 | 0.2814 | 0.2965 | 0.2814 |
| 0.50 B2 | 0.7601 | 0.3230 | 0.0697 | 0.2965 | 0.2814 | 0.2965 | 0.2814 |
| 0.50 B3 | 0.7601 | 0.3230 | 0.0697 | 0.2965 | 0.2814 | 0.2965 | 0.2814 |
| 0.75 B1 | 0.5797 | 0.3695 | 0.1833 | 0.4173 | 0.3961 | 0.4173 | 0.3961 |
| 0.75 B2 | 0.5797 | 0.3695 | 0.1833 | 0.4173 | 0.3961 | 0.4173 | 0.3961 |
| 0.75 B3 | 0.5797 | 0.3695 | 0.1833 | 0.4173 | 0.3961 | 0.4173 | 0.3961 |
| 1.50 B1 | 0.3238 | 0.4128 | 0.4388 | 0.6429 | 0.6101 | 0.7021 | 0.6662 |
| 1.50 B2 | 0.3238 | 0.4128 | 0.5760 | 0.7465 | 0.7084 | 0.7465 | 0.7084 |
| 1.50 B3 | 0.3238 | 0.4128 | 0.5760 | 0.7465 | 0.7084 | 0.7465 | 0.7084 |
| 3.45 B1 | 0.1450 | 0.4253 | 0.5341 | 0.7243 | 0.6874 | 1.1420 | 1.0837 |
| 3.45 B2 | 0.1450 | 0.4253 | 0.5747 | 0.7550 | 0.7164 | 1.0522 | 0.9985 |
| 3.45 B3 | 0.1450 | 0.4253 | 0.5747 | 0.7550 | 0.7164 | 0.9035 | 0.8574 |

Table 7. Energetic analysis for the location of Porto.

| **Installed PV Power (kW) / Parameters** | **SCR (Self-consumption Ratio)** | **SSR (Self-supply Ratio** | **BU (Battery Use)** | **SMR (Saved Money Rate)** | | | |
|---|---|---|---|---|---|---|---|
| | **Case I and Case II** | | | **Case I** | | **Case II** | |
| | *Tariff independent* | | | **Flat** | **Bi-hourly** | **Flat** | **Bi-hourly** |
| 0.50 | 0.7901 | 0.2964 | N/A | 0.2238 | 0.2356 | 0.2448 | 0.2556 |
| 0.75 | 0.6070 | 0.3416 | N/A | 0.2579 | 0.2659 | 0.3165 | 0.3219 |
| 1.50 | 0.3489 | 0.3927 | N/A | 0.2965 | 0.2998 | 0.4906 | 0.4853 |
| 3.45 | 0.1569 | 0.4061 | N/A | 0.3066 | 0.3082 | 0.8852 | 0.8606 |
| **Installed PV Power (kW) / Parameters** | **SCR (Self-consumption Ratio)** | **SSR (Self-supply Ratio** | **BU (Battery Use)** | **Saved Money Rate (SMR)** | | | |
| | | | | **Flat** | **Bi-hourly** | **Flat** | **Bi-hourly** |
| | **Case III, Case IV** | **Case III** | **Case III, Case IV** | **Case III** | | **Case IV** | |
| 0.50 B1 | 0.7901 | 0.2964 | 0.0538 | 0.2644 | 0.2509 | 0.2644 | 0.2509 |
| 0.50 B2 | 0.7901 | 0.2964 | 0.0538 | 0.2644 | 0.2509 | 0.2644 | 0.2509 |
| 0.50 B3 | 0.7901 | 0.2964 | 0.0538 | 0.2644 | 0.2509 | 0.2644 | 0.2509 |
| 0.75 B1 | 0.6070 | 0.3416 | 0.1512 | 0.3720 | 0.3531 | 0.3720 | 0.3531 |
| 0.75 B2 | 0.6070 | 0.3416 | 0.1512 | 0.3720 | 0.3531 | 0.3720 | 0.3531 |
| 0.75 B3 | 0.6070 | 0.3416 | 0.1512 | 0.3720 | 0.3531 | 0.3720 | 0.3531 |
| 1.50 B1 | 0.3489 | 0.3927 | 0.3889 | 0.5901 | 0.5600 | 0.6338 | 0.6015 |
| 1.50 B2 | 0.3489 | 0.3927 | 0.5011 | 0.6748 | 0.6404 | 0.6748 | 0.6404 |
| 1.50 B3 | 0.3489 | 0.3927 | 0.5011 | 0.6748 | 0.6404 | 0.6748 | 0.6404 |
| 3.45 B1 | 0.1569 | 0.4061 | 0.5249 | 0.7028 | 0.6670 | 1.0599 | 1.0059 |
| 3.45 B2 | 0.1569 | 0.4061 | 0.5939 | 0.7550 | 0.7164 | 0.9545 | 0.9058 |
| 3.45 B3 | 0.1569 | 0.4061 | 0.5939 | 0.7550 | 0.7164 | 0.8825 | 0.8375 |

Table 8. Energetic analysis for the location of Azores.

| **Installed PV Power (kW) / Parameters** | **SCR (Self-consumption Ratio)** | **SSR (Self-supply Ratio** | **BU (Battery Use)** | **SMR (Saved Money Rate)** | | | |
|---|---|---|---|---|---|---|---|
| | **Case I and Case II** | | | **Case I** | | **Case II** | |
| | *Tariff independent* | | | **Flat** | **Bi-hourly** | **Flat** | **Bi-hourly** |
| 0.50 | 0.8664 | 0.2829 | N/A | 0.2314 | 0.2449 | 0.2432 | 0.2568 |
| 0.75 | 0.6748 | 0.3305 | N/A | 0.2703 | 0.2789 | 0.3126 | 0.3223 |
| 1.50 | 0.3958 | 0.3877 | N/A | 0.3171 | 0.3177 | 0.4731 | 0.4789 |
| 3.45 | 0.1841 | 0.4147 | N/A | 0.3392 | 0.3368 | 0.8229 | 0.8375 |
| **Installed PV Power (kW) / Parameters** | **SCR (Self-consumption Ratio)** | **SSR (Self-supply Ratio** | **BU (Battery Use)** | **Saved Money Rate (SMR) (€)** | | | |
| | | | | **Flat** | **Bi-hourly** | **Flat** | **Bi-hourly** |

| | **Case III, Case IV** | **Case III** | **Case III, Case IV** | Case III | | Case IV | |
|---|---|---|---|---|---|---|---|
| 0.50 B1 | 0.8664 | 0.2829 | 0.0298 | 0.2558 | 0.2648 | 0.2558 | 0.2648 |
| 0.50 B2 | 0.8664 | 0.2829 | 0.0298 | 0.2558 | 0.2648 | 0.2558 | 0.2648 |
| 0.50 B3 | 0.8664 | 0.2829 | 0.0298 | 0.2558 | 0.2648 | 0.2558 | 0.2648 |
| 0.75 B1 | 0.6748 | 0.3305 | 0.1089 | 0.3594 | 0.3722 | 0.3594 | 0.3722 |
| 0.75 B2 | 0.6748 | 0.3305 | 0.1089 | 0.3594 | 0.3722 | 0.3594 | 0.3722 |
| 0.75 B3 | 0.6748 | 0.3305 | 0.1089 | 0.3594 | 0.3722 | 0.3594 | 0.3722 |
| 1.50 B1 | 0.3958 | 0.3877 | 0.3702 | 0.6199 | 0.6419 | 0.6339 | 0.6564 |
| 1.50 B2 | 0.3958 | 0.3877 | 0.4048 | 0.6482 | 0.6712 | 0.6482 | 0.6712 |
| 1.50 B3 | 0.3958 | 0.3877 | 0.4048 | 0.6482 | 0.6712 | 0.6482 | 0.6712 |
| 3.45 B1 | 0.1841 | 0.4147 | 0.5259 | 0.7693 | 0.7966 | 1.0368 | 1.0736 |
| 3.45 B2 | 0.1841 | 0.4147 | 0.5853 | 0.8179 | 0.8469 | 0.9732 | 1.0077 |
| 3.45 B3 | 0.1841 | 0.4147 | 0.5853 | 0.8179 | 0.8469 | 0.8543 | 0.8847 |

## 5. Discussion

As a general comment, cases I and II, which consider the PV-only configurations, are the most profitable. PV+battery configurations are already profitable in very specific conditions, and only with the configuration which has the highest PV power installation (3.45 kW), being slightly better with the bi-hourly tariff. The bi-hourly tariff is the most profitable electric tariff to use in all the cases. Generally, the Azores site configurations are the less profitable and the Évora site are the most profitable, mostly due to the available solar irradiation levels and consequently higher PV power generation. Although energy management strategies are relevant for PV+battery configurations profitability, the geographical location and electric tariff choice are essential factors in the configuration's economic and energetic viability. The 25 years analysis period considers the investment in two batteries units over that time period. This decision was made considering the useful lifecycle of the lithium-ion batteries available indicated in the consulted bibliography and warranty by the battery manufacturers.

In the following, the main three obtained economic indicators are discussed. Regarding NPV, the three locations have similar scenarios, in the sense of a go/no go decision regarding the investment, as can be observed in Fig. 10, Fig. 11 and Fig. 12. Case II is profitable in all configurations regardless of the electricity tariff or location, although in some locations this result is more positive than others. Including a battery is only economically viable when the generated PV energy is the biggest, namely in the IVB1 configuration with 3.45 kW installed PV power, and only for the by-hourly tariff. Case I

presents one unviable project, the 3.45 kW size, regardless tariff, since the oversizing of the installation.

Payback time is depicted in Fig. 13, Fig. 14 and Fig. 15. As general remark, the payback time is positive for cases I and II, and mostly negative for cases III and IV. With the considered conditions, case III is unprofitable in all locations. This case doesn't consider the potential additional costs of a RESP connection, generally associated with off-grid connections (since off-grid configurations are usually characterized by being distant from the available grid point of connection), and which would have had impact in the economic indicators in all the studied locations. The best PV+battery scenario for the Évora site is the bi-hourly tariff with 3.45 kW PV installation IVB1, although still considered slightly high - 16 years - compared with a 25 year investment. An interesting aspect is the difference between the obtained results of case IV in Évora, Porto, and in Azores, because of the different (higher) electricity tariff in this last location, and even though associated with the smallest solar resource, presents the worst scenarios, concluding that although having a higher electricity tariff still can't compensate the lowest solar irradiation. Case I average payback is 9.5 years for the location of Évora, 10 years for Porto and 9.8 years for Azores. Case II average payback is 7.8 years for Évora, 8.6 years for Porto and 9.0 years for Azores. This result shows that the grid-connected installations in Portugal have better payback, location independent, due to the increased income of selling the energy surplus to the grid. This means that in average, its 22 % more economic to invest in a grid-connected installation (case II) in Évora, 16 % in Porto and 9 % in Azores.

Considering all sites, in some of the studied situation's grid-parity is achieved, observing the obtained LCOE values (Fig. 16, Fig. 17 and Fig. 18). The lowest values, and so best results, are observed in cases I and II, for all PV configurations and all the locations. The use of the batteries presents positive economic interest in case IVB1 for the 3.45 kW PV installation. The lowest PV+battery energy profit occurs in Azores. The most striking economically unviable cases are the case scenarios IIIB3 and IVB3 0.50 kW, due to the low usage of the battery capabilities, and high cost (inexistence of a balanced trade-off). The same comment regarding the case III because of the absence of additional costs associated with the connections with RESP, related to off-grid configurations, which aren't considered in this work.

The IRR obtained results are presented in Table A2, Table A3 and Table A4, and a general comment can be done regarding the high obtained values in the unprofitable configuration's cases. The B/C ratio, present in Table A5, Table A6 and Table A7, and the higher value, the better project viability. The indicator corroborates the three main

discussed economic indicators in this analysis. The energy analysis made, presented in Table 6, Table 7 and Table 8 allows a more detailed analysis of the generated energy use. The SCR decreases with the increase of the PV installed power, which confirms the existing trade-off between PV generation and effective consumption of this energy. SCR indicator is showing how much of the produced energy is effectively self-consumed and is always dependent of the load diagram and PV generation. In Évora case I, SCR is lower than the one in Porto, and Azores has the highest because the PV generation is the lowest, so the energy ratio is more influenced, compared to the other locations. SSR increases with the increase of the PV installed power, because the biggest the PV generated electricity, the biggest the consumed energy, and considering the energy load constant. The BU indicator helps in the evaluation of need of a battery system, and its value is high when its use is high. In the cases III and IV, the BU indicator confirms that the 0.50 kW and 0.75 kW PV installed power, the PV generation is too low to justify a battery acquisition, so its size is irrelevant in the final gross of energy, in the three locations. With the 1.50 kW and 3.45 kW PV installed power, the use of the battery increases a lot and helps the energy independency. For most of the locations, SMR is smaller for the bi-hourly tariff cases. This indicator compares the energy saved with the current configuration, considering the energy prices at which the electricity is effectively sold, and the electricity bill, in one year, after the payback achievement. The relevance of the introduction of this indicator is mostly to represent the major differences among the use of different electric prices and different electric companies' prices of the contracted power and of energy (EDP commercial and EDA). The fact that Azores has a distinct tariff is well observed in the SMR indicator, because it has the lowest PV generation, but the highest remuneration for the energy makes it have some of the best SMR values. For the case IV, it is noticeable that values above the unity means that one is earning money with the configuration, even though the configuration is already paid. The 23$^{rd}$ article of the DL 153/2014 doesn't establish a limit for the UPAC's injection in RESP, so this configuration is very interesting. The biggest differences between cases III and IV is prominent in the higher PV installed power, as the grid injection remuneration is very low.

## 6. Conclusion

The main aim of this study was the evaluation of the viability of different solar PV configurations in different situations. Four cases were investigated, two cases with PV-only configurations, differing from each other by the injection of the surplus to the grid, and two PV+battery configurations which differ also from the injected surplus, and the

inclusion of batteries. The most profitable PV-only configurations for the locations of Évora, Porto and Azores is the case II (0.50 kW PV power with bi-hourly tariff). These are followed in a general way by case I (0.50 kW PV power). The most profitable PV+battery configuration for Évora, Porto and Azores is case IVB1 (3.45 kW PV installed power + 3.3 kWh battery). Although these are very positive results from a PV-only configuration perspective, most of the studied cases of PV+battery are not profitable, but the scenario shows a very positive future perspective. The bi-hourly tariff presents better results, with the used load profile, which doesn't have a profile with striking load variations. The energy management strategy used in this study was the simplest, but the usage of an intelligent energy management strategy can, by itself, improve the results obtained in this study, particularly considering a multi optimization strategy.

Current average price of the batteries considered in this study is 492 €/kWh, which is still a very high value, and makes the CAPEX of the PV+battery configuration a competitive value, compared with other alternatives. Further decrease of the battery costs which are expected in the following years will be needed to improve the profitability of PV residential applications, although this study is a remark of that beginning. Independent of the technology chosen, battery energy storage has been quickly evolving, with technical improvements being achieved, as for the capacity, performance, efficiency and the response that manufacturers are giving to the market.

All the configurations implemented self-consumption, considered to be the current most adequate context to implement PV solar energy in Portugal in the residential sector, regarding the Portuguese legislation. A revision of the current DL is ongoing due to the evolution that PV technology and batteries have been showing since 2014 (year of the DL prevalence), following the example of different and more profitable residential schemes, as net-metering or community sharing PV generation, from an economic, energetic and social well-being point of view.

**Acknowledgements**

This work was supported by the project AGERAR (Ref. 0076_AGERAR_6_E), co-financed by the European Regional Development Fund (ERDF), within the INTERREG VA Spain-Portugal cooperation programme (POCTEP).

## References

[1] IEA-ETSAP; IRENA, "Renewable Energy Integration in Power Grids - Technology Brief," 2015.

[2] Solar Power Europe, "Global Market Outlook for Solar Power 2017-2021," 2017.

[3] Publication Office of the European Union, "Future and Emerging Technologies Workshop on Future Battery Technologies for Energy Storage," Luxembourg, 2018.

[4] BNEF, "A Behind the Scenes Take on Lithium-ion Battery Prices | BloombergNEF." [Online]. Available: https://about.bnef.com/blog/behind-scenes-take-lithium-ion-battery-prices/. [Accessed: 07-Mar-2022].

[5] International Energy Agency, "Policy database – Data & Statistics - IEA," *Policies database*, 2020. [Online]. Available: https://www.iea.org/policies?qs=united&country=United Kingdom&status=In force&jurisdiction=National. [Accessed: 07-Mar-2022].

[6] P. S. MOLINA, "Spain's new rules for self-consumption come into force," *PV Magazine*, 2019. [Online]. Available: https://www.pv-magazine.com/2019/04/08/spains-new-rules-for-self-consumption-come-into-force/. [Accessed: 07-Mar-2022].

[7] E. Bellini, "Italy offers incentives for EVs – pv magazine International." [Online]. Available: https://www.pv-magazine.com/2019/04/08/italy-offers-incentives-for-evs/. [Accessed: 07-Mar-2022].

[8] G. Lorenzi, R. da Silva Vieira, C. A. Santos Silva, and A. Martin, "Techno-economic analysis of utility-scale energy storage in island settings," *J. Energy Storage*, vol. 21, no. August 2018, pp. 691–705, 2019.

[9] S. Dhundhara, Y. P. Verma, and A. Williams, "Techno-economic analysis of the lithium-ion and lead-acid battery in microgrid systems," *Energy Convers. Manag.*, vol. 177, no. May, pp. 122–142, 2018.

[10] A. Lahnaoui, P. Stenzel, and J. Linssen, "Techno-economic analysis of photovoltaic battery system configuration and location☆," *Appl. Energy*, vol. 227, no. September 2017, pp. 497–505, 2018.

[11] D. Shaw-Williams, C. Susilawati, and G. Walker, "Value of residential investment in photovoltaics and batteries in networks: A techno-economic analysis," *Energies*, vol. 11, no. 4, 2018.

[12] E. Tervo, K. Agbim, F. DeAngelis, J. Hernandez, H. K. Kim, and A. Odukomaiya, "An economic analysis of residential photovoltaic systems with lithium ion battery storage in the United States," *Renew. Sustain. Energy Rev.*, vol. 94, no. January, pp. 1057–1066, 2018.

[13] F. Cucchiella, I. D'Adamo, and M. Gastaldi, "Photovoltaic energy systems with battery storage for residential areas: An economic analysis," *J. Clean. Prod.*, vol. 131, pp. 460–474, 2016.

[14] G. Cerino Abdin and M. Noussan, "Electricity storage compared to net metering in residential PV applications," *J. Clean. Prod.*, vol. 176, pp. 175–186, 2018.

[15] F. M. Camilo, R. Castro, M. E. Almeida, and V. F. Pires, "Economic assessment of residential PV systems with self-consumption and storage in Portugal," *Sol. Energy*, vol. 150, pp. 353–362, 2017.

[16] C. H. Villar, D. Neves, and C. A. Silva, "Solar PV self-consumption: An analysis of influencing indicators in the Portuguese context," *Energy Strateg. Rev.*, vol. 18, pp. 224–234, 2017.

[17] J. C. Solano, M. C. Brito, and E. Caamaño-Martín, "Impact of fixed charges on the viability of self-consumption photovoltaics," *Energy Policy*, vol. 122, pp. 322–331, 2018.

[18] J. R. Martín, "Exclusive: Portugal in energy storage push as PV auction calendar builds | PV Tech," *PV Tech*, 2019. [Online]. Available: https://www.pv-tech.org/news/exclusive-portugal-to-hold-50-100mw-energy-storage-auction-in-2020.

[19] E. Bellini, "EDP to build Portugal's first MW-sized PV plant coupled with storage – pv magazine International," *pv magazine*, 2019. [Online]. Available: https://www.pv-magazine.com/2019/04/11/edp-to-build-portugals-first-mw-sized-pv-plant-coupled-with-storage/. [Accessed: 08-Mar-2022].

[20] M. C. Pacheco, B. C. Ferreira, and C. R. P. & Arnaut, "Electricity regulation in Portugal: overview | Practical Law," *Thomson Reuters Practical Law*, 2020. [Online]. Available: https://uk.practicallaw.thomsonreuters.com/6-564-1565?transitionType=Default&contextData=(sc.Default)&firstPage=true#co_anchor_a916055. [Accessed: 08-Mar-2022].

[21] República Portuguesa, *Decreto-Lei n.º 162/2019 de 25 de outubro*. Portugal, 2019, pp. 45–62.

[22] República Portuguesa, *Decreto-Lei n.º 153/2014 | DRE*. Portugal, 2014.

[23] "Publicações | OMIE." [Online]. Available: https://www.omie.es/pt/publicacoes. [Accessed: 08-Mar-2022].

[24] EDP Comercial, "EDP Comercial," *Electricity Tariffs*. [Online]. Available: https://www.edp.pt/particulares/energia/tarifarios/. [Accessed: 14-Dec-2020].

[25] EDA, "Períodos Horários EDA." [Online]. Available: https://www.eda.pt/Clientes/AMinhaEmpresa/TarifasBaixaTensaoNormal/Períodos Horários.pdf. [Accessed: 08-Mar-2022].

[26] EDP Distribuição, "Atualização dos perfis de consumo , de produção e de autoconsumo para o ano de 2018 Documento Metodológico," 2017.

[27] "DGEG." [Online]. Available: https://www.dgeg.gov.pt/. [Accessed: 08-Mar-2022].

[28] "PVGIS Photovoltaic Geographical Information System." [Online]. Available: https://joint-research-centre.ec.europa.eu/pvgis-photovoltaic-geographical-information-system_en. [Accessed: 08-Mar-2022].

[29] "Solar resource maps and GIS data for 200+ countries | Solargis." [Online]. Available: https://solargis.com/maps-and-gis-data/download/portugal. [Accessed: 08-Mar-2022].

[30] W. Short, D. J. Packey, and T. Holt, *A Manual for the Economic Evaluation of Energy Efficiency and Renewable Energy Technologies*. 1995.

[31] "Home Page - Simulação de PV." [Online]. Available: https://www.sisifo.info/pt/default. [Accessed: 08-Mar-2022].

[32] "Ecosist - Sistemas de Poupança - O seu parceiro de confiança." [Online]. Available: https://www.ecosist.net/. [Accessed: 08-Mar-2022].

[33] "SOLARIMPACT." [Online]. Available: https://loja.solarimpact.pt/. [Accessed: 08-Mar-2022].

[34] "Module Price Index – pv magazine International." [Online]. Available: https://www.pv-magazine.com/features/investors/module-price-index/. [Accessed: 08-Mar-2022].

[35] "ERSE - Tarifas e preços - eletricidade," *Tarifas e preços para a energia elétrica e outros serviços em 2018*, 2018. [Online]. Available:

https://www.erse.pt/atividade/regulacao/tarifas-e-precos-eletricidade/#a2018. [Accessed: 08-Mar-2022].

[36] "MeterBoost - Baterias de Lítio." [Online]. Available: https://www.meterboost.pt/produtos. [Accessed: 08-Mar-2022].

## Appendices

Table A1. Lithium-ion battery characterization data, given by the manufacturer [36]

| Battery Identification | B1 (3.0 kW/3.3 kWh) |
|---|---|
| Model | METERBOOST-48-LTO6-3.3 |
| Nominal Voltage (V) | 48.0 |
| Maximum/minimum Voltage (V) | 32.0-58.4 |
| Nominal Capacity (Ah) | 63 |
| Nominal Capacity (kWh) | 3.3 |
| Nominal Power (kW) | 3.0 |
| Weight (Kg) | 17 |
| Length x Width x Height (mm) | 430x360x76 |
| Useful lifecycle (years) | >17 |

Table A2. Results of the Internal Rate of Return economic indicator, for the studied configurations cases, for the location of Évora.

| *Location of Évora* | | | | | | | | |
|---|---|---|---|---|---|---|---|---|
| *Electric Tariff* | *Flat* | | | | *Bi-hourly* | | | |
| *Configuration* | *0.5* | *0.75* | *1.5* | *3.45* | *0.5* | *0.75* | *1.5* | *3.45* |
| *I* | 13.0 | 8.41 | -2.42 | -188 | 14.7 | 9.65 | -1.17 | -115 |
| *II* | 14.0 | 12.0 | 8.08 | 5.78 | 15.6 | 13.0 | 8.69 | 6.13 |
| *IIIB1* | -200 | -199 | -194 | -194 | -196 | -195 | -78.0 | -193 |
| *IIIB2* | -202 | -202 | -200 | -200 | -201 | -201 | -200 | -200 |
| *IIIB3* | -203 | -203 | -202 | -201 | -202 | -202 | -202 | -201 |
| *IVB1* | -200 | -199 | -194 | -195 | -106 | -60.1 | -19.0 | -4.66 |
| *IVB2* | -202 | -202 | -200 | -199 | -201 | -200 | -199 | -85.6 |
| *IVB3* | -203 | -203 | -202 | -201 | -202 | -202 | -201 | -200 |

Table A3. Obtained results regarding the IRR economic indicator, for the studied configurations cases, for the location of Porto.

| *Location of Porto* | | | | | | | | |
|---|---|---|---|---|---|---|---|---|
| *Electric Tariff* | *Flat* | | | | *Bi-hourly* | | | |
| *Configuration* | *0.5* | *0.75* | *1.5* | *3.45* | *0.5* | *0.75* | *1.5* | *3.45* |
| *I* | 11.3 | 6.96 | -3.60 | -191 | 13.3 | 8.49 | -2.11 | -187 |
| *II* | 12.0 | 10.1 | 6.27 | 3.72 | 13.9 | 11.4 | 7.04 | 4.17 |
| *IIIB1* | -201 | -200 | -196 | -195 | -196 | -196 | -194 | -194 |
| *IIIB2* | -203 | -202 | -200 | -200 | -201 | -201 | -200 | -200 |
| *IIIB3* | -203 | -203 | -202 | -201 | -202 | -202 | -202 | -201 |
| *IVB1* | -201 | -200 | -194 | -195 | -194 | -120 | -29.5 | -7.12 |
| *IVB2* | -203 | -202 | -200 | -198 | -201 | -201 | -199 | -196 |
| *IVB3* | -203 | -203 | -202 | -201 | -202 | -202 | -201 | -200 |

Table A4. Internal Rate of Return economic indicator results, for the studied configurations cases, for the location of Azores.

| *Location of Azores* | | | | | | | | |
|---|---|---|---|---|---|---|---|---|
| *Electric Tariff* | *Flat* | | | | *Bi-hourly* | | | |
| *Configuration* | *0.5* | *0.75* | *1.5* | *3.45* | *0.5* | *0.75* | *1.5* | *3.45* |
| I | 12.2 | 8.08 | -1.71 | -83.4 | 12.63 | 8.02 | -2.46 | -184 |
| II | 12.2 | 10.1 | 5.86 | 2.58 | 12.56 | 10.04 | 5.44 | 2.24 |
| IIIB1 | -201 | -200 | -195 | -134 | -196 | -195 | -194 | -194 |
| IIIB2 | -203 | -202 | -200 | -199 | -201 | -201 | -200 | -200 |
| IIIB3 | -203 | -203 | -202 | -201 | -202 | -202 | -202 | -201 |
| IVB1 | -201 | -200 | -194 | -191 | -162 | -74.19 | -38.4 | -9.72 |
| IVB2 | -203 | -202 | -200 | -199 | -201 | -200 | -200 | -197 |
| IVB3 | -203 | -203 | -202 | -201 | -202 | -202 | -202 | -201 |

Table A5. Obtained results of the Benefit-to-Cost Ratio economic measure, for each of the studied configurations, for the location of Évora.

| *Location of Évora* | | | | | | | | |
|---|---|---|---|---|---|---|---|---|
| *Electric Tariff* | *Flat* | | | | *Bi-hourly* | | | |
| *Configuration* | *0.5* | *0.75* | *1.5* | *3.45* | *0.5* | *0.75* | *1.5* | *3.45* |
| I | 4.35 | 3.42 | 1.97 | 0.97 | 4.76 | 3.65 | 2.08 | 1.02 |
| II | 1.34 | 1.54 | 1.78 | 2.07 | 1.41 | 1.58 | 1.80 | 2.08 |
| IIIB1 | 0.59 | 0.79 | 1.07 | 1.02 | 1.06 | 1.07 | 1.14 | 1.05 |

| | | | | | | | | |
|---|---|---|---|---|---|---|---|---|
| IIIB2 | 0.38 | 0.51 | 0.83 | 0.75 | 0.68 | 0.70 | 0.85 | 0.77 |
| IIIB3 | 0.28 | 0.38 | 0.62 | 0.58 | 0.50 | 0.52 | 0.64 | 0.59 |
| IVB1 | 0.45 | 0.61 | 0.85 | 0.83 | 0.87 | 0.90 | 1.07 | 1.45 |
| IVB2 | 0.32 | 0.43 | 0.70 | 0.64 | 0.61 | 0.64 | 0.78 | 0.99 |
| IVB3 | 0.25 | 0.33 | 0.55 | 0.51 | 0.47 | 0.50 | 0.61 | 0.68 |

Table A6. Results of the BC Ratio, for each of the studied configurations, for the location of Porto.

| *Location of Porto* | | | | | | | | |
|---|---|---|---|---|---|---|---|---|
| *Electric Tariff* | *Flat* | | | | *Bi-hourly* | | | |
| *Configuration* | *0.5* | *0.75* | *1.5* | *3.45* | *0.5* | *0.75* | *1.5* | *3.45* |
| I | 3.99 | 3.16 | 1.87 | 0.93 | 4.43 | 3.43 | 2.00 | 0.98 |
| II | 1.21 | 1.39 | 1.61 | 1.86 | 1.29 | 1.45 | 1.64 | 1.88 |
| IIIB1 | 0.53 | 0.71 | 0.99 | 0.99 | 1.03 | 1.04 | 1.08 | 1.03 |
| IIIB2 | 0.34 | 0.46 | 0.75 | 0.75 | 0.67 | 0.68 | 0.79 | 0.76 |
| IIIB3 | 0.25 | 0.34 | 0.57 | 0.58 | 0.49 | 0.50 | 0.59 | 0.59 |
| IVB1 | 0.41 | 0.55 | 0.78 | 0.80 | 0.84 | 0.87 | 0.99 | 1.35 |
| IVB2 | 0.29 | 0.39 | 0.64 | 0.64 | 0.59 | 0.62 | 0.72 | 0.89 |
| IVB3 | 0.22 | 0.30 | 0.50 | 0.51 | 0.46 | 0.48 | 0.57 | 0.66 |

Table A7. Results of the Benefit-to-Cost Ratio, for the location of Azores, for the studied configurations.

| *Location of Azores* | | | | | | | | |
|---|---|---|---|---|---|---|---|---|
| *Electric Tariff* | *Flat* | | | | *Bi-hourly* | | | |
| *Configuration* | *0.5* | *0.75* | *1.5* | *3.45* | *0.5* | *0.75* | *1.5* | *3.45* |
| *I* | 4.19 | 3.36 | 2.03 | 1.04 | 4.28 | 3.34 | 1.96 | 1.00 |
| *II* | 1.48 | 1.64 | 1.78 | 1.89 | 1.48 | 1.61 | 1.72 | 1.84 |
| *IIIB1* | 0.52 | 0.70 | 1.05 | 1.10 | 1.05 | 1.05 | 1.06 | 1.03 |
| *IIIB2* | 0.34 | 0.46 | 0.74 | 0.82 | 0.68 | 0.69 | 0.73 | 0.76 |
| *IIIB3* | 0.25 | 0.34 | 0.56 | 0.64 | 0.50 | 0.51 | 0.55 | 0.59 |
| *IVB1* | 0.43 | 0.57 | 0.87 | 0.93 | 0.91 | 0.94 | 1.01 | 1.33 |
| *IVB2* | 0.30 | 0.40 | 0.65 | 0.73 | 0.63 | 0.66 | 0.72 | 0.90 |
| *IVB3* | 0.23 | 0.31 | 0.50 | 0.58 | 0.48 | 0.50 | 0.56 | 0.62 |

## 3.3.1. Testing and evaluation of batteries for commercial and residential applications

E. López González[1], L. Fialho[2], L. Vargas Vázquez[1], A. Foles[2], J. Saénz Cuesta[1], M. Collares Pereira[2]

In *VII Symposium on Hydrogen, Fuel Cells and Advanced Batteries, HYCELTEC 2019*

***Keywords*:** Renewable Energy, Li ion battery, Vanadium Redox Flow Battery (VRFB), micro grids

### 1. Introduction

Renewable energy sources have demonstrated in recent years their ability to reduce the dependence on fossil fuels, contribute to the security of energy supply and play an important role in reducing greenhouse gas emissions. However, an important challenge in the use of renewable energy is the generalisation of distributed generation, where generation and consumption are usually located in the nearness. In addition to the reduction in the need for large infrastructures, distributed generation offer the additional advantage of reducing transmission losses.

The concept of micro grid has been considered as a solution for the reliable integration of distributed generation, including energy storage systems, and controllable loads [1]. A micro grid is a bidirectional electricity generation system that allows the distribution of electricity from suppliers to consumers, with the aim of optimizing the management and saving of energy, as well as reducing costs and increasing reliability [2].

Many of these renewable energy sources are intermittent resources and thus require complementary systems to adjust the necessary real time equilibrium between generation and consumption. That equilibrium can be reached through a combination of demand response measures and storage, but also by connecting these micro grids to the main electrical grid. In this context, energy storage systems (ESS) are key in the way

[1]Instituto Nacional de Técnica Aeroespacial (INTA), Área de Energías Renovables-CEDEA, Ctra, S. Juan-Matalascañas, km.34, 21130, Mazagón (Huelva), Spain
[2]Universidade de Évora, Cátedra Energias Renováveis, Palácio do Vimioso, Largo Marquês de Marialva, 7002-554, Évora, Portugal

towards decarbonisation of the energy system. Finding solutions to energy storage issues is a key element for achieving the EU's energy policy objectives [3]. Different energy storage technologies coexist because their characteristics make them attractive to different applications. Electrical energy storage includes a broad range of technologies, which either directly or indirectly provide electrical energy storage via an electrical input and output.

In this framework, the AGERAR project (Storage and management of renewable energies in commercial and residential applications) aims to research, develop and evaluate technical solutions to promote energy efficiency and sustainability criteria in commercial and residential micro grids. These solutions could increase the use and management of renewable energies in these applications, thanks to innovative energy storage systems and the massive implementation of information and communication technologies (ICTs). To achieve these objectives, one of the activities of the project focuses on the test, evaluation and comparison of main key performance indicators (KPIs) for different battery technologies, suitable for commercial and residential applications, from cells and modules to complete systems up to 60 kWh of energy storage capacity. This technological validation will provide reliable information to the public bodies, private companies and final users, based on experimental data, about the real performance and potential benefits of these technologies, in terms of efficiency, lifetime, costs, and safety, among others.

## 2. Testing and evaluation of batteries for commercial and residential applications

The University of Évora (UÉvora) and the Spanish National Institute for Aerospace Technology (INTA) will be responsible for the testing and evaluation of batteries in the AGERAR project. To cover a wide range of technologies, power and energy storage capacities, UÉvora is focused on commercial Li-ion based systems and Vanadium Redox Flow Batteries (VRFB), while INTA is testing Li-ion cells and packs with lithium titanium oxide (LTO) anode, as well as Aluminium ion secondary battery cells.

### 2.1 Testing of batteries at UÉvora

The Renewable Energies Chair of the University of Évora is developing activities focused on solar energy and energy storage. In these experimental facilities there are two microgrids:

I) VRFB microgrid for rehearsing and characterisation of PV + storage systems and integration into the grid/building in real scale. Equipped with a vanadium redox flow

battery (5 kW/60 kWh), rooftop PV generation (6.74 $kW_p$), precision monitoring and control systems.

II) Li-Ion microgrid for rehearsing and characterisation of PV + storage systems and integration into the grid in real scale. Equipped with advanced lithium-ion batteries (30 kWh + 9.8 kWh), PV generation (3.3 $kW_p$), precision monitoring and control systems. Table 1 presents the installed vanadium redox flow battery technical specifications:

Table 1 - VRFB manufacturer technical specifications.

| | **Units** | **Value/Range** |
|---|---|---|
| Number of cells in the stack | | 40 |
| Electrical connection | | Three-phase |
| Operating voltage | V | 50-60 |
| Volume | $m^3$ | 1.8x2 |
| Weight | Kg | 3800 |
| Depth of discharge | % | 95 |
| Lifetime | | +10,000 deep charge/discharge cycles |

Regarding the Li ion battery, its main specifications (provided by the manufacturer), are presented in Table 2, as follow:

Table 2 - Li-ion battery manufacturer technical specifications.

| | **Units** | **Value/Range** |
|---|---|---|
| Total Energy Capacity | kWh | 9.8 (25ºC, 100% SOC) |
| Usable Energy Capacity | kWh | 8.8 |
| Battery Nominal Capacity | Ah | 189 |
| Volume | $m^3$ | 0.05 |
| Weight | Kg | 75 |
| Voltage Range | VDC | 42.0-58.8 |
| Nominal Voltage | VDC | 51.8 |
| Max. Current | A | 119 A at 42 V |
| Nominal / Max. Power | kW | 3.3 / 5.0 |
| Peak Power | kW | 7.0 kW for 3 sec. |
| Peak Current | A | 166.7 A for 3 sec. |
| Lifetime (80% DOD, 25ºC) / (90% DOD, 25ºC) | | 10000 / 6000 |
| Battery Pack Round-Trip Efficiency | % | >95% (under specific conditions) |

Both technologies, VRFB and Li-Ion battery were tested according to the manufacturer's specifications and operational limits, with all the control and datalogging done with in-house developed software.

### 2.2 Testing of batteries at INTA

The Laboratory of the INTA's Renewable Energy Area in El Arenosillo (Huelva) has in their facilities different test benches for the evaluation and demonstration of electrochemical technologies for the storage and generation of electrical energy (batteries, supercapacitors and fuel cells) at cells and modules scale, for stationary and mobile applications. An experimental micro grid, where the most promising technologies are integrated and validated at pilot plant scale, complements these test facilities. The objective of these testing facilities is to support demonstration and evaluation projects in this field, collaborating with companies and other R&D centers in the development and demonstration of their products and systems. The tests performed in the AGERAR project involve the use of a battery/supercapacitor test bench. This test station has 4 channels for high voltage (up to 400 A in a range of 0 to 60V, with 6 kW maximum power per channel), and other 4 channels of low voltage (up to 10 A in a range of 0 to 5V and a maximum power per channel of 50 W). The test bench is complemented with a climate chamber of 300 litters capacity (internal measurements 700 x 700 x 625 mm), able to operate from -40 to 150 °C and equipped with sensors and gas detectors. In a first phase, two different technologies of batteries have been tested at INTA: commercial LTO based Li-ion cells and prototypes of Al-ion cells. Regarding the Li ion cells, its main specifications, according to the manufacturer, are detailed in Table 3.

Table 3 - LTO Li-ion cells specifications.

| | **Units** | **Value/Range** |
|---|---|---|
| Rated Capacity | Ah | 46 (charge @ 0.2C, 23±3℃, discharge@0.2C, 23±3 ºC) |
| Specific Energy | Wh/kg | 143 |
| Energy Density | Wh/L | 334 |
| Weight (per cell) | Kg | Max. 1.190 |
| Cell Dimensions | Mm | 226 x 227 x 12.5 @ 3.7 ± 0.1V |
| Voltage | V | 3.7 (nominal); 2.7 (lower limit); 4.2 (upper limit) |
| Current | A | Max. charge cont. 138.0 (3C); Max. discharge cont. 552.0 (12C); Max. discharge Peak. 690.0 (15C, <10 sec, > SOC 50%) |
| Cycle life to 80% of remaining capacity | Cycles | ≥5,000 (1C/1C) |

These cells have been individually characterized to verify the technical data provided by the manufacturer, using them as reference data, and assembled in a 13S1P pack (AGERAR pack, nominal voltage 48.1 V, min. voltage 35.1 V, max. voltage 54.6 V, energy capacity 2.21 kWh, max. power 26,6 kW). This pack has been tested according to different load profiles, representative of typical power consumption in the South of Spain and Portugal under different assumptions and operating conditions.

Regarding the prototypes of Al ion cells, they have been developed and supplied by the company Albufera Energy. Its main specifications are listed in Table 4.

Table 4 - Al ion cells specifications.

| | **Units** | **Value/Range** |
|---|---|---|
| Rated Capacity | mAh | 25 |
| Voltage | V | 1.7 (nominal); 1 (lower limit); 2.3 (upper limit) |

These cells have been tested according to the manufacturer specifications, with 25 mA (1C) max. charge current and 2.5 mA (C/10) max. discharge current, both cycles at $23 \pm 2$ ºC.

## 3. Results and Discussion

The LTO based Li ion pack has been tested at INTA for more than 500 hours, in successive cycles with different daily charging and load profiles, obtained from real data and simulations, for Spain and Portugal. To fit the testing campaigns with the scope of the project, four different profiles have been developed and programmed in the battery test bench: Spain summer, Spain winter, Portugal summer and Portugal winter. Each of these profiles has into account average daily power consumptions, as well as power generation, supposing the contribution of 1 kW PV field to the charge of the batteries.

The Figure 1 shows an example of a 65-hour test with the Spain summer profile, performed in a climatic chamber at 30 ºC and 65 % relative humidity.

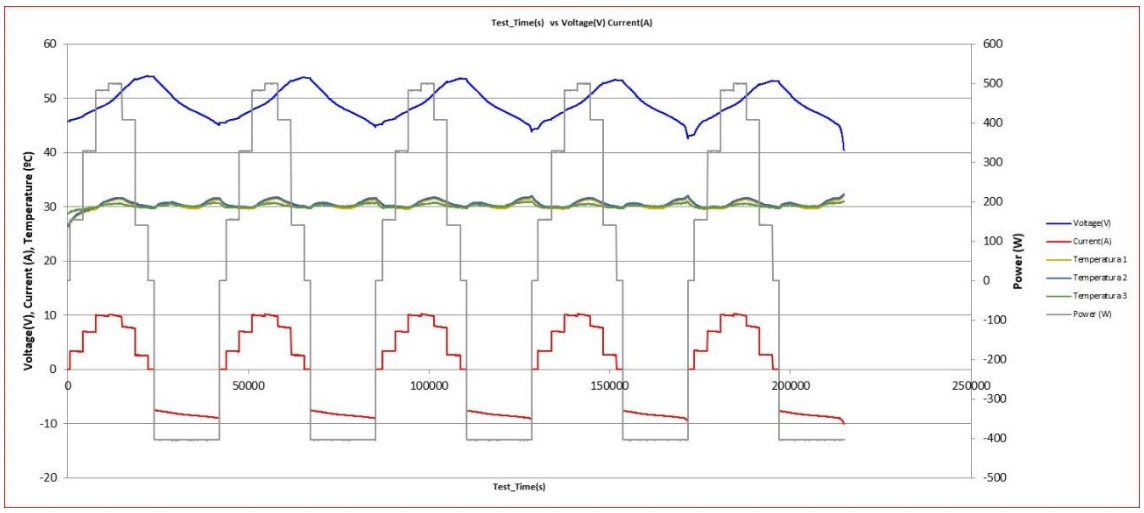


Figure 1 - Performance of AGERAR Li-ion pack in a 65 h test.

The energy charged and discharged is around 2 kWh, operating the pack in safe conditions (11 A max. discharge current, 11 A max. charge current), according to the manufacturer specifications, in order to ensure the maximum cycle life of the cells. After 400 hours of operation, the cells have been again individually characterised, without significant changes in their performance, in comparison with the initial reference tests. Regarding Al ion cells, they have been also successfully tested in more than 10 charge/discharge cycles, achieving the performance criteria defined for these tests.

The Vanadium Redox Flow Battery (redT) has been tested in 6 consecutive full charge-discharge cycles with a total duration of 600h, as shown in the Figure 2.

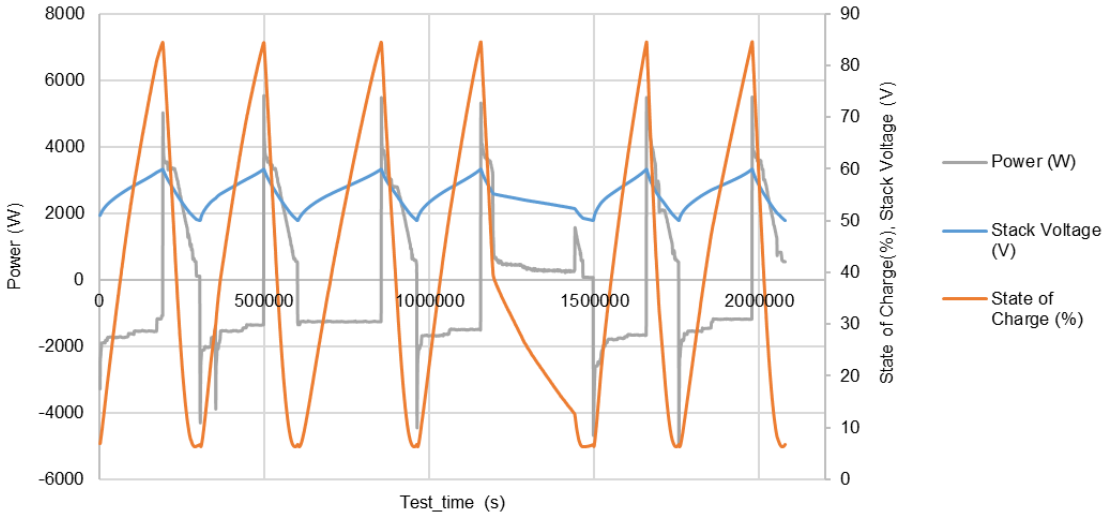


Figure 2 - Performance of the VRFB during the characterisation test.

In order to accomplish the current energy performance of the VRFB, average values from the previous analysis were calculated. The most relevant parameters are summarized in Table 5, shown below.

Table 5 - VRFB performance results under the operated conditions.

| | **Units** | **Value/Range** |
|---|---|---|
| Total Capacity (Charge Capacity) | kWh | 86.3 ± 2.30 |
| Max. Useful Capacity (Discharge Capacity) | kWh | 66.5 ± 4.26 |
| Energy Density (per unity of mass) | Wh/Kg | 18.5 ± 4.26 |
| Energy Density (per unity of volume) | Wh/L | 17.5 ± 4.26 |
| Fastest/Slowest Charge | | 51h41min. / 70h10min. |
| Fastest/Slowest Discharge | | 26h54min. / 109h7min. |
| Charge and Discharge Efficiency (complete cycles) | % | 77.1 ± 3.36 |
| Max. Charge and Discharge Power | kW | 7.20 |
| Response Time | | Seconds (s) |
| Cell voltage in the operating range | V | 1.25-1.51 |
| Typical discharge time | | Hours (h) |

The domestic scale lithium-ion battery of UÉvora was supplied by LG and has been rehearsed according to a different test plan. The charges and discharges correspond to a period of 27 complete cycles, at constant power rates (from minimum power up to the maximum limit of 3.3kW), using the range from 20% to 90% of state of charge. Each power setting was repeated 4 times, obtaining this way, a greater precision and accuracy of the results. Figure 3 shows an example compilation of the obtained data in the set, as well as the correspondent standard deviation.

The current energy performance of the Li-ion battery gathered throughout the performed tests is presented in Table 6.

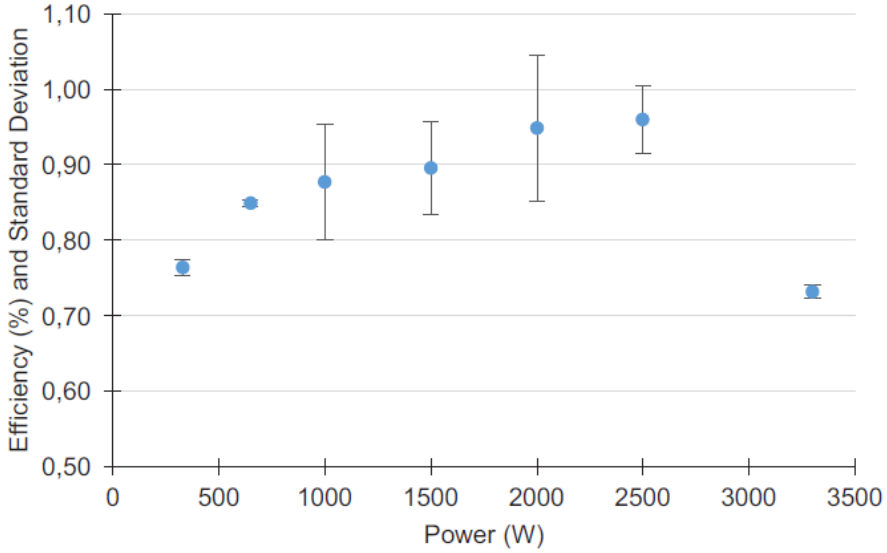


Figure 3 - Li-ion battery DC charge-discharge efficiency and corresponding standard deviation value.

Table 6 - Li-ion battery performance results under the operated conditions.

| | **Units** | **Value/Range** |
|---|---|---|
| Total Capacity (Charge Capacity) | kWh | 6.52 ± 7.47 |
| Max. Useful Capacity (Discharge Capacity) | kWh | 5.34 ± 2.39 |
| Energy Density (per unity of mass) | Wh/Kg | 73.5 ± 9.00 |
| Energy Density (per unity of volume) | Wh/L | 103 ± 20.9 |
| Fastest/Slowest Charge | | 2h25min / 10h09min |
| Fastest/Slowest Discharge | | 1h36min / 11h13min |
| Charge and Discharge Efficiency (complete cycles) | % | 86.1 ± 14.9 |
| Max. Charge and Discharge Power | kW | 3.30 |

## 4. Conclusions

Preliminary conclusions demonstrate the technical feasibility of LTO based Li ion and VRF batteries for the commercial and residential applications considered in the AGERAR project. Nevertheless, in addition to the suitability of the batteries, there are other critical components to take into account in the design, development and installation of adequate battery energy storage systems for these applications, in particular the battery monitoring and management system (with cell balancing capabilities) and the power conditioning system.

The measured technical parameters of characterisation proved to be non-negligible in the development of these technologies and will allow the development of improved strategies for energy management with optimisation of the systems' performance, benefiting the end user and the overall economic results of these energy storage solutions.

VRF and Li-Ion batteries performed according to the manufacturers' specifications, while the VRFB even surpassed some of the values announced in its specifications sheet.

Regarding Al ion batteries, the technology is very promising, mainly regarding cost and environmental issues, but it is currently at TRL 3-4, and an important effort is still necessary to implement it in commercial and residential applications.

## Acknowledgements

The project AGERAR (Ref. 0076_AGERAR_6_E) is co-financed by the European Regional Development Fund (ERDF), within the INTERREG VA Spain-Portugal cooperation programme (POCTEP).

## References

[1] B. Lasseter, "Microgrids [distributed power generation]," in *2001 IEEE Power Engineering Society Winter Meeting, PES 2001 - Conference Proceedings*, 2001, vol. 1, pp. 146–149.

[2] D. E. Olivares *et al.*, "Trends in microgrid control," *IEEE Trans. Smart Grid*, vol. 5, no. 4, pp. 1905–1919, 2014.

[3] "Energy storage." [Online]. Available: https://energy.ec.europa.eu/topics/research-technology-and-innovation/energy-storage_en. [Accessed: 08-Mar-2022].

## 3.3.2. 2nd Life Lithium-ion batteries - operation, testing and outcomes

- Part of this work was submitted in *8th World Conference on Photovoltaic Energy Conversion* (WCPEC-8), p. 1496 – 1503, 2022, ISBN: 3-936338-86-8, DOI: 10.4229/WCPEC-82022-5CO.10.4, and an oral presentation was given.

### 1. Introduction

This subchapter presents the work developed with the second-life lithium-ion battery (SLIB) prototype. The work has been ongoing under the scope of the POCITYF project (GA 864400) [1], and preliminary results were submitted to a conference proceeding for publication.

The SLIB is integrated into the microgrid of the University of Évora and was subjected to performance testing at its pack level, intending to obtain a complete performance characterisation of the product. The testing obeyed a specifically designed protocol in order to operate the batteries at their general operating conditions, supported by the development of a dedicated LabVIEW programming as the software control. The control unit is a computer responsible for real-time communication with the inverter to acquire data. This set allows the SLIB to be evaluated regarding its technical evaluation, electrical performance, and suitability to several use-case scenarios. The results are analysed, and key performance indicators (KPIs) are calculated to characterise the product, such as energy capacity and efficiencies. The KPIs obtained are presented as relevant data for the state-of-the-art of second-life lithium-ion batteries, allowing further comparisons with other energy storage technologies and further modelling developments.

The initial characterisation tests determine the battery parameters within the defined state of charge (SOC) and voltage ranges, considering the guidelines of the manufacturer. In this way, it is possible to calculate the KPIs. The most relevant are the coulombic efficiency, useful energy capacity, maximum charge/discharge power, energy and power densities, charge/discharge power and energy efficiencies, and typical discharge time.

The second part of the tests pertains to use-case scenarios in an off-grid setup. The operational limits of the batteries are chosen to consider the security margins associated with the depth of discharge (DOD). In that sense, the batteries are fully charged and discharged at defined constant power limits (although those power levels obey a

particular power-SOC curve, further explained) to evaluate their response at different power (current) levels at the defined operating conditions. The tests are supported by DC and AC measurement devices (to execute, for example, current and voltage monitoring) and temperature sensors.

Additional testing with use-case scenarios provides technical key indicators regarding its performance in a real-operational environment under stress conditions enabling the further finetuning and validation of this product, reaching a higher TRL. Output test data enables further model development and validation or improved state of health estimation.

## 2. Framework

With future perspective growing estimation scenarios, the IEA states that the electric automotive industry is expected to increase from 2020 to 2030 with an average annual growth rate of nearly 30 % [2]. The graphical example of Figure 26 presents the global market forecast of the second-life lithium-ion battery, expected to represent 20 GWh in 2023 and 1552 GWh in 2032.

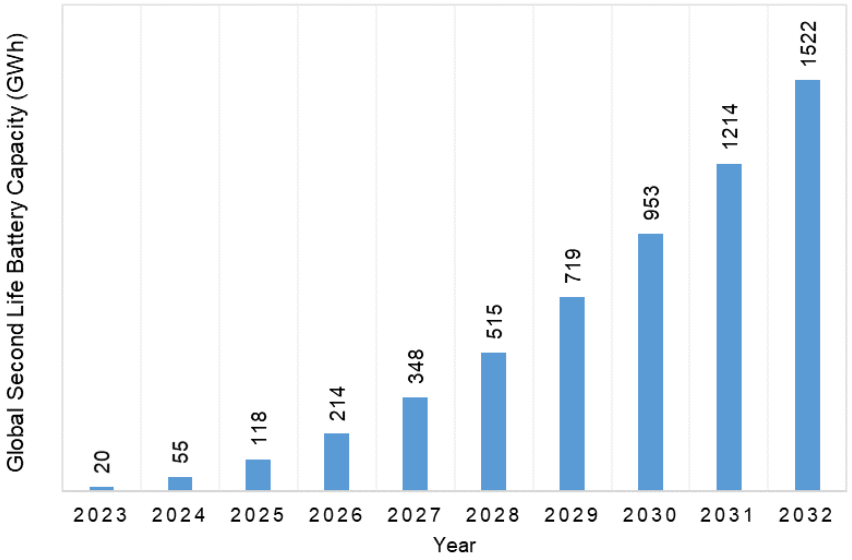


Figure 26. Expected global second-life battery capacity and electric vehicle stock. Adapted from [3].

The batteries that compose the EVs present an energy capacity degradation upon cycling. Their remaining energy capacity could serve lower intensive applications, like stationary ones, represented in Figure 27. The still-useful batteries can create significant value and ultimately increase the sustainability of the battery value chain. In that sense,

a secondary market arises for the second application use of the EV batteries before their end of life (EOL) (recyclability or landfill).

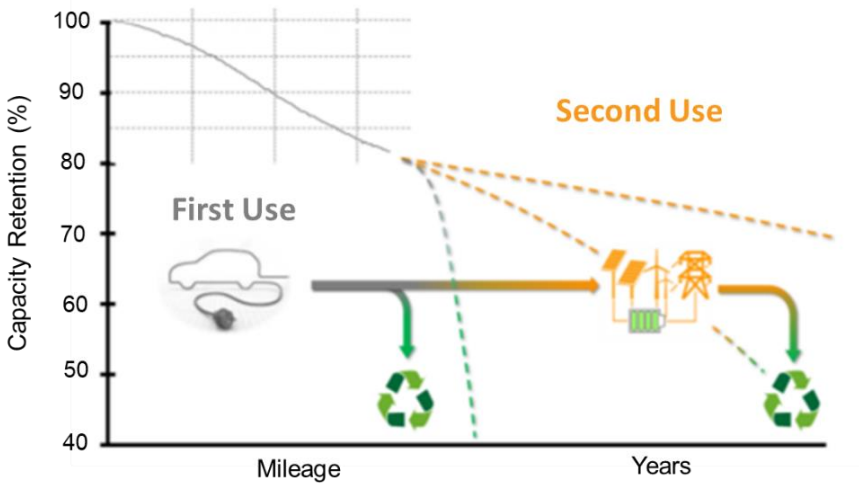


Figure 27. Energy capacity retention (%) during the lifecycle of the first application of an EV-lithium-ion battery and its potential second use. Adapted from [4].

The delay of the battery EOL translates into adding a step in the life cycle assessment (LCA). Different authors, [4] and [5], agree that using a SLIB combined with renewable energy sources provides environmental benefits, helping reduce the environmental footprint: avoid the manufacturing of first-life LIB and avoid the use of natural gas or coal-based power generation. In [5], the investigation also concludes that the environmental effects of SLIB implementation rely on their expected lifetime and ageing behaviour. Figure 28 presents the lifecycle of first and second-life LIBs.

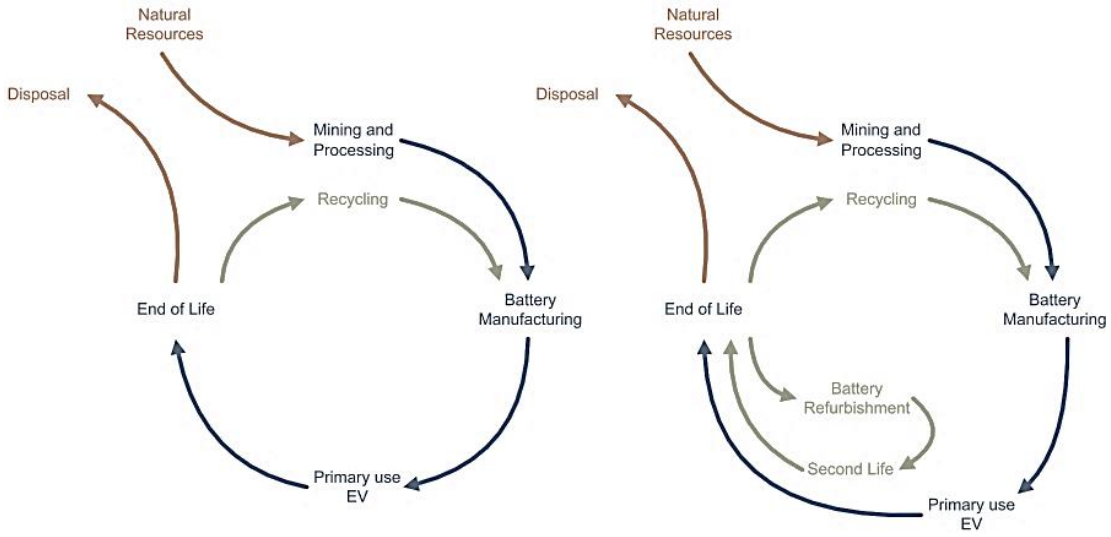


Figure 28. Lifecycle of an EV battery pack: first life (left) and second life (right) [5].

The need for cost-effective, affordable, and flexible solutions to compose the distributed energy storage conjuncture makes the SLIB a solution. SLIB can represent an opportunity to meet this demand and an option for residential and off-grid applications at possibly lower costs than the other commercial batteries. SLIBs can be applied to improve grid performance and be integrated with renewable energy or charge EVs. However, the SLIB application still needs to overcome several challenges to become technically and economically viable. This is due mainly to the uncertainty associated with their performance and degradation behaviour. Research has focused on understanding the early stages of degradation (commonly described as first-life lithium-ion batteries). Also, proper policies and incentives for business models must be developed [6].

A prototype of a SLIB has been built as part of other energy storage technologies at the University of Évora. The prototype from *betteries AMPS GmbH* [7] was connected to the Renewable Energies Chair microgrid through a commercial inverter. The specific SLIB presented a preliminary power and energy capacity of 2.0 kW/2.3 kWh, a voltage operating range of 45-64 V, and an approximate weight of 35 kg. With an advisable DOD of 80%, the expected lifetime is 7-10 years. The second-life lithium-ion battery state of health (SOH) is within 70 to 90 %, depending on the user, use, and road conditions (aspects related to its first-use application) [10]. It has a passive balancing system.

The case of the *betteries AMPS GmbH* solution aims to be applied to off-grid solar PV installations, with the possibility of applying it in certain residential test cases. In contrast to other technological approaches, *betteries AMPS GmbH* solution has a modular design: the modules can be stacked on each other, increasing the usable energy capacity output up to 5 kW/9.2 kWh (with the stacking of 4 modules).

## 3. Methodology

This work proposes the calculation of performance parameters of the *betteries AMPS GmbH* second-life lithium-ion prototype, a portable 48V battery. The *betteries AMPS GmbH* integrated four battery modules of SLIB the Renewable Energies Chair microgrid. Figure 29, below presented, schematises the individual integration of the technology into the existing microgrid.

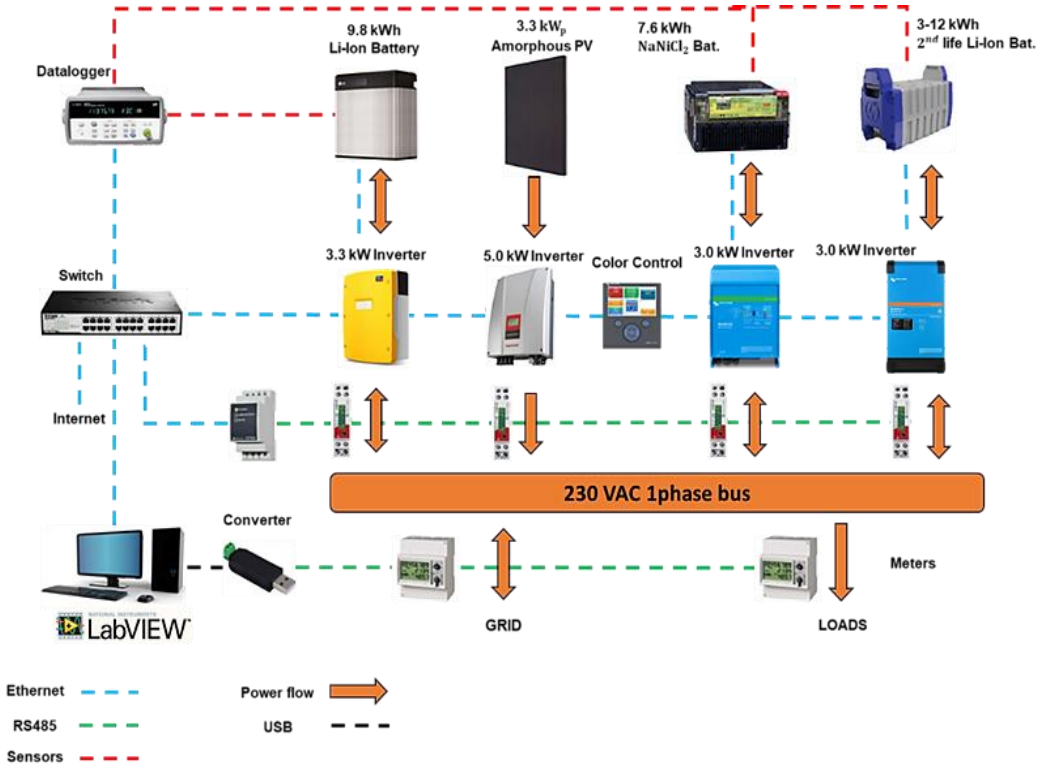


Figure 29. General scheme of the installed equipment and representation of the energy fluxes in the Renewable Energies Chair microgrid.

The University of Évora tested three battery modules (BMs) from the *betteries AMPS GmbH* first developed solution and one betterPack (BP) from the newest version of the product. The preliminary specifications given by the provider are gathered in Table 3 below.

Table 3. Reference conditions and main characteristics of one single module, available by the manufacturer *betteries AMPS GmbH*, where first and second versions of the product are differentiated [1].

| Variable | Units | BM-0015<br>BM-00018<br>BM-00022 | BP-0075<br>(betterPack - Single) |
|---|---|---|---|
| Electrical performance and Lifetime | | | |
| Nominal voltage (external) | V | 49 | 52.5 |
| Pack voltage range | V | 45 to 64 | 42 to 57.68 |
| Weight | Kg | 35 | 31 |
| Dimensions (height x length x width) | mm | 407 x 498 x 277 | 321 x 558 x 227 |
| Balancing | - | Active | Not specified |
| Cycle lifetime | cycles | 1500 | 1500 |
| Calendric lifetime | years | 7 | 7 |

| Energy and Power | | | |
|---|---|---|---|
| Nominal energy capacity | kWh | 3.0 | 2.3 |
| Useful energy capacity | kWh | 2.4 (80% DoD) | 1.8 (80% DoD) |
| Nominal charge power | kW | 1.4 | 1.4 |
| Nominal discharge power | kW | 2.0 | 2.0 |
| Maximum power output | kW | 3.0 | 4.0 |
| Environmental conditions | | | |
| Cooling | - | Natural convection | Natural convection |
| Venting | - | Pressure equalising & overpressure | Pressure equalisation & overpressure relief |
| Ambient operating temperature | ºC | -10 to +40 | -10 to +40 |
| Non-operating temperature (storage) | ºC | -20 to +70 | -20 to +50 |
| Ingres protection | - | IP67 | IP67 |

## 3.1. Test conditions

### 3.1.1. Rates of testing

C-rates are reasonable limits to characterise lithium-ion batteries, justified to normalise the battery energy capacity (distinct characteristic among different batteries). Lithium-ion batteries are generally tested with constant current over the voltage range (and state of charge range), resulting in a discharge and charge rate. Another term used generally in the battery field is the E-rate, which is an equivalent term compared to C-rate. The E-rate expresses the charge or discharge power (in watts).

In the absence of a current controller device that effectively sustains the current at a constant value, the controller had to be developed through the control of the AC power setpoint (depending on the connected load), which is the controllable variable on the inverter connected to the battery. This fact conducts to relatively different outputs of these tests to the ones generally achieved by the manufacturers. Given the absence of strict standards, testing with the E-rates is considered valued. Moreover, the testing on these conditions reflects the operating conditions of the batteries in a real-case scenario.

The charging and discharging output data was gathered considering the most similar AC and DC average power output and the most similar average current output. Those values of AC constant power are slightly different in the charge and the discharge operating states, although this approach seemed the more consistent in comparing charged and discharged power/ energy figures. An example of this approach is presented in Table 4. The grey area represents the data considered to calculate efficiencies given the similarity of average current and power levels overcharges and discharges operating states.

Table 4. Example of the data gathering for treatment, considering the E-rates of charge and discharge obtained outputs.

| State | AC Constant Power | AC Average Power | DC Average Power | Average current (A) | Duration (hours) |
|---|---|---|---|---|---|
| Charge | 220 | 174.05 | -177.59 | -3.08 | 12.40 |
| Discharge | 130 | -173.45 | -173.42 | 3.01 | 11.78 |
| Charge | 220 | 174.55 | 174.55 | -3.18 | 12.45 |
| Discharge | 130 | -172.73 | -172.72 | 3.00 | 11.79 |
| | | | | | |
| Charge | 390 | 295.96 | 296.02 | -5.33 | 7.28 |
| Discharge | 300 | -341.27 | -341.31 | 6.06 | 6.26 |
| Charge | 390 | 293.93 | 293.93 | -5.30 | 7.34 |
| Discharge | 300 | -343.01 | -343.07 | 6.09 | 6.31 |
| Charge | 390 | 295.96 | 296.02 | -5.33 | 7.28 |
| Discharge | 300 | -344.11 | -344.12 | 6.08 | 6.30 |
| | | | | | |
| Charge | 780 | 516.46 | 516.42 | -9.17 | 4.23 |
| Discharge | 600 | -568.05 | -568.19 | 10.25 | 3.71 |
| Charge | 950 | 564.82 | 564.90 | -9.95 | 3.90 |
| Discharge | 600 | -585.03 | -585.09 | 10.60 | 3.50 |
| | | | | | |
| Charge | 1260 | 568.39 | 568.30 | -10.06 | 3.17 |
| Discharge | 740 | -644.21 | -644.27 | 11.68 | 3.27 |
| Charge | 1880 | 503.80 | 503.74 | -8.87 | 4.42 |
| Discharge | 740 | -648.10 | -648.02 | 11.73 | 3.25 |
| | | | | | |
| Charge | 1880 | 710.82 | 710.81 | -12.45 | 3.13 |
| Charge | 1880 | 490.50 | 490.62 | -8.63 | 4.51 |
| Charge | 780 | 412.15 | 412.15 | -7.35 | 5.28 |
| Charge | 950 | 454.85 | 454.87 | -8.06 | 4.80 |
| Charge | 1260 | 474.67 | 474.67 | -8.41 | 4.60 |
| | | | | | |
| Discharge | 1000 | -770.50 | -770.51 | 14.01 | 2.73 |
| Discharge | 1000 | -753.78 | -754.05 | 13.69 | 2.80 |
| Discharge | 1300 | -827.74 | -827.83 | 15.12 | 2.52 |
| Discharge | 1300 | -843.65 | -843.53 | 15.45 | 2.47 |
| Discharge | 1300 | -849.26 | -849.56 | 15.55 | 2.46 |

### 3.1.2. Levels of charge and discharge

The performance and lifetime of lithium-ion batteries are affected by charge and discharge rates and ambient temperature, which is the motive for the power setpoints command of the second-life lithium-ion battery being carefully chosen. Figure 30 (a) and (b) present the charge and discharge limits for current, respectively, and Table 5 the maximum current limits, given the number of stacked battery modules.

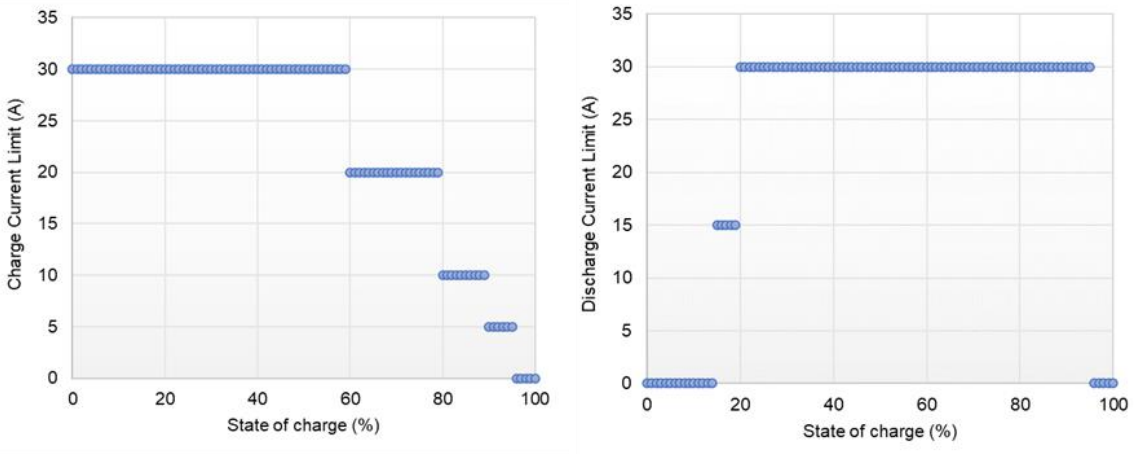


(a) (b)

Figure 30. Charge current limits (a) and discharge current limits (b) according to the state of charge of the battery.

Table 5. Maximum current limitation, in accordance with the stacked number of battery modules associated with the same inverter.

| Number of battery modules | Maximum acceptable current (A) |
|---|---|
| 1 | 30.0 |
| 2 | 44.3 |
| 3 | 53.6 |
| 4 | 63.0 |

### 3.1.3. Related test conditions

The reference conditions are the storage typical operating conditions in which the characterisation tests occur. The inverter connected to the battery limits the maximum charge and discharge power limits, which in this case, is upper limited to 3.0 kW. The characterisation tests occur at a temperature range from 15 ºC to 25 ºC. In the case of the use-cases tests, the temperature is aimed to obey the provider's advised temperature range (-10 ºC to +40 ºC).

For the older batteries' versions, the operating ranges of charge-discharge curves depletions and full charge states were based on the state of charge ranges: the BM-0015 and BM-0022 state of charge operation range was from 15 % to 94 % (DOD of 80 %), and the BM-0018 charge-discharge tests occurred in the SOC range of 20 % to 90 % (DOD of 70 %), in agreement with the battery provider. In the case of BP-0075, the

tests occurred between the 51.1-57.68 V, representing this newer version pack voltage range (depletion and full-charge states). The difference in operation ranges among the different batteries is justified by the different SOC calculating methods achieved by the battery BMU and the battery BMS, which do not match the newer version (BP-0075).

## 3.2. LabVIEW programming control

The tests entail the development of a programming control whose objective is to communicate with the inverter, which communicates with the battery. The communication is achieved through the Modbus TCP/IP protocol, and the programming was fully developed in the LabVIEW environment. The timeframe of the control application was defined as being three seconds, including the sending of requests, executing intermediate measurements, receiving the communication response from the battery and the inverter, and registering the acquired data (both from the inverter and the external monitoring devices, such as the precision multimeter).

The desired E-rates are either automatically or manually defined in real-time, adapted to the relation of power-SOC, given the previously presented limits in Table 5 and Figure 30. An example of the final developed software interface to achieve the characterisation is illustrated in Figure 31 below.

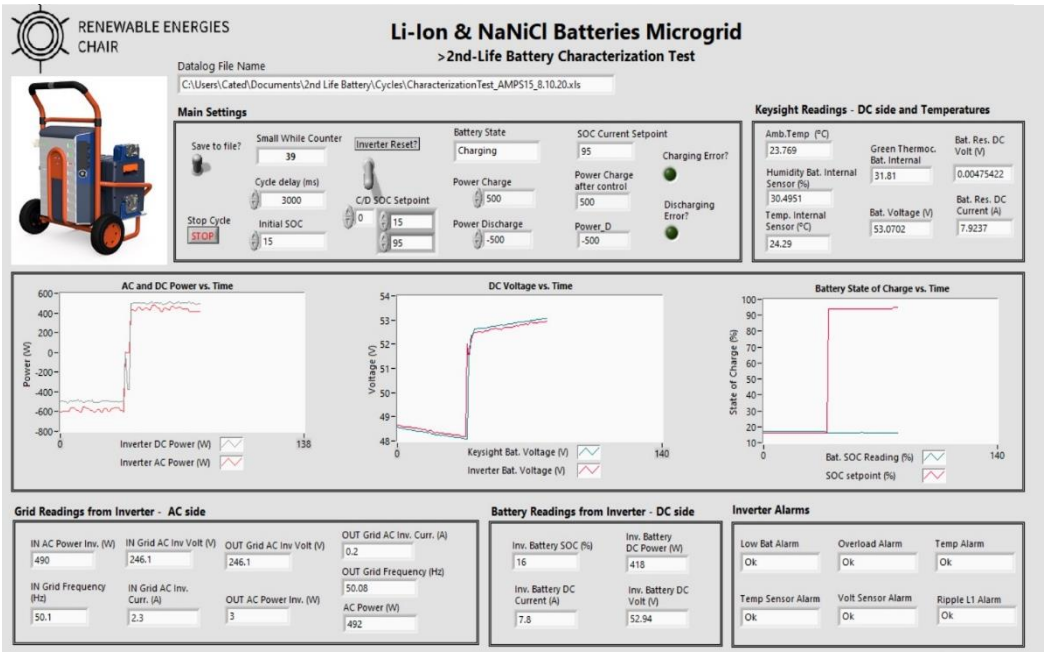


Figure 31. LabVIEW interface of the characterisation tests of the second-life lithium-ion batteries.

### 3.3. Battery performance efficiencies' calculations

A battery-suited evaluation can be achieved by determining performance indicators related to investment and energetic perspectives. As the most relevant performance indicators, the analysis relies on the determination of the following indicators: voltage efficiency, coulombic efficiency, energy efficiency and power efficiency, charge and discharge energy capacities (Wh), energy densities (Wh/kg and Wh/L), power densities (W/kg) and fastest/slowest charge and discharge.

The battery performance is characterised by executing tests from the defined range of the state of charge or voltage operation limits (from depletion to full charge). The operating limits of the battery to perform these tests are chosen regarding the security margins associated with the DOD and degradation, considering the SLIB characteristics. Next, the efficiency evaluation KPIs are detailed – Eq. (1)-(4):

- ✓ Voltage efficiency is the ratio of cell voltage during discharge to that during charge [8]:

$$\theta_v = \frac{U_{discharge}}{U_{charge}} \quad (1)$$

- ✓ Coulombic (charge) efficiency is the ratio of electrical charge capacity during discharge to that during charge:

$$\theta_q = \frac{q_{discharge}}{q_{charge}} \quad (2)$$

- ✓ Energy efficiency is the ratio of electrical energy during discharge to that during charge:

$$\theta_E = \frac{U_{discharge} \times q_{discharge}}{U_{charge} \times q_{charge}} \quad (3)$$

- ✓ Power efficiency is the ratio of electrical power during discharge to that during charge:

$$\theta_W = \frac{I \times U_{discharge}}{I \times U_{charge}} \quad (4)$$

The other calculated KPIs are explained in the following. The total energy capacity is the sum of the energy used to charge the battery. The useful energy capacity is the sum of the energy drawn from the battery (discharged from the battery). The energy densities are only calculated for discharged energy. They result from averaging the obtained discharged energy from the battery at the different power levels, rated by the weight or

volume of the battery. For the case of the power densities, one could use the averaging of the three maximum discharged power levels (rated at 1300 W AC), rated by the weight and volume of the battery. The slowest and fastest charge and discharge were calculated through the minimum and maximum values, respectively, of the sum of the period whereby the test occurred.

The charge-discharge repetition at each power level allows the averaging of the results, helping reduce the error of the result. After that, the KPIs were calculated for each full charge-discharge of the battery.

### 3.4. Inverter efficiency

In order to understand the inverter input/output influence on the battery performance output, a dedicated inverter efficiency test occurred. The commercial inverter connected to the SLIB is from the Victron brand, model MultiPlus-II 48/3000/32. In order to reduce the load power consumption of the inverter, the manufacturer defined improvements in this model compared to previous versions [11]. Figure 32 presents the inverter efficiency curve and dissipation influence regarding output power, made available by the manufacturer.

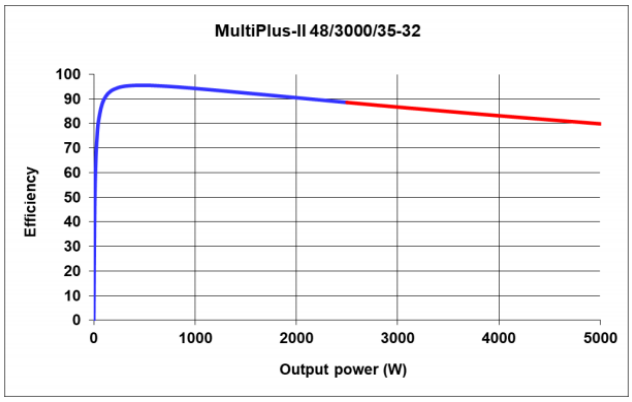


| Output power (W) | Dissipation (W) | Efficiency (%) |
|---|---|---|
| 0 | 11 | 0 |
| 10 | 11 | 47,6 |
| 20 | 11 | 64,5 |
| 30 | 11 | 73,1 |
| 50 | 11 | 81,8 |
| 100 | 12 | 89,7 |
| 200 | 13 | 93,9 |
| 400 | 19 | 95,5 |
| 800 | 43 | 94,9 |
| 1600 | 139 | 92,0 |
| 2500 | 324 | 88,5 |
| 3000 | 461 | 86,7 |
| 4000 | 811 | 83,1 |
| 5000 | 1261 | 79,9 |

Figure 32. Inverter Multi-Plus-II curve efficiency on the left, and dissipation and efficiency at each power level, on the right [11].

The inverter AC-DC (battery operation in the state of charge) and DC-AC (battery operation in the state of discharge) efficiencies are calculated, for charge and discharge states, respectively:

- ✓ DC-AC and AC-DC conversion efficiency – Considers energy conversion losses from DC to AC energy and from AC to DC energy, respectively, are presented in Eqs. (5) and (6).

$$\eta_{conv(DC-AC)} = \frac{E_{AC}}{E_{DC}} \quad (5)$$

$$\eta_{conv(AC-DC)} = \frac{E_{DC}}{E_{AC}} \quad (6)$$

The inverters operate according to an efficiency profile related to the power level set. In the solar photovoltaic field, the inverter efficiency can be generally characterised by the EU efficiency and CEC (California Energy Commission) efficiency, with equations composing weight factors. CEC efficiency is generally used in a location with higher annual irradiation levels. Since the inverter coupled with the SLIB is not connected to a solar PV system, the inverter efficiency used in this work is calculated through Eq. (5), considering different power levels. In this context, a LabVIEW program was developed to operate the inverter at specific power levels (from 150 to 3000 W) to calculate the efficiency profile and evaluate its performance output. The program was chosen to operate at 15-minute intervals for each power level, regarding its nominal power. The LabVIEW-developed interface is presented in Figure 33.

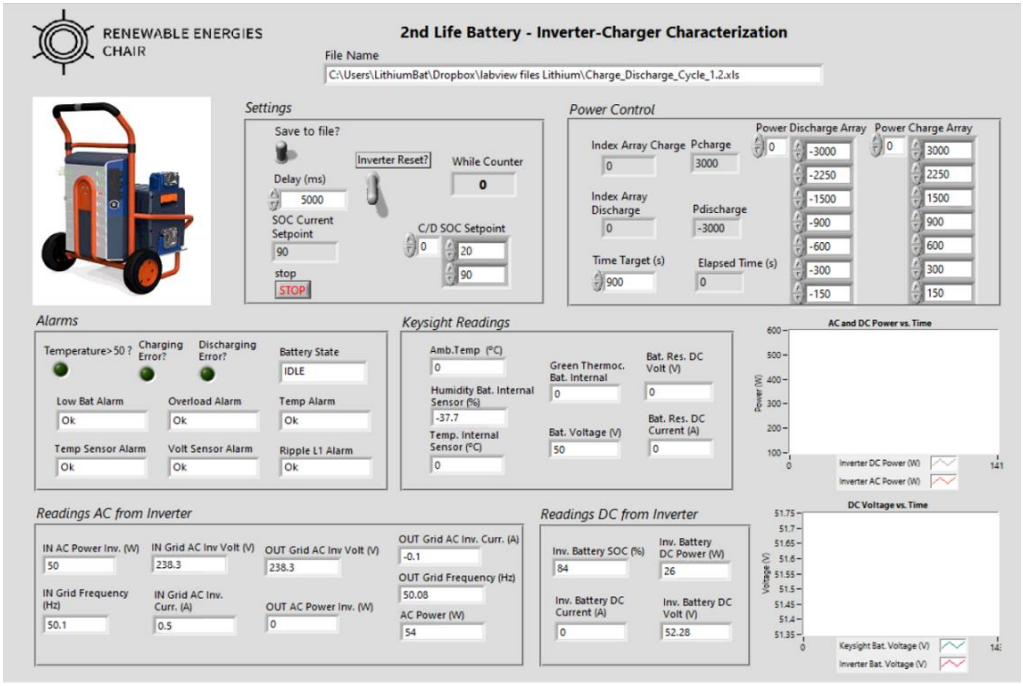


Figure 33. LabVIEW programming interface Victron Multiplus II for its efficiency tests.

### 3.5. Use-cases testing

This work proposes use-case scenario testing to provide technical performance output in a real-operational environment under stress conditions. To this end, a portable data acquisition unit was constructed to include the data acquisition station, measurement devices, DC protections and a UPS-type station, so the tests are done in isolated locations.

Figure 34 presents the use-cases testing setup, including the portable data acquisition unit, the used sensors (precision resistor, thermocouple, and humidity sensor), the AC power analyser, the protections, the inverter and the battery.

The use-cases testing includes the equipment's use in general conditions, including an electric chainsaw, power drill and grinding wheel with the function of "grinding" and "cut". The tests evaluate the application suitability of the battery unit to satisfy the use of this equipment and check possible optimisation paths.

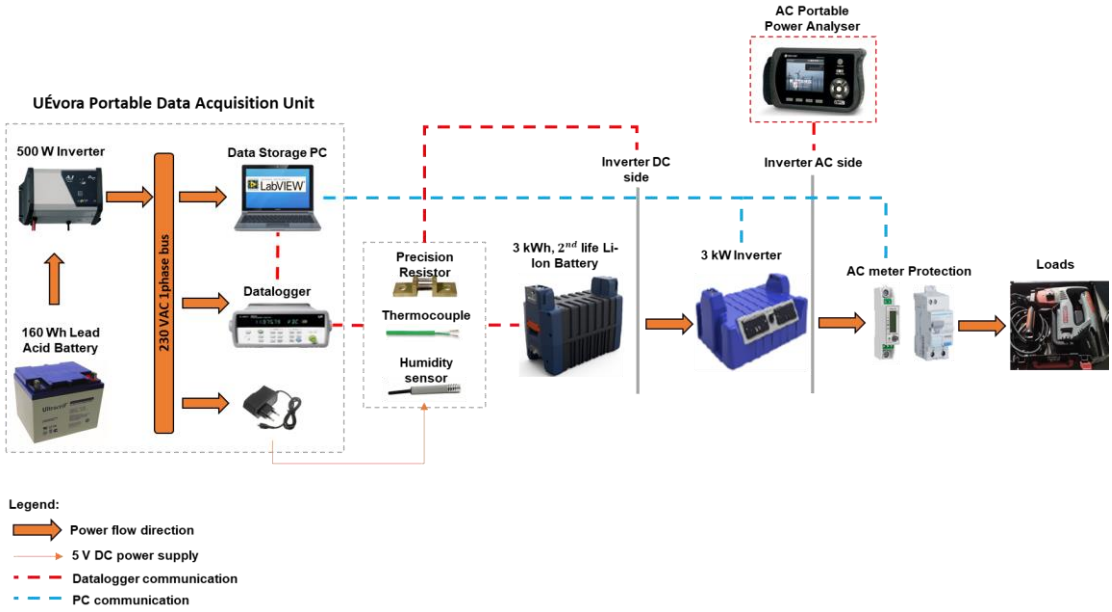


Figure 34. General scheme of the microgrid connected equipment to achieve the use-cases testing, respective energy fluxes' representation.

## 4. Results

### 4.1. Batteries' KPIs

Each E-rate was averaged for two or three repeated tests to diminish the testing-related errors.

Table 6 presents the four batteries' efficiencies, calculated with the help of Equations (1) to (4). The remaining KPIs were calculated and are presented in Table 7.

Table 6. Efficiency results of the BM-0022, BM-0018, BM-0015 and BP-0075.

| | | Coulombic efficiency | Energy efficiency | Power efficiency | Voltage efficiency |
|---|---|---|---|---|---|
| **BP-0075** | Average efficiency | 0.925 | 0.830 | 0.766 | 0.864 |
| | Standard deviation | 0.040 | 0.124 | 0.283 | 0.078 |
| | Variance | 0.002 | 0.015 | 0.080 | 0.006 |
| **BM-0015** | Average efficiency | 0.954 | 0.802 | 0.822 | 0.746 |
| | Standard deviation | 0.027 | 0.086 | 0.114 | 0.077 |
| | Variance | 0.001 | 0.007 | 0.013 | 0.006 |
| **BM-0018** | Average efficiency | 0.948 | 0.852 | 0.938 | 0.898 |
| | Standard deviation | 0.056 | 0.107 | 0.177 | 0.097 |
| | Variance | 0.003 | 0.011 | 0.031 | 0.009 |
| **BM-0022** | Average efficiency | 0.903 | 0.599 | 0.702 | 0.817 |
| | Standard deviation | 0.054 | 0.088 | 0.084 | 0.047 |
| | Variance | 0.003 | 0.008 | 0.007 | 0.002 |

Table 7. Energy performance main results of the SLIB.

| BM / Characteristic | 0015 (15-95 % SOC) | 0018 (20-90 % SOC) | 0022 (15-95 % SOC) | 0075 (~50-57 V) |
|---|---|---|---|---|
| Total energy capacity (charge capacity) (kWh) | 2.30 ± 0.337 | 2.18 ± 0.559 | 2.40 ± 0.600 | 2.15 ± 0.106 |
| Useful energy capacity (discharge capacity) (kWh) | 2.14 ± 0.321 | 1.92 ± 0.209 | 1.84 ± 0.715 | 2.05 ± 0.601 |
| Energy density (discharge) (Wh/kg) | 54.9 ± 8.23 | 49.3 ± 14.3 | 52.6 ± 17.1 | 66.0 ± 10.3 |
| Energy density (discharge) (Wh/L) | 38.3 ± 5.73 | 34.3 ± 9.99 | 32.9 ± 10.7 | 49.9 ± 7.76 |
| Power density (discharge) (W/L) | 20.7 ± 2.57 | 22.8 ± 1.01 | 20.6 ± 0.741 | 20.4 ± 0.203 |
| Power density (discharge) (W/kg) | 33.1 ± 4.11 | 36.5 ± 1.62 | 33.0 ± 1.18 | 27.1 ± 0.268 |
| Slowest/ fastest charge (h) | 3.0 / 13.7 | 1.9 / 10.7 | 3.05 / 12.7 | 3.13 / 12.5 |
| Slowest/ fastest discharge (h) | 1.7 / 14.3 | 1.5/ 12.6 | 1.65 / 10.9 | 2.46 / 11.8 |

Where ± indicates the percentual error.

A more extensive set of battery modules tested would improve the average results found, probably minimising the STD values of the results.

Figure 35 and Figure 36 presents an example of the voltage and current-energy capacity curve in the charging operating state, while Figure 37 and Figure 38 show an example of the voltage and current-energy capacity in the discharging state.

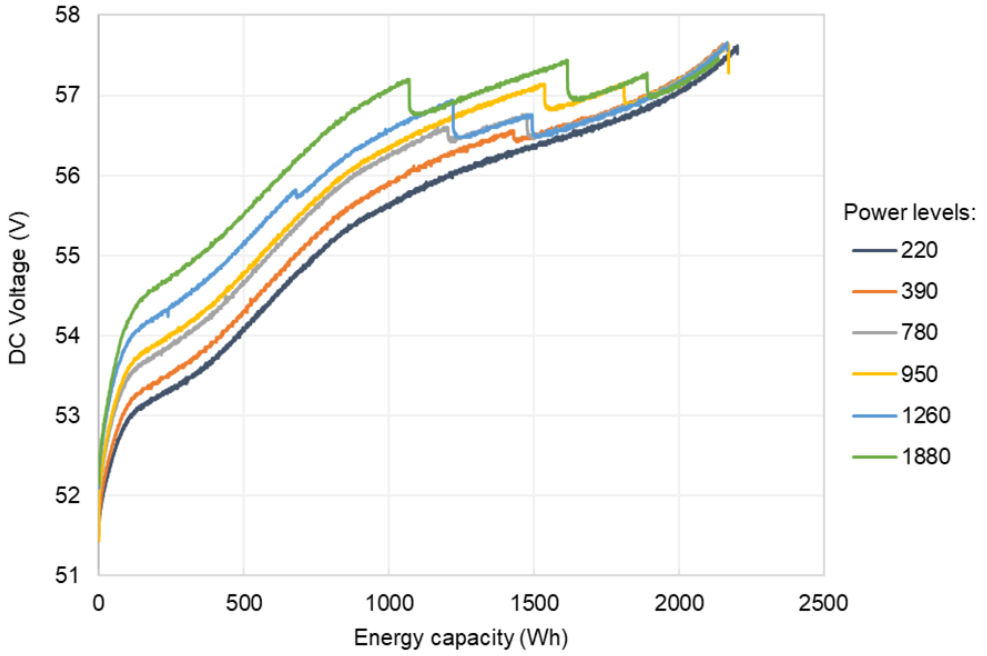


Figure 35. The voltage-energy capacity exemplary curve of BP-0075 in charging.

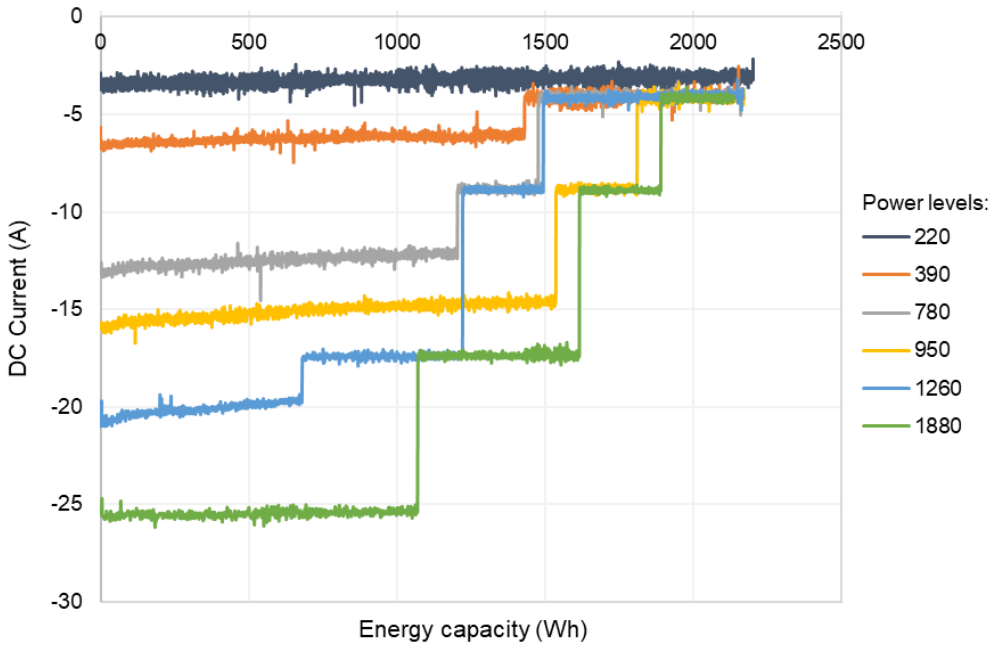


Figure 36. The current-energy capacity exemplary curve of BP-0075 in charging.

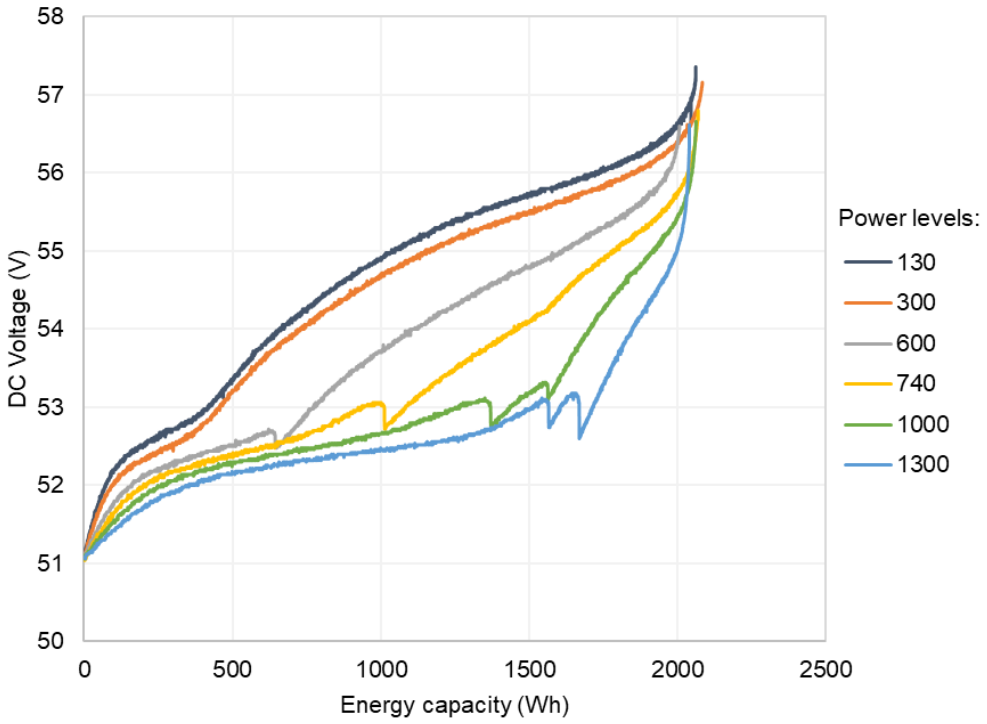


Figure 37. The voltage-energy capacity exemplary curve of BP-0075 in discharging.

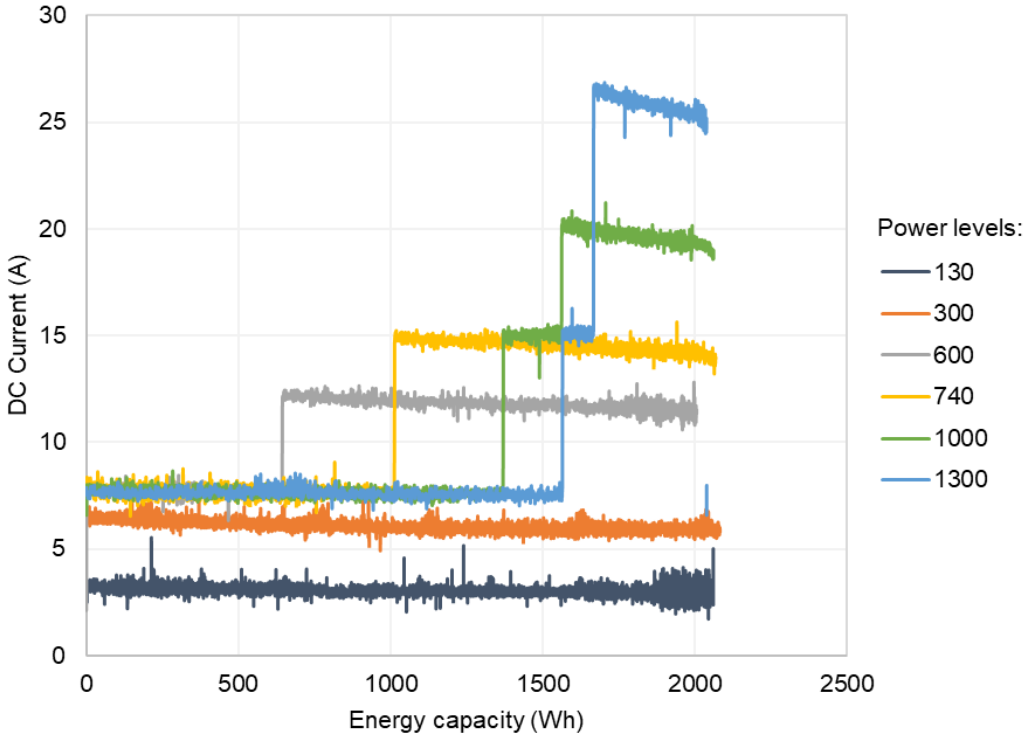


Figure 38. The current-energy capacity exemplary curve of BP-0075 in discharging.

### 4.2. Inverter efficiencies results

The LabVIEW developed control allowed to plot the charge and discharge efficiency curves, Figure 39 and Figure 40, respectively.

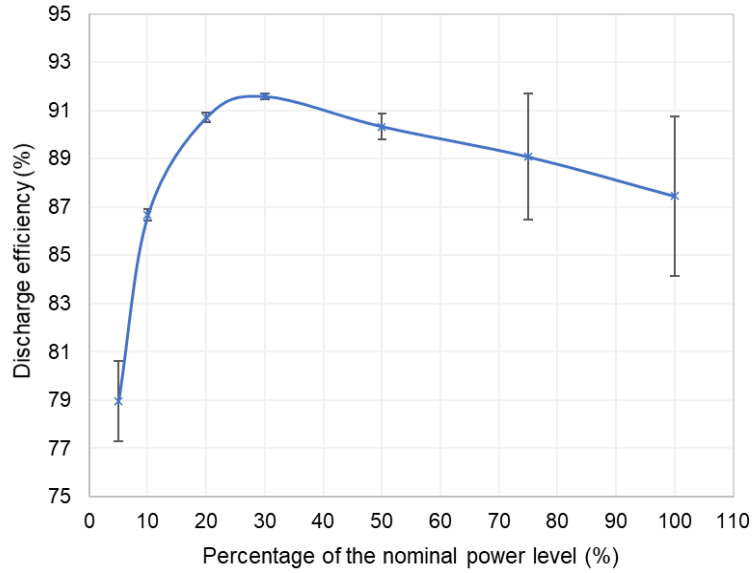


Figure 39. Inverter discharge efficiency as a function of the power level.

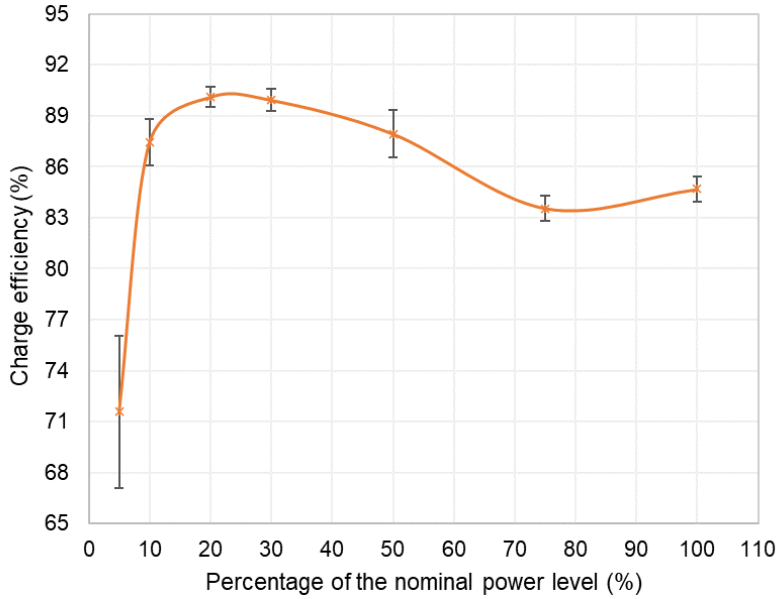


Figure 40. Inverter charge efficiency as a function of the power level.

Figure 39 and Figure 40 output results can be related to the inverter available manufacturer data of Figure 32 [9]. There, one can observe that for the 400-5000W power levels range, a corresponding increase in energy dissipation is observed (from the low to the highest power level), decreasing the efficiency values.

Additional tests and higher granular power settings would lead to a curve with less associated error.

### 4.3. Use-cases Results – BMs versions

This section presents a resume of the performance tests realised with three power tools – a chainsaw, a driller, and a grinding wheel. The data presented have a temporal resolution of 3 seconds.

#### 4.3.2. Electric Chainsaw

The batteries BM-00015, BM-00018 and BM-00020 were used to test an electric chainsaw from Black and Decker. The chainsaw operates at a 230 VAC voltage, and the manufacturer defines a maximum rated current of 6 A. Figure 41 (a) presents a representative image of the chainsaw, and (b) presents the field-testing setup. The electric chainsaw test was used under general user operating conditions, with the data acquisition of temperatures, currents, voltages, grid frequency, and battery state of charge. These data are presented in Figure 42.


(a)

(b)

Figure 41. a) Electric chainsaw used as a representative load, and b) chainsaw exterior use-case test.

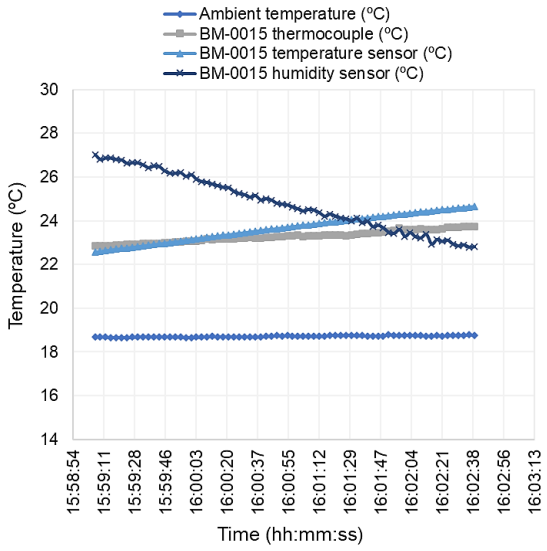
Ambient temperature (ºC)
BM-0015 thermocouple (ºC)
BM-0015 temperature sensor (ºC)
BM-0015 humidity sensor (ºC)
Temperature (ºC)
Time (hh:mm:ss)

(a)

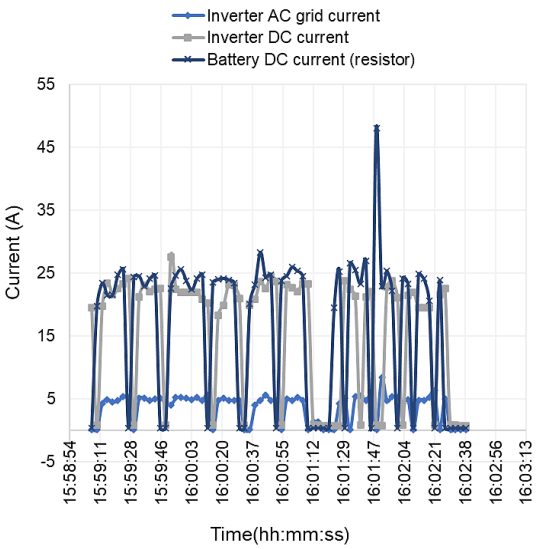
Inverter AC grid current
Inverter DC current
Battery DC current (resistor)
Current (A)
Time(hh:mm:ss)

(b)

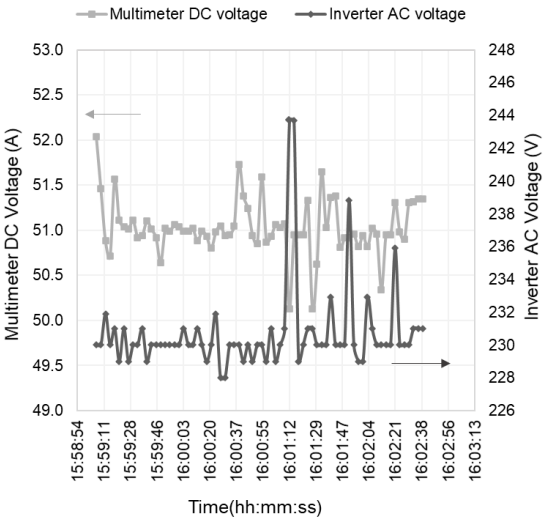
Multimeter DC voltage
Inverter AC voltage
Multimeter DC Voltage (A)
Inverter AC Voltage (V)
Time(hh:mm:ss)

(c)

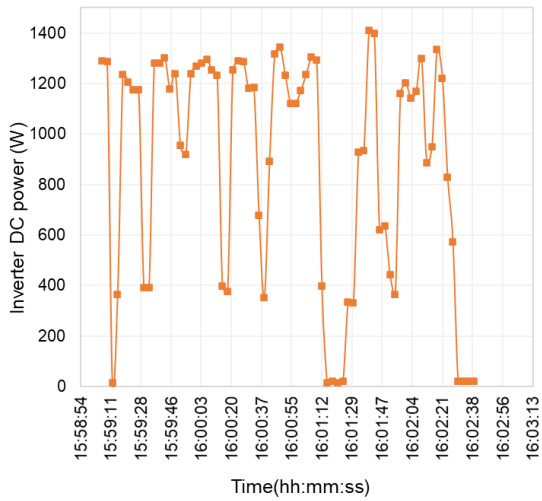
Inverter DC power (W)
Time(hh:mm:ss)

(d)

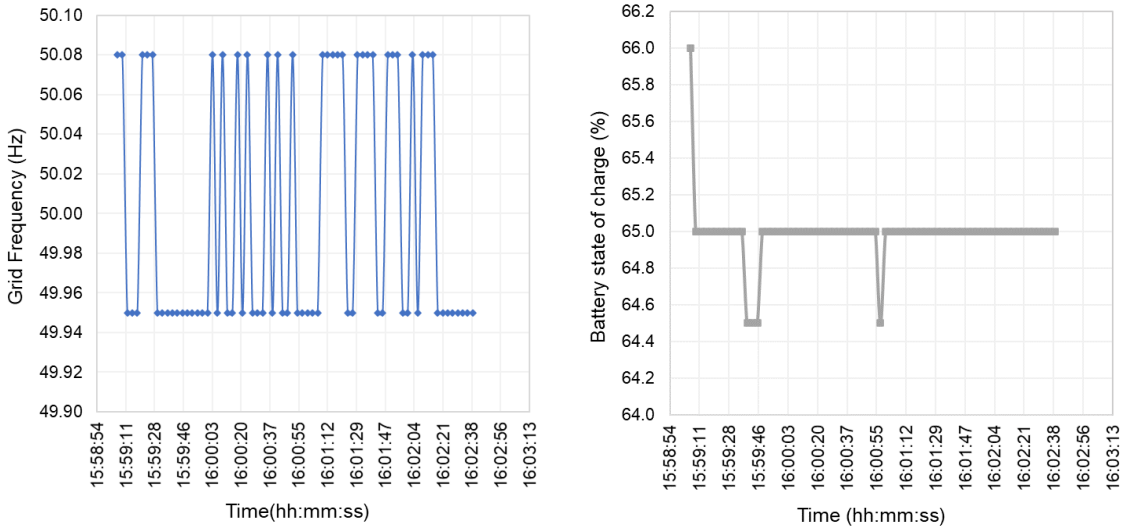


(e) (f)

Figure 42. Electric chainsaw use-case test output: (a) temperatures acquired by the precision multimeter (ºC); (b) DC and AC currents read through the inverter and the precision multimeter device; (c) voltages read by the precision multimeter device (DC) and inverter (AC); (d) DC power measurement read through the inverter; (e) grid frequency read through the inverter (Hz); (f) state of charge obtained through the inverter (%).

### 4.3.2. Power Drill

The batteries BM-00015 and BM-00018 were used to test a Kress brand power drill, model SDS-Plus. The equipment operates at a 230 VAC voltage, and the manufacturer defines a maximum rated power of 800 W. The test used the power drill under general user operating conditions, with the same data acquisition as the previously presented tool. Figure 43 is a representative image of the used power drill, and Figure 44 shows the output of the use-case tests.


Figure 43. Used power drill as a representative load.

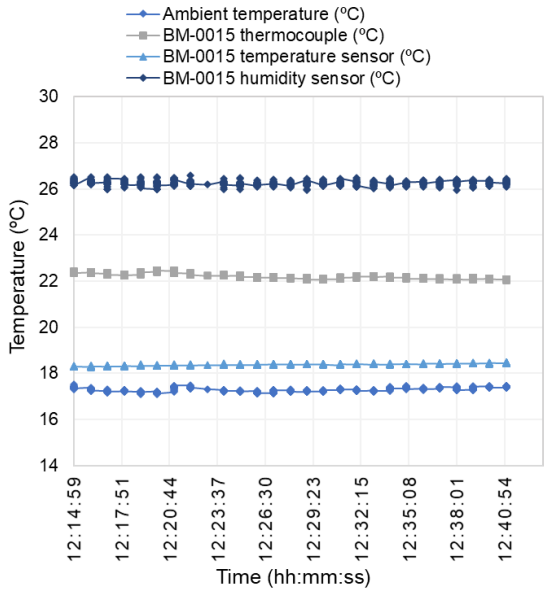
Ambient temperature (ºC)
BM-0015 thermocouple (ºC)
BM-0015 temperature sensor (ºC)
BM-0015 humidity sensor (ºC)
Temperature (ºC)
Time (hh:mm:ss)

(a)

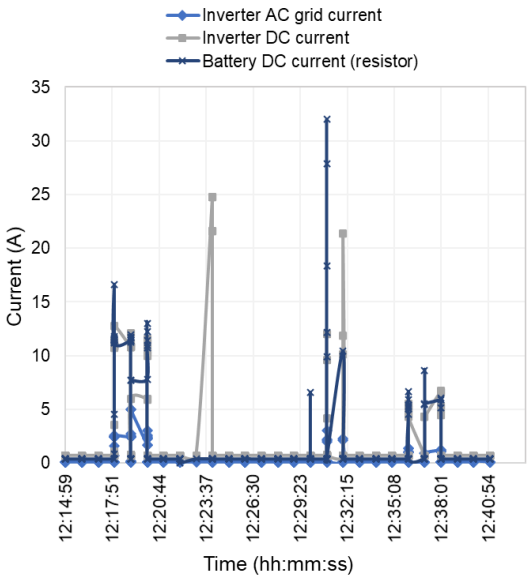
Inverter AC grid current
Inverter DC current
Battery DC current (resistor)
Current (A)
Time (hh:mm:ss)

(b)

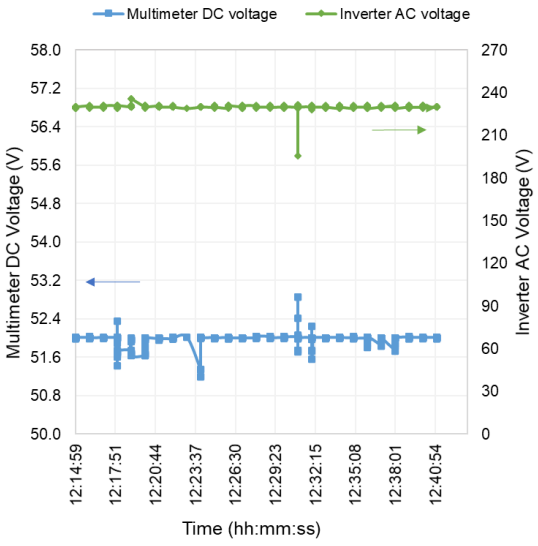
Multimeter DC voltage
Inverter AC voltage
Multimeter DC Voltage (V)
Inverter AC Voltage (V)
Time (hh:mm:ss)

(c)

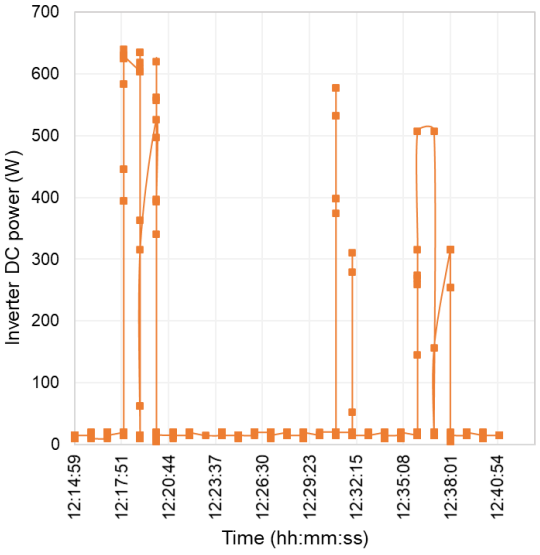
Inverter DC power (W)
Time (hh:mm:ss)

(d)

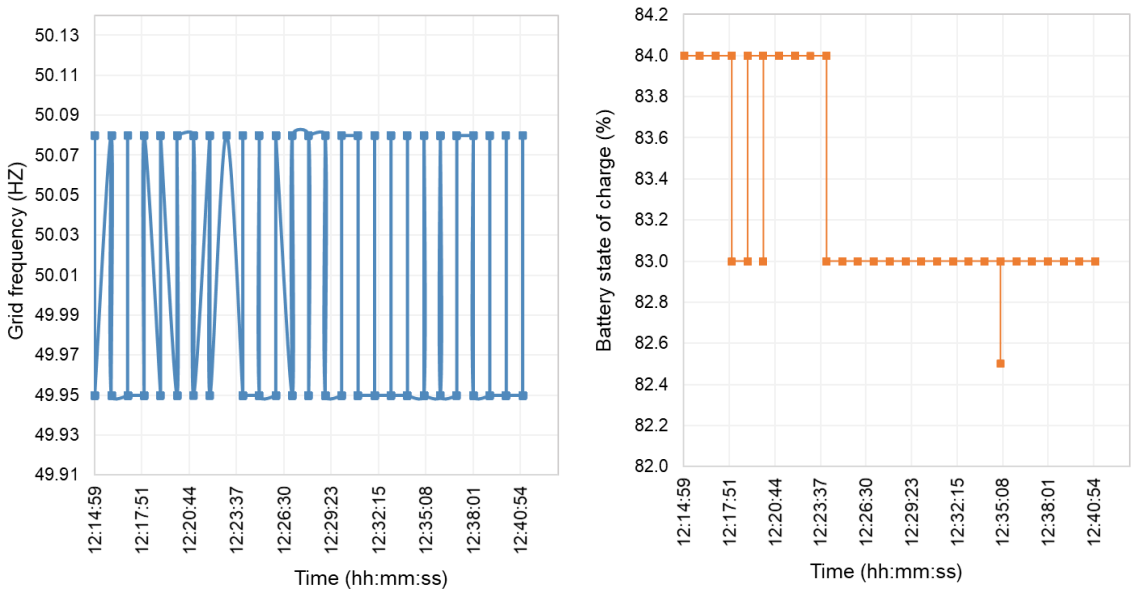


(e) (f)

Figure 44. Use-case test output of the power drill: (a) temperatures acquired by the precision multimeter (ºC); (b) DC and AC currents read through the inverter and the precision multimeter device; (c) voltages read by the precision multimeter device (DC) and inverter (AC); (d) DC power measurement read through the inverter; e) grid frequency read through the inverter (Hz); f) state of charge obtained through the inverter (%).

### 4.3.3. Grinding Wheel

The BM-00015 and BM-00018 were used to test the grinding wheel from Fein's brand, model WSS14-125. This equipment operates at a 230 VAC voltage. The manufacturer defines a maximum rated power of 1200 W. This equipment is tested in its two functions of work, which differ in energy performance: cut and grinding. Figure 45 is a representative image of the used power drill, and Figure 46 presents the output of the use-case tests.

✓ Function of grinding

(a) (b)

Figure 45. (a) Grinding wheel as a use-case representative load, and (b) use-case testing of the grinding wheel.

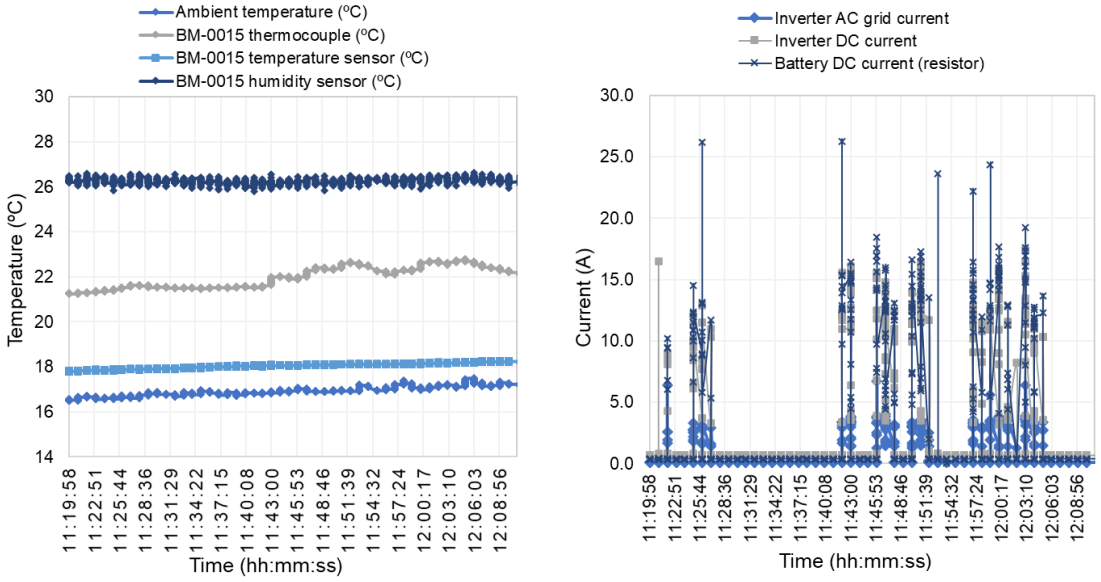


(a) (b)

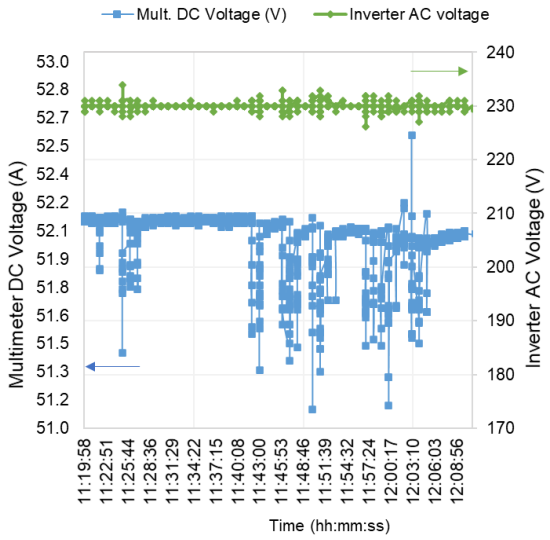


(c)

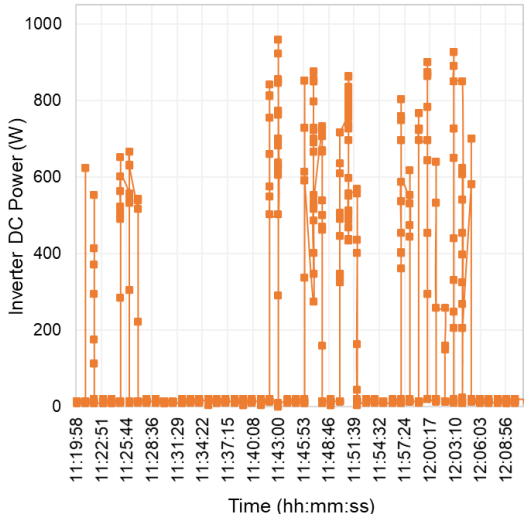


(d)

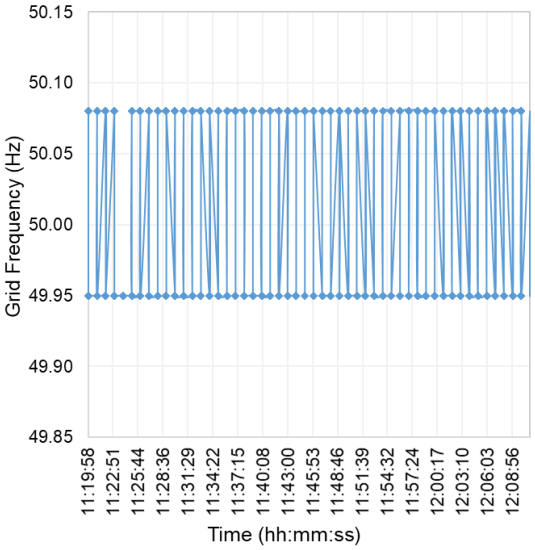


(e)

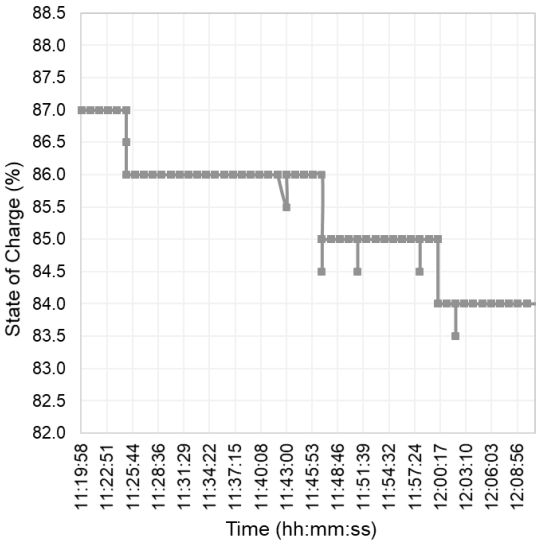


(f)

Figure 46. Grinding wheel, with the function of grinding, use-case result of (a) Temperatures (ºC); (b) DC and AC currents from inverter; (c) Voltages measured by multimeter (DC) and inverter AC voltage; (d) inverter DC power; (e) grid frequency (Hz); and (f) state of charge (%).

✓ Function of cutting

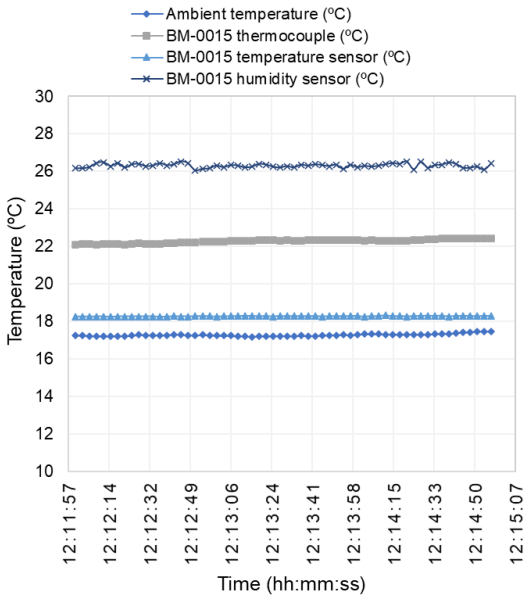


(a)

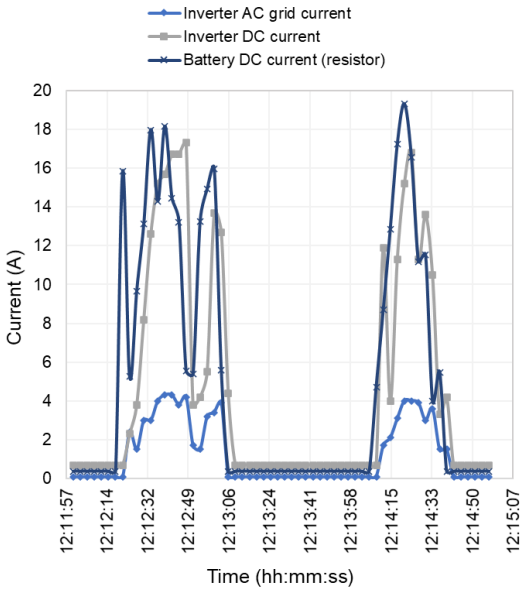


(b)

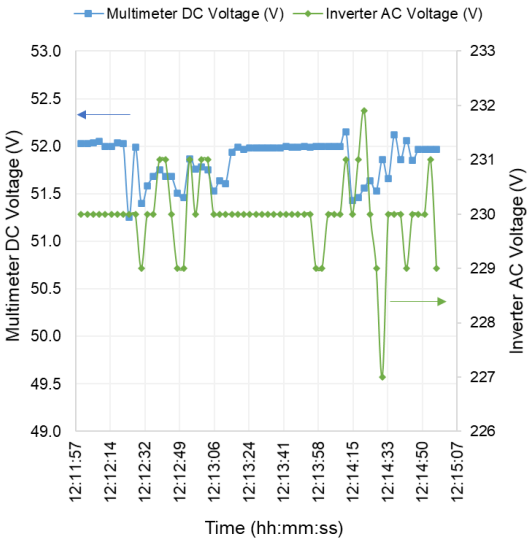


(c)

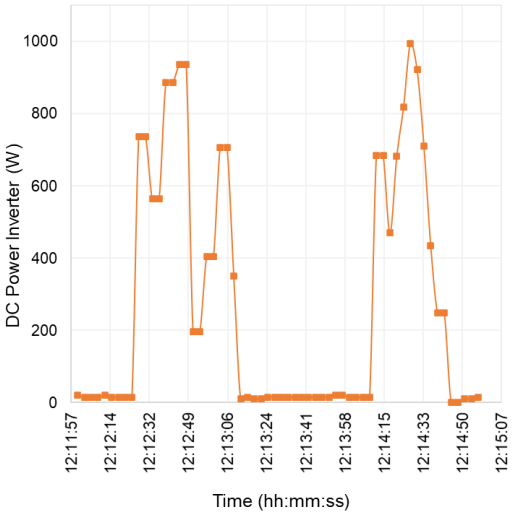


(d)

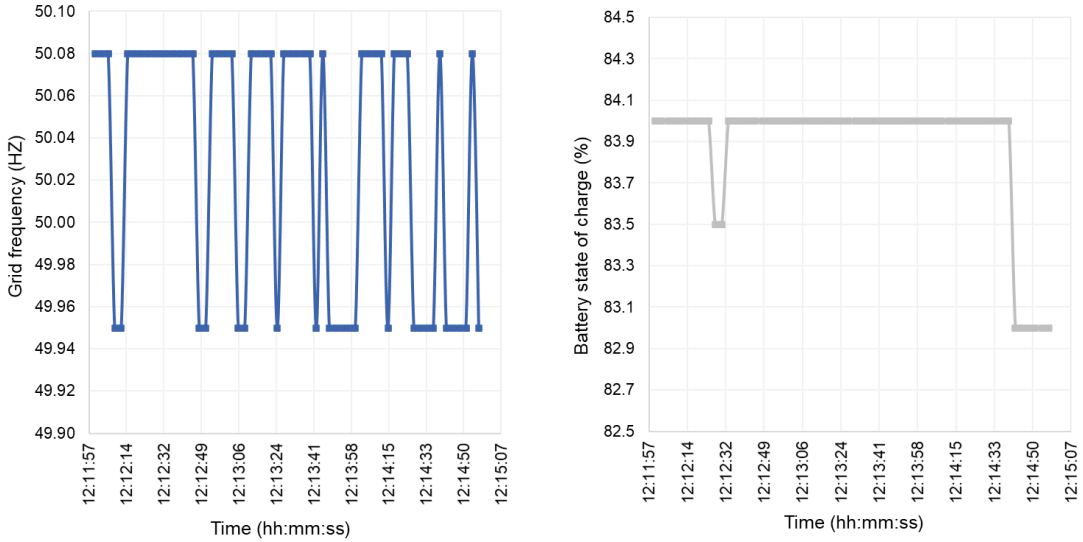


(e) (f)

Figure 47. Grinding wheel, the function of cut, use-case result of (a) Temperatures (ºC); (b) DC and AC currents from inverter; (c) Voltages measured by multimeter (DC) and inverter AC voltage; (d) inverter DC power; (e) grid frequency (Hz); and (f) state of charge (%).

## 3. Contributions to the prototype development, improvements in the testing control and final remarks

The operation of the battery prototype in the Renewable Energies Chair installations allowed the improvement of the product, with the continuous outputs being feedbacked to the battery provider. As a result of the collaboration, the main contributions from prototyping to the last versions of the product are summarised.

In many of the executed characterisation tests, at higher power levels, the inverter shut at nearly 45 % of the state of charge, as shown in Figure 48, with BM-0015.

From the observation of Figure 48, the most probable cause of this issue could be related to the battery temperature measurement. The thermocouple, placed in the BMS board, registers the temperature anomaly, which causes the battery BMS to shut down in the power bus. Investigation into this issue should be pursued to avoid it happening.

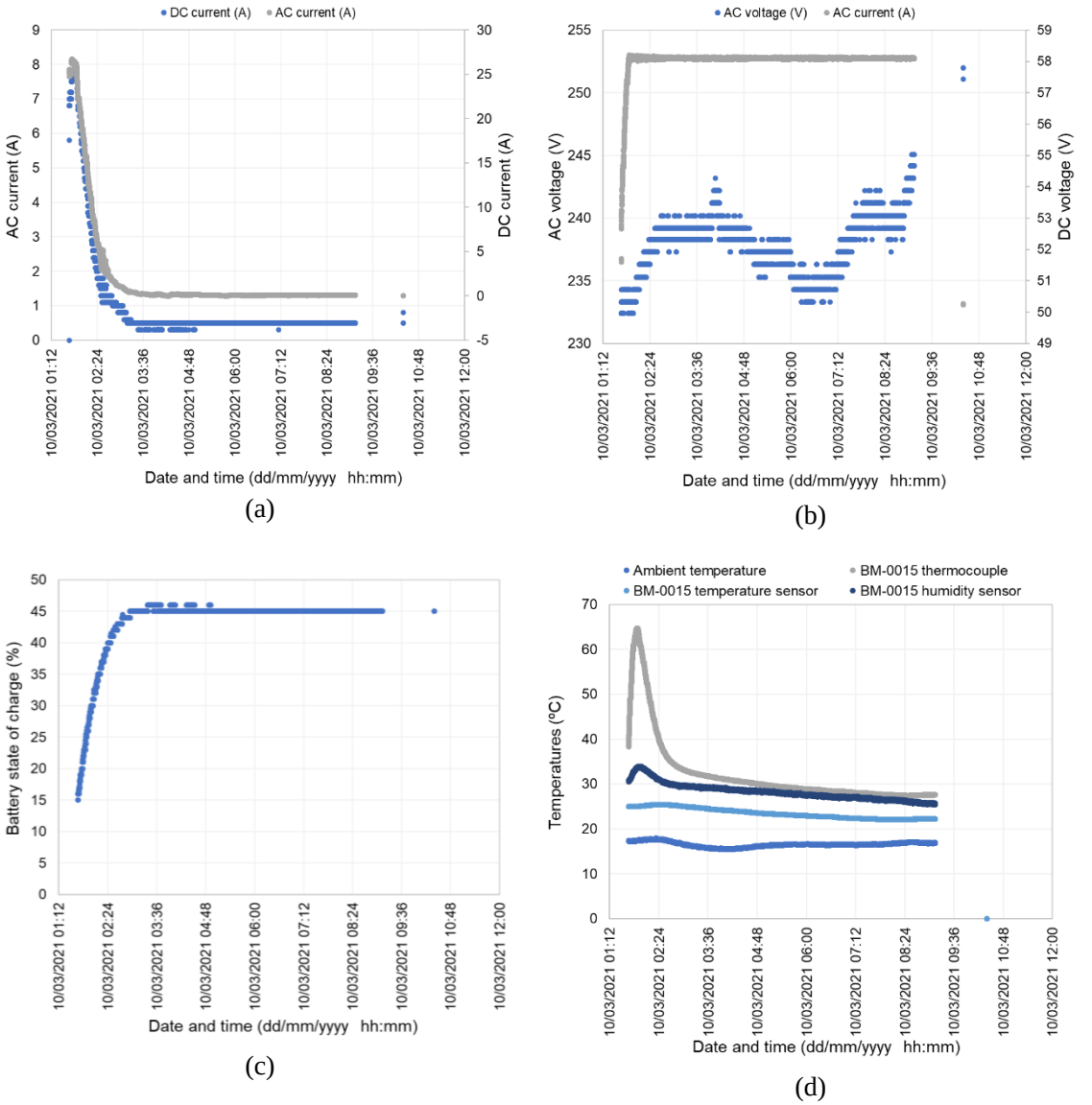


Figure 48. Example of the occurrence with BM-0015, with: (a) current (A); (b) voltage (V); (c) state of charge (%); and (d) temperatures (ºC).

The first tests were achieved using the battery SOC range of 20-90%, later updated to 15-94 % for the prior versions. Further improvements were added to the LabVIEW control to prevent the battery from disconnecting from the power bus. In the following, the obstacles faced in the control implementation phase are detailed, next to the mitigation measures:

- Pack voltage drop (inverter disconnection in "end of charging/discharging"): The SLIB consists of 32 cells (with increased internal resistance compared to first-life lithium-ion batteries), where the pack voltage drops below 30% SOC. In first life, it generally occurred at around 15 % SOC. The reduction of the

power discharge rate at SOC below 30% was implemented in control to avoid this from happening (Table 5).

- BMS disconnect at high temperatures: This issue was previously discussed as the reason for the inverter disconnection. If the temperature of 75°C is reached, the BMS is disconnected from the power bus – rigid BMS control. The inverter also monitors the battery temperature (the temperature at the BMS board, ~10–20 °C above the cell temperature). For this case, a mitigation measure should be implemented to avoid the temperature reaching and BMS disconnection. In this case, the AC power level at the inverter is reduced when a temperature of 65°C is measured. The lower power level is held until the temperature is below 50°C.
- Achieve the higher SOC imposed limit: When the operational state of charge surpasses the SOC of 95%, the battery disconnects from the power bus and cannot be externally controlled by LabVIEW. The most probable cause is the safety limits imposed by the battery provider. In order to proceed with the performance testing, the LabVIEW upper SOC limit was reduced to 94%.

The ambient temperature influences the operation of a lithium-ion battery. In general operation, its operational temperature range should be strictly respected. With the help of the air-conditioning unit, the characterisation tests of the prototypes were achieved with a controlled environmental temperature, within 10 to 25 °C.

The use-case scenarios' testing occurred outdoors, without ambient temperature control. In that case, the ambient temperature, and consequently the temperature inside the enclosure of the battery, influences the demanded current drawn by the battery.

A relationship of opposing objectives between inside battery temperature control and the system's degree of environmental protection (IP65) exists; however, it seems an essential constraint regarding its operation in outdoor conditions, for example, in the summer in the Mediterranean/African countries.

The realisation of the battery prototype testing under use-cases (battery state discharging-only) found constraints in the testing periods, which were not always achievable in an isolated situation, extending the testing calendar. Moreover, the use-cases performance tests were carried out with two batteries to avoid battery disconnection.

In a finalised product, it is peremptory to solve the restart of the battery if the SOC decays to values below 10%. In the regular operation of the battery, these values should not be reached to prolong the lifetime of the SLIB. Nevertheless, the restart of the battery in testing conditions should be achieved to control failure and control self-

discharge better. In the University of Évora installations, the batteries are not being operated daily, compromising the further integration of this battery in future research lines. Installing the batteries in the residences in Valverde will increase the probability of this situation occurring. One solution that could prevent the battery from reaching SOC values below the lower limit is to remotely control the SOC and prioritise slow charging in this situation in order to avoid battery disconnection.

The prototype solution, "inverter+battery", is a heavy solution for a general user. The transport is not smooth. Since it is a heavy solution, stability and steps are an issue. The application in the open field raises mobility difficulties regarding transport, especially on muddy or uneven ground.

The second version of the product is lighter than the previous, while the inverter (*betterGen*) transport is more effortless. Although heavy, the metallic betterGen enclosure offers stability and protection for outdoor applications.

### 5.1. Final remarks

The current work methodology allows the quantification of the relevant KPIs, characterising the technology in real operating conditions and opening a path to its electrical modelling. The performance output facilitates comparing the electrical performance of the SLIB with the commercial and documented energy storage technologies.

The prior versions of the product demonstrate a set of technical issues that are currently solved. The performance results demonstrate the product's suitability for stationary applications (both off-grid and residential). The realisation of the tests allowed the gathering of information that contributed to the improvement of the prior versions of the product for building a more robust solution, reaching a higher TRL.

The development of the testing unit in the present context and respective changes in the LabVIEW programming control allowed the integration of the SLIB in the developed energy management strategies set, allowing its inclusion in further project proposals. Additional testing with use-case scenarios provides technical key indicators regarding its performance in a real-operational environment under stress conditions, enabling further finetuning and validation of the product.

The developed test setup will allow dedicated energy management strategies to produce experimental validation data and contribute to current ageing modelling approaches.

## 6. References

[1] Pocityf, “Leading the smart evolution of historical cities,” 2022. [Online]. Available: https://pocityf.eu.

[2] IEA, “Global EV Outlook 2021,” Paris, 2021.

[3] S. A. berylls, “BATTERY PRODUCTION TODAY AND TOMORROW,” 2018.

[4] J. Falk, A. Nedjalkov, M. Angelmahr, and W. Schade, “Applying Lithium-Ion Second Life Batteries for Off-Grid Solar Powered System—A Socio-Economic Case Study for Rural Development,” *Zeitschrift für Energiewirtschaft*, vol. 44, no. 1, pp. 47–60, 2020.

[5] E. Martinez-Laserna *et al.*, “Battery second life: Hype, hope or reality? A critical review of the state of the art,” *Renew. Sustain. Energy Rev.*, vol. 93, no. February 2017, pp. 701–718, 2018.

[6] E. Hossain, D. Murtaugh, J. Mody, H. M. R. Faruque, M. S. H. Sunny, and N. Mohammad, “A Comprehensive Review on Second-Life Batteries: Current State, Manufacturing Considerations, Applications, Impacts, Barriers Potential Solutions, Business Strategies, and Policies,” *IEEE Access*, vol. 7, no. June, pp. 73215–73252, 2019.

[7] betteries AMPS GmbH, “Technical data betterPack,” 2022. [Online]. Available: https://betteries.com/wp-content/uploads/2022/11/betterPacks_technical_data.pdf.

[8] H. F. Gibbard, “Redox Flow Batteries for Energy Storage,” *28th Int. Batter. Semin. Exhib. 2011*, vol. 2, pp. 394–406, Jan. 2022.

[9] “Technical notes on output rating, operating temperature and efficiency.” [Online]. Available: https://www.victronenergy.com/upload/documents/Output-rating-operating-temperature-and-efficiency.pdf.

## 3.4. Validation of a Lithium-ion Commercial Battery Pack Model using Experimental Data for Stationary Energy Management Application

Ana Foles[1,2], Luís Fialho[1,2], Pedro Horta[1,2], Manuel Collares-Pereira[1,2]

In *Open Research Europe, Research article, Vol. 2, p. 1-15, 2022,*

https://doi.org/10.12688/openreseurope.14301.2

**Abstract**

A cost-effective solution for the design of distributed energy storage systems implies the development of battery performance models yielding a suitable representation of its dynamic behaviour under realistic operation conditions. In this work, a lithium-ion battery (LIB) is tested to be further modelled and integrated into an existing energy management control system. This specific LIB (5.0 kW /9.8 kWh) is integrated with a commercial inverter and solar photovoltaic (PV) system (3.3 kWp) as part of a microgrid that is also encompassing other energy storage technologies at the University of Évora, Pole of INIESC – National Research Infrastructure for Solar Energy Concentration. A testing protocol fully characterizes the battery and the inverter efficiency to describe their performance better. Then, a battery model is built upon both the existent LIB description and experimental fitting regression. The model allows to obtain the voltage curve, the internal resistance (i.e., to describe instantaneous voltage drop/rise and transients), and the state of charge (SOC) and/or energy capacity based on the current input. The developed model is validated through the comparison with the experimental results. The model approach presented a higher voltage RMSE (root mean square error) of 5.51 V and an MRE (maximum relative error) of 5.68 % in the discharge state. Regarding SOC, the MRE obtained was approximately 6.82 %. In the charge state, the highest RMSE voltage was 5.27 V, with an MRE of 6.74 %. Concerning SOC, the MRE obtained was approximately 6.53 %. The developed model is validated through the comparison with experimental results. Based on computational effort, simplicity of use and the associated model error, the approach is validated to the regular conditions of the commercial battery pack to be incorporated in the next research step, following a bottom-up modelling approach for an increasingly more complex smart grid.

[1] Renewable Energies Chair, University of Évora, 7000-651, Évora, Portugal
[2] Institute of Earth and Sciences, University of Évora, Rua Romão Ramalho, 7000-671, Évora, Portugal

**Nomenclature**

| | |
|---|---|
| BESS | Battery Energy Storage Systems |
| BMS | Battery Management System |
| DOD | Depth of Discharge |
| DSM | Demand Side Management |
| DSO | Distributor System Operator |
| ECM | Electric Circuit Model |
| EES | Electrical Energy Storage |
| EMS | Energy Management Strategy |
| ESS | Energy Storage System |
| EV | Electric Vehicle |
| LIB | Lithium-ion Battery |
| R&D | Research and Development |
| RES | Renewable Energy Sources |
| SOC | State of Charge (%) |
| TSO | Transmission System Operator |
| VRE | Variable Renewable Energy |

**Keywords:** Electrical energy storage, Lithium-ion battery, Characterization tests, Battery model

## 1. Introduction

In 2019, 2.9 gigawatts (GW) of energy storage worldwide were added, almost less than 30 % compared with 2018. The result is justified by the early maturity stage of some energy storage technologies – with presence in a few specific markets – and high dependence on support from appropriate policies [1]. In the electrical sector, the energy storage can be applied to different goals: meeting the demand and reliability in the grid peak hours or as an asset on the liberalised electricity markets, benefit from price arbitrage depending on the fluctuation in spot prices, from capacity credit as transmission congestion relief or resource suitability, or for ancillary resources as voltage or frequency regulation and spinning or non-spinning reserves [2]. On a smaller scale, these storage technologies can also directly benefit the consumer, namely, for solar photovoltaic (PV) self-consumption maximization, in the electricity shift from low demand to peak times or helping stabilize intermittent renewable energy sources (RES). They can also help in the demand-side management (DSM) or flexible power demand and in the smart-charging of electric vehicles (EVs) [3]. Energy storage comprises different technologies, and in this work, the electrical sector application of a lithium-ion electrochemical energy storage technology will be discussed.

Lithium-ion battery (LIB) continues to be the most deployed electrical energy storage (EES) technology, driven mainly by the downward trend in costs [4] [5]. Characterized by a) high efficiencies, b) moderated lifetime, c) low volume and weight per kWh of storage, d) temperature sensibility, and by being associated with low maintenance compared to other battery technologies, LIB are the state-of-art technology for electric vehicles (EVs) with across-the-globe investments by large market player battery manufacturers [5]. It is a mature technology in the mobile device market, currently deployed in the automotive sector and is at an early stage in stationary applications. Nowadays, the automotive market is ten times greater than the grid-scale market. The research and development (R&D) efforts made, and the diminishing costs of the EV batteries could boost the commercial and residential market. The search for alternative battery chemistries (post-lithium) to allow for better performance (power/energy rates, for example) could also offer a solution for the market, with possible declining battery costs. The ongoing scale-up allowed LIBs to present a downward trend regarding costs in the past years [1][4], and they are forecasted to reach a cost potential of 70 $/kWh in 2050 [5]. The optimized cost reduction path goes along the further improvements of energy and economic indicators, such as the energy density, along the industrialization value chain.

A battery model is essential for designing and optimizing an electric power system and smart management. As non-ideal equipment, the battery response is affected by the state of charge or charge/discharge rates. The models allow for a more accurate analysis of the real system, which enriches the development of systems' analysis of performance and costs, allowing the faster application of commercial batteries in smarter residential markets. Predicting its performance allows estimating its use and durability, optimizing its energy use, and determining the applications that best fit the performance. Each microgrid equipment can be modelled, and the smaller the modelling error compared to the experimental performance, the better the description of the system's performance in real operating conditions. The traditional lithium-ion modelling approach generally relies on the existing models in MATLAB/Simulink. However, it is possible to identify some limitations of this modelling approach: the challenge in obtaining more accurate results (model is embedded in the code), difficulty in applying to another programming language, and verifying if the model aligns with the experimental result of the general battery. This work contributes to constructing a database with pre-defined experimental setups and validated models that allow the easier optimization of the use of a commercial lithium-ion battery, accessible to any residential user.

This work is focused on the LIB characterization testing and modelling for real-time application in future battery control scenarios and energy management strategies. In the literature, the modelling of LIB for EV application is broad, but for stationary applications, e.g., solar photovoltaic systems (validated with experimental results), the scientific literature found is scarce. This work aims to use a model to represent the dynamic behaviour of the battery with an adequate error, considering the interface with the power electronics and validating it through results experimentally obtained to allow the possibility of model integration into a more complex control system or algorithm. In the medium term, the developed model will later be integrated with models of other storage technologies to optimize the control and global operation of a complex but flexible and intelligent grid system, allowing it to respond to the objectives of future electrical networks.

This paper is organized as follows: Section 2 delivers a bibliographic literature review on lithium-ion battery technology and the existing modelling approaches that better describe the LIB in focus in this work. Section 3 presents the methodology used: the experimental microgrid description, the LIB and inverter characterization testing plan, and the model's detailed description. Section 4 presents the results obtained, including the experimental data and the battery modelling results. Based on the methods used and the results obtained, a discussion is carried out in Section 5, followed by the conclusions of the work in Section 6.

## 2. Literature review

This section briefly describes the lithium-ion technology and the technology modelling approaches used throughout the bibliographic references.

### 2.1. The lithium-ion technology

The lithium-ion battery (LIB) was conceived and developed by the Japanese Asahi Kasei Corporation and released commercially in 1991 by Sony Corporation, followed by A&T Battery Co. in 1992 [7], especially for low-power portable applications. The technology was well accepted given its characteristics of high energy density, good performance, less heat generation, small dimension, lightweight (Wh/kg) [8], and no memory effect, compared with nickel-cadmium or nickel-hydride batteries. The low atomic number of lithium is the cause of the high electrode potential, which results in

higher energy density. Over 90% of the worldwide production of LIBs is based in Japan, Korea and China [9].

Developing new high-energy-density lithium batteries has been challenging, requiring new anodes, cathodes, and nonaqueous electrolytes [7]. Generally, a lithium-ion battery has two electrodes and an organic electrolyte, nonaqueous, containing dissolved lithium salts. The cathode is lithium metal oxide and the anode is from graphitic carbon. Inside the cell, the materials are ionically and not electrically connected by an electrolyte, and it has an insulating membrane. The reaction occurs with a characteristic electrochemical potential difference (voltage). LIB cathode materials can be associated with a variety of multiple chemistries, such as lithium cobalt oxide (LCO), lithium nickel manganese cobalt oxide (NMC), lithium manganese oxide (LMO), nickel cobalt aluminium oxide (NCA), and lithium iron phosphate (LFP). Recently, besides graphite, the anode can be composed of lithium titanate (LTO). NMC is the typical chemistry used in grid-scale ESS [10]. Overall characteristics depend on the cell chemistry. However, it generally has higher gravimetric and volumetric energy density, high efficiency, high power capability, long cycle, and long calendar lifetime than other battery technologies [11].

Lithium-ion batteries (LIBs) allow fast and slow charging-discharging operation states, have high energy densities and have reasonable power densities. The technology has a battery management system (BMS) which monitors its general operating conditions – a range previously defined by the manufacturer, due to sensibility to high-temperature operation and high depth of discharge (DOD). Those factors are usually linked to faster degradation conditions (ageing), permanent damage or unsafe operation. The response time of this technology is usually in the millisecond's timescale, a fast response compared to the average. It is also easily scalable in terms of power or energy. In recent years, R&D has evolved using non-flammable and/or flame-retardant additives (non-flammable electrolytes) [7]. . LIBs are sensitive to temperature. Usually, an active cooling system is integrated within the building/container of the battery (or in the EV refrigeration battery system) to reach its optimal temperature range (or move away from extreme temperature ranges). Generally, LIBs are designed to operate at about 21°C so that a heating-cooling active system can be used.

Improvements of this technology are related to its core aspects as energy storage, mainly from its competitiveness in the market since they are still associated with a high production cost. The technology still presents challenges in the 2 $^{nd}$ life usage or at the end-of-life /recycling process, being its salvage value lower than the processing cost [12]. After high-intensity applications, as in EVs application, LIBs present generally

good condition to be further used in high energy density applications, such as in grid storage [13][14]. LIB recycling is limited at present, having recycling figures below 3% [15][16], but this will be a vital issue in its future deployment. Different LIB technologies are recycled through similar processes to recover materials like lithium, copper, cobalt, nickel, iron, aluminium, and manganese. The level of toxicity of the substances used in LIB is lower than other battery technologies, and in some countries, these are still disposed of in landfills [16]. For LIBs, lithium appears to be the only critical raw material. In contrast, other critical elements are being studied to reduce their need to incorporate the battery, e.g., the use of manganese instead of critical cobalt is expected to be used for electrode coatings in the future [17].

### 2.1.1. Standards for battery operation

The following standards are the currently most relevant in force for the technology:

- UL 1642 [18] is a standard that expresses guidelines for manufacturers, with procedures on construction, performance, and electrical, mechanical, environmental, and marking tests.
- LIB's transport guidelines are described in IEC 62281 and ST/SG/AC.10/27/ [19], with the United Nations recommendations.

Furthermore, the general standards for secondary batteries are highlighted in the following:

- UL 2054 [20] is a reference for household and commercial batteries for understanding the considerations made for residential sector application regarding construction and testing for the electrical, mechanical, enclosure, fire, and environmental performance and conditions and marking.
- IEC 61427-1 and 2 refer to the photovoltaic off-grid application and on-grid application, respectively, and IEC 62933-5-2 ED1 describes the safety requirements for grid integrated EES systems – electrochemical based systems [19].

Policies and the regulatory framework for batteries are still under development. For instance, the European Parliament is currently preparing the proposal for a regulation on batteries and waste batteries, including raw materials, carbon footprint and end-of-life handling, setting the sustainability requirements for EES technologies [21]. The regulation is missing for different application scenarios and, for the relevance of this work, critical aspects of the integration, testing and operation of this specific

technology, such as the controls and BMSs, temperature, degradation, and safety measures, among others.

## 2.2. Modelling a lithium-ion battery

LIB models are being emphasized in the current battery's panorama [22]–[26], , most of them fostered by the research in the automotive sector field [27]–[29]. A battery model predicts the performance of the battery unit to be used on a simulation framework, allowing the optimization of the system itself and its integrated control within a microgrid. Generally, it starts at a single-cell level, progressing to a unit system description, using the nominal energy capacity and voltage characteristics. The efficiency losses due to racking, hardware for control and safety, and power converter elements should also be considered. The voltage curve depends on the battery state of charge, operating current, resistance, and energy capacity. The internal resistance increases over time, conducting to a decreasing usable voltage range. Operating the battery at higher currents is related to a higher rate of voltage decrease, reducing the available bulk capacity. The thermal behaviour could be described using a heat transfer coefficient with the environment for instantaneous thermal effects on capacity and resistance. The temperature effect is usually described as a function of ambient temperature and operating current, resulting in a resistance parameter.

A brief review of available LIB models was made, and different approaches were found. In article [30], a description of LIB models and parameter identification techniques is made; the authors of [23] compared different LIB models; in reference [29] the authors present LIB models for automotive applications, and the authors of [22] provide a review of models for generic batteries. Modelling approaches based on MATLAB/Simulink are presented in studies [28], [31], [32]. Battery testing based on pulse-charging is carried out by the authors of [33] and by the authors of [34]. In the case of model approaches emphasising on chemical modelling, the authors of [35] explored parameters identification techniques for a LIB model. In [25] an extended Kalman filter is used to estimate the SOC of a LIB. The authors of [36] estimate parameters of the electric model, such as the resistances and capacitors, directly from measurements.

LIB models research in the literature outnumbers those for stationary applications, justified by the EV's continuously increasing deployment. The design of future smart grids relies on robust battery modelling and field validated approaches. Many research

activities are devoted to optimising energy efficiency and energy management for smarter energy systems and designing scenarios for battery applications, such as in buildings or EV charging stations, where the battery performance influences the investment. The generated model can be replicated and, among the possibilities, be used to study different energy management strategies, such as PV ramp-rate relief or energy arbitrage or investigate the possible integration with other energy storage technologies within microgrid or building scenarios.

The voltage equation modelling is based on the charging and discharging efficiency. Three main approaches are found in the literature: Shepherd's battery model, electric circuit models, and the modified Shepherd's battery model. These three approaches are briefly presented below.

### 2.2.1. Electric circuit models (ECMs)

Equivalent electric circuit models can be applied to describe different battery technologies [22]. The ECMs for lithium-ion batteries found in the literature review showed satisfactory output results, following simple and fast algorithms and representing the battery in permanent and transient states [28] [32][36]. Their suitability for stationary applications is considered a good approach. The model shown in Figure 1 has a constant voltage source in series with a resistor and is the straightforward ECM representation.

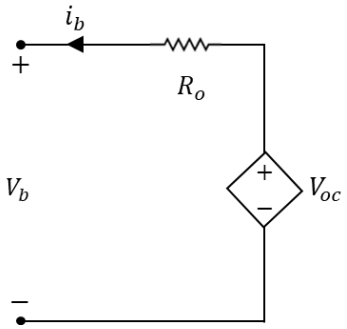


Figure 1 - Equivalent circuit representation to the lithium-ion battery model.

The current $i_b$ represents the dynamic internal current, $R_o$ represents the internal ohmic resistance, $V_b$ is the battery voltage in its terminals, and $V_{oc}$ is the applied input voltage [22]. The battery voltage is obtained through the simple circuit analysis of this equivalent circuit, expressed in Eq. (1).

$$V_{battery}(t) = V_{oc} - R_o i_b(t) \quad (1)$$

Among the ECMs, it is possible to find simple models, Thevenin-based models, impedance-based models, combined ECM and generic based models [22]. The presented model includes the determination of the SOC as a function of the open-circuit voltage ($V_{OC}$), and others could also include bias effects. Although more accurate, capacitors represent significant additional computational times.

### 2.2.2. Shepherd's battery model

Shepherd's battery model is a widely known model that describes a battery's terminal voltage over the current inputs. It is generally described through a constant current discharge, expressed in Equation (2) [28],

$$V_b(t) = E_0 - K\frac{Q}{Q - it}i(t) - R_o i(t) \quad (2)$$

Where,

$V_b$ is the terminal voltage of the battery, in V, at instant $t$.

$E_0$ is the battery constant voltage, in V.

K is the polarization constant, in $V/Ah$.

Q is the battery energy capacity, described in units of Ah.

$it$ is the discharge energy capacity, in Ah.

$R_0$ is the battery internal resistance, in **Ω**.

$i(t)$ is the dynamic current (A) in instant $t$.

The voltage equation parameters – $E_0$, $K$, $R_0$ – can be obtained through the relation established on three points of the battery discharge curve given by the manufacturer (($V_{full}$, $Q_{full}$), ($V_{exp}$, $Q_{exp}$) and ($V_{nom}$, $Q_{nom}$)), illustrated in Figure 2, below shown.

Shepherd's model is usually studied in the literature to describe the automotive batteries behaviour.

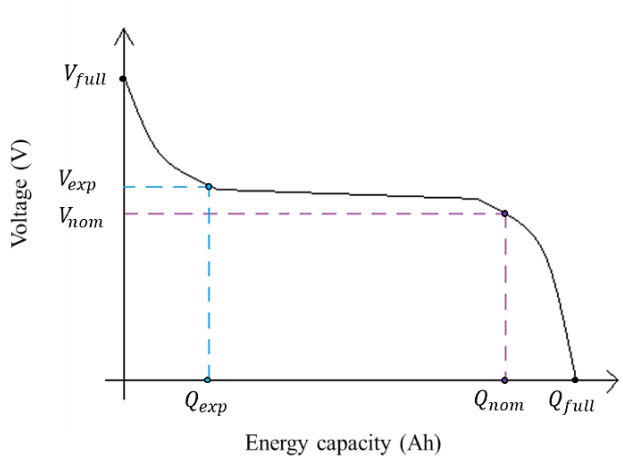


Figure 2 – Example of an ideal discharge curve, where the three points can be extracted: the ( V full , Q full ) are the voltage (V) and energy capacity (Ah) of the completely charged battery; the ( V exp , Q exp ) are the voltage (V) and energy capacity (Ah) at the end of the exponential zone; and ( V nom , Q nom ) are the voltage (V) and energy capacity (Ah) at the end of the nominal zone. This image has been reproduced with permission from [28].

### 2.2.3. Shepherd model modified versions

Shepherd's battery model can be modified to better describe the dynamic battery behaviour through an exponential function, previously presented in the work developed by the authors of [32]. The modified Shepherd's model charge and discharge voltage curves are based on Eq. (2) and are represented below in Eq. (3) and Eq. (4).

$$V_{batt\_ch}(t) = E_0 - K\frac{Q}{it - 0.1Q}\left(it + i(t)\right) + Ae^{-B\,it} - R_o i(t) \quad (3)$$

$$V_{batt\_dis}(t) = E_0 - K\frac{Q}{Q - it}\left(it + i(t)\right) + Ae^{-B\,it} - R_o i(t) \quad (4)$$

Where, $V_{batt\_ch}$ represents the charge voltage and $V_{batt\_dis}$ represents the discharge voltage. The rest of the parameters present in Eq. (3) and Eq. (4) ($E_0$, K, A, B) can be determined through the manufacturer discharge curve and being directly determined with the use of the equations of Table 1, shown below.

Table 1 - Parameter's description of equations (3) and (4).

| Model parameter | Description | Equation representation |
|---|---|---|
| A, Exponential Voltage Amplitude Constant, in V | The amplitude of the exponential region. | $A = V_{full} - V_{exp}$ |
| B, Time Constant Inverse, in $Ah^{-1}$ | Charge at the end of the exponential zone of the battery's discharge curve. The scalar value of 2.3 was used in [32] to improve the fit to the specific battery used. | $B = \frac{2.3}{Q_{exp}}$ |
| K, Polarization Constant, in $V/Ah$ | Calculated using $V_{full}$ and the end of the nominal zone of the discharge curve. The scalar value of 0.065 was used in [32]. | $K = X\left[V_{full} - V_{nom} + A(e^{-BQ_{nom}} - 1)\right]\frac{Q_{full} - Q_{nom}}{Q_{nom}}$ |
| R, Internal Resistance, in Ω | The internal resistance of the battery at steady-state current. $\upsilon$ is the efficiency of the battery, and $V_{nom}$ and $Q_{nom}$ are the nominal values for voltage (V) and energy capacity (Ah), respectively, of the curve (see Figure 2). | $R = V_{nom}\left(\frac{1-\upsilon}{0.2 \times Q_{nom}}\right)$ |
| $E_0$, Battery Constant Voltage, in V | Represents the value when the battery is close to completely discharged and no current is flowing. | $E_0 = V_{full} + K + R \times i - A$ |

The three points of the discharge curve are used (see Figure 2) to calculate the voltage-current curve. In the work developed by the authors of [32], the proposed model considers this approach, including the battery lifetime. Moreover, the authors test the model within a SOC operating range in the linear region of the battery discharge curve (to operate within the 20–85 % SOC range) and consider the temperature operating range to be maintained within the -10°C to 45°C range.

## 3. Methodology

In this work, the authors aim to develop a model for a commercial LIB that allows its real-time description for stationary applications. An experimental setup is developed to characterize the battery, and further model validation against the experimental data

acquired is carried out. The methodology follows the steps described in Figure 3, which detail the input parameters subjacent to the model construction and development.

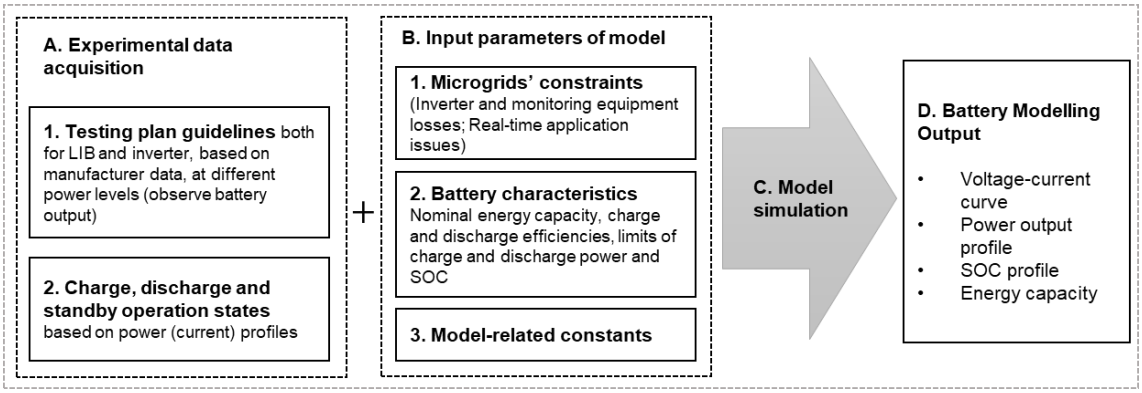


Figure 3 - Methodology to describe the lithium-ion battery under study.

LIB, lithium-ion battery; SOC, state of charge.

The following subsections describe the key aspects of the experimental data acquisition and the model approach.

### 3.1. University of Évora microgrid infrastructure

The LIB characterization process aims at verifying the performance and dynamic behaviour of the selected battery: 5.0 kW/ 9.8 kWh (189 Ah) LIB energy storage from the LG Chem manufacturer [37] , model RESU 10, with a nominal voltage of 48 V. The LIB and the SMA Sunny Island [38] 4.4M inverter (3.3 kW nominal power) are integrated into one of the University of Évora (UÉvora) microgrids. The integration consisted of connecting the systems to the grid, installing AC meters, DC measurement devices and temperature sensors (in the battery's two surface parts – above and lateral - and environmental temperature). The next step consisted in establishing a communication set with the inverter through the Modbus TCP/IP protocol (see Section 3.2.for further details). The current microgrid schematic is shown in Figure 4, including a 3.3kW solar amorphous photovoltaic installation, a 3.0 kW/ 7.6 kWh sodium-nickel chloride battery, and a 3.0 kW/ 3.0 kWh 2 $^{nd}$ life lithium-ion battery, and monitoring equipment (AC and DC meters and temperature sensors) on each relevant point of the microgrid. This research infrastructure was designed for the systems' operation study and development, where a communication and control platform were developed. The manufacturer data [39] of the commercial battery is displayed in Table 2.

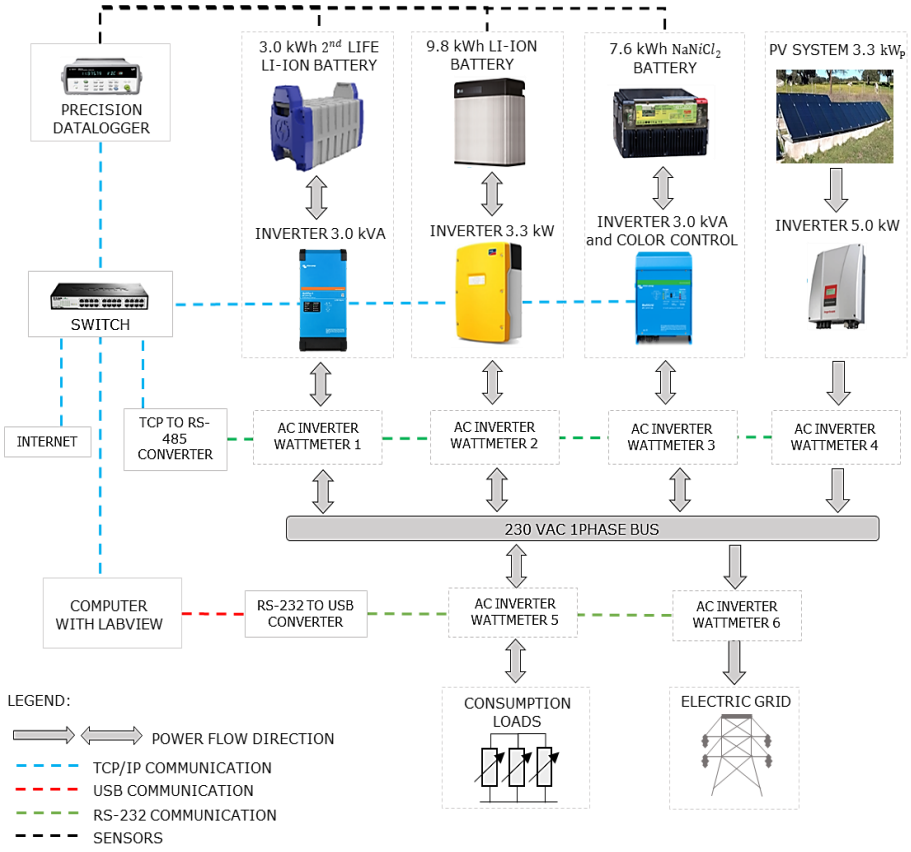


Figure 4 - General schematic of the equipment and control platform of the microgrid of the Renewable Energies Chair at the University of Évora.

In the figure, PV is the solar photovoltaic generation; AC is alternating current; TCP/IP is the Transmission Control Protocol/Internet Protocol (to allow communication on a network); RS-232 is a protocol for the exchange of data (generally used in the serial ports of the computers).

Table 2 - Reference operating conditions and main characteristics available by the manufacturer of the LG Chem Resu10 48 V LIB [39].

| Variable | Unit | Value |
|---|---|---|
| General | | |
| DC voltage operating range | V | 42.0~58.8 |
| Volume (exterior box) | $m^3$ | 0.05 |
| Weight | Kg | 75 |
| Average environmental temperature | °C | 20 |
| Depth of discharge | % | 80 |

| Energetic | | |
|---|---|---|
| Nominal energy / useful | kWh | 9.8 (25°C, 100% SOC) / 8.8 |
| Nominal power / maximum / peak (in 3 s) | kW | 3.3 / 5.0 / 7.0 |
| Nominal Capacity | Ah | 189 |
| Maximum Current | A | 119 at 42V |
| DC nominal Voltage | V | 51.8 |
| Cycles number (90% DOD, 25°C) | - | 6000 |
| Cycles number (80% DOD, 25°C) | - | 10000 |
| Environmental conditions | | |
| Cooling | - | Natural convection |
| Operating Temperature | °C | -10 a 45 |
| Optimal Operating Temperature | °C | 15 a 30 |
| Storage temperature | °C | -30 a 60 |
| Humidity | % | 5 a 95 (no condensation) |
| Altitude | m | < 2000 |

### 3.2. LIB and inverter testing description

In the consulted bibliography, battery testing procedures generally consist of a battery discharge at a constant current, known as C-rate [28][32]. It is generally encountered in literature for the batteries' description to normalize it with the battery capacity, which might be variable. The test consists of discharging the battery at a calibrated current relative to its maximum capacity, which led the battery modelling to be developed based on the manufacturer discharge curve at constant current, one of the most widespread models found in the literature [28][32][40]. In the absence of both a manufacturer curve and the option of testing the LIB at a fully controlled constant current discharge (due to the inability to control all the inverter parameters, which satisfies the relation of power-voltage-current at each instant), the charge and discharge curves were obtained through the available points of control of the battery inverter, which is the alternating current (AC) delivery point. This case consists of the battery testing procedure with an E-rate [41] - measuring the power rate at which a battery is discharged relative to its maximum capacity, in Wh.

The experimental tests and respective data acquisition are presented in the following paragraphs. The outlined test plan considers the manufacturer's operating conditions (see Table 2), with a 20–90% SOC range. The operation of the battery within the

referred range includes a safety margin closely related to the depth of discharge (DOD) and the technology degradation. The air-conditioning unit controls the environment temperature within 15–25°C.

A battery-inverter communication control was developed to conduct the testing plan and real-time data monitoring. The communication is based on the Modbus TCP/IP protocol [42][43] , with the help of the LabVIEW 2014 programming environment (the communication can be established in a similar routine through open-sourced software such as Python). In that sense, the inverter needs to be connected to the Ethernet, detaining an IP address. It relies on the Modbus mapping addresses available from the inverter manufacturer, SMA Sunny Island 4.4M [43], that is available from reference [44] (“ Technical Information – Modbus® Interface” and consult the .xlsx file choosing the model of the inverter). Through the communication establishment, the inverter is asked to, periodically (at 2-second intervals), retrieve and send commands (based on the power profiles at the AC point connection). An example of the communication establishment is detailed in Figure 5.

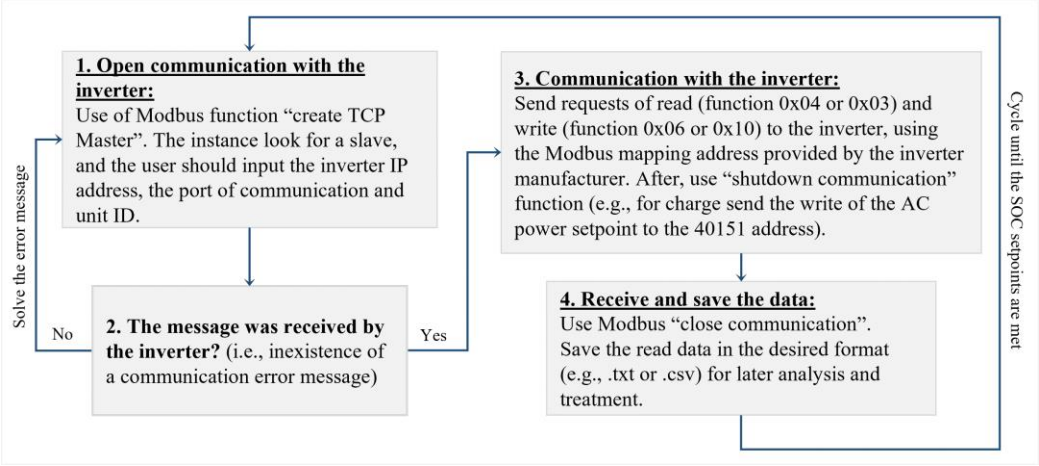


Figure 5 – Communication establishment with the inverter to perform the charge-discharge tests.

The data acquisition is achieved by reading the parameters of the inverter from the high precision AC wattmeter [45], and the measuring precision datalogger [46] . The acquired parameters include current, voltage, power, temperatures, and battery and inverter alarms.

The battery cycling tests were conducted after assuring reliable data measurement acquisition and optimization of the control program (definition of timeframe, prioritization of specific readings, organizing the different equipment readings). The

cycling corresponded to about 30 complete charge-discharge cycles at predefined constant power levels throughout the SOC range (from nominal power to low operating power: 330-3300). The obtained average data for each power level is made available in *Underlying data* [47]. An example of a full charge and discharge battery test is shown in Figure 6, at a constant power level of 2.7 kW, throughout the mentioned SOC range.

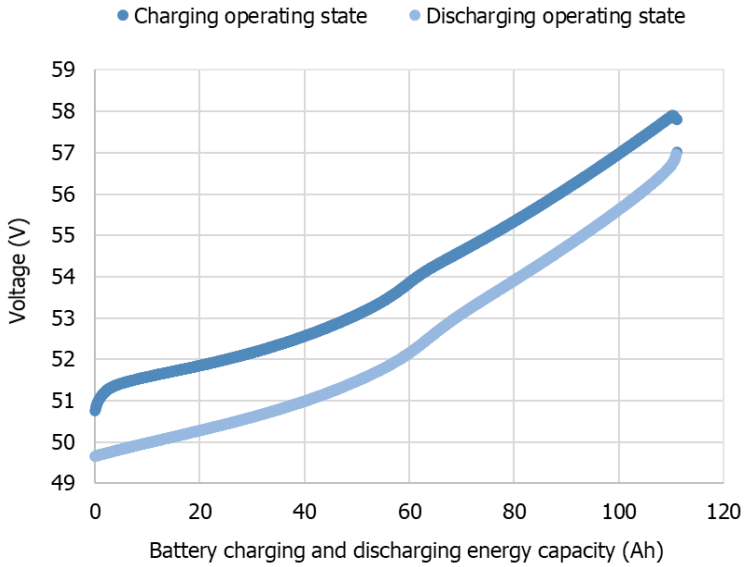


Figure 6 – Complete battery charge-discharge cycle at a constant power level of 2.7 kW at the AC delivery point, from 20-90 % SOC range.

The inverters operate at different power levels and according to a power-related efficiency profile. Given the integrated battery-inverter use, it is essential to consider the efficiency curve of the inverter, which varies throughout its power range (either charging or discharging). For that reason, it is relevant to acquire its experimental efficiency curves since they will impact the overall battery system results.

To evaluate the performance of the SMA Sunny Island 4.4M inverter, a test control was implemented in the LabVIEW 2014 programming interface, fully reproducible through open-source software, e.g., Python. It used Modbus TCP/IP and was achieved by the mapping of addresses given by the inverter manufacturer (in this case, SMA) [43]. The test control made was similar to the previous, where only the remaining time at a certain level of power was variable. The protocol consisted of operating the inverter at different rates of its nominal power (5% to 100% rate) during periods of 15 minutes. DC and AC electrical parameters were monitored. The test's main objective was to calculate the charge and discharge efficiencies over the power operating levels, presented in the next section of this work (Section 4).

### 3.3. LIB modelling application

Using the previously obtained experimental data to describe the LIB, a LIB model was developed considering modelling adaptations of Shepherd's model, described in Section 2.2.3. The authors of [32], describe the battery through the manufacturer-provided curves. In the present work, the battery is described by the results of the experimental testing at different constant power levels over the complete charging and discharging operating states. The modified version of Shepherd's model was computed to obtain the dynamic battery behaviour, using Equation (3) and Equation (4), considering the dynamic current over the state of charge range at a particular power level.

In addition, the state of charge parameter of the battery at each instant *t* is generally estimated by the following Equation (5) and Equation (6),

$$SOC(t) = SOC(t-1) + \frac{i(t) \times \Delta t}{Q} \quad \text{, if Q is in the unit of Ah} \tag{5}$$

$$SOC(t) = SOC(t-1) + \frac{P(t) \times \Delta t}{Q} \quad \text{, if Q is in the unit of Wh} \tag{6}$$

Where Q is the energy capacity of the battery, and the $\Delta t$ the difference of the step time: $t-1$ (last instant of $t$) and $t$. The $Q$ values are bounded by its real defined range of minimum and maximum energy capacity values. Using the model described in Section 2.2.3 to describe the LIB understudy better, some adaptations were made. In Equation (3), a multiplication factor of 0.65 for Q was used instead of the 0.1 described. Regarding the rest of the parameters, the used time constant inverse of 2.3/ $Q_{exp}\ Ah^{-1}$ was maintained, and a polarization constant with a scalar value of 7.3 was used instead of 0.065 (see Table 1). For the obtained voltage to be described by Equation (3) and Equation (4), the curve has a constant fit of a scalar value of +41.2 (obtained through the observation of a mismatch of the initially computed voltage curve and experimental voltage values obtained).

The model was computed using MATLAB (2017b) programming and is fully reproducible through alternative software, e.g. Python (see *Software availability* [48]). As a first approach, the operation of the battery at constant power levels, acquired experimentally, was chosen to validate it. The model was used to suit both charge and discharge curves from the experimental values, given the need to describe the overall battery behaviour. For the intermediate power values, a technique of regression fittings

was used, taking advantage of the MATLAB fitting tool (also existing in alternative software, such as the open-sourced software Python).

The proposed model uses the current as input to represent the LIB voltage behaviour. Regarding the practical model application within a more extensive model regarding all microgrid systems (and to implement energy management strategies), it is generally helpful to have the battery output in terms of the energy and power domains. The cp-rate can be defined by the rate of constant power that will cause the battery to discharge in a certain amount of time, as explained in [32].

### 3.4. LIB ageing model

The battery lifetime depends on the operation conditions based on temperature, SOC and total energy throughput (electrochemical operating ranges), charge and discharge rates [49] and the total number of cycles. In the case of the present work, particular emphasis will be given to the description of the battery in its current state through the validation of the model approach against the experimental results. The main goal is to have the battery model in its current operational state, validating this model approach with the experimental results. Nevertheless, the LIB ageing effects should be included in the modelling used for real-time predictive optimization control modelling for wider timeframes of simulation. There is no standard model for LIB ageing, although this model should describe the fade mechanisms triggered by cycling patterns, storage, and others. Lifetime fade or degradation (capacity decrease) and cycling fade affect the performance and battery lifetime, impacting its financial results (given the high upfront cost).

The present work approach allows for updating the values of internal resistance (depending on temperature and state of charge) and energy capacity (depending on temperature, T, and cycle count, $N_{cell}$) based on the National Renewable Energy Laboratory (NREL) lifetime model [49]. This model will be included in detail in further work application of this model. The final complete LIB long-term use model is shown in Figure 7.

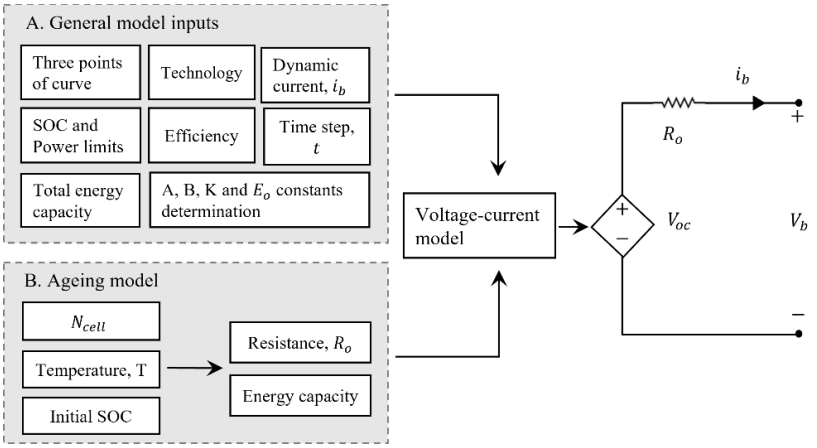


Figure 7 - Complete model of the lithium-ion battery technology approach.

In this figure, A is the exponential voltage amplitude constant (V); B is the time constant inverse (Ah); K is the polarization constant (V/Ah); $E_0$ is the battery constant voltage (V); $N_{cell}$ the number of cells in series; SOC is the state of charge of the battery; $R_0$ is the series resistance of the equivalent model (Ω); $V_{oc}$ is the open-circuit voltage (V) and $V_b$ is the battery terminals voltage (V).

## 4. Results

This section summarizes the main output results of this work, firstly concerning the battery pack and inverter characterization performance, and secondly, the developed model which fits the experimental data previously obtained.

### 4.1. Battery testing and inverter results

Based on the methodology described in Section 3, the battery and inverter characterization data were obtained, and the battery performance indicators were calculated (see *Underlying data* [47] ). The characterization included the realization of at least three cycles for each power level to obtain greater precision and accuracy within the results.

Concerning the inverter charge efficiency (coulombic), it was possible to obtain an average value of 94.8 %, with an STD of 1.4, and regarding discharge, the obtained average value was 95.6 % with an STD of 2.7. The efficiencies defined by the manufacturer are an IEC efficiency of 94.0 % and a maximum efficiency of 95.3 %. Figure 8 presents the data from the inverter manufacturer in the technical document (a) [50] and the experimental data obtained for different power levels for discharge (b) and charge (c).

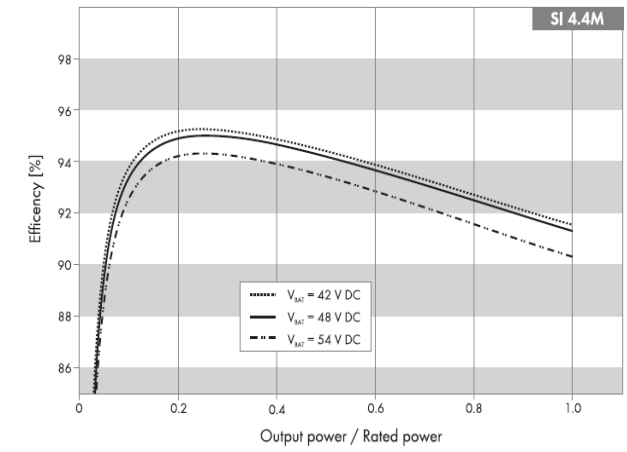


(a)

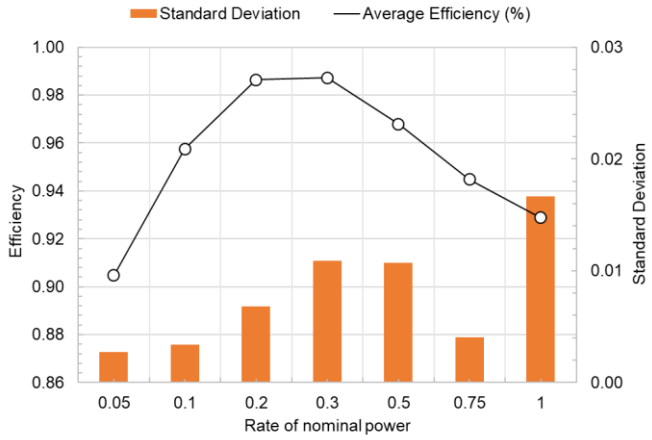


(b)

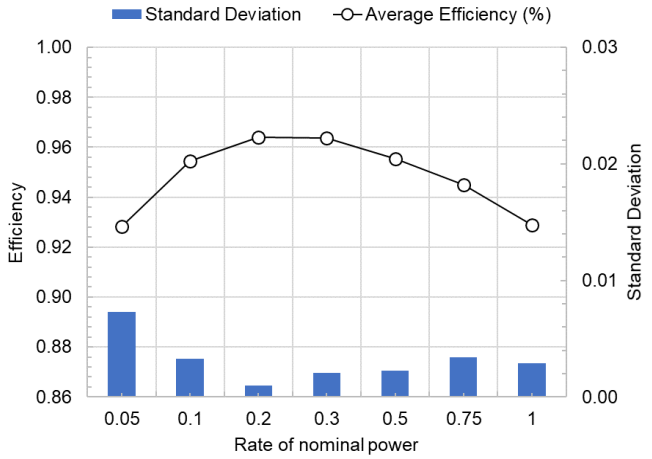


(c)

Figure 8 – Inverter efficiency curve as a function of the power level ( a) given by the manufacturer [50], ( b) from the experimental results of discharge, and ( c) from the experimental results of charge. In this figure, (a) has been reproduced with permission from [50].

Regarding the battery, the charge and discharge efficiencies calculation was based on the DC measurements acquired throughout the tests, presented in Table 3.

Table 3 - Charge and discharge battery cycling results, at constant values of power over the state of charge range.

| Rate of nominal power | AC Power (W) | DC Energy | |
|---|---|---|---|
| | | Average efficiency | Standard deviation |
| 10 | 330 | 0.75 | 0.05 |
| 15 | 500 | 0.84 | 0.01 |
| 20 | 650 | 0.85 | 0.00 |
| 30 | 1000 | 0.84 | 0.07 |
| 50 | 1650 | 0.90 | 0.03 |
| 60 | 2000 | 0.95 | 0.10 |
| 75 | 2500 | 0.96 | 0.05 |
| 80 | 2700 | 0.79 | 0.00 |
| 100 | 3300 | 0.74 | 0.01 |

Figure 9 presents the average battery efficiency at each power level and the correspondent STD. The experimental results made it possible to obtain an overall average battery efficiency of 84.6 % with an STD of 7 %. In Figure 9, the influence of the inverter efficiency dependency on power rating is noticeable.

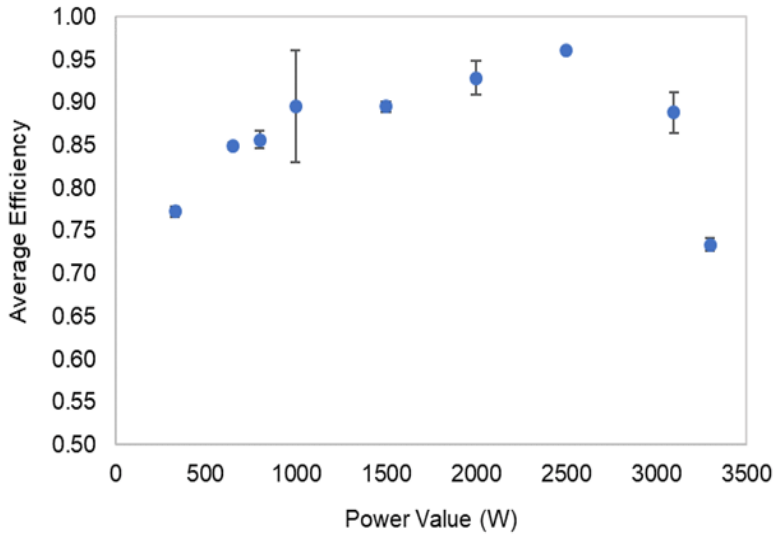


Figure 9 - Battery efficiency at each level of power, and respective standard deviation results.

The tests performed allowed the calculation of other battery indicators besides efficiencies, such as energy capacities, energy densities, full charge and discharge spent times, response times, and typical discharge power. These indicators are presented in Table 4.

Table 4 – Battery performance indicators resulting from the experimental tests.

| Battery Performance Parameters | Units | Results |
|---|---|---|
| Total Capacity (Charge capacity) | kWh | $6.6 \pm 0.5$ |
| Useful maximum capacity (Discharge capacity) | kWh | $5.5 \pm 0.4$ |
| Energy Density in charge by unit of mass | Wh/kg | $86 \pm 6.0$ |
| Energy Density in discharge by unit of mass | Wh/kg | $73 \pm 5.0$ |
| Energy Density in charge by unit of volume | Wh/L | $129 \pm 10$ |
| Energy Density in discharge by unit of volume | Wh/L | $109 \pm 8.0$ |
| Fastest/slowest charge | h | 2h04min / 10h46min |
| Fastest/slowest discharge | h | 1h33min / 3h48min |
| Charge/discharge efficiency (complete cycles) | % | $84.6 \pm 0.1$ |
| Charge/discharge maximum power | kW | 3.3 |
| Response Time | Seconds | < 1s |
| Typical discharge time | h | Hours |

The experimental acquired voltage-current data in function of the battery energy capacity (or SOC) were used to validate the modelling approach of the following Subsection (4.2). Figure 10 exemplifies some of the experimental results obtained.

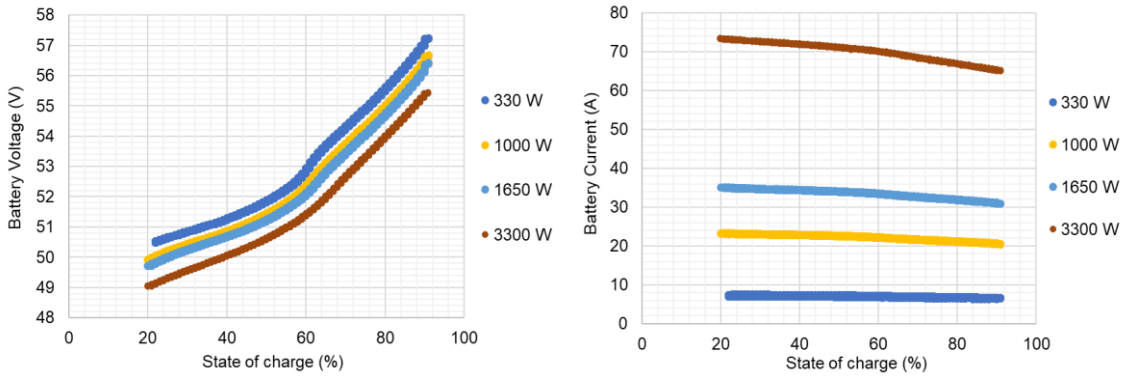


Figure 10 – Lithium-ion battery voltage and current data from the experimental test plan, for complete charge-discharge cycles, at different constant power levels (due to readiness, only few power levels are represented).

## 4.2. Modelling approach to the overall battery operating states

In the literature is common to find references on the battery modelling for one C-rate [28][32] or one E-rate [41]. However, it lacks a solution to describe the battery behaviour over its overall operating frame required to meet the aim of this work: the use for smart power applications' management. The validation of a single power level charge and discharge curve, chosen as the nominal power, was conducted. Regarding the rest of the data validated with different power levels, it was possible to find a regression fit for each, based on the variation of the three extracted points from the curves but keeping all the other variables constant. Below, the approach is detailed.

### 4.2.1. Battery behaviour representation for a single power level

The voltage curve was profiled and used for later model validation for the nominal inverter power level, 3300 W, over the defined SOC range and at a constant ambient temperature of 20°C (measured). For both experimental curves of charge and discharge – the contrary to the manufacturer curves as the modified Shepherd's model defined – the three extracted points of voltage and energy capacity are hereinafter enunciated for the charge in Equation (7),

$$\begin{cases} (V_{full}, Q_{full}) = (60.90, 169) \\ (V_{exp}, Q_{exp}) = (57.35, Q_{full} \times n_{\text{exp\_}c}) \\ (V_{nom}, Q_{nom}) = (52.60, Q_{full} \times n_{nom}) \end{cases} \quad (7)$$

And discharge, in Eq. (8),

$$\begin{cases} (V_{full}, Q_{full}) = (60.90, 169) \\ (V_{exp}, Q_{exp}) = (58.50, Q_{full} \times n_{\text{exp\_}d}) \\ (V_{nom}, Q_{nom}) = (54.60, Q_{full} \times n_{nom}) \end{cases} \quad (8)$$

Where $n_{\text{exp\_}c}$ is a percentage of the $Q_{full}$ to obtain the value of $Q_{exp}$ in the case of charge, and $n_{\text{exp\_}d}$ in the case of discharge. The $n_{nom}$ is a percentage of the $Q_{full}$ to obtain the value of $Q_{nom}$. In the case of the discharge state, the same percentage is given both for charge and discharge.

The values of Equation (7) and Equation (8) were obtained by implementing an iterative cycle. The three values of voltage should obey three conditions: they should be different from each other, obey the order $V_{full}$>$V_{exp}$>$V_{nom}$, and should be in the range of 49 to 61 V. The iterative cycle is initiated with three guessed values made variable within the range of centesimal digits. The iterative cycle tests different values among the

conditions referred, and the obtained curves are then compared with the experimental curve, where the one with the minor error compared with experimental values is used, and the guessed three points (V, Q) are its the correspondent values (presented in Equation (7) and (8) for inverter nominal power). Then, the correspondent energy capacity ($Q_{full}$, $Q_{exp}$, $Q_{nom}$) for that voltage value is obtained. The same procedure took place for the attributed values $n_{\text{exp\_}c}$, $n_{\text{exp\_}d}$ and $n_{nom}$ but now within the 0.1 to 1 range.

This power level's charge and discharge voltage curve presented a root mean square error (RMSE) of near 0.1 V and a maximum relative error of near 1.0 %. The obtained SOC values presented a maximum relative error of near 2.5 %. The experimental and simulated voltage curves for this power level are shown in Figure 11.

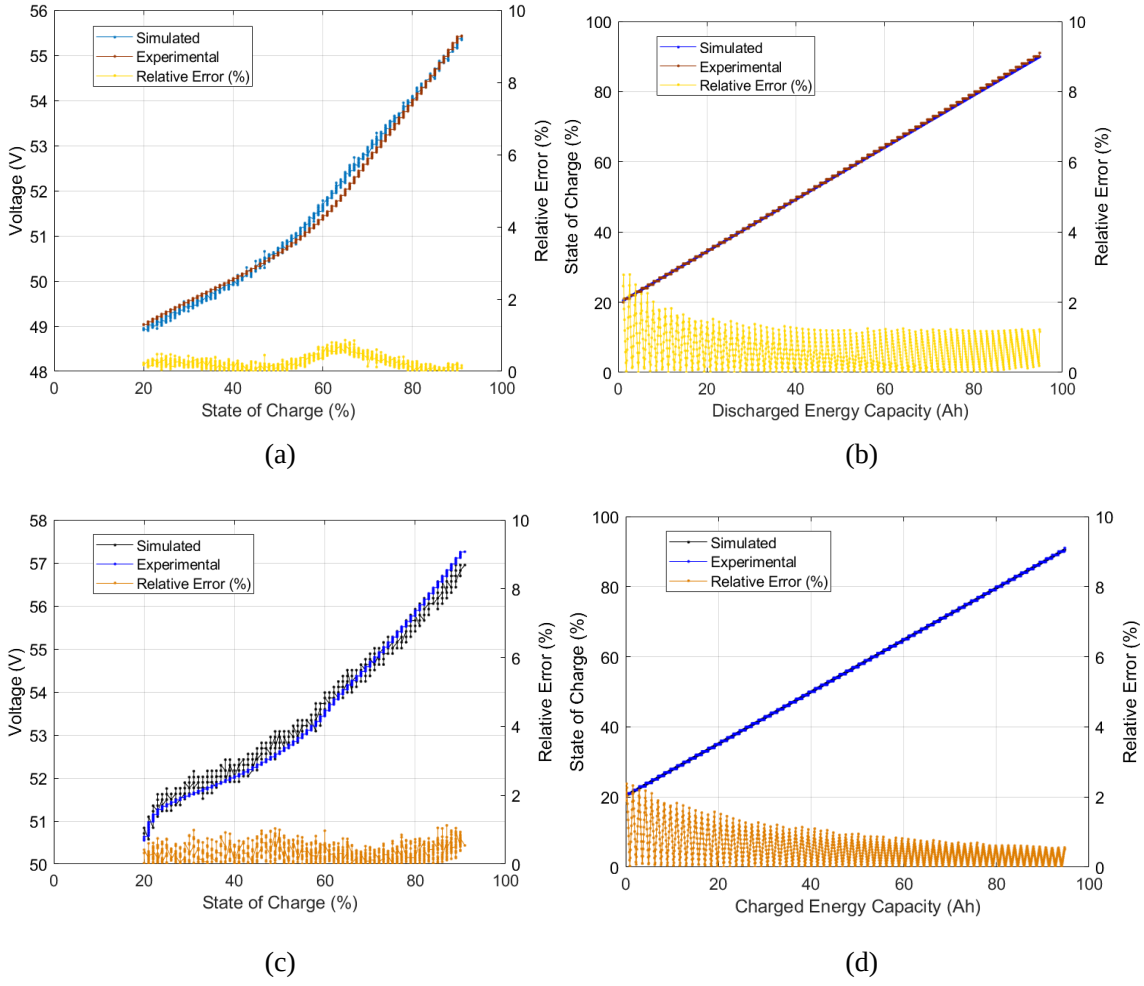


Figure 11 – Model validation simulated vs experimental results for the 3300 W level of power: ( a) discharge voltage- State of Charge (SOC) curve, ( b) discharge SOC-energy capacity curve, ( c) charge voltage-SOC curve, and ( d) charge SOC-energy capacity curve.

### 4.2.2. Battery behaviour representation for all power levels (regression fit)

Figure 11 shows the battery voltage curve over the different states of charge and SOC vs energy capacity of a single power level. For an overall battery description, distinct experimental power level curves should be tested within the simulated model. For the model to describe the different operating power levels of the battery, the three points of voltage and energy capacity (see Equation (7), Equation (8) and Figure 2) correspond to the experimental charge and discharge curves of each power level (or different current level), should be extracted (guessed). In that sense, the following approach aims to adjust the simulated model curves of each power level to the experimental results obtained, as Equation (9) indicates,

$$\begin{aligned}(V_{full}, Q_{full})_{power\_level(soc)} &= (V_{full} + Y, Q_{full} + Z)\\ (V_{exp}, Q_{exp})_{power\_level(soc)} &= (V_{exp} + Y, Q_{exp} + Z)\\ (V_{nom}, Q_{nom})_{power_{level(soc)}} &= (V_{nom} + Y, Q_{nom} + Z)\end{aligned} \quad (9)$$

Equation (9) was used to check the existence of a relationship of Y and Z with the extracted points (guessed) that better describe each power level experimental data. As firstly made to the first power level (Section 4.2.1), points from the experimental curves of each power level were guessed, and afterwards, the values of Y and Z that better fit that data are obtained. A curve-fitting on the best-guessed values that described the battery's experimental data was achieved with the help of the MATLAB curve fitting tools (also existing in alternative software, such as the open-sourced Python), both for charge and discharge operation state. Through the curve fitting, it was possible to find a function that describes the values of Y and Z that should be added/subtracted to the initial guessed three points of the curves. The functions' representations are shown in Figure 12.

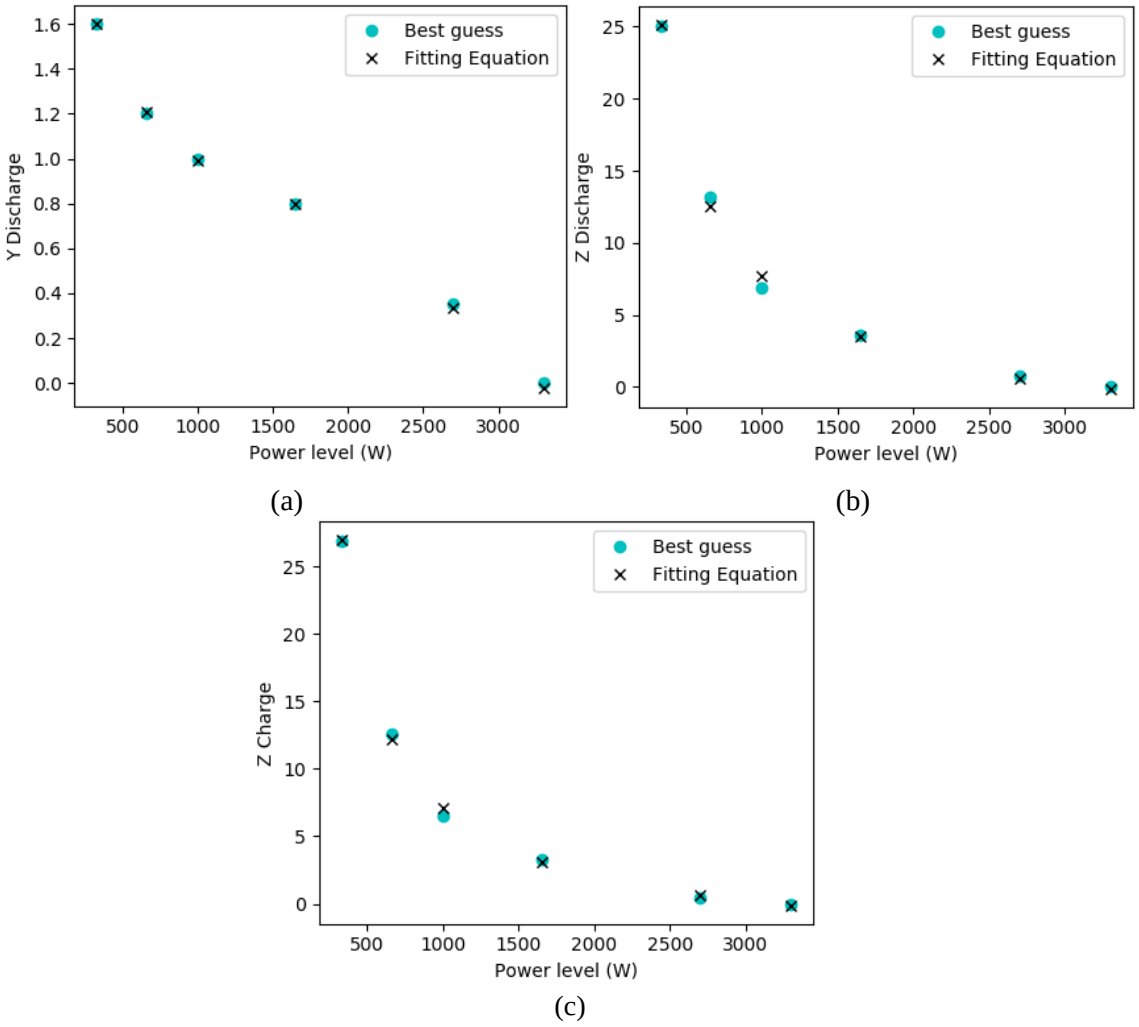


Figure 12 – Y and Z regression fitting values obtained for the charge and discharge operating states, in function of the power levels of the battery operation.

The guessed values that better described the three extracted points were compared with the best-fit function in these figures. The determination of Y and Z for both charge and discharge states offer, in this way, a full battery behaviour description within the experimental values obtained. To observe the voltage regression fit accuracy of the simulated values against the experimental acquired values, Table 5 and Table 6 present the RMSE and maximum relative errors of each fitting point with its correspondent experimental value for discharge and charge operating states, respectively. The obtained regressions allow the battery's description through its distinct operation states in the regular operating conditions. The state of charge at each of the power level obtained values can be observed in Table 7. The developed model is made available in *Software availability* [48].

Table 5 - Comparison of the simulated against experimental voltage values on discharge state, and respective errors (root mean square error (RMSE) and minimum and maximum relative errors).

Where, $n_{exp\_d}$ is a percentage of the $Q_{full}$ to obtain the value of $Q_{exp}$ in the case of discharge curve; $n_{nom}$ is a percentage of the $Q_{full}$ to obtain the value of $Q_{nom}$; $Y_d$ and $Z_d$ are the values to be added to the voltage and energy capacity, respectively, extracted discharged curves.

| Power level (W) | $n_{exp\_d}$ | $n_{nom}$ | $Y_d$ | $Z_d$ | RMSE error (V) | Maximum Relative Error (%) |
|---|---|---|---|---|---|---|
| 330 | 0.77 | 0.98 | 1.60 | 25.1 | 0.74 | 4.81 |
| 660 | | | 1.21 | 12.5 | 5.51 | 5.68 |
| 1000 | | | 0.99 | 7.65 | 1.28 | 3.11 |
| 1650 | | | 0.80 | 3.51 | 0.48 | 2.12 |
| 2700 | | | 0.35 | 0.73 | 0.05 | 1.17 |
| 3300 | | | 0.01 | 0.13 | 3.84 | 4.78 |

Table 6 - Comparison of the simulated against experimental voltage values on charge state, and respective errors (root mean square error (RMSE) and minimum and maximum relative errors).

Where, n exp_ c is a percentage of the Q full to obtain the value of Q exp in the case of charge curve; n nom is a percentage of the Q full to obtain the value of Q nom ; Y c and Z c are the values to be added to the voltage and energy capacity, respectively, extracted charged curves.

| Power level (W) | $n_{exp\_c}$ | $n_{nom}$ | $Y_c$ | $Z_c$ | RMSE error (V) | Maximum Relative Error (%) |
|---|---|---|---|---|---|---|
| 330 | 0.60 | 0.98 | 0.00 | 26.9 | 1.34 | 5.57 |
| 660 | | | 0.00 | 12.2 | 5.27 | 6.74 |
| 1000 | | | 0.00 | 7.07 | 1.06 | 2.75 |
| 1650 | | | 0.00 | 3.05 | 1.02 | 3.02 |
| 2700 | | | 0.00 | 0.60 | 0.47 | 3.78 |
| 3300 | | | 0.00 | 0.12 | 0.10 | 1.61 |

Table 7 - Comparison of the simulated against the experimental SOC values errors (root mean square error (RMSE) and minimum and maximum relative errors).

| Operating state | Charge | | Discharge | |
|---|---|---|---|---|
| Power level (W) | RMSE error (V) | Maximum Relative Error (%) | RMSE error (%) | Maximum Relative Error (%) |
| 330 | 0.78 | 3.12 | 0.60 | 3.90 |
| 660 | 0.37 | 2.97 | 0.25 | 3.67 |
| 1000 | 0.30 | 6.53 | 0.31 | 3.60 |
| 1650 | 1.15 | 2.61 | 0.48 | 5.02 |
| 2700 | 0.20 | 2.62 | 0.79 | 6.02 |
| 3300 | 1.05 | 2.44 | 0.30 | 6.82 |

## 5. Discussion

In this work, a commercial LIB battery pack was the object of experimental tests through its complete charge and discharge at constant levels of a power testing plan. The manufacturer data helped to track the operating range limits and, in the testing, the definition of the overall condition. The establishment of inverter communication allowed the battery testing under controlled conditions. For that reason, the testing output is influenced by this unit. The LIB testing results, which enabled the energetic performance calculation presented in Table 4 and Figure 9, follow the expected results for the tested technology [51][52]. The values obtained for the inverter efficiencies are close to the manufacturer-provided data, with a calculated STD of 2.7 %.

A LIB model is commonly found in literature, mostly based on the MATLAB/Simulink pre-existing model [28][30][31][53]. The reproduction/justification of the model to be applied for a stationary application which could fit the obtained experimental data was not found. Thus, in this work, the authors based the modelling approach on one of the modified Shepherd's models and adapted it to describe the real-time battery dynamic behaviour of the battery integrated into the microgrid.

The results obtained within the model approach used show satisfactory adequacies for all the values experimentally obtained with the LIB. In the discharge state, the higher voltage RMSE is 5.51 V, and the maximum relative error (MRE) is 5.68 %. The MRE obtained for the SOC is about 6.82 %. In the charge state, the highest RMSE for voltage is 5.27 V and an MRE of 6.74 %. The MRE obtained for SOC is 6.53 %. Given the equation fitting and the experimental data errors obtained, generally, the model describes the battery behaviour. The standby operation (self-discharge and inverter

auxiliary consumption) will also be considered in future work for the final complete model.

The temperature effects were not fully considered in this approach. The higher the charge and discharge rates and ambient temperatures, the higher the internal resistance and generally, more heat is generated by the Joule effect. In this case, voltage and energy capacity are affected. The lack of details regarding this present battery composition makes it more challenging to include parameters that could describe those effects. The battery is operated under a controlled ambient temperature range, and the authors believe that the obtained figures for the curves include the slight temperature variations within the obtained errors. Moreover, the temperature dependence variation within the series resistance impacts LIB lifetime. This phenomenon will be approached in further research by considering the model describing the battery behaviour over time (to be used in future energy and economic assessments) and including temperature and SOC effects in the resistance calculation and the temperature and cycling effects in the calculation of battery energy capacity.

The achieved model describes, with small computational effort and fast runtime, the main characteristics of the battery, which facilitates its application within larger models of energy management strategies. The model is validated with different power levels and experimental battery data, improving its modelling of the battery behaviour with variable input profiles.

Similarly to most commercially available LIBs, the LIB manufacturer does not provide information regarding the internal construction, missing information such as the number of cells, parallel and series connections, voltage equalization algorithms, or temperature control algorithms. Missing important information limits the modelling accuracy, generating a higher error in the simulation results. Nevertheless, the maximum error obtained is considered low, being the model accurate to represent the battery performance, even with relevant battery data not being provided by the manufacturer.

## 6. Conclusion

This work applies and validates a model to a 9.80 kWh (189 Ah) lithium-ion commercial battery pack behaviour – voltage-current curves, energy capacity and SOC profiles with real-time variation – to give a potential modelling application to optimization and predictive microgrid programming control (including additional assets

and corresponding models, such as PV systems), specifically for commercial and residential applications.

The correspondence between the general voltage-current models and the operating conditions matching the battery is usually a complex task. In this work, a LIB and inverter experimental setup was built to characterize performance and behaviour with precision monitoring. Communication was established with the battery inverter, enabling it to send real-time commands and get readings. This setup allowed performing the necessary characterization tests under real operating conditions.

Several curve fittings representing the battery behaviour under different operating states with a lower error were obtained. Charge and discharge errors were calculated and observed in Table 5, Table 6, and Table 7, with a maximum relative error of 6.74 % for simulated voltage.

Future work development will include applying this model within a larger simulation model, considering other systems present in the residential and commercial sectors. Further development should also include an ageing model and an energy management strategy, contributing to the technical and economic evaluation. Lithium-ion battery technology will continue to increase within its typical application in the automotive market, with the expectation that the technology will also be used in a second market for stationary applications. Accurate models for stationary application of LIB will provide significant advantages to the market uptake, in particular, for the residential and commercial sectors.

**Data availability**

Underlying data:

Zenodo: Lithium-ion battery charge and discharge testing data - current, voltage, soc, ta - at constant levels of power. https://doi.org/10.5281/zenodo.5196334 44 .

This project contains the following underlying data:

- Lithium_Ion_Battery_Testing_Data.csv (this dataset was used in the composition of the lithium-ion battery testing and modelling validation. The file contains the charge and discharge testing acquisition data - current, voltage, soc, ta - at constant levels of power. The legend of the text is given in the final column “BI” of the .csv file.)

**Software availability**

Source code available from: https://github.com/catSelof/Batteries

Archived source code at time of publication: https://doi.org/10.5281/zenodo.5814884 45

License: LGPL-2.1

**Acknowledgements**

The authors would like to thank the support of this work, developed under the European POCITYF project, financed by 2020 Horizon under grant agreement no. 864400. The authors also thank the support provided by INIESC – Infraestrutura Nacional de Investigação em Energia Solar de Concentração -, FCT / PO Alentejo / PO Lisboa, Candidatura: 22113 – INIESC AAC 01/SAICT/2016 (2017-2021). This work was also supported by the PhD. Scholarship (author Ana Foles) of FCT – Fundação para a Ciência e Tecnologia –, Portugal, with the reference SFRH/BD/147087/2019.

**7. References**

[1] Luis Munuera; Claudia Pavarini, "IEA," *Energy Storage - more efforts needed*, 2020. [Online]. Available: https://www.iea.org/reports/energy-storage. [Accessed: 20-May-2021].

[2] J. Liu, C. Hu, A. Kimber, and Z. Wang, "Uses, Cost-Benefit Analysis, and Markets of Energy Storage Systems for Electric Grid Applications," *J. Energy Storage*, vol. 32, no. February, p. 101731, 2020.

[3] B. Zakeri and S. Syri, "Electrical energy storage systems: A comparative life cycle cost analysis," *Renew. Sustain. Energy Rev.*, vol. 42, pp. 569–596, 2015.

[4] C. Curry, "Lithium-ion Battery Costs and Market Squeezed margins seek technology improvements & new business models," 2017.

[5] L. Mauler, F. Duffner, W. G. Zeier, and J. Leker, "Battery cost forecasting: a review of methods and results with an outlook to 2050," *Energy Environ. Sci.*, vol. 14, no. 9, pp. 4712–4739, Sep. 2021.

[6] K. Mongird, V. Viswanathan, J. Alam, C. Vartanian, V. Sprenkle, and R. Baxter, "2020 Grid Energy Storage Technology Cost and Performance Assessment," 2020.

[7] M. Yoshio, R. J. Brodd, and A. Kozawa, *Lithium-ion batteries: Science and technologies*. Springer New York, 2009.

[8] X. Luo, J. Wang, M. Dooner, and J. Clarke, "Overview of current development in electrical energy storage technologies and the application potential in power system operation," *Appl. Energy*, vol. 137, pp. 511–536, 2015.

[9] Publication Office of the European Union, "Future and Emerging Technologies Workshop on Future Battery Technologies for Energy Storage," Luxembourg, 2018.

[10] T. Aquino, M. Roling, C. Baker, and L. Rowland, "Battery Energy Storage Technology Assessment Platte River Power Authority," p. 27, 2017.

[11] D. Parra *et al.*, "An interdisciplinary review of energy storage for communities: Challenges and perspectives," *Renew. Sustain. Energy Rev.*, vol. 79, no. May 2016, pp. 730–749, 2017.

[12] N. S. Wales, J. Robinson, E. Darmanin, S. Christie, and M. Weirich, *i am your battery guide*. .

[13] E. Hossain, D. Murtaugh, J. Mody, H. M. R. Faruque, M. S. H. Sunny, and N. Mohammad, "A Comprehensive Review on Second-Life Batteries: Current State, Manufacturing Considerations, Applications, Impacts, Barriers Potential Solutions, Business Strategies, and Policies," *IEEE Access*, vol. 7, pp. 73215–73252, 2019.

[14] E. Martinez-Laserna *et al.*, "Battery second life: Hype, hope or reality? A critical review of the state of the art," *Renew. Sustain. Energy Rev.*, vol. 93, no. February 2017, pp. 701–718, 2018.

[15] H. V. S. D. M. Höök, "Lithium availability and future production outlooks." [Online]. Available: https://reader.elsevier.com/reader/sd/pii/S0306261913002997?token=12601FE1ADF103AFD9E3955BE27387573503998DFCC033C2857B815BFF7A70D0BEA153777F369AEA7BF521E773F6CAB9&originRegion=eu-west-1&originCreation=20211202170841. [Accessed: 02-Dec-2021].

[16] A. R. Dehghani-Sanij, E. Tharumalingam, M. B. Dusseault, and R. Fraser, "Study of energy storage systems and environmental challenges of batteries," *Renew. Sustain. Energy Rev.*, vol. 104, no. January, pp. 192–208, 2019.

[17] P. Viebahn, O. Soukup, S. Samadi, J. Teubler, K. Wiesen, and M. Ritthoff, "Assessing the need for critical minerals to shift the German energy system towards a high proportion of renewables," *Renew. Sustain. Energy Rev.*, vol. 49, pp. 655–671, 2015.

[18] UL, *Ul 1642*. 2012.

[19] IRENA, *Quality Infrastructure for Smart Mini-Grids*. 2020.

[20] N. O. T. Authorized, F. O. R. Further, R. Or, D. Without, and P. From, *Ul 2054*. .

[21] European Parliament, "New EU regulatory framework for batteries - Setting sustainability requirements," no. July, 2021.

[22] S. M. Mousavi G. and M. Nikdel, "Various battery models for various simulation studies and applications," *Renew. Sustain. Energy Rev.*, vol. 32, pp. 477–485, 2014.

[23] H. Hinz, "Comparison of lithium-ion battery models for simulating storage systems in distributed power generation," *Inventions*, vol. 4, no. 3, 2019.

[24] F. Saidani, F. X. Hutter, R. G. Scurtu, W. Braunwarth, and J. N. Burghartz, "Lithium-ion battery models: A comparative study and a model-based powerline communication," *Adv. Radio Sci.*, vol. 15, pp. 83–91, 2017.

[25] Y. Diab, F. Auger, E. Schaeffer, and M. Wahbeh, "Estimating Lithium-Ion Battery State of Charge and Parameters Using a Continuous-Discrete Extended Kalman Filter," *Energies*, vol. 10, no. 8, 2017.

[26] A. A. H. Hussein and I. Batarseh, "An overview of generic battery models," *IEEE Power Energy Soc. Gen. Meet.*, no. 4, pp. 4–9, 2011.

[27] Z. Pei, X. Zhao, H. Yuan, Z. Peng, and L. Wu, "An Equivalent Circuit Model for Lithium Battery of Electric Vehicle considering Self-Healing Characteristic," *J. Control Sci. Eng.*, vol. 2018, 2018.

[28] O. Tremblay and L. A. Dessaint, "Experimental validation of a battery dynamic model for EV applications," *World Electr. Veh. J.*, vol. 3, no. 2, pp. 289–298, 2009.

[29] J. Meng, G. Luo, M. Ricco, M. Swierczynski, D. I. Stroe, and R. Teodorescu, "Overview of Lithium-Ion battery modeling methods for state-of-charge estimation in electrical vehicles," *Appl. Sci.*, vol. 8, no. 5, 2018.

[30] S. Barcellona and L. Piegari, "Lithium ion battery models and parameter identification techniques," *Energies*, vol. 10, no. 12, 2017.

[31] Z. Gao, C. S. Chin, W. L. Woo, J. Jia, and W. Da Toh, "Lithium-ion battery modeling and validation for smart power system," *I4CT 2015 - 2015 2nd Int. Conf. Comput. Commun. Control Technol. Art Proceeding*, no. I4ct, pp. 269–274, 2015.

[32] E. Raszmann, K. Baker, Y. Shi, and D. Christensen, "Modeling stationary lithium-ion batteries for optimization and predictive control," *2017 IEEE Power Energy Conf. Illinois, PECI 2017*, pp. 1–7, 2017.

[33] S. S. Madani, E. Schaltz, and S. K. Kær, "An electrical equivalent circuit model of a lithium titanate oxide battery," *Batteries*, vol. 5, no. 1, 2019.

[34] R. M. S. Santos, C. L. G. D. S. Alves, E. C. T. Macedo, J. M. M. Villanueva, and L. V. Hartmann, "Estimation of lithium-ion battery model parameters using experimental data," *INSCIT 2017 - 2nd Int. Symp. Instrum. Syst. Circuits Transducers Chip Sands, Proc.*, Nov. 2017.

[35] Y. Cui *et al.*, "State of health diagnosis model for lithium ion batteries based on real-time impedance and open circuit voltage parameters identification method," *Energy*, vol. 144, pp. 647–656, 2018.

[36] D. Dvorak, T. Bauml, A. Holzinger, and H. Popp, "A Comprehensive Algorithm for Estimating Lithium-Ion Battery Parameters from Measurements," *IEEE Trans. Sustain. Energy*, vol. 9, no. 2, pp. 771–779, 2018.

[37] "LG ESS Battery | Europe." [Online]. Available: https://www.lgessbattery.com/eu/main/main.lg. [Accessed: 03-Dec-2021].

[38] SMA, "SMA Solar Technology AG - Inverter & Photovoltaics solutions." 2016.

[39] LG Chem, "Residential Energy Storage Unit for Photovoltaic Systems," Seoul, Korea, 2016.

[40] A. Baczyńska, W. Niewiadomski, A. Gonçalves, P. Almeida, and R. Luís, "LI-NMC batteries model evaluation with experimental data for electric vehicle application," *Batteries*, vol. 4, no. 1, pp. 1–16, 2018.

[41] MIT Electric Vehicle Team, "A Guide to Understanding Battery Specifications," 2008. [Online]. Available: https://web.mit.edu/evt/summary_battery_specifications.pdf. [Accessed: 30-May-2022].

[42] "O protocolo Modbus em detalhes - NI." [Online]. Available: https://www.ni.com/pt-pt/innovations/white-papers/14/the-modbus-protocol-in-depth.html. [Accessed: 03-Dec-2021].

[43] "Modbus protocol interface | SMA Solar." [Online]. Available: https://www.sma.de/en/products/product-features-interfaces/modbus-protocol-interface.html#c457833. [Accessed: 26-May-2022].

[44] "Modbus protocol interface | SMA Solar." [Online]. Available: https://www.sma.de/en/products/product-features-interfaces/modbus-protocol-interface.html. [Accessed: 03-Dec-2021].

[45] Circutor, "Circutor," *CVM-1D Series*. [Online]. Available: http://circutor.com/en/products/measurement-and-control/fixed-power-analyzers/power-analyzers/cvm-1d-series-detail. [Accessed: 14-Dec-2020].

[46] "34970A Data Acquisition / Data Logger Switch Unit | Keysight." [Online]. Available: https://www.keysight.com/zz/en/products/modular/data-acquisition-daq/digital-acquisition-benchtop-system/34970a-data-acquisition-control-mainframe-modules.html#KeySpecifications. [Accessed: 28-Sep-2021].

[47] A. Foles, "Lithium-ion battery charge and discharge testing data - current, voltage, soc, ta - at constant levels of power," *Zenodo*. [Online]. Available: https://doi.org/10.5281/zenodo.5196334.

[48] A. Foles, "catSelof/Batteries: LIBcode," *Zenodo*. [Online]. Available: https://doi.org/10.5281/zenodo.5790174.

[49] "Battery Lifespan | Transportation and Mobility Research | NREL." [Online]. Available: https://www.nrel.gov/transportation/battery-lifespan.html. [Accessed: 02-Jul-2021].

[50] S. A. Solar Technology, "Installation Manual - SUNNY ISLAND 3.0M / 4.4M / 6.0H / 8.0H," 2016.

[51] R. Amirante, E. Cassone, E. Distaso, and P. Tamburrano, “Overview on recent developments in energy storage: Mechanical, electrochemical and hydrogen technologies,” *Energy Convers. Manag.*, vol. 132, pp. 372–387, 2017.

[52] M. Aneke and M. Wang, “Energy storage technologies and real life applications – A state of the art review,” *Appl. Energy*, vol. 179, pp. 350–377, 2016.

[53] I. Baboselac, T. Benšić, and Ž. Hederić, “MatLab simulation model for dynamic mode of the Lithium-Ion batteries to power the EV,” *Teh. Glas.*, vol. 11, no. 1–2, pp. 7–13, 2017.

## 3.5. Vanadium redox flow battery modelling and PV self-consumption management strategy optimization

Ana Foles[1], Luís Fialho[1], Manuel Collares-Pereira[1], Pedro Horta[1]

In *37th European Photovoltaic Solar Energy Conference and Exhibition*, p. 1418-1425, 2020, ISBN: 3-936338-73-6, 10.4229/EUPVSEC20202020-5EO.2.1

**Abstract**

This work aims to maximize the photovoltaic solar electricity's self-consumption, through the development and validation of an equivalent electric model of a vanadium redox flow battery and its implementation in an energy management strategy. The first phase of the work presents the modelling of the 5.0 kW/60 kWh VRFB integrated in a solar photovoltaic microgrid - 3.5 kWp monocrystalline plus 3.2 kWp polycrystalline technology – at the University of Évora. The model is based in the equivalent electric circuit model built upon the consulted bibliographic references allowing to calculate the battery parameters on the desired power. It considers the auxiliary power consumption and operational parameters and despite its simplicity attains for a good match with experimental results. Upon its validation, the model is further enhanced as to better describe the VRFB real response in its regular operating conditions. Assessment of the enhanced model is based on key performance indicators such as self-consumption rate, rate of battery usage or electric grid independence. In this work an approach to best fit the battery modelling and simultaneously the energy management strategy for a PV+VRFB system is presented, based on actual operating conditions and on a prescribed EMS goal.

**Keywords:** Characterisation, Storage, Strategy

[1] Renewable Energies Chair, University of Évora, Plataforma de Ensaio de Concentradores Solares, Herdade da Mitra – Valverde, 7000-083, Nossa Senhora da Tourega, Évora, Portugal

## 1. Introduction

In 2017 the solar photovoltaic (PV) reached a total installed capacity 98 GW. For 2019 the PV stood for 3 % of the total global power generation mix, with a 2050 forecast of 23 % [1]. Its relevance is being noticed in the countries' national plans worldwide. Increased PV capacity in the power generation system, combined with higher capacity of other low dispatchability renewable electricity sources such as wind, raise the importance of electricity storage as the power distribution system requires a due management of dispatchability.

Despite its importance, battery storage technologies still face challenges as turnkey solutions. Fostering the study and demonstration of different electricity storage technologies, and in the framework of the project PVCROPS 2012-2015 [308468], the Renewable Energies Chair of the University of Évora (CER-UÉvora) has installed and fully integrated a Vanadium Redox Flow Battery (VRFB), 5kW/60kWh, manufactured by REDT company [2] in a microgrid – Figure 1 and 2. This microgrid is currently exclusively devoted for its testing and systems operation study, and integration with the building at real scale.


**Figure 1:** VRFB by manufacturer REDT, 60/5 kWh/kW, installed in the University of Évora.

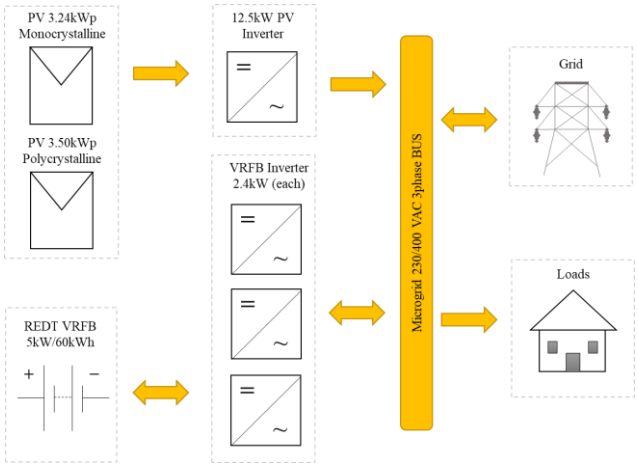


**Figure 2:** VRFB microgrid.

This microgrid is equipped with a PV system with 3.5 $kW_p$ of polycrystalline technology and 3.2 $kW_p$ of monocrystalline technology – Figure 3 –, precision monitoring equipment and the control system. The RFBs are a promising choice for stationary electricity storage in electric grids, regarding power quality and energy management services:

- Power rating depends on stack sizing and stored-energy rating depends on the volume of the tanks. The decoupling of power rating and storage capacity is a competitive advantage of RFBs towards other battery technologies.
- Its response is usually fast, and it is associated to longer lifetimes and low maintenance requirements. It stores energy in two electrolytic solutions with two different redox couples.
- The stack, the energy conversion unit, is made of several cells, forming two electrodes separated by a proton selective membrane. The electrolyte is pumped from the tanks to the stack, where the half-electrochemical reactions occur [3].

The present RFBs have different chemistries: bromine-polysulphide, hydrogen-bromine, magnesium-vanadium, vanadium-bromine, vanadium-cerium, vanadium-oxygen, vanadium polyhalide, vanadium-vanadium, zinc-bromine, zinc-cerium. Although all these configurations, the vanadium-vanadium chemistry is the most mature so far. Introduced in the 1970s and already marketed, there are still some aspects of its operation to explore and improve. The VRFB has the vanadium element in four oxidation states mixed in an aqueous solution of sulfuric acid:

Negative electrode

- $V^{2+}$ (bivalent)
- $V^{3+}$ (trivalent)

Positive electrode

- $VO^{2+}$ (tetravalent)
- $VO_2{}^{+}$ (pentavalent)

Being the electrochemical reactions the following:

- In charge operation:

Negative electrode: $V^{3+} + e^{-} \rightarrow V^{2+}$

Positive electrode: $VO^{2+} + H_2O \rightarrow VO_2{}^{+} + 2H^{+} + e^{-}$

- In discharge operation:

Negative electrode: $V^{2+} \rightarrow : V^{3+} + e^{-}$

Positive electrode: $VO_2{}^{+} + 2H^{+} + e^{-} \rightarrow VO^{2+} + H_2O$

The electrodes are a highly porous carbon/graphite felts, properly treated to improve its hydrophilic capacity, and achieve catalytic effects. This bipolar plate (which exists between each cell), creates the electrical connection between the two opposite poles.

**Figure 3:** University of Évora's PV installation.

The VRFB's stack is a dynamic system, and its performance depends on multiple effects: electrochemical, fluid dynamics, electric and thermal. To obtain the system description, non-linear equations are used, as follows [3]:

- Butler-Volmer equation – Describes electrochemical kinetics and activation overpotentials, as a function of the current density.
- Nernst-Plank equation – Describe the mass transport and ions in the electrodes.
- Vogel-Tammam-Fulcher equation – Considers the ions transport in the membrane.
- *Lattice-Boltzmann model* – Considers the non-linear superdiffusive behaviour of the ions in mesoscale, in anisotropic porous media.

These models are the basis of the multiphysics models which are currently used to describe the VRFB [4]. The level of detail of the model determines the computational resource and processing time to simulate the battery operation [5].

A detailed electric equivalent model considers the loss in the membrane, electrochemical activation in the positive and negative electrodes and the mass flow in the electrodes as resistances, and capacitors representing the double layer effects on the reaction surfaces inside the electrodes. Controlled current sources are used to represent the species crossover between the two electrodes (diffusion e electroosmotic drag), the energy absorption of pumps in circulation as controlled current sources, and an equivalent shunt resistance to account the shunt currents in the solutions.

The aim of this work is to use a model which represents the battery system with adequate precision and that considers the interfaces with the power converters, the battery BMS, and the active components (pumps and valves). To model these components, simpler models are used, such as equivalent circuits that have reduced complexity and satisfying results. In a more simplified approach, it can be concluded that the losses of electrochemical activation are much lower than the ohmic losses of the membrane at full load. Concentration losses are important when the rated current density is exceeded.

Some VRFB models are found in literature, depending on the desired degree of detail. A very detailed modelling review is made by Chakrabarti et al [6], although a simpler model is needed for real world fast computing applications. Chahwan et al. [7] investigated a simple model application, evaluating the fitting for one charge and discharge, achieving satisfactory results. Similar models are the ones developed by D'Agostino et al [5], Nguyen et al [8] and Qiu et al [9], with interesting results on field validations. With an extended Kalman filter, Mohamed [10] explored a model for a unit cell. Wei et al [11] developed an online adaptative model of a VRFB to better reproduce its dynamics. Bhattacharjee et al [12] studied a general electrical model, and also an online SOC estimation. The reviewed models are important benchmarks for the VRFB modelling and were the starting point of this work, giving more emphasis to operational and controlling real-time aspects, in conjunction with the modelling. Considering the aim of developing a model to integrate in an energy management strategy (EMS) for the microgrid as a whole, a compromise between accuracy, simplicity and computational effort possible was assumed in for the model herein presented, implemented in MATLAB [13], and further compared against real data for charge and discharge. The application of the developed model to the EMS is evaluated and discussed, and the strategy merit factors are investigated.

## 2. Battery characterization

The manufacturer REDT made available the data presented in Table I, which is very important information, but not enough to an accurate model. To achieve a robust model, additional details should be used to the battery general characterization. Aiming at gathering data and sensibility to real scale / real-time operation performance, the battery was subjected to characterization tests: six successive full cycles of charge and discharge under reference operating conditions, ranging the state of charge (SOC) from

5% to 90%. To achieve this characterization a dedicated control was developed and implemented in LabVIEW, communicating and registering all the microgrid data with a timestep of 4-5 seconds. This program is followed by precision monitoring to compare the obtained data and correct possible errors in real-time. It registers active and reactive power, voltage, current and many other variables, along the power exchanged with the microgrid.

VRFB is composed by a reference cell, Figure 4, which is hydraulically connected in parallel with the stack, subjected to the same electrolyte flux, without being subjected to charge or discharge, with the aim of making direct real-time voltage measurements. This voltage represents the battery real voltage, since it is only affected by the electrolyte real oxidation state. Through this measurement it is possible to know the real SOC of the battery, through a manufacturer given relation SOC-one cell voltage.

**Table I:** REDT available data.

| **Manufacturer technical specifications** | |
|---|---|
| Rated energy capacity (kWh) | 60 |
| Number of cells in the stack | 40 |
| Operating voltage range (V) | Up to 65 |
| Volume ($m^3$) | 1.8 (each tank) |
| Depth of discharge (%) | 95 |
| Lifetime (cycles) | +10000 |

**Figure 4:** Stack of the VRFB and its reference cell.

Battery characterization test data was analyzed, and average results are presented in Table II.

**Table II:** Experimental obtained parameters.

| **VRFB performance** | **Results** |
|---|---|
| Total capacity (kWh) | 86.3 ± 2.30 |
| Useful maximum capacity (kWh) | 66.5 ± 4.26 |
| Energy density (Wh/L) | 17.5 ± 4.26 |
| Fastest charge (h) | 51h41 |
| Fastest discharge (h) | 26h54 |
| Charge/discharge efficiency | 77.1 ± 3.36 |
| Maximum power (kW) | 5.0 |
| Response time | Seconds (s) |
| Cell voltage operating range (V) | 1.249-1.513 |
| Typical response time | Hours |

The values obtained were compared with bibliographic references, [14]–[19], and show consistency.

## 3. Electrical VRFB model

To determine the electrical requirements for the power battery management system (BMS), the main effects to be considered are the drop in resistive voltage in the membrane, allowing a simple estimation of the cell voltage, through the Eq. (1) [3]:

$$v_c \cong E(s) - \Delta v_t = E(s) - r_t j \quad (1)$$

The stack losses and battery efficiency are influenced by two main factors: pumps and shunt currents, further discussed. A simplified modelling approach considers cells internal losses and all the battery external losses, since the aim is to detail its electrical behaviour. The model is built upon already existent models of the vanadium redox flow battery, adapting it to the real operation of this battery. In Figure 5 the equivalent electric model is shown.

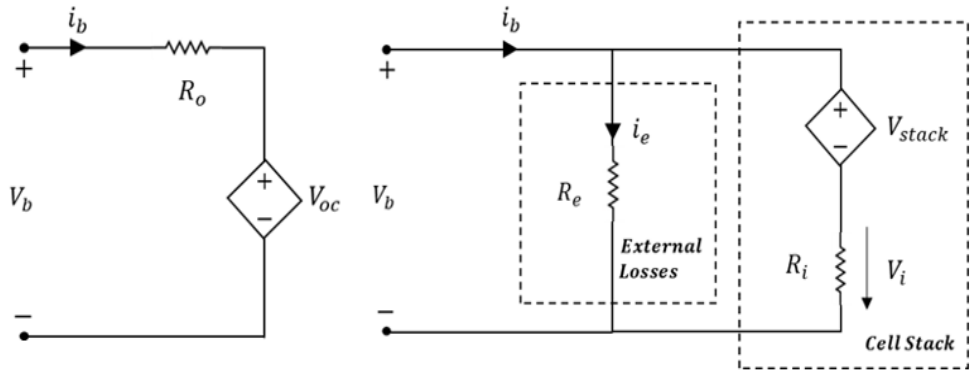


**Figure 5**: Equivalent electric model scheme used to describe the VRFB operation.

### 3.1. Stack Voltage

The battery voltage, $V_b$, is calculated after Eq. (2):

$$V_b = V_{Stack} + i_{stack} R_i \tag{2}$$

Where $V_{Stack}$ is the stack voltage and $i_{stack}$ is the stack current. The stack current is obtained through the application of the Kirchhoff's first law, as Eq. (3) presents:

$$i_{stack} = i_b - i_e \tag{3}$$

Where $i_b$ is the battery current, and $i_e$ the current of the external losses.

The voltage of the stack depends on the SOC, temperature (T, in K), and the number of cells of the stack, $n_{cells}$. The open circuit voltage is given by the Nernst equation, shown in Eq. (4), which includes the knowing of the electrolyte ions concentration and determines the solution modularity,

$$E = E^0 + \frac{R \times T}{F} \times \ln\left[\frac{C_{VO_2^+}(C_{H^+})^2 C_{V^{2+}}}{C_{VO^{2+}} C_{V^{3+}}}\right] \tag{4}$$

Where, $E^0$represents the Gibbs potential, $R$ the universal gas constant (8.314 J/mol.K), T is the temperature in Kelvin, F the Faraday constant (96485 sA/mol). The vanadium ions concentration is given by Eq. (5) and by Eq. (6):

$$C_{V^{2+}} = C_{VO_2^+} = C_V \, SOC \tag{5}$$

$$C_{V^{3+}} = C_{VO^{2+}} = C_V(1 - SOC) \tag{6}$$

The voltage of a single cell of the stack can be approximated to Eq. (7):

$$\frac{V_{Stack}}{n_{cells}} = V_{SOC,50\%} + \frac{R \times T}{F} \times \ln\left[\frac{SOC^2}{(1 - SOC)^2}\right] \tag{7}$$

Being the $V_{SOC,50\%}$ the voltage of a single cell at the SOC of 50%. Finally, the total stack voltage is given by Eq. (8),

$$V_{Stack} = n_{cells} \times \left\{ V_{Soc,50\%} + \frac{R \times T}{F} \times \ln\left[ \frac{SOC^2}{(1 - SOC)^2} \right] \right\} \quad (8)$$

### 3.2. Resistances

The selected model has a time resolution in the order of microseconds, which is satisfactory for the solar photovoltaic and loads response time as well as our control running time. The cell stack losses are described as one single resistance of Thevenin, $R_i$, representing the reaction resistive losses. The equivalent resistance is estimated as quasi-constant in processes of charge and discharge, and is represented through Eq. (9),

$$R_i = \sum_{1}^{k} \frac{V_{b,k} - V_{stack,k}}{i_{stack,k}} \quad (9)$$

Being $V_{b,k}$ the battery terminal voltage, $V_{stack,k}$ the stack voltage, $i_{stack,k}$ the stack current, all at instant k. The external losses (pumps) could be achieved using Eq. (10):

$$R_e = \frac{V_b}{i_e} \quad (10)$$

### 3.3. State of charge

The battery SOC can be calculated through Eq. (11) and Eq. (12).

$$SOC_{t_n} = SOC_t + \Delta SOC_{t_k - t} \quad (11)$$

$$SOC_{t_n} = SOC_t + \int_t^{t_k} \frac{V_{stack}(t) i_s(t)}{E_{Capacity}} \, dt \quad (12)$$

Being the $E_{Capacity}$ (Wh) the total capacity of the battery. This model was compared with experimental data, through the full characterization data obtained of the VRFB real operation, and some adaptation of the model was made to better fit our goal.

## 4. Model adaptations and simulation results

### 4.1. Voltage at 50% of SOC and Resistances

Given the manufacturer SOC curve of the VRFB described in [20], the cell reference voltage is 1.400 V, at 50% of SOC, as can be observed with the help of Figure 6. For

comparison, the obtained SOC of the battery in the studied interval is calculated through the manufacturer curve, as shown in the work developed in [20].

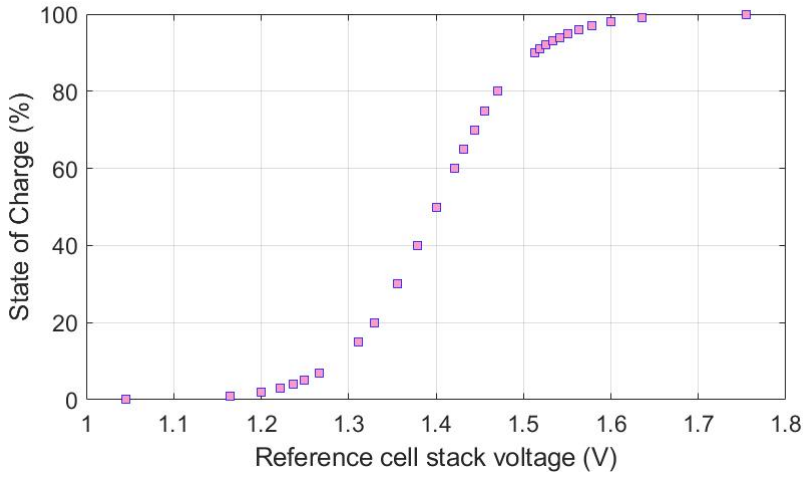


**Figure 6:** SOC (%) in function of the reference cell stack voltage (V).

After the tests and comparison with the experimental data, the calculation of the resistance after Equation 8 was improved for charge and discharge. An average for each resistance was obtained, with a value of 0.07Ω for charge and 0.20Ω for discharge.

The current needed to power the pumps of the VRFB is considered constant in this work, since its consumption varies very little within the stack voltage of the battery, i.e., the SOC. This value was, on average, 1.8702 A, as can be observed in the following Figure 7, for real charge and discharge data.

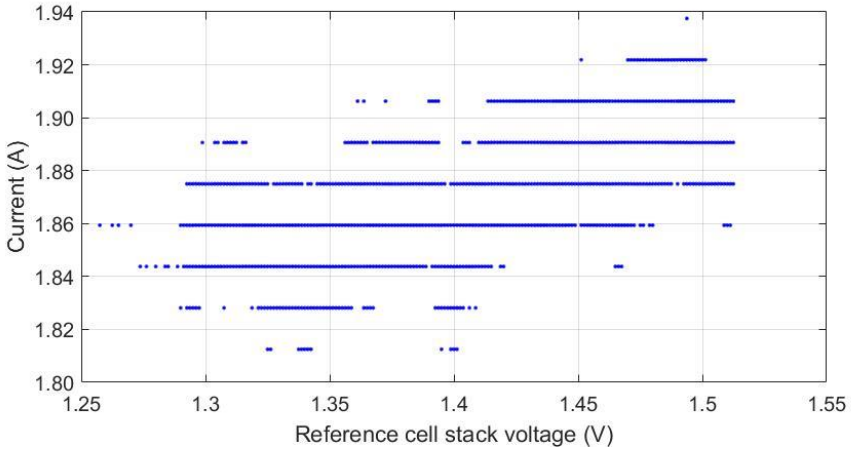


**Figure 7:** Auxiliar current in function of the reference cell stack voltage.

Besides this adaptation, a sensibility analysis of the obtained results and parameters of the model was made. The relation of the reference cell voltage-SOC had good results, so it does not need further improvements. The $V_{soc50}$ was the value which offered the best fitting.

Unfortunately, the experimental stack current was not measured during the tests, since the sensor was malfunctioning, so this parameter was not evaluated in the scope of the present paper.

### 4.2. Implementation and validation

The battery was fully characterized within the operational range for the SOC from 5% to 90%, given the operational available power of charge and discharge for that range. The maximum power of either charge or discharge is 5000 W. In the battery room, an air conditioning is working to maintain an ambient temperature of 24ºC. We assume a constant storage temperature of 26ºC. The model input data is shown in Table III. In Figure 8 the obtained values of the voltage stack are given, in conjunction with its relative error.

According to the model application, simulation, and overall control, it is possible to present the obtained parameters of the battery model in Table IV.

**Table III:** Model input parameters.

| **Input parameter** | **Data** |
|---|---|
| Power profile (W) | - |
| Initial SoC (%) | 7.5 |
| Vsoc50 (V) | 1.400 |
| Parasitic resistance charge (RPC) | 0.05 |
| Parasitic resistance discharge (RPC) | 0.07 |
| Losses resistance charge (RCC) | 0.04 |
| Losses resistance discharge (RCD) | 0.20 |
| Temperature (K) | 26+273.15 |
| Number of cells in the stack | 40 |
| Faraday constant (As/mol) | 96485 |
| Pump DC power (W) | 300 |
| Pump AC power (W) | 350 |
| Gas constant | 8.314 |

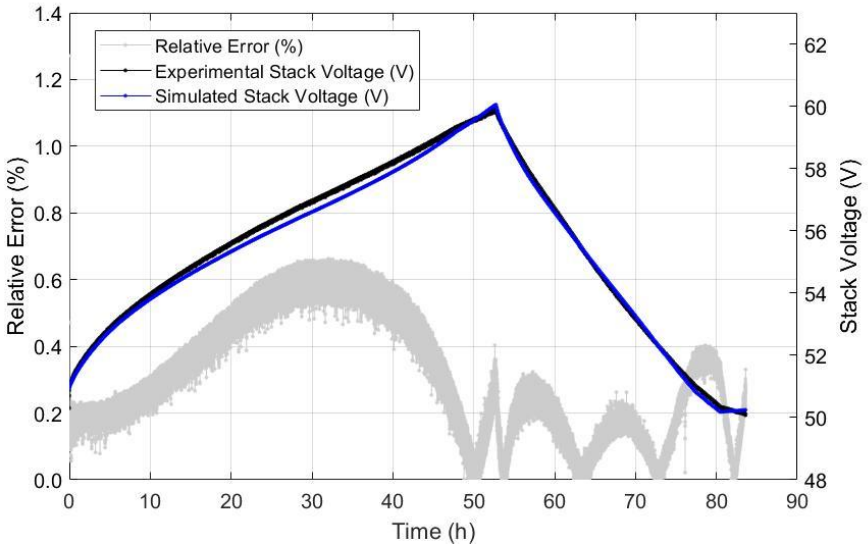


**Figure 8:** Stack voltage experimental and simulated, and the respective relative error.

**Table IV:** Obtained model parameters errors.

| Parameter | RMSE | Mean relative error |
|---|---|---|
| Stack voltage | 0.4143 V | 0.2991 |
| Voltage terminal | 1.3716 V | 0.6141 |
| Current terminal | 2.8858 A | 0.0180 |

## 5. EMS – Self-consumption strategy

### 5.1. EMS

Portugal has in force the Decree-Law 162/2019 (25$^{th}$ October) which gives a very strong emphasis to the renewable energy self-consumption. In that context, we choose to evaluate this model using this EMS, since it is the most suitable strategy for a residential scale. The PV self-consumption maximization with the use of a battery was explored to check the suitability of the application methods in real time operation. A specially devoted LabVIEW programme was developed for this control strategy, with internal implementation of the VRFB model. The user interface is showed in Figure 10.

For this strategy application, real-time data of the PV system over 6 days was tested. The decision to eliminate some parts of the null PV generation was made in order to shorten the time duration of the test in real-time. The load profile is made available by EDP Comercial website and corresponds to an estimation for 2019 average Portuguese loads, for BTN C (normal low voltage, residential) [21]. This publicly available data is a

fifteen-minute average, based on the year-before loads. This data is published at unit scale and was scaled to fit the PV installed power in the microgrid. The resulting load profile is presented in Figure 9.

After some simulations, a response time window of 3-5 seconds is achieved with success allowing real time control to be possible. In each control cycle the commands are sent, all the variables read and registered. To proper evaluate the strategy application, the best suited key-performance indicators were calculated.

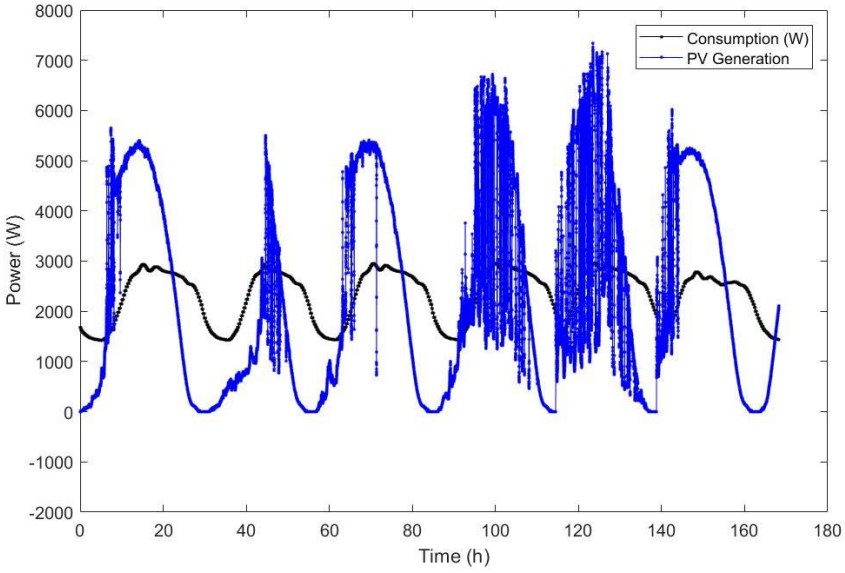


**Figure 9:** PV profile and load consumption.

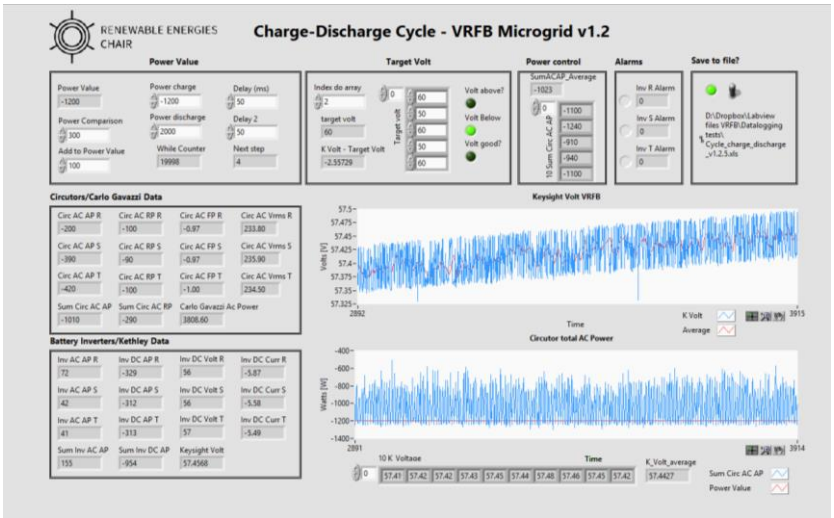


**Figure 10:** LabVIEW EMS implementation.

### 5.2. Key-performance indicators

- **Self-consumption ratio (SCR)** – Share of the PV generation consumed by the installation from the total of the PV energy generation.

$$SCR = \frac{E_{PVconsumed}}{E_{PVgenerated}} \tag{13}$$

Where, $E_{PVconsumed}$ is the PV energy generation consumed directly or indirectly (e.g., battery auxiliary consumption), and the $E_{PVgenerated}$ is the total PV energy generated by the PV system.

- **Self-sufficiency ratio (SSR)** – Share of the consumed PV energy generation in the total load consumption needs.

$$SR = \frac{E_{PVconsumed}}{E_{Load}} = \frac{E_{Load} - E_{Grid}}{E_{Load}} \tag{14}$$

Where, $E_{Load}$ is the total load consumption needs, and the $E_{Grid}$ is the sum of the energy, which is injected and extracted from the network grid, in the overall strategy.

- **Grid-relief factor (GRF)** – The grid relief factor offers a measure of the total grid use in the overall load consumption needs.

$$GRF = \frac{E_{Load} - E_{Grid}}{E_{Load}} \tag{15}$$

- **Overall battery use (OBU)** – Share of energy of the power battery command in the overall energy consumption.

$$OBU = \frac{E_{Load} - (E_{charge} + E_{discharge})}{E_{Load}} \tag{16}$$

Where, $E_{charge}$ is the total energy used to charge the battery, and the $E_{discharge}$ is the total energy used to discharge the battery, in the overall strategy.

- **Battery charge ratio (BCR)** – Total energy used to charge the battery, in the overall power battery commands sent to the battery.

$$BCR = \frac{E_{charge}}{E_{battery\_command}} \tag{17}$$

Where, $E_{battery\_command}$ is the total energy sent to charge and discharge the battery, in absolute values.

- **Energy from the grid (EG)** – Amount of energy extracted from the grid, considering the total grid use.

$$G = \frac{E_{fromGrid}}{E_{Grid}} \tag{18}$$

Where, $E_{fromGrid}$ is the energy needed to extract from the grid to supply the energy needs, in the overall strategy.

- **From grid use (FGU)** – Amount of energy extracted from the grid in the overall energy needs.

$$FGU = \frac{E_{fromGrid}}{E_{Load}} \tag{19}$$

- **To grid use (TGU)** - Amount of energy injected into the grid in the overall energy needs.

$$TGU = \frac{E_{toGrid}}{E_{Load}} \tag{20}$$

Where, $E_{toGrid}$ is the energy sent to the grid.

- **From battery use (FBU)** – Amount of energy extracted from the battery in the overall energy needs.

$$FBU = \frac{E_{fromBattery}}{E_{Load}} \tag{21}$$

Where, $E_{fromBattery}$ is the energy used to discharge from the battery.

- **To battery use (TBU)** – Amount of energy sent to the battery in the overall energy needs.

$$TBU = \frac{E_{toBattery}}{E_{Load}} \tag{22}$$

Where, $E_{toBattery}$ is the energy used to charge the battery.

### 5.3. EMS results evaluation

Regarding the overall EMS evaluation, the key-performance indicators obtained for this test are presented in Table V. One of the most important parameters for the battery control is the SOC at each point for the EMS to run accordingly. Figure 11, below shown, presents the obtained SOC evolution during the test timeframe, and Figure 12 represents the power exchanged with the battery and the power exchanged with the grid, over the experiment.

**Table V:** Resulting model Key Performance Indicators, over the 6 days of implementation.

| **Parameter** | Value [%] |
|---|---|
| Self-consumption ratio (SCR) | 67.02 |
| Self-sufficiency ratio (SSR) | 64.66 |
| Grid-relief factor (GRF) | 15.71 |
| Overall battery use (OBU) | 52.02 |
| Battery Charge Ratio (BCR) | 52.26 |
| Energy from the grid (EG) | 70.65 |
| From grid use (FGU) | 11.10 |
| To grid use (TGU) | 4.612 |
| From battery use (FBU) | 26.72 |
| To battery use (TBU) | 25.29 |

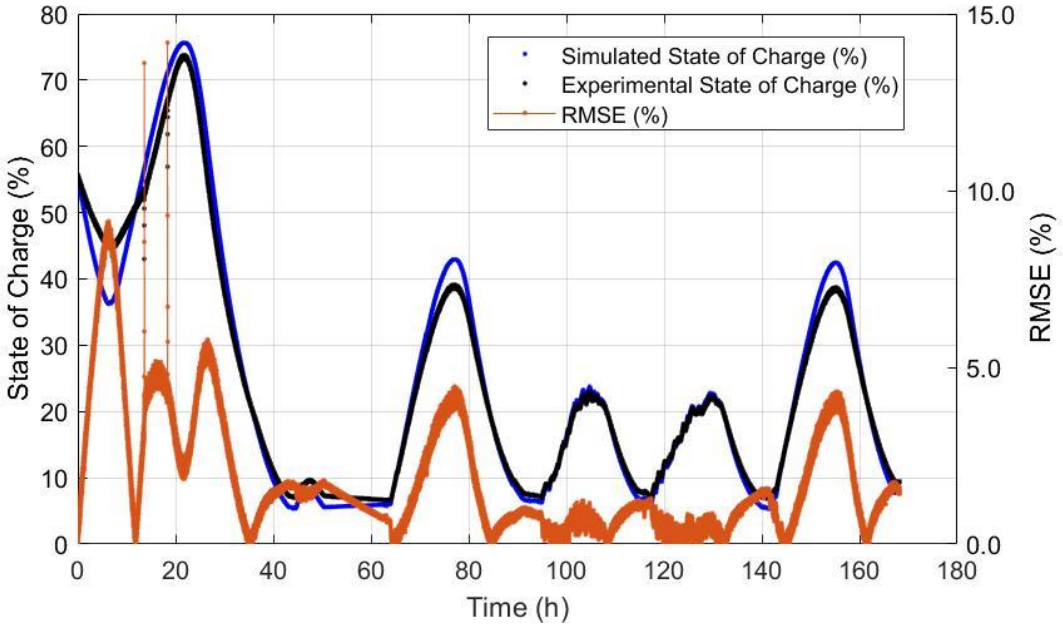


**Figure 11:** SOC of the VRFB along the EMS test period.

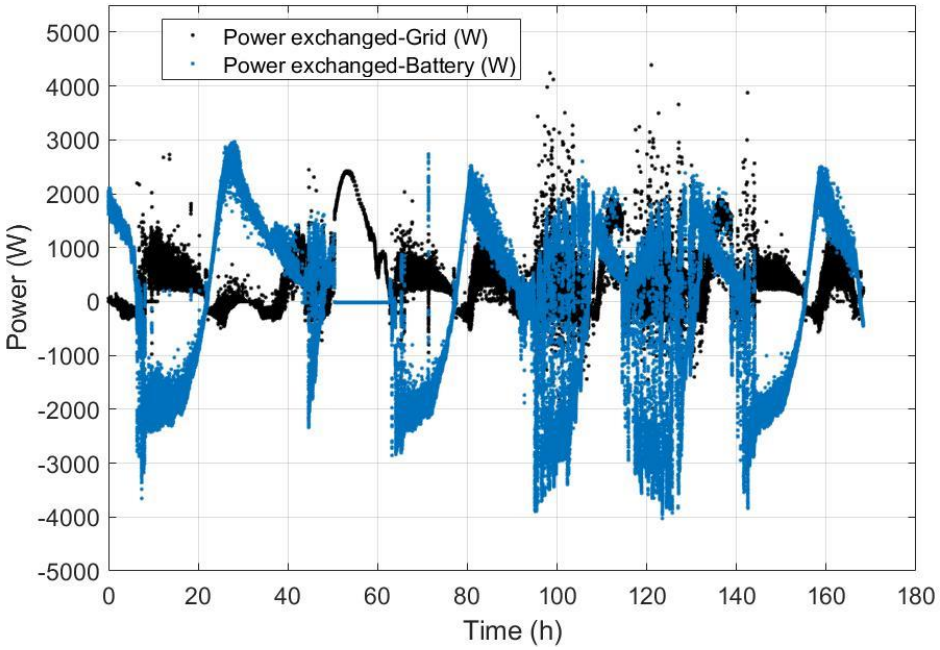


**Figure 12:** Power exchanged with the battery and the power exchanged with the grid, in the test period.

### 5.4. Results discussion

The equivalent electric circuit model of the VRFB has generated low error results for the key parameters (stack voltage, terminal voltage and terminal current), with increased computational simplicity and efficiency, as shown in the Figure 8 and Table IV. It accounts for the major VRB issues including thermal effects, transients, and dynamic SOC. The model seems to be suited for long term operation with lower computational effort, being validated by the presented results.

One of the problems in the battery characterization tests was the malfunctioning of the stack current sensor. This issue was already addressed and ongoing work on the model will also fine-tune this model parameter, lowering even further the error results presented here.

The validation of this model for the VRFB with experimental data in real operating conditions and at full scale, allowed to validate an equivalent electric circuit model requiring less computational resources, and implementing it within a microgrid EMS.

This EMS was tested and the resulting KPIs are consistent with good performance of the overall goal of self-consumption maximization. It resulted in values of SCR and SSR of 67% and 65% (respectively). TBU and FBU, indicators related to battery usage

achieved 25% and 27%, to and from battery use respectively, over all the energy flow in the microgrid. With this strategy, a value of GRF of around 16% points to good results, given the PV generation with heavy intermittency due to clouds (Figure 9).

The simulated SOC presented low error (Figure 11), pointing to good model performance, thus validating it. Even though it is not an important simulation parameter for real control, since VRFB technology allows to measure this quantity in real time of battery operation, this is an important result for validation of the developed model.

The overall results obtained, point to a good approximation of the key parameters by the developed model and a good performance of the energy management strategy, reaching a self-consumption rate of 67%, even with very cloudy days.

The way of operating, control and test the battery are crucial aspects to achieve a good match among the simulation model and the real-time response. The developed control was made to achieve the best key-performance indicators and respecting the general operating limits of the battery.

## 6. Conclusions

Literature lacks optimal VRFB modelling, including ancillaries and power electronics solutions, modelling the electric, chemical and fluid-dynamic parameters according to the electric input and output power requirements. The fact that the VRFB has an online SOC real-time measurement, based on the reference stack voltage, allows a more precise control to be made, regarding other storage technologies, increasing its lifetime and reliability.

The presented results validate the developed simplified VRFB model and its implementation within a EMS was fully concluded achieving good final KPIs.

Implementing lower computational effort models allows the development of more intelligent energy management strategies, taking into account the optimization of internal battery model operating parameters. Implementing this EMS with fast response times (control loop under 3-5s) enable to deal with rapid intermittency or fast power ramps due to the load characteristics to be supplied.

In this work we chose to work with the simplest model with the highest accuracy, and the obtained results are as expected. The aim of the model is to be used in energy management strategies, and the results validate this assumption. Future work can

include fine-tuning of internal model parameters and inclusion in other EMS or even EMS for hybrid battery systems.

**Acknowledgements**

The authors would like to thank the support of this work, developed under the European GRECO project, financed by 2020 Horizon under the grant agreement no. 787289. This work was also supported by the PhD. Scholarship (author Ana Foles) of FCT – Fundação para a Ciência e Tecnologia –, Portugal, with the reference SFRH/BD/147087/2019.

## 7. References

[1] Arina Anisie *et al.*, "Innovation landscape for a renewable-powered future: Solutions to integrate variable renewables," 2019.

[2] "redT energy storage." [Online]. Available: http://www.redtenergy.com.au/.

[3] M. Guarnieri, P. Mattavelli, G. Petrone, and G. Spagnuolo, "Vanadium Redox Flow Batteries," *IEEE Ind. Electron. Mag.*, no. december, pp. 20–31, 2016.

[4] P. Alotto, M. Guarnieri, and F. Moro, "Redox flow batteries for the storage of renewable energy: A review," vol. 29, pp. 325–335, 2014.

[5] R. D'Agostino, L. Baumann, A. Damiano, and E. Boggasch, "A Vanadium-Redox-Flow-Battery Model for Evaluation of Distributed Storage Implementation in Residential Energy Systems," *IEEE Trans. Energy Convers.*, vol. 30, no. 2, pp. 421–430, 2015.

[6] B. Chakrabarti *et al.*, "Modelling of redox flow battery electrode processes at a range of length scales: a review," *Sustain. Energy Fuels*, 2020.

[7] J. Chahwan, C. Abbey, and G. Joos, "VRB Modelling for the Study of Output Terminal Voltages , Internal Losses and Performance," pp. 387–392, 2007.

[8] T. A. Nguyen, X. Qiu, J. David, G. Ii, M. L. Crow, and A. C. Elmore, "Performance Characterization for Photovoltaic-Vanadium Redox Battery Microgrid Systems," vol. 5, no. 4, pp. 1379–1388, 2014.

[9] X. Qiu, T. A. Nguyen, J. D. Guggenberger, M. L. Crow, and A. C. Elmore, "A field validated model of a vanadium redox flow battery for microgrids," *IEEE Trans. Smart Grid*, vol. 5, no. 4, pp. 1592–1601, 2014.

[10] M. R. Mohamed, H. Ahmad, M. N. A. Seman, S. Razali, and M. S. Najib, "Electrical circuit model of a vanadium redox flow battery using extended Kalman filter," *J. Power Sources*, vol. 239, pp. 284–293, 2013.

[11] V. Viswanathan *et al.*, "Cost and performance model for redox fl ow batteries," *J. Power Sources*, vol. 247, pp. 1040–1051, 2014.

[12] A. Bhattacharjee and H. Saha, "Design and experimental validation of a generalised electrical equivalent model of Vanadium Redox Flow Battery for interfacing with renewable energy sources," *J. Energy Storage*, vol. 13, pp. 220–232, 2017.

[13] "MathWorks." [Online]. Available: https://www.mathworks.com/products/matlab.html.

[14] IEC, "Electrical Energy Storage."

[15] EASE, "Flow Battery."

[16] R. Amirante, E. Cassone, E. Distaso, and P. Tamburrano, "Overview on recent developments in energy storage: Mechanical, electrochemical and hydrogen technologies," *Energy Convers. Manag.*, vol. 132, pp. 372–387, 2017.

[17] H. Lopes, R. Garde, G. Fulli, W. Kling, and J. Pecas, "Characterisation of electrical energy storage technologies," *Energy*, vol. 53, pp. 288–298, 2013.

[18] G. L. Kyriakopoulos and G. Arabatzis, "Electrical energy storage systems in electricity generation: Energy policies, innovative technologies, and regulatory regimes," *Renew. Sustain. Energy Rev.*, vol. 56, pp. 1044–1067, 2016.

[19] X. Luo, J. Wang, M. Dooner, and J. Clarke, "Overview of current development in electrical energy storage technologies and the application potential in power system operation," *Appl. Energy*, vol. 137, pp. 511–536, 2015.

[20] L. Fialho, T. Fartaria, L. Narvarte, and M. C. Pereira, "Implementation and validation of a self-consumption maximization energy management strategy in a Vanadium Redox Flow BIPV demonstrator," *Energies*, vol. 9, no. 7, 2016.

[21] EDP Distribuição, "Atualização dos perfis de consumo , de produção e de autoconsumo para o ano de 2018 Documento Metodológico," 2017.

# CHAPTER 4

# Energy Management Strategies of VRFB and LIB and their Hybridisation

---

## 4.1. Introduction

Chapter 4 introduces concepts of operating the batteries using energy management strategies algorithms under real-time operation. At the residential and buildings scale, the batteries provide flexibility to the novel networks and increase the decentralisation of energy generation with the integration of variable renewable energy. Moreover, they provide a sustained role to couple smart home appliances and their innovative management. Among the various technologies composing the Renewable Energies Chair microgrid, this work focuses on the VRFB and lithium-ion batteries based on their recognised potential in the current and future scenarios for stationary energy storage. This chapter discusses the role of distributed energy storage with VRFB management. In addition, the inclusion of a lithium-ion battery in the VRFB single case is added to check the economic impact, which leads to the concepts of ESS hybridisation and power allocation and energy management strategies investigation. The investigated concepts developed throughout this thesis are relevant contributions to the HyBRIDSTORAGE project in developing a software simulation tool supported by constructing a real-scale prototype.

## 4.2. An approach to implement photovoltaic self-consumption and ramp-rate control algorithm with a vanadium redox flow battery day-to-day forecast charging

Ana Foles[1,2], Luís Fialho[1,2], Manuel Collares-Pereira[1,2], Pedro Horta[1,2]

In *Sustainable Energy, Grids and Networks, 2022, vol. 30, 100626, ISSN 2352-4677,*
https://doi.org/10.1016/j.segan.2022.100626
*Open access version in ArXiv:* https://doi.org/10.48550/arXiv.2012.11955

**Abstract**

The variability of the solar resource is mainly caused by cloud passing, causing rapid power fluctuations on the output of photovoltaic (PV) systems. The fluctuations can negatively impact the electric grid, and smoothing techniques can be used as attempts to correct it. However, the integration of a PV+VRFB to deal with the extreme power ramps at a building scale is underexplored in the literature, as well as its effectiveness in combination with other energy management strategies (EMSs). This work is focused on using a VRFB to control the power output of the PV installation, maintaining the ramp rate within a non-violation limit and within a battery state of charge (SOC) range, appropriate to perform the ramp rate management. Based on the model simulation, energy key-performance indicators (KPI) are studied, and validation in real-time is carried. Three EMSs are simulated: a self-consumption maximisation (SCM), and SCM with ramp rate control (SCM+RR), and this last strategy includes a night battery charging based on a day ahead weather forecast (SCM+RR+WF). Results show a battery SOC management control is essential to apply these EMSs on VRFB, and the online weather forecast proves to be efficient in real-time application. SCM+RR+WF is a robust approach to manage PV+VRFB systems in wintertime (studied application), and high PV penetration building areas make it a feasible approach. Over the studied week, the strategy successfully controlled 100% of the violating power ramps, also obtaining a self-consumption ratio (SCR) of 59% and a grid-relief factor (GRF) of 61%.

**Keywords:** Photovoltaic solar energy; energy storage; self-consumption; ramp rate; VRFB; energy management strategies

[1]Renewable Energies Chair, University of Évora. Pólo da Mitra da Universidade de Évora, Edifício Ário Lobo de Azevedo, 7000-083, Nossa Senhora da Tourega, Portugal
[2]Institute of Earth Sciences, University of Évora, Rua Romão Ramalho, 7002-554, Évora, Portugal

**Nomenclature**

| | |
|---|---|
| API | Application Programming Interface |
| AROME | Application of Research to Operations at MesoscalE |
| BAPV | Building Applied Photovoltaics |
| BCR | Battery Charge Ratio |
| BESS | Battery Energy Storage System |
| BTN | Normal Low-Voltage |
| CRR | Controlled Ramps Ratio |
| DL | Decrew-Law |
| DOD | Depth of Discharge (%) |
| DSM | Demand Side Management |
| DSO | Distributor System Operator |
| ECMWF | European Centre for Medium-Range Weather Forecasts |
| EDP | Electricity of Portugal |
| EG | Energy from the Grid |
| EMS | Energy Management Strategy |
| ENTSO-E | European Network of Transmission System Operators for Electricity |
| ESS | Energy Storage System |
| FBU | Overall From Battery Use |
| FGU | Overall From Grid Use |
| GRF | Grid Relief Factor |
| IPMA | Portuguese Institute for Sea and Atmosphere |
| JSON | JavaScript Object Notation |
| KPI | Key-performance Indicator |
| MA | Moving Average |
| MPP | Maximum Power Point |
| MPPT | Maximum Power Point Tracker |
| PV | Solar Photovoltaic |
| RFB | Redox Flow Battery |
| RR | Ramp Rate (%/min per nameplate capacity) |
| SCM | Self-Consumption Maximization |
| SCM+RR | Self-Consumption Maximization with Ramp Rate Control |
| SCM+RR+WF | Self-Consumption Maximization with Ramp Rate Control with Weather Forecast VRFB Charging |
| SCR | Self-Consumption Ratio |
| SOC | State of Charge (%) |
| SSR | Self-Sufficiency Ratio |
| TBU | Overall To Battery Use |
| TGU | Overall To Grid Use |
| TMY | Typical Meteorological Year |
| TSO | Transmission System Operator |
| UÉvora | University of Évora |
| UPS | Uninterruptible Power Supply |
| UTC | Coordinated Universal Time |
| VRE | Variable Renewable Energy |
| VRFB | Vanadium Redox Flow Battery |
| WF | Weather Forecast |

## 1. Introduction

At the end of 2019, the global installed renewable energy capacity reached 2,537 GW, more 176 GW compared with 2018 [1]. In the same year, solar photovoltaic (PV) energy had a 3% share in the world generation mix, with a 2050 forecast of 23% [2]. With the significant share of renewable energy, which is variable (VRE), it is necessary to impose limits for its integration into the grid [3]. The integration of VRE obeys a regulation that defines the conditions of the parameters to be exchanged with the grid (quality). The parameters are, for instance, the voltage and frequency operating ranges, reactive power capacity for voltage control, active power gradient limitations, among others. The fluctuation of primary energy from VRE is concerned with the limitations of the active energy gradient. The increase in VRE's contribution to final energy consumption can be resolved by creating a ramp rate limit, which is already in the legislation of some countries around the world [3]. Countries with a significant number of solar PV installations have limitations in supplying energy to the grid. The ENTSO-E (European Network of Transmission System Operators) requires the ramp rate to be specified by the regional Transmission System Operator (TSO), if necessary. In Germany, the grid code establishes that if the installed capacity of a PV generator is greater than 1 MVA, the ramp rate limit is 10% of the rated power per minute. In Puerto Rico island, the PREPA 2012 regulation imposes as well a 10% of nameplate capacity per minute as a ramp rate limitation of grid injection [4]. In Ireland, the EirGrid Plc regulation establishes that the wind farm power stations must be able to control the ramp rate of their active power output over a range of 1-100% of their nominal capacity per minute. The wind turbines must be able to restrict ramping [3]. In the Philippines, the grid code establishes an active power limit during over-frequency. The largest plants must be able to limit ramps, and in China, a National Standard was created to control the maximum ramp range of PV power stations to be less than 10% of the installed capacity per minute [5].

Short-term energy fluctuations are directly related to the area of the PV plant and its geographical dispersion, and for this reason, in general, the small area, associated with a building PV installation, becomes especially subject to severe fluctuations in PV energy [6]. Ramp rate negative impact is related to matters as the extension of household appliances lifetime, and the contribution to the grid stability. To characterize the impact that the 6740 W of one of the UÉvora Building Applied PV (BAPV) systems has on the building, a calculation was made for the ramp rate, for 1 minute with one year of PV recorded data (2018). The monitoring data is collected through an in-house developed

software using the LabVIEW environment, with a 2-second time frame, using a precision power analyser (Circutor CVM-1D [7]) and the PV inverter. The ramp rate was calculated for the entire year for values of ramp rates of 5% and 10% as current references, and the results are shown in Table 1, below.

Table 1 – Ramp rate in %/min of the nameplate capacity of the PV system (UÉvora, 2018 data).

| Ramp rate (%/min) in the year 2018 | Percentage of total ramp rate in one year (%) |
|---|---|
| $<$ 5 %/min | 78.5 |
| $\geq$ 5 %/min | 8.09 |
| $\geq$10 %/min | 5.16 |
| $>$ 10 %/min | 4.83 |
| $\geq$ 50 %/min | 0.65 |

From the observation of Table 1, about 8% are above the 5%/min ramp rate and about 5% are higher or equal to 10%/min of the PV nameplate capacity, which is an expected result given the PV installation size. These ramp rate values have probably low impact on the grid, although should not be ignored. To increase the degree of confidence of these results, a substantially greater data period is required, ideally, several years. The existence of systems with monitoring of long-term PV generation data with high frequency (as, for instance, data logging at 2s) is rare and should be an effort to be implemented in the future of experimental installations. The results of Table 1 are representative of the location and specifications (tilt, azimuth, among others) of this single PV system, due to the direct relationship between this solar radiation data and the occurrence of power ramps, as the analysis of the solar radiation meteorological data.

To tackle the PV fluctuations the ramp rate control can be achieved through three main techniques, namely, operation of the PV system below its nominal capacity, bypassing the MPP [8], or through the use of a Battery Energy Storage System (BESS) to absorb or inject the excess of generated PV energy when the ramp rate is violated [9]. BESS helps in the regard of self-consumption and self-generation of energy and grid auxiliary. It also contributes to energy loss reduction, reliability increase, stability, power quality increase and energy efficiency, help in the systems operation and frequency regulation and balance establishment among energy demand and supply [10]. Ramp rate limitations are generally studied to apply in large PV installations, where their effects

are more noticeable, due to the reduction or sudden increase in the power injected into the grid. Although, with the increase of PV installations number in the buildings sector, this issue should be addressed. In the literature, the authors of [11] approach the ramp rate control application to deal with PV fluctuations at a real scale using a BESS to compensate sizing to deal with ramping. The authors of [9] explore the PV ramping application with a battery state of charge (SOC) reference calculation. Previous works are references in the field, although there is a clear lack of studies devoted to the domestic and services (buildings) sector and real-time application, given the previous studies focused on large-scale solar PV plants and BESS sizing. The authors of [12] developed the ramp rate and self-consumption algorithm validation with a DC controller for an ultracapacitor as BESS in a microgrid, although the building integration at real scale is still lacking and being the control devoted for DC microgrids. The authors of [13] present the comparison of different ramping smoothing filter techniques using a BESS, exploring time intervals of 2.5, 5, 7.5, and 10 minutes, evaluating the number of fluctuations and their impact on the application, and the authors of [14] consider a time interval of 15 minutes. Both works have considered large sets which is not the case of the present work, where the time frame of seconds is considered, as further discussed. On the contrary, the research conducted by [15] considers a 250 ms PV and wind data, explaining the lower intervals impact.

A BESS is generally managed optimally if applying energy management strategies (EMSs) in its control and operation, involving the generation and the consumption of energy. PV for self-consumption is the most studied and applied strategy to operate a PV system with or without a battery (depending on the consumption needs). In the context of the Portuguese legislation in force, the Decree-Law 169/2019 [16], PV self-consumption is highly promoted, being a starting point of this work. Within this topic, a greater volume of works has been developed, not only for PV-only configurations, as much as integrating a BESS, at buildings scale, with different final objectives improvements, namely, economic, technic, or energetic. The variety of works in literature present energy management strategies as the PV self-consumption maximization in [17], demand-side management (DSM) in [18] and [19], the use of load forecasts to optimize the operation of PV and the battery in [20], load-scheduling [21], peak-shaving and power curtailment [22], or battery charging controls [23] as battery operating scheduling [24], among others. In the case of the present work, the more significant EMS under study is the self-consumption maximization combined with a ramp rate control, considering a PV installation and a BESS.

In this work, the BESS technology under study is a redox flow battery (RFB), considered promising for stationary energy storage in electric grids [25]. The RFB electrochemical processes occur as redox reactions in its conversion unit, the stack. The stack is made of several cells, which form two electrodes separated by a proton selective membrane. The electrodes are made of porous graphite felts, and the bipolar plate between each cell creates the electrical connection between the two opposite poles. The electrolyte is pumped from the tanks to the stack, where the half-electrochemical reactions occur. RFB technology has advantages in the decoupling of power and energy ratios, large cycle life, low maintenance, and limited self-discharge. As for disadvantages, it has a low power density. Different chemistries of RFBs exist, as the example of zinc-bromine, hydrogen-bromine, among others, although vanadium-vanadium chemistry is the most mature so far, introduced in the 1970s and already commercialized.

The vanadium redox flow battery (VRFB) has the vanadium element in four oxidation states mixed in an aqueous solution of sulfuric acid. The storage of energy is made in two electrolytic solutions with two different redox couples: the negative electrode is composed of bivalent $V^{2+}$ and trivalent $V^{3+}$ ions; the positive electrode is composed of tetravalent $VO^{2+}$ and pentavalent $VO_2{}^{+}$ ions [26]. VRFBs are suited for applications requiring security of energy supply, energy/power quality, load levelling, and renewable energy compensation as time-shift, grid efficiency and off-grid applications [27], peak shaving, and uninterrupted power supply (UPS). Details of costs can be consulted in [28] – a 1 MW/4 MWh VRFB ESS states at 391 $/kWh in the 2020 year, with a projection of 318 $/kWh for the 2030 year. In literature, VRFB as a BESS is being investigated, and in the following, the most relevant for this context are highlighted. In the scale of MW VRFB, the potential integration of VRFBs with wind farms is investigated by the authors of [29] to mitigate power grid and market integration issues, and although the simulation results of the economic study are compelling, the solution is not validated at a real-scale. In [30] the authors combine a 1 kW/6 kWh VRFB with a 10 kW solar PV, a 15 kVA biomass infrastructure, and a 1kW of wind for different EMSs purposes, and operation control is designed and simulated through LabVIEW, although the study lacks general EMSs evaluation indicators. The same issue is lacking in the work developed by the authors of [31], with relevant inputs of controlling the charging current and flow rate of the 6 kWh/ 1kW VRFB integrated with a PV maximum power point tracker (MPPT). The work is validated through some hours of operation. Authors of [32] explore modelling and operation of a VRFB strictly for PV

application. There, a PV+VRFB model is explored, based on its typical operation characteristics, in conjunction with a charge controller unit, to ensure safe operation. The simulation is carried to the battery balancing the load to ensure firm power output at the load, although the real-time validation and building integration is missing.

In this work, three energy management algorithm strategies are studied, explained in the following. Self-consumption maximization (SCM – strategy 1) is a strategy that maximizes the usage of the PV generation throughout the day and can benefit from the VRFB to increase the PV power consumption. The second strategy is self-consumption maximization with ramp-rate control (SCM+RR – strategy 2) is strategy 1 including a ramp rate control accommodated by the VRFB if it presents suitable capacity (within the allowed SOC range) and power, and any SOC control is carried. The third strategy is a Self-consumption maximization with Ramp-rate control and VRFB charging based on a weather forecast (SCM+RR+WF – strategy 3) and is strategy 2 with a battery SOC control implementation. This work aims to control PV fluctuation and still execute self-consumption to benefit from the Portuguese legislation in force. The strategy is a theoretical simple approach, and if the VRFB SOC control turns effective with the local weather forecast (WF), the VRFB application is effective as well and can be applied to any VRFB+PV self-consumption scenario. Using UÉvora's microgrid as a building sector case study, this work investigates the possibility to develop and implement the real-time multipurpose algorithm control, to improve the integrated system, assuring the security of supply and solving a predicted regionally high PV penetration scenario already in force in some countries, in this case for the location of Évora, Portugal. The evaluation is carried through dedicated key-performance indicators (KPI), to check if the WF adding on the PV+VRFB operation improves (not worsens) any of the studied KPI. In this work, the exploitation of the conjunction of the SCM and the ramp rate control with the local daily WF with a VRFB as a solution for building integration is a novelty, both in simulation, as well as in the application.

This work is structured as follows: Section 2 presents the overall methodology of the work, starting with the description of the microgrid architecture and setup (2.1), as well as the VRFB modelling (2.2). Section 2.3 presents the PV generation and load profiles used for the EMSs simulations. The next section (2.4) shows the ramp rate calculation method and the filter technique used and the time frame chosen for the ramp rate control effectiveness. To assess the EMSs' performance, KPIs were defined and used, as depicted in Section 2.5. Section 2.6 presents the original control implementation methodology, divided into three main sections: the upfront VRFB WF online

explanation for implementation (2.6.1), the VRFB operational constraints for LabVIEW implementation (2.6.2) and the algorithm implementation section which better details its functionality (2.6.3). Section 3 provides the main simulation results of the work and its related discussion, as the resulting of the SOC control (3.1), the energy KPIs (3.2), and other related outcomes from the experimental approach (3.3 and 3.4), with a final remark on further work (3.5). Finally, the fundamental conclusions of this work are detailed in Section 4.

## 2. Methodology

The work approach follows the steps of Figure 1, which specifies the input parameters subjacent to the simulation model and the output of the energy analysis (A), and the details regarding the experimental validation for the EMS's feasibility (B).

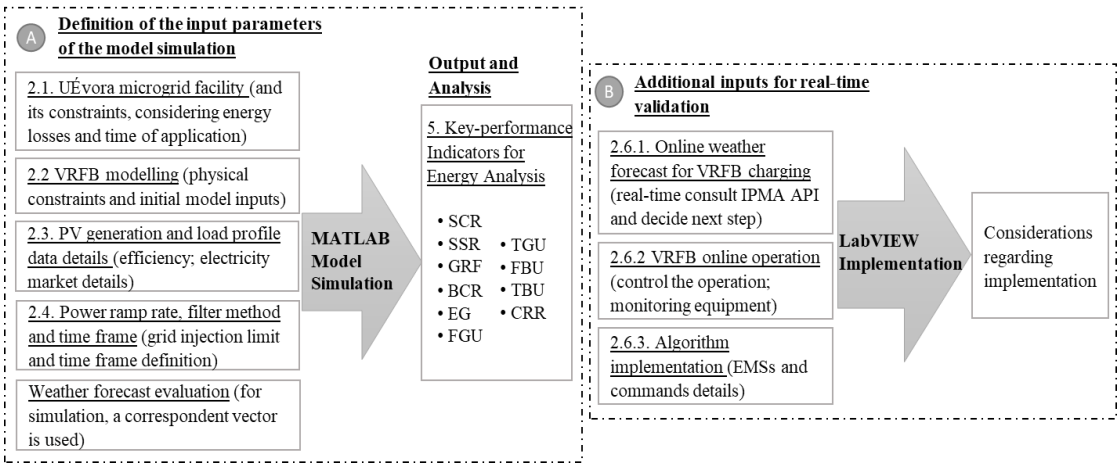


Figure 1 – Overview of the architecture underlying present work methodology. The definition of KPIs is detailed in Section 2.5.

The simulation of the three EMSs algorithms is developed in MATLAB. The inputs of the simulation model include the constraints details of the UÉvora microgrid, the PV generation and load profiles, the developed VRFB electrical model, and the ramp rate calculus and its premises. The evaluation of each strategy is made through dedicated energy KPIs. After the evaluation and optimization of the simulation model, SCM+RR+WF – strategy 3 is implemented in real-time using LabVIEW in the UÉvora microgrid, where the required inputs of the weather forecast are online consulted.

Hence, the validation of the proposed EMS is achieved, through control with the monitoring equipment. Each of the marked text points of Figure 1, concerning the MATLAB simulation modelling (A) and the LabVIEW implementation (B), that allowed the construction of the modelling and the real-time microgrid operation are presented in the subsequent sections: the UÉvora microgrid facility corresponds to subsection 2.1, and so on successively.

### 2.1. UÉvora microgrid facility

The building scale VRFB (5 kW/ 60kWh) from redT is integrated into a three-phasic microgrid test facility of Renewable Energies Chair of the University of Évora, in operation since 2012. The roof facility is equipped with a polycrystalline technology of 3.5 kWp and a monocrystalline technology of 3.2 kWp PV systems, separated by strings, directed through another AC/DC Ingeteam PV inverter. AC metering is installed in several points of the microgrid (before and after each piece of equipment), and the DC measurements of voltages, currents, and temperature are achieved through a data precision multimeter. The power management system that operates the VRFB is composed of bidirectional inverters from Ingeteam, with an operation above 48 DC voltage, which also executes AC and DC data measurement. A desktop computer equipped with the LabVIEW environment is the control unit, which in real-time operation, gather the data under the chosen (or possible) time frame. Its main components are schematized in Figure 2, below.

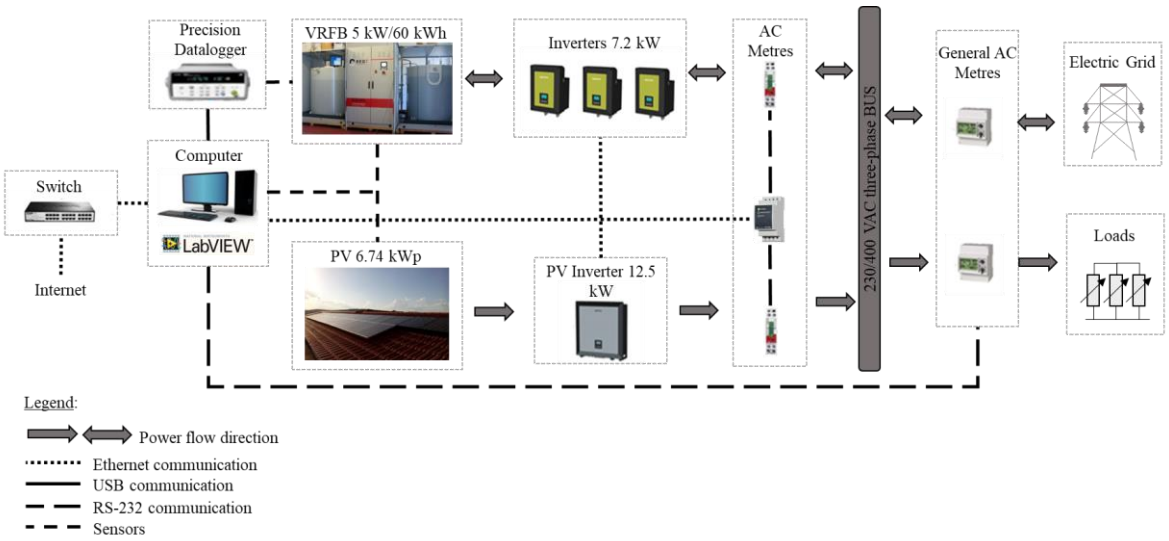


Figure 2 – Representation of UÉvora's VRFB microgrid equipment's connection and energy fluxes.

The microgrid general equipment's measurement uncertainty and communication delays should be accounted as a constraint of the real-time application. The AC/DC efficiency of the VRFB's integrated inverters was included in the developed simulation model (AC/DC efficiency of 0.88, resulting from previous experiments). The standby value of 30 W was considered.

### 2.2. VRFB modelling

For the simulation of the EMSs through MATLAB, a dedicated VRFB model was included. VRFB architecture allows its replication in other facilities, with the increased advantage of being an easily scalable product. The technology has two electrolyte tanks containing a mixture of vanadium ions and sulfuric acid, two pumps for electrolyte flowing, and the stack as the energy conversion unit, with 40 cells electrically connected in series, and hydraulically connected in parallel. The 5-kW stack is a dynamic system, and its performance depends on multiple effects: electrochemical, fluid dynamics, electric and thermal. This specific 60 kWh VRFB was the object of study in previous works, and the most recent include the battery electrical modelling, developed, and validated on a real operation scale, considering its general operating conditions in the UÉvora. The model is fully detailed in the research conducted in [33], and it was implemented and used in the developed simulation model to test the implementation of these EMSs. The use of this validated battery model helps the control implementation with the smallest possible error.

### 2.3. PV-generation and load profile data

To compose the buildings scenario, the PV profile used corresponds to the data obtained with the UÉvora's PV installations, during one week from the 1st to the 7th day of January of 2018, with 2-second intervals data logging. The load profile used is made available by EDP Distribuição – Portuguese DSO company – with 15 minutes of average load data for the year 2018 [34]. With the help of the MATLAB software, the data were treated to correspond to the PV data sampled time frame. The PV and load profiles collected data for the first seven days of January 2018 can be seen in Figure 3, below.

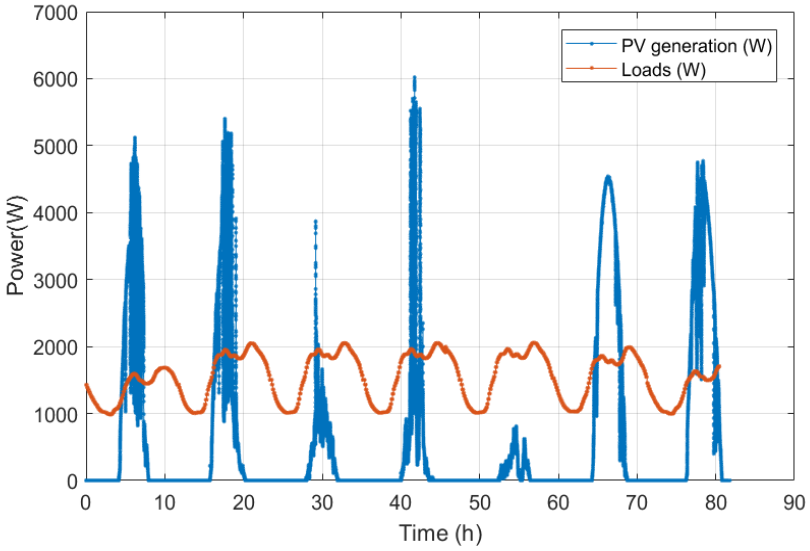


Figure 3 – Solar PV profile obtained by the measured data of the UÉvora's PV installation, and load profile, obtained by [34] estimation for BTN B sector, for 1 week of January, from day 1-7 day of 2018.

### 2.4. Power ramp rate, filter method and time frame

In general, the classic way of representing the ramp rate is defined as RR, as presented in Eq. (1),

$$RR = \frac{\frac{P_{PV}(t) - P_{PV}(t - \Delta t_R)}{P_N}}{\Delta t_R} \times 100 \quad (1)$$

where, $P_{PV}$ – PV power (W) and $t - \Delta t_R$ – time differential of the ramp rate, typically equal to the unit (min).

In this work, the authors focus on the Moving Average (MA) filter technique type, which is considered the most traditional filter technique, although it can lead to increased battery cycling. This is also the reason why the present study was chosen to apply the MA filter to a VRFB, with a high energy capacity of 60 kWh. This BESS technology, although a battery with moderate energy density, allows (if necessary) a high number of cycles without significantly reducing its performance, capacity, or life. The moving average time frame should be sensibly weighted. The contribution developed in [35] investigates the PV time averaging impacts on the small and medium-sized PV installations and concludes that a time frame of 15-minute averages describes the ramps poorly. For the week considered in this study, the theoretically controlled

ramps were calculated using the 10%/min ramp rate with an average of different periods of PV intervals. The obtained values are presented in Figure 4, below.

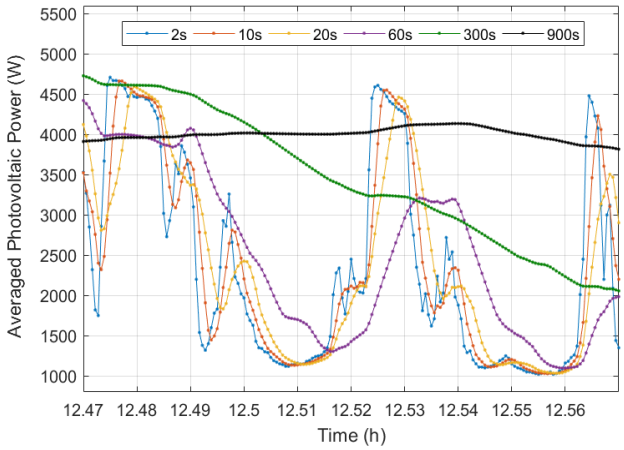


(a)

| Time frame | Controlled ramps in the chosen week (RR ≥ 10%/min) |
|---|---|
| 2 s (without averaging) | 5716 |
| 10 s | 5751 |
| 20 s | 5660 |
| 60 s (1 min) | 5039 |
| 300 s (5 min) | 364 |
| 900 s (15 min) | 0 |

(b)

Figure 4 – (a) PV average of the time frames studied. The 2s correspond to the raw data extracted from the PV installation under study. The remaining time frames are the PV averaging corresponding to each of that time frames. (b) The number of controlled ramps for the studied week, over different time frames of PV average values.

Figure 4 (b) results obtained support the study previously referred to in [35], for the domestic PV installations: as the average time frame increases, fewer ramps are detected and controlled. Alternatively, if the average time frame is too small, the impact will be low. The simple implementation of MA and low computational effort can let through unexpected artefacts such as peaks in the results. In accordance, and considering the microgrid constraints, a time frame of 20 seconds was chosen. This method functions with the averaging of the previous PV measurements, in a chosen period, $t$. The battery command, $P_{battery}$ , at a $k^{th}$ instant, can be calculated from Eq. (2) [13]:

$$P_{battery}(k) = \frac{\sum_{i=0}^{t-1} P_{PV}(k) - P_{PV}(k-i)}{t} - P_{PV}(k) \quad (2)$$

### 2.5. Energy Key-Performance Indicators

To properly evaluate the EMSs, suited key-performance indicators are calculated. The parameters are based on the sum of the energy used throughout the days of the strategy application. In the following Table 2, the indicators are enunciated, below.

Table 2 – Energy key-performance indicators for the evaluation of the EMS.

| KPI | Description | Equation |
|---|---|---|
| Self-consumption ratio (SCR) | Share of the PV energy consumed within the installation over the total PV energy generated. The PV energy produced can be consumed indirectly by the battery (including losses). | $SCR = \frac{E_{PVconsumed}}{E_{PVgenerated}}$ |
| Self-sufficiency ratio (SSR) | Share of the consumed PV energy generation over the total consumption needs. | $SSR = \frac{E_{PVconsumed}}{E_{Load}} = \frac{E_{Load} - E_{Grid}}{E_{Load}}$ |
| Grid-relief factor (GRF) | The measure of the total energy of the installation loads, which is exchanged with the grid. | $GRF = \frac{E_{Grid}}{E_{Load}}$ |
| Battery charge ratio (BCR) | Total energy used to charge the battery, over the overall energy sent and received to/by the battery. | $BCR = \frac{E_{charge}}{E_{battery}}$ |
| Energy from the grid (EG) | Amount of energy extracted from the grid, considering the total energy exchanged with the grid | $EG = \frac{E_{fromGrid}}{E_{Grid}}$ |
| Overall from grid use (FGU) | Amount of energy extracted from the grid in the overall installation consumption needs | $FGU = \frac{E_{fromGrid}}{E_{Load}}$ |
| Overall to grid use (TGU) | The amount of energy injected into the grid, over the overall installation consumption needs | $TGU = \frac{E_{toGrid}}{E_{Load}}$ |
| Overall from battery use (FBU) | Amount of energy extracted from the battery in the overall installation load profile | $FBU = \frac{E_{fromBattery}}{E_{Load}}$ |
| Overall to battery use (TBU) | Amount of energy sent to the battery, over the overall installation load profile | $TBU = \frac{E_{toBattery}}{E_{Load}}$ |
| Controlled ramps ratio (CRR) | Rate of the total number of the ramps (up and downs) controlled with the use of the battery using the EMS, over the total number of ramps (up and downs) without the use of an EMS | $CRR = \frac{Nr_{strategy}}{Nr_{original}}$ |

Where: $E_{PVconsumed}$ is the PV energy generation consumed directly or indirectly; $E_{PVgenerated}$ is the total PV energy generated by the PV installation; $E_{Load}$ is the total load consumption; $E_{Grid}$ is the injected and extracted energy to/from the grid; $E_{battery}$ represents the total energy sent to charge and discharge the battery, in absolute values; $E_{fromGrid}$ is the energy needed to extract from the grid to supply the energy consumption needs, in the overall strategy; $E_{Grid}$ the total amount of energy exchanged with the grid; $E_{toGrid}$ is the sum of the energy sent to the grid; $E_{fromBattery}$ is the energy used to discharge the battery; $E_{toBattery}$ is the energy used to charge the battery; $Nr_{strategy}$ is the total number of ramps controlled using the EMS; and $Nr_{original}$ the number of ramps that occur without an EMS.

## 2.6. Control Implementation

The proposed strategy 3 combined with the online WF and the VRFB is a complex task to orchestrate in real-time operation. Through the seven-day experimental validation, the feasibility of its application in real-time can be properly assessed. PV fluctuation has a seasonal-dependent characteristic, occurring in Portugal mostly in periods from winter to spring. By these means, the authors decided to evaluate this strategy application in one particularly fluctuation week (1-7$^{th}$ of January). The real-time operation of the SCM+RR+WF (strategy 3) and experimental validation details are presented in this section. The study made in [36] validated the SCM (strategy 1) using the same experimental setup and battery. Strategy number 2 is a simplification of strategy number 3. Being the SCM+RR+WF (strategy 3) the most complex strategy, both on algorithm or control implementation, when compared to strategy 1 and strategy 2, it was decided to implement the SCM+RR+WF only and validate it at full scale and real operating conditions in the experimental microgrid of the VRFB, using LabVIEW, a graphical programming code, which combines visualization results and interactive tools to allow a real-time controller interface, check the course of the algorithm and act if needed.

### 2.6.1. Weather forecast for VRFB charging

In strategy 3, SCM+RR+WF, the battery will be charged to values near the 50 % SOC when needed, with data input from weather forecast (ramp-rate occurrence), using data forecast produced by IPMA (*Instituto Português do Mar e da Atmosfera*). IPMA is a Portuguese public body, which is responsible for, among other many tasks, forecasting the states of the weather and sea, for all necessary needs. The forecasted data, associated with the geographical and seismic events, are made available in their Application Programming Interface (API) in a JSON format [37]. The data is obtained automatically through a forecast statistic process with forecasts of two numerical models – ECMWF (European Centre for Medium-Range Weather Forecasts) [38] and AROME (Application of Research to Operations at MesoscalE) [39]. These forecasts are updated two times per day, at 00 UTC (available at 10 am) and 12 UTC (available at 8 pm). In the summertime, the Portuguese legal hour is UTC+1, and in the wintertime, the legal hour is equal to UTC. In the referred online API, daily meteorological data forecast up to 5 consecutive days by region can be found with aggregated information per day. IPMA forecasts roughly 41 regions, both onshore and offshore. Every twelve hours, the forecast information on the website is updated, for each region. In this work, relevance

was given to the "id weather type", for which a number is attributed, corresponding to a weather description, which can be observed in Table 3.

Table 3 – IPMA API ID weather type [37], to allow the construction of a correspondence map. The bold values correspond to the ones used for the 50 % battery SOC target of strategy 3, SCM+RR+WF.

| Number | Correspondence | Number | Correspondence |
|---|---|---|---|
| --- | -99 | ***14*** | ***Intermittent heavy rain*** |
| 0 | No information | 15 | Drizzle |
| 1 | Clear sky | ***16*** | ***Mist*** |
| 2 | Partly cloudy | ***17*** | ***Fog*** |
| 3 | Sunny intervals | **18** | **Snow** |
| ***4*** | ***Cloudy*** | 19 | Thunderstorms |
| ***5*** | ***Cloudy (High cloud)*** | 20 | Showers and thunderstorms |
| 6 | Showers | 21 | Hail |
| 7 | Light showers | 22 | Frost |
| ***8*** | ***Heavy showers*** | ***23*** | ***Rain and thunderstorms*** |
| 9 | Rain | ***24*** | ***Convective clouds*** |
| 10 | Light rain | ***25*** | ***Partly cloudy*** |
| ***11*** | ***Heavy rain*** | ***26*** | ***Fog*** |
| 12 | Intermittent rain | ***27*** | ***Cloudy*** |
| 13 | Intermittent light rain | | |

With the help of this information, the battery SOC is prepared for the next day, as needed, through battery charging during the night hours (in general there is low energy consumption from domestic users during those hours). For that reason, this control type is optimal for the Portuguese bi-hourly and tri-hourly household tariffs, with lower electricity prices during the night [40].

### 2.6.2. VRFB operation

For continuous operation control and alarm detection, the battery terminals, cells of the stack, and the reference cell have installed electric sensors, which variables are real-time acquired. The variables are voltage and current, temperature (high accuracy probes), pressure, and mass flow, watt meters, and many possible alarms. The SOC of the

battery is obtained in the course of the operation, through the real-time acquisition of the open-circuit voltage, as detailed in [36]. UÉvora's VRFB is generally operated at a depth of discharge of 85 %, in previous characterization tests it was possible to obtain a specific energy density of near 18.5 ± 4.2 Wh/Kg, a maximum useful capacity of 66.5 ± 4 kWh, a battery efficiency of 77.1 ± 3.36 %, and a response time of seconds [41]. Considering the small relative error of the model when calculating the VRFB key parameters, including the SOC, and the availability of power (charge/discharge), a battery operating range of 20% and 70% of SOC was selected (battery depth of discharge, DOD, of 50%), to avoid states of charge next to the extreme limits. The maximum power is constrained to the maximum inverter and battery limits and the real-time state of charge. The VRFB Power-SOC relation is considered for maximum charge and maximum discharge levels of power. Due to the Power-SOC characteristics of the BESS technologies the available power to charge/discharge is severely constrained near the upper and lower SOC limits. These available power technical restrictions hinder the full control of power ramps.

### 2.6.3. Algorithm implementation

The night charging only happens if the next day's forecast indicates a cloudy day, considering the map developed in Table 3. The cloudy day indicates a higher probability of the occurrence of PV power ramps. The flowchart of this algorithm part is presented in Figure 5. The ramp rate algorithm is activated when its real-time calculated result is equal to or larger than the 10 %/min of the PV nameplate capacity value. Every day at 1:30 am, the algorithm consults the IPMA API, to decide if it should act on the battery charging-only, to avoid the VRFB SOC being near to its lowest limit at the end of the day. If none of the conditions is satisfied - near lowest limit SOC, or "bad" weather day - the EMS continue its algorithm course, the self-consumption maximization.

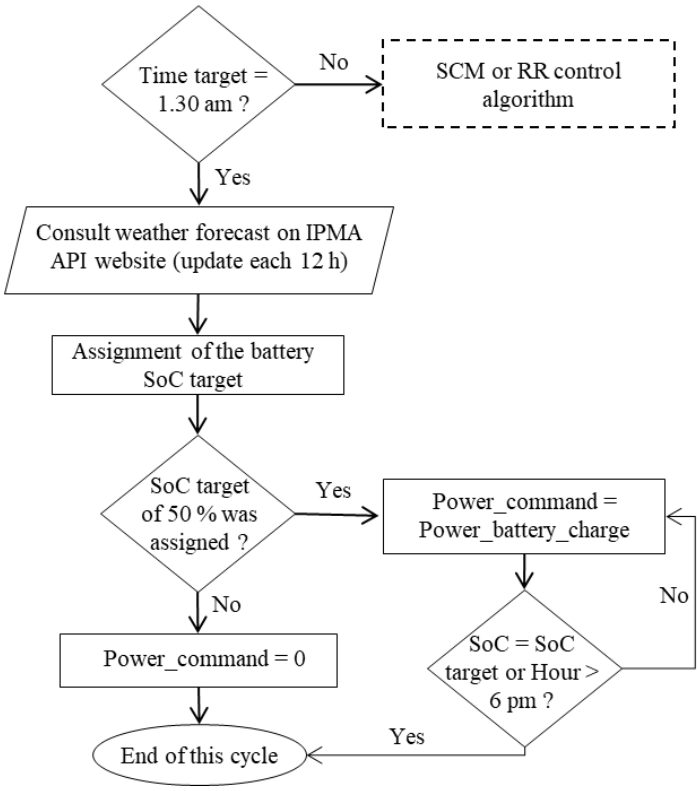


Figure 5 – Algorithm flowchart of the weather forecast with the IPMA API and SoC control. Where: Time_target – Initial hour for the beginning of the night charge (h); SoC target – Target to which the SoC should achieve, set as 50 %; Power_command – Power command value sent/received to/from the battery (W); and P_battery_charge – Constant charge power sent to charge the battery, in nightly hours (W).

Figure 6 presents the algorithm performing the ramp rate control when the defined maximum ramp value is violated. Given the inputs, at every 2 s the PV data is read lido and the ramp rate is calculated. If it violates the 10%/min of the PV nameplate capacity, the SOC is observed, and if possible, the battery compensates the PV deviation, with either a charge or a discharge (depending on the slope of the deviation). If the ramp rate violates the defined limit, the battery will only accommodate charges if its SOC is lower than the SOC lower limit, and discharges if its SOC is higher than the SOC higher limit. If the ramp rate is lower than the 10%/min of the PV nameplate capacity, the EMS becomes the self-consumption maximization (SCM). The SCM algorithm was presented and validated in the work of [11], wherefore will not be detailed in this work.

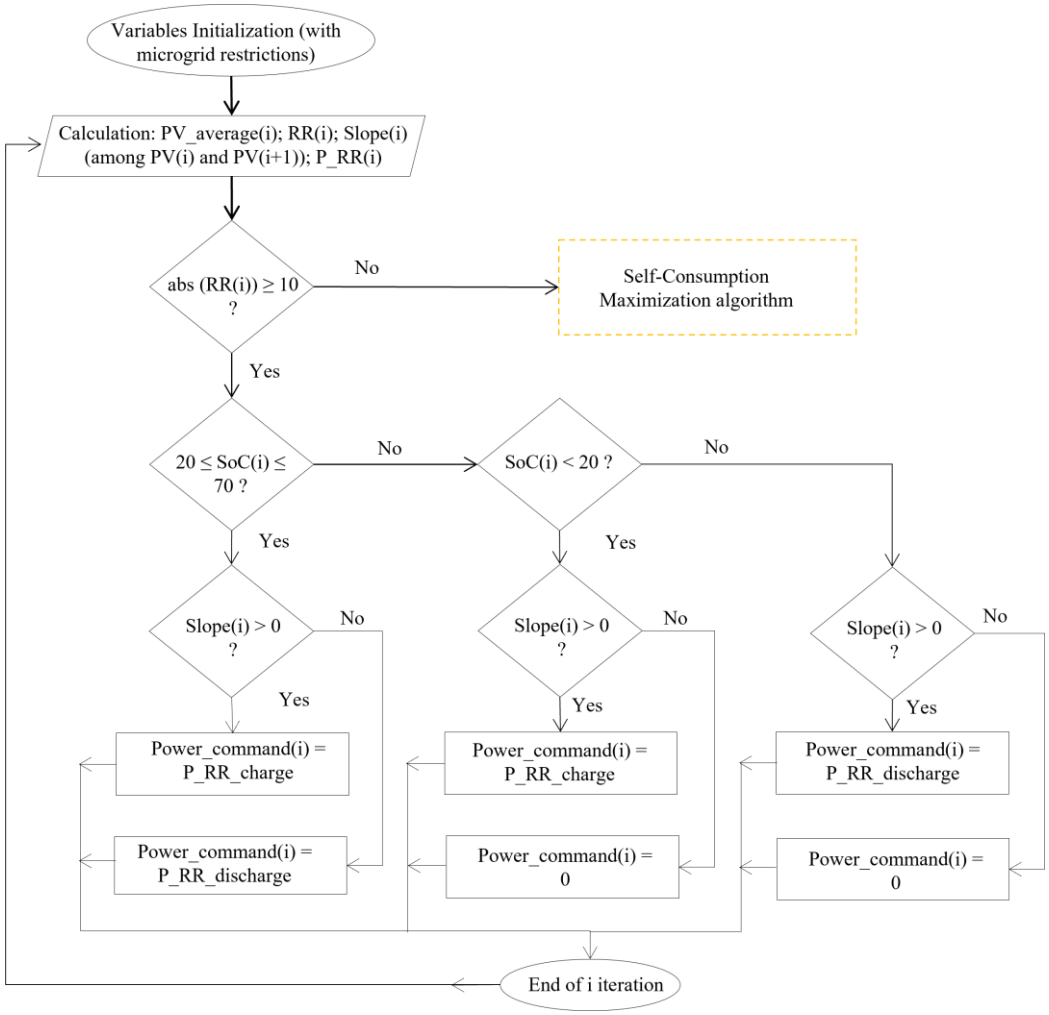


Figure 6 - Ramp-rate control algorithm flowchart, highlighting the battery power command power calculated at each iteration, with a cycle time frame of 2s. Where: i – Cycle iteration number; PV_average – PV values average of samples correspondent to 20 s (W); P_RR – Equivalent to the $P_{battery}$ of Equation (2) presented in Section 2.4 (P_RR_charge - $P_{battery}$ is a battery charge command and P_RR_discharge - $P_{battery}$ is a battery discharge command; and Slope – Slope of the two consecutive values of PV.

## 3. Results and Discussion

This section summarizes the main results and its related discussion obtained within this study, considering the consulted and described studies mentioned in Section 1 and the purpose of this investigation.

### 3.1. Weather Forecast VRFB charging

Power ramp rate control earns value if a state of charge control is implemented. Figure 7 presents the impact of having this battery charging for the SOC management in the current SOC of the battery over the course of the studied days where the control is applied. For the chosen week (1-7 January 2018), the IPMA API weather forecast was consulted for the next day forecasts, resulting in an active SOC control (night battery charge) on days 2, 3, 4 and 5. On days 1, 6, and 7, due to the weather forecast, the active SOC control was not activated.

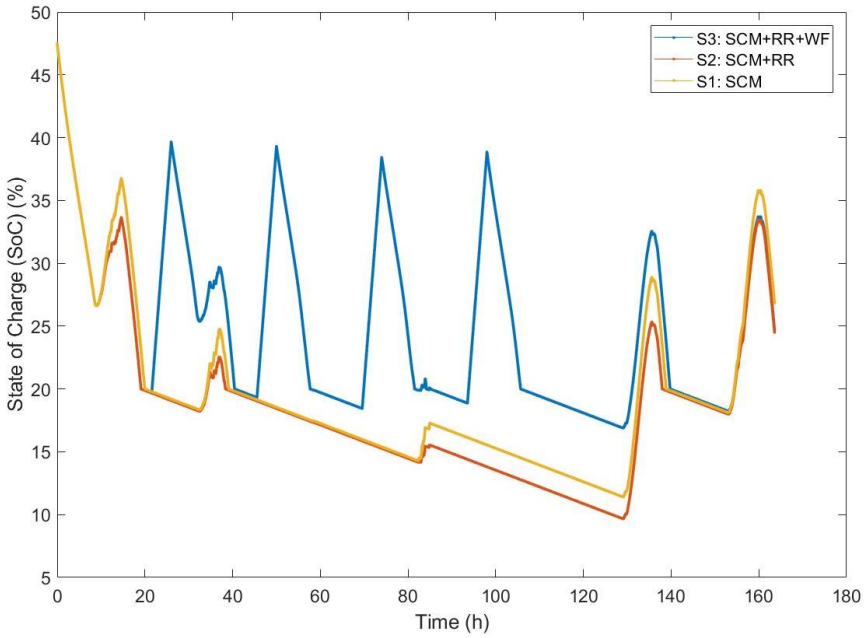


Figure 7 – Simulation of the battery SOC for the three strategies, over the same week PV-generation and load profiles.

If the VRFB SOC is near its extreme limits, the ramp rate control cannot be correctly applied, approaching the results of Strategy 2 to Strategy 1. The VRFB night charging based on the WF maximizes the amount of energy that flows to and from the VRFB (see TBU and FBU indicators, further discussed). Strategy 3, SCM+RR+WF, allows to deal with a bigger percentage of PV fluctuations, can successfully control all power ramps (CRR) with a ramp rate limit of 10%/min. On the other hand, Strategy 2 only control about 86% of the total power ramps occurring in the test period.

The WF control type relates the geographical location of the PV installation with the management of the battery. The developed approach allowed the battery SOC to be effectively controlled, allowing enough energy capacity for the next day's absorption or

injection PV ramping needs. Improvements in the forecasts will impact the improvement of the EMS. The night battery charging power setpoint should be adapted for the considered technology type and energy capacity. The night charging is attractive for bi-hourly and tri hourly tariffs, given the cheapest price for off-peak energy. The SOC management could be achieved through other algorithm types, such as linear or dynamic ramp-rate limiter control, depending on the required speed and efficiency of the application. The WF VRFB charging method, based on locally projected forecasts proves to be a good method to use in Portugal, and certainly could be reproduced in other countries. A further sensitivity analysis of the SOC different controls should be addressed in future building sector studies.

### 3.2. Energy KPIs

The KPIs were calculated for each of the simulation environments, for the one week of January. For the reader to be engaged with the significance of the key performance indicators, a best-case scenario for the prosumer (self-consumption user/installation owner) point-of-view is presented. This reference value can help the reader to understand how close or distant a strategy is from its ideal (best-case) scenario. The best-case for one indicator could imply the worst case of another. The week chosen in this study can also influence some of the KPIs. The results can be observed in Table 4, presented below.

Table 4 – Results obtained of the KPIs and their respective best-case-scenario, for the simulation study, of the 1st week of January 2018.

| KPI | 1 SCM (%) | 2 SCM+RR (%) | 3 SCM+RR+ WF (%) | Ideal best value (%) | Ideal best value direct meaning, from the point of view of the prosumer |
|---|---|---|---|---|---|
| SCR | 58.6 | 58.7 | 59.2 | 100 | The amount of PV energy produced meets with the PV energy consumed |
| SSR | 21.8 | 22.9 | 21.8 | 100 | The amount of PV energy consumed meets the energy consumed |
| GRF | 57.9 | 63.3 | 60.8 | 100 | Level of independence from the grid, from the user point-of-view (if equal to 100 %, there is no energy to the grid). |
| BCR | 38.7 | 37.4 | 40.9 | 50 (with 100% of battery efficiency) | Maximum possible energy used to charge the battery. Dependent on the battery energy capacity |
| EG | 98.8 | 95.2 | 94.9 | 100 (should | Quantification of the amount of energy |

| | | | | | |
|---|---|---|---|---|---|
| | | | | be weighted) | coming from the grid or going to the grid. Equal to 100 % means the energy sent to the grid is 0 %. |
| FGU | 57.2 | 60.2 | 57.7 | 0 | Equal to 100 % means that all the overall consumed energy comes from the grid. |
| TGU | 0.71 | 3.06 | 3.09 | 0 | Equal to 100 % means that the energy injected into the grid is equal to the load profile. |
| FBU | 13.2 | 10.8 | 22.2 | 100 | Equal to 100 % means that all the consumed energy comes from the battery. |
| TBU | 20.9 | 18.1 | 32.0 | 0 | Equal to 100 % means that all the energy sent to the battery (charge) is equal to the load energy needs. |
| CRR | 0.00 | 85.9 | 100 | 100 | Equal to 100 % means all ramps that violate the ramp rate reference are controlled. |

To improve the readability of the previous enunciated indicators, a graphical representation is presented in Figure 8 with the results of the resultant KPIs of the EMSs and the best-case scenario from the point-of-view of the prosumer.

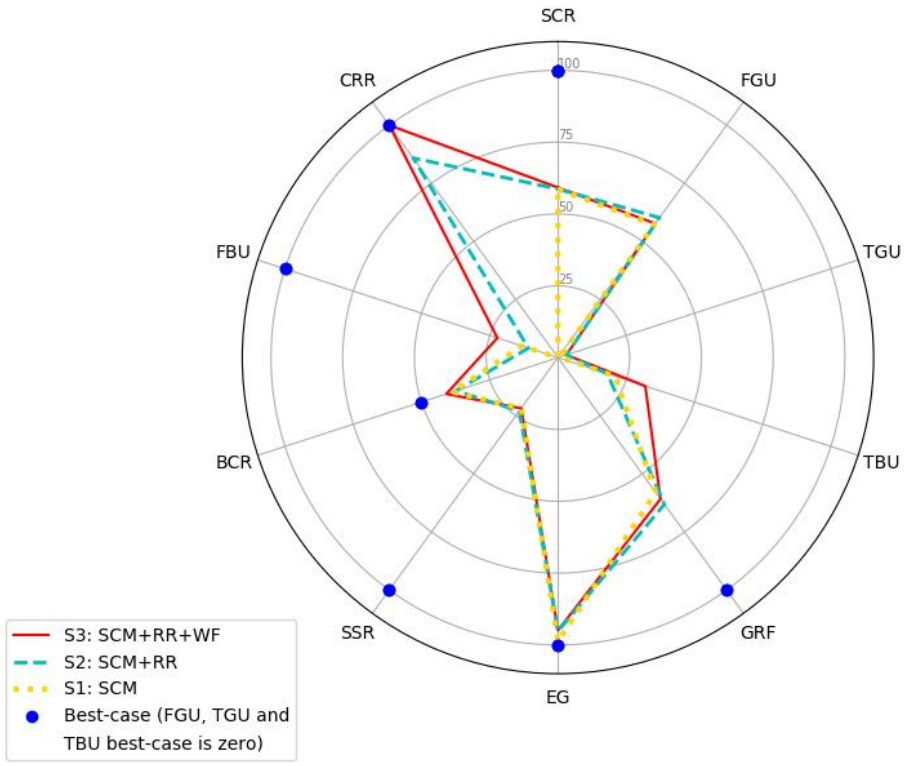


Figure 8 – Representation of the results of the KPIs for each of the simulated strategies, with the best-case scenario illustration inclusion.

Given this configuration context and the obtained best-case values, no strategies could achieve it, although some can get close. From the KPI results for all the strategies, the SCR parameter is consistent. Besides the PV-generated energy that is consumed directly by the installation, SCR is dependent on the availability of the battery to charge or discharge, and the main reason that the strategy 2 and 3 present a slightly higher value than the approach of strategy 1. Considering the understudy week, SCR is far from its theoretical maximum due to the PV generation of energy being greater than the global energy load profile and suffering a wide variation throughout the entire year (seasonality). The energy used for ramp control tasks (PV or battery) is lower when compared with the consumption needs. This means that this objective does not greatly penalize the SCR KPI.

The SSR indicator is curiously the same on strategy 1 and strategy 3, and higher than strategy 2. Similar behaviour to the previous indicator is observed regarding the best-case scenario. This indicates the ramp rate control does not affect the consumed PV energy, which was a priority to follow within the three strategies. Given the PV-generation and load profiles, the GRF is marginally higher for strategy 2 (SCM+RR). This KPI relates the energy extracted from the grid and the energy needed to supply the load. The night battery charging of strategy 3 could have led to the highest total energy exchanged to the grid, which did not happen. The strategy with the highest EG parameter in the overall grid use is Strategy 1 (SCM) mainly due to a lower weekly total of energy exchanged with the grid. The TGU indicator presents a growth from the simplest to the most complex strategy, meaning increased energy injected into the grid, although the grid injection of strategies 2 and 3 is smoothed since the ramp rate control is activated whenever a violation of the ramp rate limit occurs. TGU results offered a near value to its appointed best-case scenario. The energy extracted from the grid over the load profile is represented by FGU, which presents a distant value from the pointed best-case. Strategy 2 presents the highest value since it makes less use of the battery interaction with the loads (when devoted to the ramp rate control). BCR addresses the energy used to charge the battery over the total energy exchanged with the battery. It offers a clear representation of the energy fluxes in and out of the battery, and its pointed best-case is close to the obtained results.

This work focused to evaluate energetic KPIs, although the importance of economic indicators is recognized. Nevertheless, it was intended to minimize the cost of charging the VRFB (to control SOC when needed) overnight using the cheapest electricity tariffs (bi-hourly or tri-hourly tariffs).

### 3.2.1. Type of battery impact on energy indicator – ageing and capacity fading

The implementation of the WF VRFB charge for SOC ramp rate control causes an increase in the battery utilization rate, as expected, noticeable in the increase of the TBU and FBU indicators. In the case of the VRFB, this additional usage will not reduce its lifespan or increase its degradation, which could happen, for example, in lithium-ion battery (LIB) technology. The MA technique is a satisfactory method to approach the ramp rate calculation and was satisfactorily implemented in this VRFB. MA implies more cycling numbers than other ramp rate techniques, which is not an obstacle for this work since this VRFB presents a considered nominal energy capacity (60 kWh).

## 3.3. Combination of distinct controls aims

The PV self-consumption maximization energy management strategy could improve certain desired indicators, without compromising the main issues for which the strategy was built to solve. The analysis made concerns one week in the Portuguese winter season, a season usually characterized by several daily fluctuations in the PV power generation, and by the time of year with the lowest average daily global solar radiation. Figure 3 depicts the PV power generation over the period studied, with days characterized by high PV variability (except for day 6), posing a challenging scenario concerning power ramps. Combining distinct controls is to combine distinct aims, which should be carefully analysed to maintain the primary objective and not conduct to misleading results. In this work case, the combined strategy provides solves issues of grid quality, does not worse the PV self-consumption rate.

## 3.4. VRFB charge based on WF Validation Analysis

One important demand of the energy management strategies real-time application is the response of the system to the algorithms' commands, due to the importance of the simulation versus actuation. The online operation complicates the task, given the reliance on the data acquisition system and its real-time monitoring. Through the validation, the algorithm's performance at real-scale and real-time operation was possible to evaluate, accounting for technical constraints, data logging periods, the performance of the API of the WF, efficiencies of the equipment, and communication delays. A time frame of half a second and one second of cycling was tested, although the many variables controlled did not have time to execute all the commands, and by

this means, a control cycle time of about 2 seconds was the minimum possible time frame to execute the algorithm properly. The comparison of the validation with the simulation enables the improvement of the technical variables considered in the model under study. Figure 9, below, depicts the VRFB SOC over the validation week, so the difference between the model and the operation can be briefly checked, and the validation of the algorithm using VRFB could be assessed.

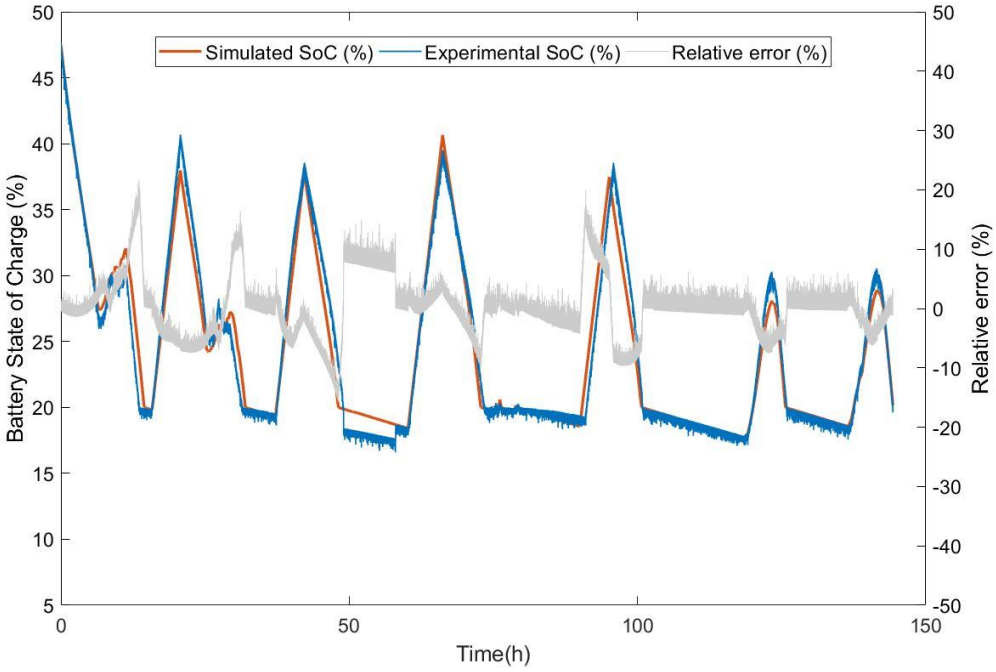


Figure 9 – SOC of the battery evolution over the period studied: SCM+RR+WF simulation vs. real-time implementation results, with a mean absolute error of 3.5%.

Considering the night battery charge in a mean value of 2700 W, and the PV-generation and load profiles, the battery SOC never exceeds 50 % for any strategy throughout the studied week. The difference between the simulation and the experimental output presents a low error (absolute average of 3.5 % over the period of study). Given the overall mentioned errors of real-time application of Strategy 3, which relies on the everyday WF, one can conclude that the EMS is possible to implement with the real-time control using the VRFB as BESS daily, and even with distinct control objectives.

### 3.5. Limitations and further work

Within the MA, the time frame has a great impact on results, as observed in Figure 4. The 20 s average time frame allowed a high number of maximum controlled ramps and

does not present a high influence by the averaging of several different measurements of PV generation fluctuations. The WF VRFB charging power setpoint should be adapted for the technology type and energy capacity. To improve confidence in this ramp rate occurrence distribution, it is necessary to collect data from a wider period, in a similar way to a Typical Meteorological Year (TMY). Its application in the generation and distribution systems is an option, which needs to be assessed. Besides the technic and energy approach followed by this work, economic evaluation still needs to be addressed. Reduction of costs will be influenced by recent analysis cost, simulation, overall efficiency optimization, anticipated flaws detection, systems characterization. Improvements in the model simulation could benefit the accuracy of the results. Economic analysis and future impacts of application in the grid should be addressed in future work. Other promising SOC management controls, to attain the similarities in aim, could be associated with, for example, seasonality.

## 4. Conclusion

This study assesses a building scenario with a PV installation, a VRFB as the electricity storage unit, and a load profile over one week of wintertime, with data from January 2018. Based on the predicted growth of the PV penetration at building scenario for the years to come, three EMSs were simulated to obtain a result improvement of the main KPIs related to the self-consumption maximization and power ramp rate control.

For the year 2018, and based on local data, it was shown that about 5% of the PV power ramps that occurred were above the rate of 10%/min of the PV nameplate capacity understudy. PV fluctuations should be carefully addressed for the buildings sector, given the increase of solar PV installations in buildings. Strategy 1, SCM, performs a simple self-consumption maximization of the PV power generation; strategy 2, SCM+RR, additionally performs a ramp rate control, imposing a 10 %/min of the PV nameplate capacity RR limit, providing additional stability over the grid energy exchange. Strategy 3, SCM+RR+WF, added a 12-hour WF based on the IPMA API, to implement a SOC control able to prepare the battery to better deal with the next-day PV power ramps. The night VRFB charging based on the WF presented an approach to follow to condition the SOC of the battery at the end of the day.

Despite the challenging scenario of occurrence of power ramps in the selected week, the SCM+RR+WF strategy demonstrated to be able to control 100% of the ramps with rates above 10%/min, maintaining the PV SCR (61%), and being able to keep the GRF close

to a value of 68%, and being implemented successfully, achieving the proposed objectives of this work. The development of multi-objective EMSs, often with competing goals such as the SCM+RR+WF, presents different system needs for power, energy, usage cycles, or response time.

**Acknowledgements**

The authors would like to thank the support of this work, developed under the European POCITYF project, financed by 2020 Horizon under grant agreement no. 864400. This work was also supported by the PhD. Scholarship (author Ana Foles) of FCT – Fundação para a Ciência e Tecnologia –, Portugal, with the reference SFRH/BD/147087/2019.

**References**

[1] Adrian Whiteman, S. Rueda, D. Akande, N. Elhassan, G. Escamilla, and I. Arkhipova, "Renewable Capacity Statistics 2020," 2020.

[2] Arina Anisie *et al.*, "Innovation landscape for a renewable-powered future: Solutions to integrate variable renewables," 2019.

[3] T. Ackermann, N. Martensen, T. Brown, P.-P. Schierhorn, F. G. Boshell, and M. Ayuso, "Scaling Up Variable Renewable Power: The Role of Grid Codes," p. 106, 2016.

[4] V. Gevorgian, M. Baggu, and D. Ton, "Interconnection Requirements for Renewable Generation and Energy Storage in Island Systems: Puerto Rico Example: Preprint," no. May, 2017.

[5] Q. Zheng, J. Li, X. Ai, J. Wen, and J. Fang, "Overview of grid codes for photovoltaic integration," *2017 IEEE Conf. Energy Internet Energy Syst. Integr. EI2 2017 - Proc.*, vol. 2018-Janua, pp. 1–6, 2017.

[6] J. M. Alvarez, I. de la P. Laita, L. M. Palomo, E. L. Pigueiras, and M. G. Solano, "Grid integration of large-scale PV plants: dealing with power fluctuations," *Large Scale Grid Integr. Renew. Energy Sources*, pp. 131–170, 2017.

[7] Circutor, "Circutor," *CVM-1D Series*. [Online]. Available: http://circutor.com/en/products/measurement-and-control/fixed-power-analyzers/power-analyzers/cvm-1d-series-detail. [Accessed: 14-Dec-2020].

[8] W. A. Omran, M. Kazerani, and M. M. A. Salama, "Investigation of Methods for Reduction of Power Fluctuations Generated From Large Grid-Connected Photovoltaic Systems," *IEEE Trans. Energy Convers.*, vol. 26, no. 1, pp. 318–327, 2011.

[9] I. de la Parra, J. Marcos, M. García, and L. Marroyo, "Control strategies to use the minimum energy storage requirement for PV power ramp-rate control," *Sol. Energy*, vol. 111, pp. 332–343, 2015.

[10] M. R. Islam, F. Rahman, and W. Xu, *Advances in Solar Photovoltaic Power Plants*. Berlin Heidelberg: Springer Nature, 2016.

[11] I. de la Parra, J. Marcos, M. García, and L. Marroyo, "Dealing with the implementation of ramp-rate control strategies - Challenges and solutions to enable PV plants with energy storage systems to operate correctly," *Sol. Energy*, vol. 169, no. March, pp. 242–248, 2018.

[12] V. Musolino, C. Rod, P. J. Alet, A. Hutter, and C. Ballif, "Improved ramp-rate and self consumption ratio in a renewable-energy-based DC micro-grid," in *2017 IEEE 2nd International Conference on Direct Current Microgrids, ICDCM 2017*, 2017, pp. 564–570.

[13] J. Martins, S. Spataru, D. Sera, D. I. Stroe, and A. Lashab, "Comparative study of ramp-rate control algorithms for PV with energy storage systems," *Energies*, vol. 12, no. 7, 2019.

[14] A. Ellis and D. Schoenwald, "PV Output Smoothing with Energy Storage," 2012.

[15] A. Allik, H. Lill, and A. Annuk, "Ramp rates of building-integrated renewable energy systems," *Int. J. Renew. Energy Res.*, vol. 9, no. 2, pp. 572–578, 2019.

[16] República Portuguesa, *Decreto-Lei n.º 162/2019 de 25 de outubro*. Portugal, 2019, pp. 45–62.

[17] A. Foles, L. Fialho, and M. Collares-Pereira, "Techno-economic evaluation of the Portuguese PV and energy storage residential applications," *Sustain. Energy Technol. Assessments*, vol. 39, no. March, p. 100686, 2020.

[18] J. Moshövel *et al.*, "Analysis of the maximal possible grid relief from PV-peak-power impacts by using storage systems for increased self-consumption," *Appl. Energy*, vol. 137, pp. 567–575, 2015.

[19] G. Lorenzi and C. A. S. Silva, "Comparing demand response and battery storage to optimize self-consumption in PV systems," *Appl. Energy*, vol. 180, pp. 524–535, 2016.

[20] J. Weniger, J. Bergner, and V. Quaschning, "Integration of PV power and load forecasts into the operation of residential PV battery systems," in *4th Solar Integration Workshop*, 2014, pp. 383–390.

[21] Y. Riffonneau, S. Bacha, F. Barruel, and S. Ploix, "Optimal power flow management for grid connected PV systems with batteries," in *IEEE Transactions on Sustainable Energy*, 2011, vol. 2, no. 3, pp. 309–320.

[22] R. Luthander, J. Widén, J. Munkhammar, and D. Lingfors, "Self-consumption enhancement and peak shaving of residential photovoltaics using storage and curtailment," *Energy*, vol. 112, pp. 221–231, 2016.

[23] G. L. Kyriakopoulos and G. Arabatzis, "Electrical energy storage systems in electricity generation: Energy policies, innovative technologies, and regulatory regimes," *Renew. Sustain. Energy Rev.*, vol. 56, pp. 1044–1067, 2016.

[24] R. Khalilpour and A. Vassallo, "Planning and operation scheduling of PV-battery systems: A novel methodology," *Renew. Sustain. Energy Rev.*, vol. 53, pp. 194–208, 2016.

[25] P. Alotto, M. Guarnieri, and F. Moro, "Redox flow batteries for the storage of renewable energy: A review," vol. 29, pp. 325–335, 2014.

[26] M. Guarnieri, P. Mattavelli, G. Petrone, and G. Spagnuolo, "Vanadium Redox Flow Batteries," *IEEE Ind. Electron. Mag.*, no. december, pp. 20–31, 2016.

[27] World Energy Council, "World Energy Resources 2016," London, 2016.

[28] K. Mongird, V. Viswanathan, J. Alam, C. Vartanian, V. Sprenkle, and R. Baxter, "2020 Grid Energy Storage Technology Cost and Performance Assessment," 2020.

[29] B. Turker *et al.*, "Utilizing a vanadium redox flow battery to avoid wind power deviation penalties in an electricity market," *Energy Convers. Manag.*, vol. 76, pp. 1150–1157, 2013.

[30] T. Sarkar, A. Bhattacharjee, H. Samanta, K. Bhattacharya, and H. Saha, "Optimal design and implementation of solar PV-wind-biogas-VRFB storage integrated

smart hybrid microgrid for ensuring zero loss of power supply probability," *Energy Convers. Manag.*, vol. 191, no. January, pp. 102–118, 2019.

[31] A. Bhattacharjee, H. Samanta, N. Banerjee, and H. Saha, "Development and validation of a real time flow control integrated MPPT charger for solar PV applications of vanadium redox flow battery," *Energy Convers. Manag.*, vol. 171, no. June, pp. 1449–1462, 2018.

[32] A. H. Fathima and K. Palanismay, "Modeling and Operation of a Vanadium Redox Flow Battery for PV Applications," *Energy Procedia*, vol. 117, pp. 607–614, 2017.

[33] A. Foles, L. Fialho, M. Collares-Pereira, and P. Horta, "Vanadium Redox Flow Battery Modelling and PV Self-Consumption Management Strategy Optimization," in *EU PVSEC 2020 - 37th European Photovoltaic Solar Energy Conference and Exhibition*, 2020.

[34] EDP Distribuição, "Atualização dos perfis de consumo , de produção e de autoconsumo para o ano de 2018 Documento Metodológico," 2017.

[35] F. P. M. Kreuwel, W. H. Knap, L. R. Visser, W. G. J. H. M. van Sark, J. Vilà-Guerau de Arellano, and C. C. van Heerwaarden, "Analysis of high frequency photovoltaic solar energy fluctuations," *Sol. Energy*, vol. 206, no. May, pp. 381–389, 2020.

[36] L. Fialho, T. Fartaria, L. Narvarte, and M. C. Pereira, "Implementation and validation of a self-consumption maximization energy management strategy in a Vanadium Redox Flow BIPV demonstrator," *Energies*, vol. 9, no. 7, 2016.

[37] IPMA, "IPMA API." [Online]. Available: http://api.ipma.pt/open-data/forecast/meteorology/cities/daily/. [Accessed: 14-Dec-2020].

[38] European Centre for Medium-Range Weather Forecasts, "ECWMF." [Online]. Available: https://www.ecmwf.int/. [Accessed: 14-Dec-2020].

[39] National Centre for Meteorological Research, "AROME." [Online]. Available: https://www.umr-cnrm.fr/spip.php?article120&lang=en. [Accessed: 14-Dec-2020].

[40] EDP Comercial, "EDP Comercial," *Electricity Tariffs*. [Online]. Available: https://www.edp.pt/particulares/energia/tarifarios/. [Accessed: 14-Dec-2020].

[41] E. López, L. Fialho, L. V. Vásquez, A. Foles, J. S. Cuesta, and M. C. Pereira, "Testing and evaluation of batteries for commercial and residential applications in AGERAR project," in *Mission 10 000: BATTERIES*, 2019.

## 4.3. Microgrid energy management control with a vanadium redox flow and a lithium-ion hybrid battery system for PV integration

Ana Foles[1], Luís Fialho[1], Manuel Collares-Pereira[1]

In *38th European Photovoltaic Solar Energy Conference and Exhibition,* p. 1464-1469, 2021, ISBN: 3-936338-78-7, 10.4229/EUPVSEC20212021-6BV.5.17

**Abstract**

Hybrid energy storage systems combine multiple energy storage technologies, to improve the overall storage's performance and lifetime expectancy, compared to a single storage unit. This work proposes an online power/energy sharing management control of a hybrid energy storage system and a simulation tool developed by the authors. The hybridized system is composed of two PV installations (3.6 kWp and 6.7 kWp), a vanadium redox flow battery (VRFB) (5.0 kW /60 kWh) and a lithium-ion battery (LIB) (3.3 kW useful /9.8 kWh). The software simulation architecture is designed using MATLAB, where three hypothetical operation scenarios are simulated, with the aim of optimizing the energy usage according to its technical characteristics, current state operation and PV generation, with a 1-year time frame. The system's overall performance is evaluated through three technical key-performance indicators. The combination of different energy storage technologies is a feasible solution that depends on the application goals and on the assurance of the accuracy and reliability of the system and its control strategy.

**Keywords:** Hybrid Energy Storage System, Energy Management, Vanadium-Redox Flow Battery, Lithium-ion battery, Solar Photovoltaic.

[1] Renewable Energies Chair, University of Évora. Pólo da Mitra da Universidade de Évora, Edifício Ário Lobo de Azevedo, 7000-083, Nossa Senhora da Tourega, Portugal

## 1. Introduction

The installed capacity for decentralized renewable energy production has been increasing. Photovoltaic (PV) self-consumption maximization is one of the most popular management strategies in the solar photovoltaic sector nowadays. Renewable energy mini-grids are new grids that combine renewable energy and loads to operate on a self-sustained basis (matching discharge time within the time frame needs) [1]. Energy storage systems (ESS) help to make this match, giving additional stability to these grids. World is looking for ESS solutions that are preferentially scalable, modular, flexible, but also cheap and reliable.

Electricity storage contributes to a flexible power system. Storage can be conceived to be applied on meeting the demand and reliability in the grid peak hours; liberalized electricity markets can benefit from price arbitrage, capacity credit, ancillary resources or having customer side benefits [2]; shifting electricity from low demand to peaks, giving support to intermittent renewable energy sources, distributed generation, or smart grid initiatives, and provide alternative solutions to increase flexibility – as, demand-side management (DSM) or flexible power demand, or even smart charging strategies for Electric vehicles (EV) [3].

The energy management strategies can help in the execution of grid services such as peak shaving and curtailment avoidance, or simply balancing of loads through the power command management. Establishing the optimal technical and economic combination of different strategies and/or services is a complex task, highly dependent on the power consumption and generation profiles, market factors, applied tariffs, the existence of a grid connection to the system, general system costs, among others.

This value-stacking approach of simultaneous usage of different energy management strategies requires making trade-offs between energy needs, power needs, battery life and degradation, specific acquisition or O&M costs, etc. The hybrid energy storage system (HESS) can effectively present advantages to this multigoal task. For instance, the vanadium redox flow batteries are well suited for low power, long discharge applications, and the lithium-ion batteries in higher power applications. A Hybrid ESS can alleviate peak power stress, allowing to optimize the lifetime of these assets. Considering other fundamental technical characteristics of these systems, such as the physical limits of the technologies (State of Charge, operation temperature, etc.), allow to achieve an improved operation that, sometimes, can have competing goals.

This work presents the online operation control of a hybrid battery system VRFB-LIB, based on power-sharing techniques, for PV integration. The use of power-sharing to allocate power is studied to achieve reasonable energy distribution between the batteries and improve the utilization of energy. In the literature, several power management methods can be found as in [4]–[8]. In this work, the control strategy is proposed in three main approaches, and its effectiveness is verified through the technic key-performance indicators results, based on one-year simulation profiles. The control considers both batteries states of charge (SOC), performance, dynamics characteristics (assured by the used battery models), charge and discharge patterns. The simulation results show the improved use of energy storage devices.

The paper is organized as follows. First, the proposed Hybridisation of VRFB-LIB ESS is presented in Section 2. In Section 3, the methodology used to simulate the power-sharing of the hybrid solution is explained. In Section 4, the simulation results are presented. Finally, Section 5 draws the conclusions of the present work.

## 2. Hybridisation of batteries

### 2.1. Interconnection of batteries

In the case of energy storage system technologies, hybridisation directly uses to the combination of more than one unit and generally is established in a single grid network. The combination is made to answer to a certain application usage case, to attend to specific needs. Hybrid battery technologies are being studied in the literature, given the distinct characteristics of each one, that can be complementary to each other. This approach can be applied for any project that combines multiple energy generation, storage, or load control technologies, co-located either physically or virtually.

Hybrid control could optimize the EMSs, allow the delivery of multiple services (“stacked”), and consider different planning horizons.

A review on Energy Storage Systems is conducted by the authors of [9], where Hybrid Energy Storage Systems (HESS) are detailed. These systems are combined considering their costs, performance, and environmental factors, emphasizing the benefits of individuals. Nevertheless, the state-of-the-art presents gaps in the development of management strategies for these systems validated with parameters and real technical restrictions in an experimental environment.

In this work, a LIB and a VRFB with different energy and power capabilities, integrated into the microgrid of the Renewable Energies Chair of the University of Évora, are studied. Table I presents the main general characteristics of each of the energy storage technologies under study. The interconnection of different energy storage systems could result in a complementary characteristics solution, to result in an overall increase of the system's performance. The selection of a specific storage type is a result of technical and/or economic optimization.

Table I: Technical characteristics of ESS systems [3][6].

| Battery/ Characteristic | VRFB | Lithium-ion |
|---|---|---|
| Power range (MW) | 0.03-3 | Up to 0.01 |
| Discharge time | s-10h | m-h |
| Overall efficiency Power | 0.65-0.85 | 0.85-0.95 |
| Power density (W/kg) | 166 | 50-2000 |
| Energy density (Wh/kg) | 10-35 | 150-350 |
| Storage durability | h-months | Min-days |
| Self-discharge (per day) | Small | 0.1-0.3 % |
| Lifetime (year) | 10-20 | 5-15 |
| Life cycles (cycles) | 10000-13000 | 1500–4500 |
| Response time | Fast | Very fast |
| Self-discharge | Null | Low |

HESS interconnection can be achieved using different approaches. The simplest and most cost efficient is through a direct DC-connection on the battery terminals, although it lacks energy management or controllability. An alternative approach is through an active power electronics interface between the different storages to a more flexible and efficient HESS [10] across the AC grid.

## 3. Methodology

In this section, the methodology which allowed the one-year simulation of the proposed hybrid configurations evaluation is explained.

### 3.1. Microgrid constraints

The HESS is a result of the combination of the LG Chem RESU 10 lithium-ion battery (LIB) of 5.0 kW /9.8 kWp, and the redT vanadium redox flow battery (VRFB) system of 5.0 kW /60 kWh, as shown in Figure 1, and the microgrid architecture is represented in Figure 2, presented below. Since the LIB inverter has a nominal power capacity of 3.3 kW, this is the assumed maximum capacity that can be retrieved from the LIB system. These technologies were chosen to be an object for this study, due to their distinct characteristics as energy capacity, efficiency, lifetime, and response time.


Figure 1: (a) Solar photovoltaic installation 6.7 kWp; (b) Solar photovoltaic installation 3.2 kWp; (c) VRFB redT 60 kWh; (d) LIB LG Chem Resu 10, 9.8 kWh.

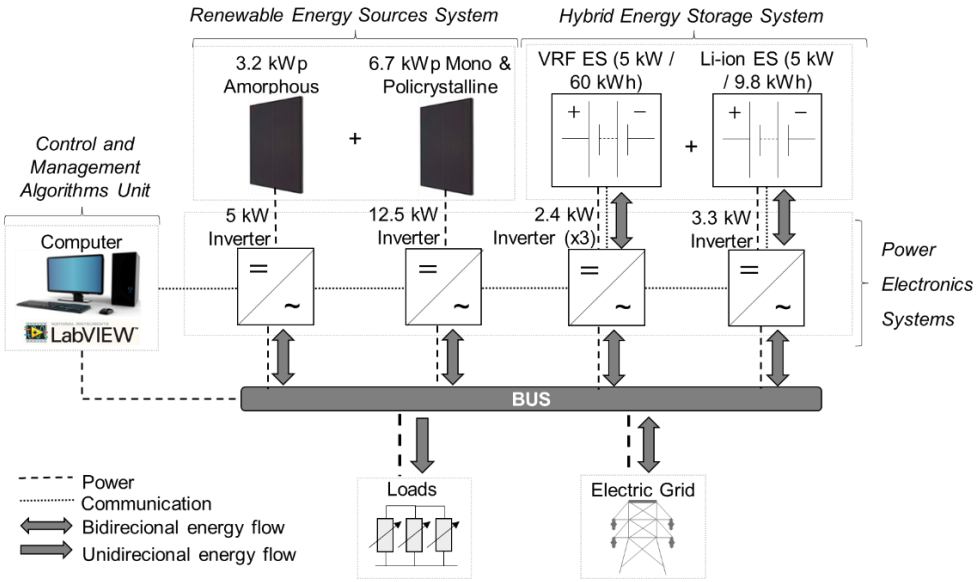


Figure 2: Scheme of the hybrid battery integration within the Renewable Energies Chair of the University of Évora's microgrid.

The power electronics efficiency of the VRFB was previously calculated and included in the developed model of the VRFB developed in [11], discussed below. In the case of the VRFB, the minimum value (limit) of the voltage is settled by the power inverter. Further development of lower voltages operation of power electronics should help the use of the battery at its fullest energy capacity. In addition, a value of 30 W total of the standby mode of the inverters was considered. The algorithms time of application is on a 1-minute basis.

### 3.2. PV and load consumption treatment output

One of the input variables is photovoltaic production. In this work, the actual PV generation curves were used, a complete year of data (2019) of the two installed PV systems (see Figure 3). The data from the two installations were treated separately and gathered for the results. The raw registered data is obtained with a 1- and 2-seconds interval, although, for this paper, a 1-minute average was achieved.

The load profile used is made available by the Portuguese DSO company E-REDES, with 15 minutes averaging of load data for the year 2019, for each of the Portuguese consumption sectors, in this case, for the BTN B sector, which corresponds to the overall consumption in buildings [12]. The data were treated to correspond to the 1-minute data sampled time frame for the PV.

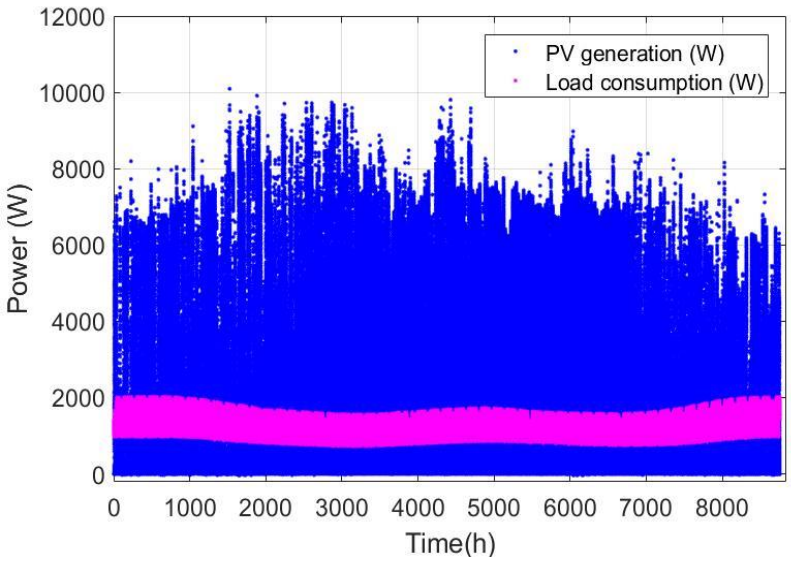


Figure 3: PV generation and load power profiles for the period of one year (2019) [12].

### 3.3. Modeling tool description

The model was developed with the help of the MATLAB programming tool, as a first approach to discuss the hybrid battery performance. The model was built to reproduce the operation of the batteries, describing their behaviour, also considering the inverters and general microgrid losses, computing the energy management systems' algorithms, and delivering the evaluation of the overall system, based on the selected key performance indicators (KPIs). In the studied scenarios, this tool provides information to evaluate whether the control offers a technically attractive solution to be considered for cost-effectiveness.

The developed model architecture was designed to be flexible to the addition of different battery units, data inputs, and model management of the overall system. The developed model allows the batteries to be operated together, to evaluate the overall HESS operation. For this purpose, the work main contribution is on the design algorithm to define HESS operation and control, the development of the energy routine for better energy performance, and the possibility of operating the HESS in a way to carry out multiple tasks.

### 3.4. Battery modelling

The operation of each BESS is achieved through its simulation model. Each battery was previously tested experimentally through characterization tests in each general operating conditions. The batteries physical constraints must be included in the model, as boundaries, such as the maximum allowable power and capacity, SOC or depth of discharge (DOD) limits, efficiencies, lifetime. Other constraints are related to the model initial definitions, being batteries-related as well. These constraints are enunciated in Table II, below.

Battery lifetime depends strongly on the operation conditions: temperature, state of charge and total energy throughput (electrochemical operating windows) and charge and discharge rates. Ageing depends on technology, usage conditions, storage conditions, and operation (temperature, charge/discharge rates, voltage operation limits). The knowledge currently available on these matters results from a vast combination of experimental and modelling approaches [14]. In this work, the time frame evaluation is of one year, and for that reason, no battery degradation was assumed.

Table II: Values of key technic parameters of the LIB and VRF batteries for modelling inputs [13].

| Quantity | Value | Value reference |
|---|---|---|
| VRFB Maximum power (W) | 5000 | According to power-SOC relation and nominal power |
| VRFB nominal energy capacity (kWh) | 60 | Nominal energy capacity |
| VRFB SOC range (%) | 10-95 | According to lifetime strategy |
| VRFB operating voltage range (V) | 50-60 | Manufacturer and inverter dependent |
| LIB Maximum power (W) | 3300 | According to power-SOC relation and nominal power |
| LIB SOC range (%) | 15-95 | According to lifetime strategy |
| LIB nominal energy capacity (Ah) | 189 | Nominal energy capacity |
| LIB operating voltage range (V) | 48-61 | Manufacturer and inverter dependent |
| Initial SOC of both LIB and VRFB | 50 | Strategy starts at the middle interval |
| Temperature (ºC) | 20-35 | General operating condition |

### 3.4.1. VRFB modelling

The VRFB is integrated with the building at a real scale, in a microgrid exclusively devoted for its testing and systems operation study. The nonlinear Nernst-Plank equation is one of the modelling approaches used to describe the multiphysics of the VRFB. The model is considered an equivalent circuit that describes the major reaction occurring in real-time operation, with reduced complexity and satisfying results. The VRFB was firstly fully experimentally characterized, and the model was validated with an energy management strategy, developed in the work in [13]. The model includes thermal effects, transients, dynamic SOC, and auxiliary consumption determination.

### 3.4.2. Lithium-ion modelling

The LIB models currently have an emphasis on the research field, most of them developed for the automotive sector. The authors of the present work developed a model of the lithium-ion battery integrated into the microgrid. Taking the bibliographical references regarding the LIB modelling for grid applications, the simple electrical equivalent model and the modified Shepperd model were used to describe the battery of this microgrid, considering the experimental characterization results, previously achieved.

### 3.5. EMS and Power command – HESS Allocation Method

In this work, the energy management strategy controls the connected power-inverters and operate the units according to the pre-defined set of rules. The goal is to have a power profile smoothing to be exchanged with the grid and the maximization of self-consumption while simultaneously protecting the battery SOC to be around the defined operational limits and the power profile limits.

A coordination block is created to virtually distribute power among the operation of the system. The filter-based power provides power splitting, as shown in Figure 4. The power-sharing strategy assigns higher power ramps to the LIB and the baseload power to the VRFB. The LIB energy capacity is lower compared with the VRFB, and its SOC can reach its extremes more often, which limits battery usability. The power-sharing ratio among the energy storage system could be dynamically adjusted for SOC regulation. The systems architecture is designed to operate the VRFB as the primary energy component, and the LIB has the primary power component. The power adjustment is achieved through the inverter control power command.

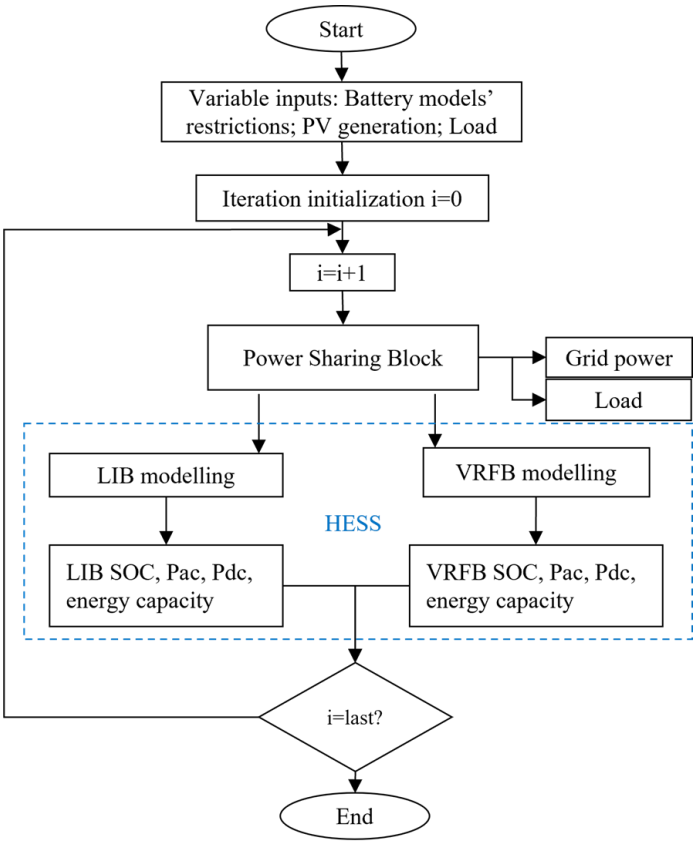


Figure 4: Modelling scheme of the hybrid energy storage system for the 3 scenarios.

The energy management strategy of self-consumption maximization is based on the HESS power allocation control. Different scenarios for the power allocation method are researched:

- **Scenario I** – The power-sharing is distributed with a fixed power ratio for each of the batteries. In this scenario, 75% of the total power is requested/retrieved from VRFB, and the rest is requested/retrieved from LIB.
- **Scenario II** – Scenario I with variable ratios. HESS is operated depending on the LIB state of charge. It obeys a power-SOC relation:

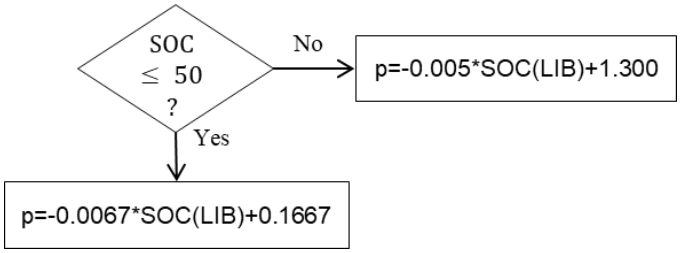


With p as the percentage. The remaining power is requested/retrieved from VRFB.

- **Scenario III** – Dynamic variability power command for LIB and fixed value for VRFB. It is the realization of two services for each battery (as if LIB executes a peak shaving strategy).

### 3.6. Key-Performance Indicators

The evaluation of the HESS power allocation control will be evaluated for a one-year time frame, using the key-performance indicators enunciated below.

- **Self-consumption ratio (SCR)** – Share of the PV generation consumed by the installation from the total of the PV energy generation.

$$SCR = \frac{E_{PVconsumed}}{E_{PVgenerated}} \tag{1}$$

- **Grid-relief factor (GRF)** – The grid relief factor offers a measure of the total grid use in the overall load consumption needs.

$$GRF = \frac{E_{Grid}}{E_{Load}} \tag{2}$$

- **Overall battery use (BU)** – Share of energy of the power battery command in the overall energy consumption

$$BU = \frac{E_{fromBattery} + E_{toBattery}}{E_{Load}} \tag{3}$$

The parameters are based on the sum of the energy used throughout the days of the strategy application. The indicators are calculated for the overall strategy output results, although the BU is calculated separately for each battery.

## 4. Simulation results

The initial state of charge is 50% for both batteries, and the simulation sample time is of 1 minute, over an entire year. The simulation tool allows for obtaining the energy fluxes that occur at each moment, which, in turn, allow for the calculation of the technical performance indicators, as the example of Figure 5, shown below.

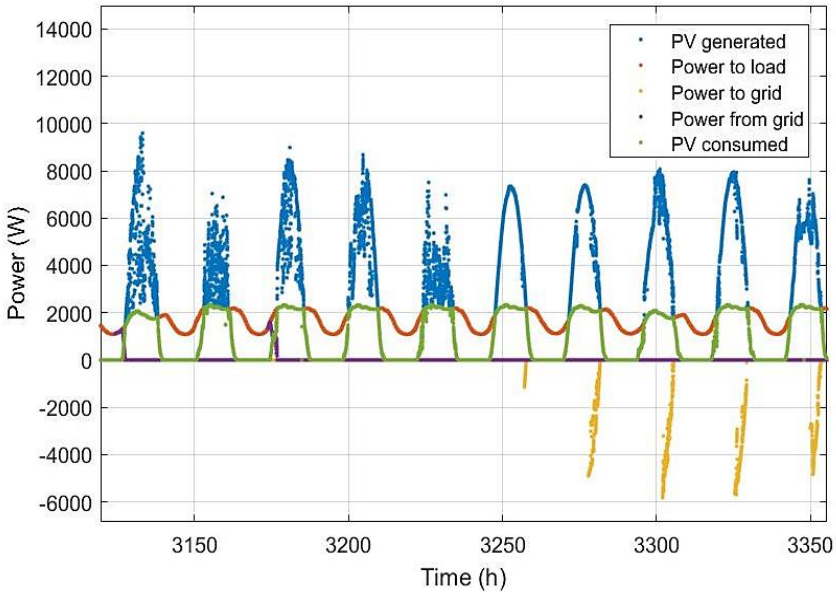


Figure 5: Output of the simulation tool, where the sum of the energy fluxes of the simulated year allows the calculation of the technical performance indicators.

The impact of the power-sharing in the studied scenarios is presented in Table III, where the calculated key-performance indicators results are shown.

Table III: Simulation results of power and energy exchange with the loads and utility grid using different power-sharing scenarios, a yearly basis.

| Scenario | SCR | GRF | BU LIB | BU VRFB |
|---|---|---|---|---|
| I | 0.53 | 0.35 | 0.55 | 0.67 |
| II | 0.53 | 0.27 | 0.63 | 0.64 |
| III | 0.53 | 0.36 | 0.54 | 0.64 |

The state of charge impact is shown in Figures 6 in (a), (b) and (c), and the AC power requested to the inverter (charge or discharge the battery) is shown in Figure 7, in (a), (b) and (c).

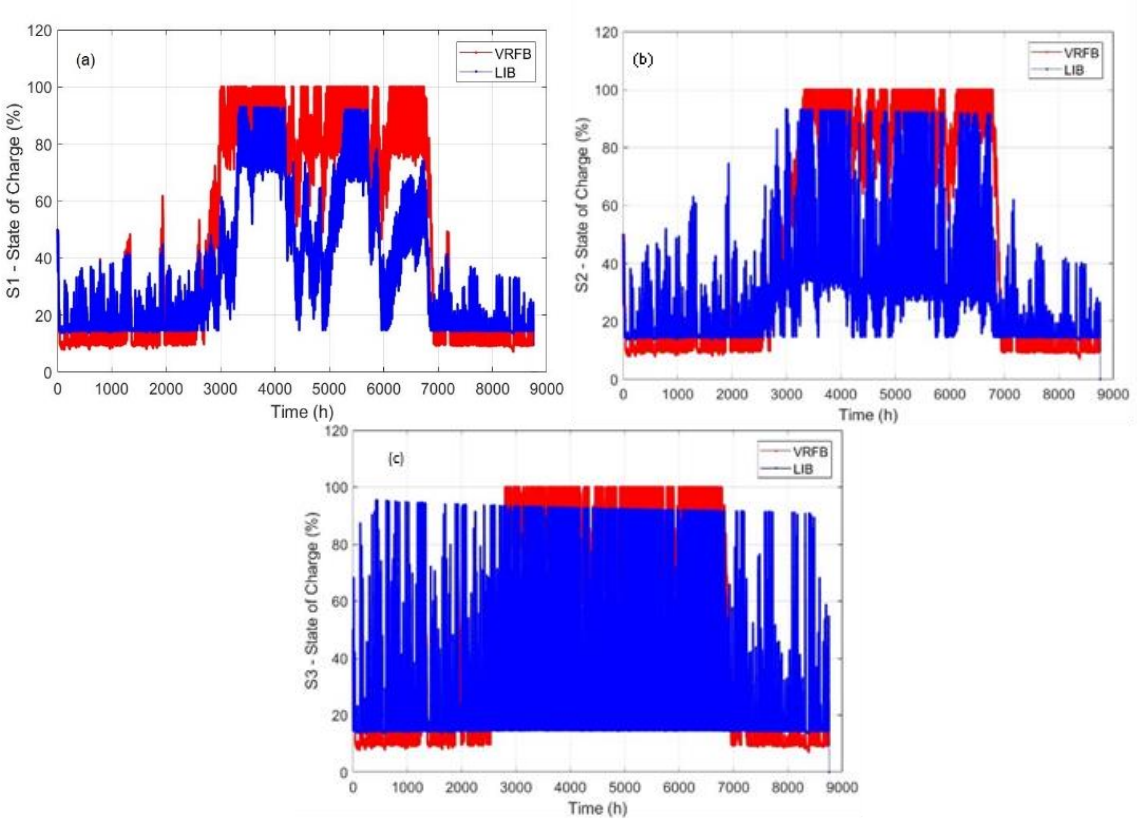


Figure 6: Output of the simulation tool: SOC evolution for both batteries for Strategy 1 (a), Strategy 2 (b) and Strategy 3 (c).

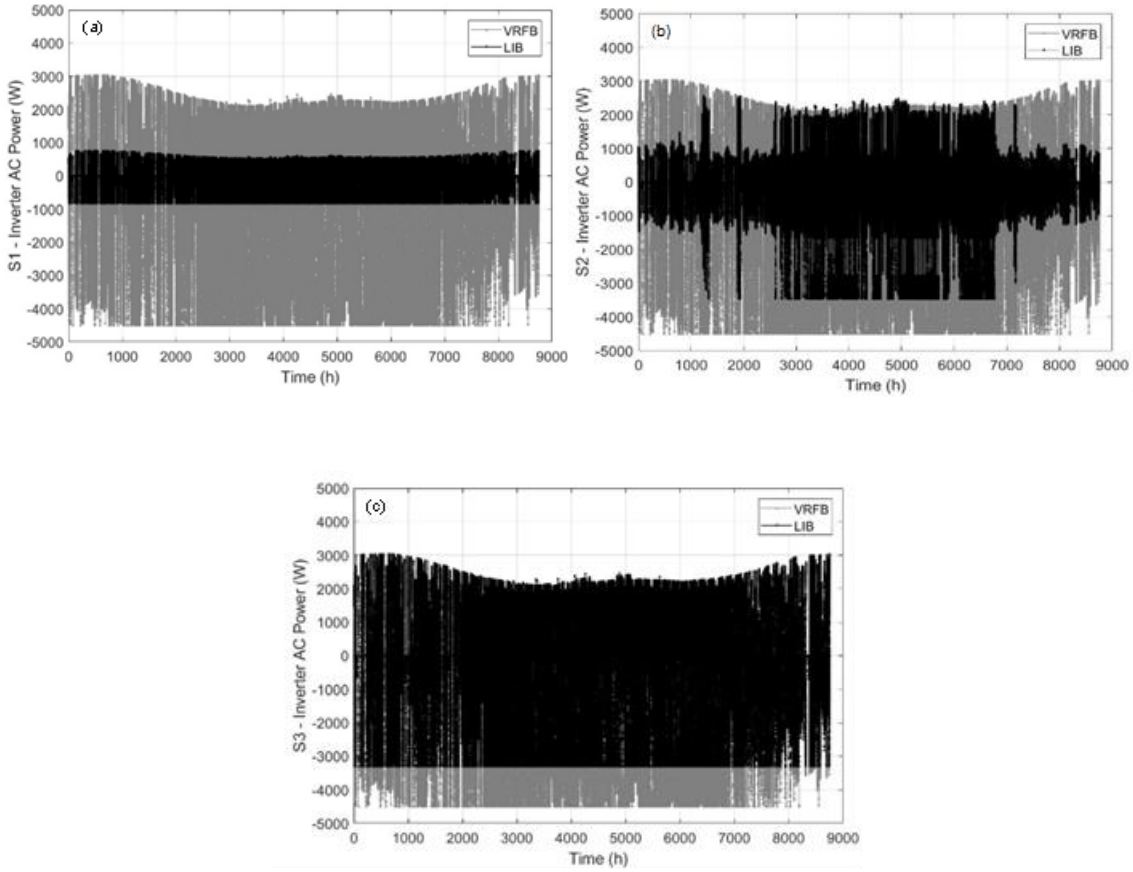


Figure 7: Output of the simulation tool: AC Power of the inverter of both batteries for Strategy 1 (a), Strategy 2 (b) and Strategy 3 (c).

## 5. Conclusions

A robust control can improve system dynamics, minimizing extreme SOC states and power levels, or peak temperatures caused by high C-rate operation. Scenario I is a rough approach as HESS power-sharing method. Scenario II improves the systems dynamic, by lowering extreme power SOC states. Scenario III offer the efficient realization of different tasks.

SCR is maintained in the three scenarios, the GRF is the smallest for Scenario II given the better batteries exploitation. VRFB executes the baseload in all the scenarios, shown by its BU indicator. The LIB BU indicator presents a higher use in Scenario 2 even though the LIB operation is controlled by the SOC-power profile. Summer-Winter differences are present regarding BU, and Scenario 3 presents a smaller LIB BU due to a smoothing of the grid power exchange operation.

Further conclusions should be drawn regarding a technical-economic analysis of this scenario comparison and considering battery ageing. Initial investment costs (CAPEX)

should be considered for complete analysis as well as a seasonal results analysis. A robust cost analysis constitutes an important goal of future work.

**Acknowledgements**

The authors would like to thank the support of this work, developed under the European POCITYF project, financed by 2020 Horizon under grant agreement no. 864400. This work was also supported by the PhD. Scholarship (author Ana Foles) of FCT – Fundação para a Ciência e Tecnologia –, Portugal, with the reference SFRH/BD/147087/2019.

## 6. References

[1] Arina Anisie *et al.*, "Innovation landscape for a renewable-powered future: Solutions to integrate variable renewables," 2019.

[2] J. Liu, C. Hu, A. Kimber, and Z. Wang, "Uses, Cost-Benefit Analysis, and Markets of Energy Storage Systems for Electric Grid Applications," *J. Energy Storage*, vol. 32, no. February, p. 101731, 2020.

[3] B. Zakeri and S. Syri, "Electrical energy storage systems: A comparative life cycle cost analysis," *Renew. Sustain. Energy Rev.*, vol. 42, pp. 569–596, 2015.

[4] Y. Ye, P. Garg, and R. Sharma, "Development and demonstration of power management of hybrid energy storage for PV integration," *2013 4th IEEE/PES Innov. Smart Grid Technol. Eur. ISGT Eur. 2013*, pp. 1–5, 2013.

[5] L. Kouchachvili, W. Yaïci, and E. Entchev, "Hybrid battery/supercapacitor energy storage system for the electric vehicles," *Journal of Power Sources*, vol. 374. Elsevier B.V., pp. 237–248, 15-Jan-2018.

[6] M. U. Mutarraf, Y. Terriche, K. A. K. Niazi, F. Khan, J. C. Vasquez, and J. M. Guerrero, "Control of hybrid diesel/PV/battery/ultra-capacitor systems for future shipboard microgrids," *Energies*, vol. 12, no. 18, pp. 1–23, 2019.

[7] Z. Bai, Z. Yan, X. Wu, J. Xu, and B. Cao, "CONTROL FOR BATTERY/SUPERCAPACITOR HYBRID ENERGY STORAGE SYSTEM USED IN ELECTRIC VEHICLES," *Int. J. Automot. Technol.*, vol. 20, p. 1287?1296, 2019.

[8] Y. Zhang, Z. Yan, C. C. Zhou, T. Z. Wu, and Y. Y. Wang, "Capacity allocation of HESS in micro-grid based on ABC algorithm," *Int. J. Low-Carbon Technol.*, vol. 15, no. 4, pp. 496–505, 2020.

[9] A. Z. AL Shaqsi, K. Sopian, and A. Al-Hinai, "Review of energy storage services, applications, limitations, and benefits," *Energy Reports*, vol. 6, pp. 288–306, 2020.

[10] S. Resch and M. Luther, "Reduction of Battery-Aging of a Hybrid Lithium-Ion and Vanadium-Redox-Flow Storage System in a Microgrid Application," *Proc. - 2020 2nd IEEE Int. Conf. Ind. Electron. Sustain. Energy Syst. IESES 2020*, pp. 80–85, 2020.

[11] L. Fialho, T. Fartaria, L. Narvarte, and M. C. Pereira, "Implementation and validation of a self-consumption maximization energy management strategy in a Vanadium Redox Flow BIPV demonstrator," *Energies*, vol. 9, no. 7, 2016.

[12] E-REDES and Q-metrics, "Update of consumption, production and of self-consumption for the year 2019," 2019. [Online]. Available: https://www.e-redes.pt/sites/eredes/files/2019-03/DocMetodologico_Perfis2019_20190111v2.pdf.

[13] A. Foles, L. Fialho, M. Collares-Pereira, and P. Horta, "Vanadium Redox Flow Battery Modelling and PV Self-Consumption Management Strategy Optimization," in *EU PVSEC 2020 - 37th European Photovoltaic Solar Energy Conference and Exhibition*, 2020.

[14] "Battery Lifespan | Transportation and Mobility Research | NREL." [Online]. Available: https://www.nrel.gov/transportation/battery-lifespan.html. [Accessed: 02-Jul-2021].

## 4.4. Economic and energetic assessment of a hybrid vanadium redox flow and lithium-ion batteries, considering power sharing strategies impact

Ana Foles[1,2], Luís Fialho[1,2], Pedro Horta[1,2], Manuel Collares-Pereira[1,2],

In *Journal of Energy Storage, 2023, vol. 71, 1008167, ISSN: 2352-152X,*
https://doi.org/10.1016/j.est.2023.108167
*Open access version in ArXiv:* http://arxiv.org/abs/2301.02535

**Abstract**

Hybrid energy storage systems (HESS) combine different energy storage technologies aiming at overall system performance and lifetime improvement compared to a single technology system. In this work, control combinations for a vanadium redox flow battery (VRFB, 5/60 kW/kWh) and a lithium-ion battery (LIB, 3.3/9.8 kW/ kWh) are investigated for the design of a HESS. A literature review presents the available energy management/ power allocation options that are being studied and applied worldwide in batteries. There is an identified need for opportunities to address better HESS configuration's economic and energy perspective for building applications. The justification of investment in such HESS should improve indicators on use scenarios based on energy management compared to single-battery scenarios. In that context, four scenarios for real-time algorithms application approaches are considered to operate the hybrid storage solution through a 15-year economic and energetic analysis using experimentally validated battery performance models. The results obtained for each scenario are compared with a single technology battery performance to analyse this HESS pair competitiveness and the relevance of the power-sharing techniques among the different ESS technologies, which should be weighted. In the definition of the scenarios, real electricity generation is considered from two solar photovoltaic installations (3.2 kWp and 6.7 kWp) and an estimated representative load of a services building. HESS performance is evaluated through specific energy and economic key performance indicators. The results indicate that using customised energy management strategies (EMSs) renders the VRFB and LIB characteristics complementary, besides enhancing the competitiveness of VRFB as a single technology. Moreover, the HESS management impacts the seasonality factor, contributing to the overall electric system smart management.

[1] Renewable Energies Chair, University of Évora, 7000-651, Évora, Portugal

[2] Institute of Earth Sciences, University of Évora, Rua Romão Ramalho, 7000-671, Évora, Portugal

**Keywords:** Solar photovoltaic energy; VRFB; lithium-ion battery; hybridisation; Energy management strategy

| **Abbreviation** | |
|---|---|
| BCR | Battery Charge Ratio |
| BESS | Battery Energy Storage System |
| BMS | Battery Management System |
| BTN | Normal Low Voltage |
| CEP | (European) Clean Energy Package |
| DOD | Depth of Discharge (%) |
| DSO | Distributor System Operator |
| EG | Energy from the Grid |
| EMS | Energy Management Strategy |
| ESS | Energy Storage System |
| EV | Electric Vehicle |
| EOL | End Of Life |
| FBU | From Battery Use |
| FGU | From Grid Use |
| FL | Fuzzy Logic |
| GRF | Grid Relief Factor |
| HESS | Hybrid Energy Storage System |
| IRR | Internal Rate of Return (%) |
| KPI | Key-Performance Indicator |
| LCOE | Levelized Cost of Energy (€/kWh) |
| LIB | Lithium-Ion Battery |
| LPF | Low-Pass Filter |
| NPV | Net Present Value (€) |
| NREL | National Renewable Energy Laboratory |
| OBU | Battery Use |
| PV | Photovoltaic |
| RES | Renewable Energy Sources |
| SAM | System Advisor Model |
| SCM | Self-Consumption Maximisation |
| SCR | Self-Consumption Ratio |
| SOC | State Of Charge (%) |
| SPB | Simple Payback (years) |
| SSR | Self-Sufficiency Ratio |
| TBU | To Battery Use |
| TGU | To Grid Use |
| TLCC | Total Life Cycle Cost (€) |
| TSO | Transmission System Operator |
| UÉvora | University of Évora |
| VAT | Value-Added Tax |
| VRE | Variable Renewable Energy |
| VRFB | Vanadium Redox Flow Battery |
| VRLA | Valve-Regulated Lead-Acid |

## 1. Introduction

In 2020, the global additional installed power of battery energy storage systems (BESS) reached 5 GW, a 50% increase compared to the previous year [1]. Despite this significant installed power capacity increase, the role of BESS in the power grid remains vague: European Clean Energy Package (CEP), published by the European Commission in October 2019 [2] distinguishes storage from generation, transmission or load, to prevent double taxes when operating a battery (charge/ discharge), yet there is slow progress in the establishment of BESS development and use regulations.

When used at the energy system level, BESS can be conceived to provide different services, such as price arbitrage, capacity credit, ancillary resources (e.g. for voltage/ frequency regulation), integration of non-dispatchable renewable electricity production or smart charging for electric mobility [3]. At smaller scales, in residential, industry or services buildings, BESS can provide both maximised PV self-consumption and overall electricity reduction costs [4]. Through battery energy and power management, a smart control strategy can favour BESS performance in the execution of grid services such as peak shaving, curtailment avoidance or balancing of loads. Establishing an optimal energetic, technical and economical combination of performance goals is a complex task, highly dependent on manifold factors, such as, e.g. generation and consumption profiles, market regulation, applied electricity tariffs, grid connection parameters or system costs.

When considering more than one BESS unit, the optimal management strategy can be described as the delivery of multiple services or the simultaneous improvement of more than one objective. Although the cost-benefit assessment of such a system might be challenging given the lack of regulation [5], if several service revenue streams are "stacked", the investment in a BESS can be profitable [6].

Among the commercially available BESS technologies, the lithium-ion battery (LIB) continues to be the most widely used [1] in view of its cost decrease over the last few years. In addition to LIB, alternative chemistry batteries with potential cost decrease in the nearest future are the ones based on sodium and redox flow.

Given this context, this work investigates whether the hybridisation of LIB and VRFB technologies improves the competitiveness of an overall generation-storage-consumption system, addressing the following questions:

1. Does the LIB+VRFB HESS configuration improve the competitiveness of single VRFB or single LIB BESS configurations?

2. Which EMSs/ power allocation can be applied to HESS?
3. Is improving or maintaining the self-consumption rate possible, considering a seasonality factor in the battery state of charge operational range?

Aiming at raising awareness of the HESS management possibilities and associated technical aspects, this work is structured as follows: Section 2 delivers a literature review on HESS, Section 3 presents the overall methodology used in this work, Section 4 provides the main simulation results, and Section 5 addresses its assessment, with a final remark on future work (5.1). Finally, the fundamental conclusions of this work are detailed in Section 6.

## 2. Literature review of HESS

For the case of energy storage technologies, hybridisation is applied to any project that combines different energy storage technologies, generation, or load control technologies, co-located physically or virtually in a single network. Each BESS is combined to complement costs, performance, and environmental factors [7]. The HESS applied to microgrids with renewable energy sources (RES) is distinguished based on the application, capacity sizing, topology, configuration, energy management and control system [8].

Next, the HESS topologies, control techniques, and real-life demonstrators are summarised, and the HESS configuration studied in this work is justified.

### 2.1. Topologies

The integration of the HESS converter is selected considering the characteristics of cost, efficiency, controllability, complexity, and flexibility. Over literature, the HESS converters are categorised by the type of control, namely passive, semi-active or active [8].

Passive control is a simple and cost-effective solution where the different ESS units are physically connected, though they are not controllable. In the semi-active control, the inverter is connected to one ESS, while the other ESS is connected to the DC bus. This type of control is limited; however, the cost is lower than the active control. In the active control, each ESS is connected to its respective power converter. It is the most efficient and reliable converter even though the cost and complexity are higher when compared to previously mentioned topologies [8] [9].

## 2.2. Control, management, and power allocation strategies

HESS management and control are generally distinguished from classical and intelligent-based methods [8]–[10]. Classical methods are based on the ESS mathematical modelling and are suitable for real-time application, given the less computational effort; intelligent-based methods aim to maximise goals through optimisation functions, though with higher computational effort. The details of existing control methods are enunciated in Figure 1.

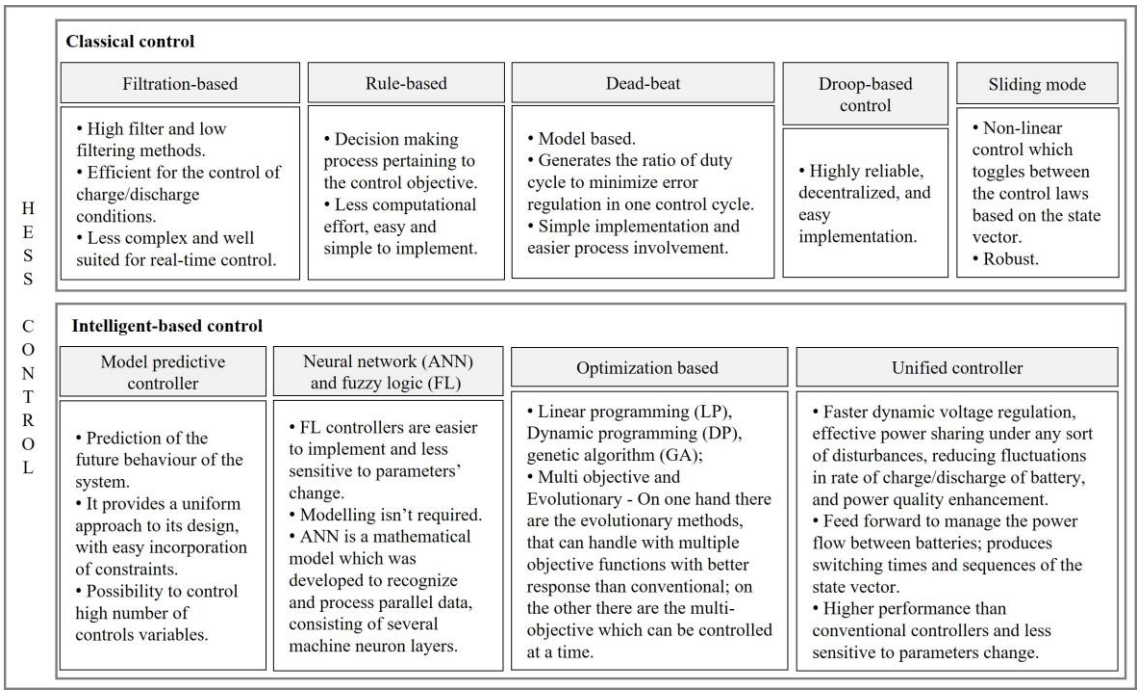


Figure 1 - HESS control methods summary, based on [8]–[10].

Relevant works on the field of energy management of energy storage and energy sources hybridisation are found in the literature but mostly for general hybrid energy systems, without a clear focus on the hybrid energy storage system, and in this case, do not approach the different ESS technologies interaction as the present work does. In [11] the authors optimise the integration of different batteries and different generation sources (PV and wind) through the use of valuable parameters such as the LCE (life cycle emission) and COE (cost of energy), although integrating single ESSs configurations. Also, the authors of [12] present a study on the predictive energy management strategy based on machine learning applied to buildings, and the authors of [13], where a novel two-step approach to deal with hybrid energy sources to optimise the techno-economic aspects, sizing the system and minimising the LCOE, considering operation and management. The authors of [14] study the optimal operation

management of a microgrid with two distinct objectives (operation cost and emission propagation), considering an optimal solution based on fuzzy logic approach.

With regards to the hybridisation of batteries (in this work approached as electrochemical and electrical devices), approached in this work as HESS, the following state of the art is described. The HESS potential has been identified for several energy-consuming sectors. For transports, the combination of batteries and supercapacitors is the most studied configuration, as referred to in work developed in [17], which considers a power allocation strategy based on a low-pass filter (LPF) and fuzzy logic (FL) control technique. Within the transport sector, lithium-ion batteries with different cathode chemistries, LFP and LTO, are addressed in [18] and further validated, demonstrating a more significant lifetime of hybridised LFP technology rather than single LFP technology. Fuel cells and lithium-ion batteries are investigated in [19], considering online and offline EMS methods to improve fuel consumption and source lifetime. The authors of [12] investigate the interaction of fuel cells, lithium-ion batteries and ultracapacitors for HEV application, which are sized as an optimisation problem. The authors of [15] address fast and short-term fluctuations of PV systems at the residential scale, including impact analysis on the battery-supercapacitor HESS group. The work focused on presenting the influence of dynamic battery operation influence in the studied KPIs, considering the optimised HESS sizing. In [16], the authors developed a techno-economic optimisation for the size and power management of a residential use-case (PV, battery, EV charger, load consumption) to optimise PV self-consumption, day-ahead and frequency containment reserve (FCR), also account for dynamic battery degradation.

A fuel cell and a nickel sodium chloride battery are studied in [20] using electrical battery models, and real-time implementation is achieved. Economic approaches are also addressed, such as in [21], where six configurations of batteries and flywheels NPV and LCOE indicators were calculated for a Greek island application and compared with single ESS scenarios. The configuration of VRFB and LIB is investigated in [22] to improve the BESS lifetime. Four scenarios are studied, with the calculation of a few energy indicators (to and from the grid). With this configuration, authors in [23] studied the HESS integration with RES, while an EMS uses a predetermined forecasted and scheduled power curve to evaluate power mismatch. Though the hybridisation of batteries is being addressed in the literature, the topic is still recent, and studies reveal a lack of complete assessment which could fairly address real-time EMSs, considering the interaction of batteries.

### 2.2.1. Demonstrators

Project commissioning validates the HESS power control allocation challenges in real-time suitability, performance, and KPIs analysis. Several HESS worldwide demonstrators can be found:

- HESS RES integration and isolated application; validation of configurations and models; technical optimisation (e.g., battery degradation, thermal stress, performance):
  - 2021, HYBRIS [24] with HESS (1 MW /0.47 MWh) demonstrators in Italy, Belgium, and The Netherlands.
  - 2020 [25] investigates high-output lithium-ion batteries with high-capacity lead-acid storage batteries to facilitate wind generation systems applied in Poland.
  - 2016, The Duke Energy Rankin Project [26] combined a battery and supercapacitor, 100 kW/ 300 kWh, installed in Gaston, North Caroline, USA.

- HESS simulation and management for control and stability purposes:
  - 2020, HyFlow [27] with a high-power vanadium redox flow battery (RFB) and a supercapacitor, advanced converter topologies and a flexible control system.
  - 2019, the SHAD project [28] developed AC and DC solutions to control different battery technologies: supercapacitors, flywheels, or fuel cells, for multiple applications.

- HESS grid services and integration – Algorithms, performance, suitability:
  - 2019 [29] studies a 2 MW/ 5 MWh RFB and LIB with 48MW/ 50MWh for grid connection in the UK.
  - 2018 [30], with a 4 MW/ 20 MWh liquid sodium-sulphur battery (NaS) and 7.5 MW/ 2.5 MWh of lithium-ion. Applied in 17 districts and four cities in Niedersachsen, Germany.
  - 2017 [31], with 300kW/ 1MWh flow batteries to hybridise with a LIB of 120 kW, Melbourne, Australia.
  - 2016 M5BAT project [32]. Study of lead batteries: one flooded and one VRLA, 1.3 MWh OCSM battery system, two strings of 1 MWh VRLA gel technology and three lithium-ion technologies.

- HESS for EV application – Fast charging and models development:
  - 2020, Hydealist [33] combines supercapacitors and conventional batteries.
  - 2019, Hybrid Battery Optimisation [34] combines lithium-ion batteries and supercapacitor to optimise energy and power.

### 2.3. Review of the hybridised batteries technologies

A BESS is defined through different performance specifications: efficiency, response time, power and energy density and capacity, ageing, and degradation effects. The interconnection of different BESS can result in a solution with complementary characteristics, resulting in an overall increase in the performance of the system [22]. Selecting a specific type of storage for an application arises from technical and economic optimisation.

This work addresses different control combinations of commercially available LIB and VRFB technologies aiming to design a HESS due to its distinct energy and power characteristics. The technologies' specifications were previously documented [35] [36] [37] and are summarised in Table 1.

Table 1 – Typical characteristics of VRFB and LIB [29] [30] [31].

| ESS Technology | Vanadium Redox Flow Battery (VRFB) | Lithium-ion Battery (LIB) |
|---|---|---|
| Power range (MW) | 0.03-3 | Up to 0.01 |
| Typical discharge time | sec-10h | min-hour |
| Overall power efficiency | 0.65-0.85 | 0.85-0.95 |
| Power density (W/L) | ~<2 | 1500-10000 |
| Energy density (Wh/kg) | 10-30 | 75-400 |
| Storage durability | hour-months | min-days |
| Self-discharge (per day) | Small | 0.1-0.3 % |
| Lifetime (year) | 5-10 | 5-15 |
| Life cycles (cycles) | 10000-13000 | 1500–4500 |

VRFBs are suited for applications that require several hours of storage, such as peak shaving, spinning reserve, stabilisation, and dispatch, mostly for stationary or mini/microgrid applications. Its main components are pumps, storage tanks, a stack composed of cells, piping, a control unit and power conversion equipment [38]. RFB technology is tolerant to over-discharge and overcharge avoidance is achieved through the control of the reference open-circuit voltage outside the stack. Vanadium ions are present in both electrolyte tanks, and crossing through the stack membrane does not lead to contamination of the electrolyte (crossover effect), which occurs in other RFB technologies, e.g., zinc-bromine.

The life expectancy of the VRFB is 10-15 years, corresponding to about 1000 annual cycles, though it can last more than 20 years [38]. VRFB have virtually no degradation (0-100 % of usable SOC) [39]. Some batteries have an inert gas on top of the electrolyte to avoid possible side reactions with the oxygen of the air, and in the case of the University of Évora VRFB, argon gas is used. VRFB cycle efficiency is in the range of 75-85 %. Its scale-up can be achieved at any power/energy rating (independently), with capacity being customisable with the sizing of electrolyte tanks and power sizing through the sizing of the stack. Vanadium's environmental restrictions are less stringent than those for lead and cadmium. Powered vanadium metal is combustible, while most of the vanadium compounds are not, and, in general, do not constitute a fire or explosion hazard [38], which stands out as an advantage of RFBs in contrast with other battery chemistries such as LIB.

LIB has a high energy density [35], making them suited for short-term and medium-term applications, such as frequency regulation, voltage support, or peak shaving [40]. Generally, it has two electrodes and an organic, non-aqueous electrolyte containing dissolved lithium salts with efficiencies between 80-90 %, with case studies of up to 97% [35] [41]. Typically presents an average life cycle of 5-15 years [41]. Its power and energy are easily scalable, and its production costs are expected to keep decreasing in the near future due to large-scale manufacturing [40]. Typically, an active cooling system is integrated to avoid extreme temperature ranges, to avoid enhanced energy storage capacity degradation. Electronic voltage control limits are crucial to prevent cell damage, SOC determination and cell operation on-stop [41].

When compared to other BESS, LIB components are less toxic, however, they are still an environmental hazard when not disposed of appropriately, which is the case in some countries where they are disposed of in landfills [42]. Given its good state after high-intensity applications, LIBs could be re-used in lower-intensity applications as grid storage or serve off-grid applications, which adds a stage to the LIB life cycle before the end of life (EOL). Recycling is crucial for sustainable technology evolution. However, currently, its recycling rate lies below 3% worldwide.

## 3. Methodology

A complete technical-economic model is developed using MATLAB software to discuss the research questions referred to in Section 1. The model reproduces the operation behaviour of BESSs and other microgrid equipment, computes the

EMS/power allocation algorithms and delivers the evaluation of the overall system based on the calculation of key performance indicators (KPIs) from an energetic and economic perspective. Over 15 years of operation are analysed, with the algorithms running on a 1-minute basis. The developed approach allows the BESS to be operated either in a single or hybrid scenario and the input data to be easily inserted. Moreover, the model addresses the combined advantages and drawbacks of the LIB and VRFB joint control and the possibility of delivering multiple tasks and still being competitive.

The following subsections describe key aspects of the model inputs and algorithm-based computation of the developed LIB and VRFB scenarios.

### 3.1. Microgrid description

The microgrid of the Renewable Energies Chair of the University of Évora allows the operation monitoring of ESSs and PV installations, controls deployment, testing, and model development. The microgrid integrates two ESSs, a 5 kW/60 kWh VRFB from redT [43] and a 5.0 kW/9.8 kWh LIB RESU10 battery pack from LG [44]. It also accounts for two PV installations, one with 6.7 kWp crystalline PV installation and the other with a 3.2 kWp amorphous BAPV system. In this work, the HESS configuration achieves an 8-kW nominal power capacity (LIB inverter limits output power) and a 70-kWh energy capacity as a result of combining the VRFB and LIB technologies referred in Section 2.3. The microgrid layout is shown in Figure 2.

The PV generation power capacity is close to 10 kW, with 6.7 kWp of monocrystalline and polycrystalline technology and 3.2 kWp of amorphous technologies; both installations are connected to individual inverters from Ingeteam. The ESSs are composed by a 5kW/ 9.8 kWh LIB connected to a 3.3 kW SMA inverter and a 5kW/ 60 kWh VRFB connected to a total of 7.2 kW monophasic inverters from Ingeteam. Each technology is connected to AC energy analysers, temperature sensors and DC measurement devices. The microgrid control is achieved by an in-house developed LabVIEW [45] program, based on Modbus TCP/IP protocol. It includes real-time data logging of energy analysers and sensors, the EMSs and power-sharing algorithms.

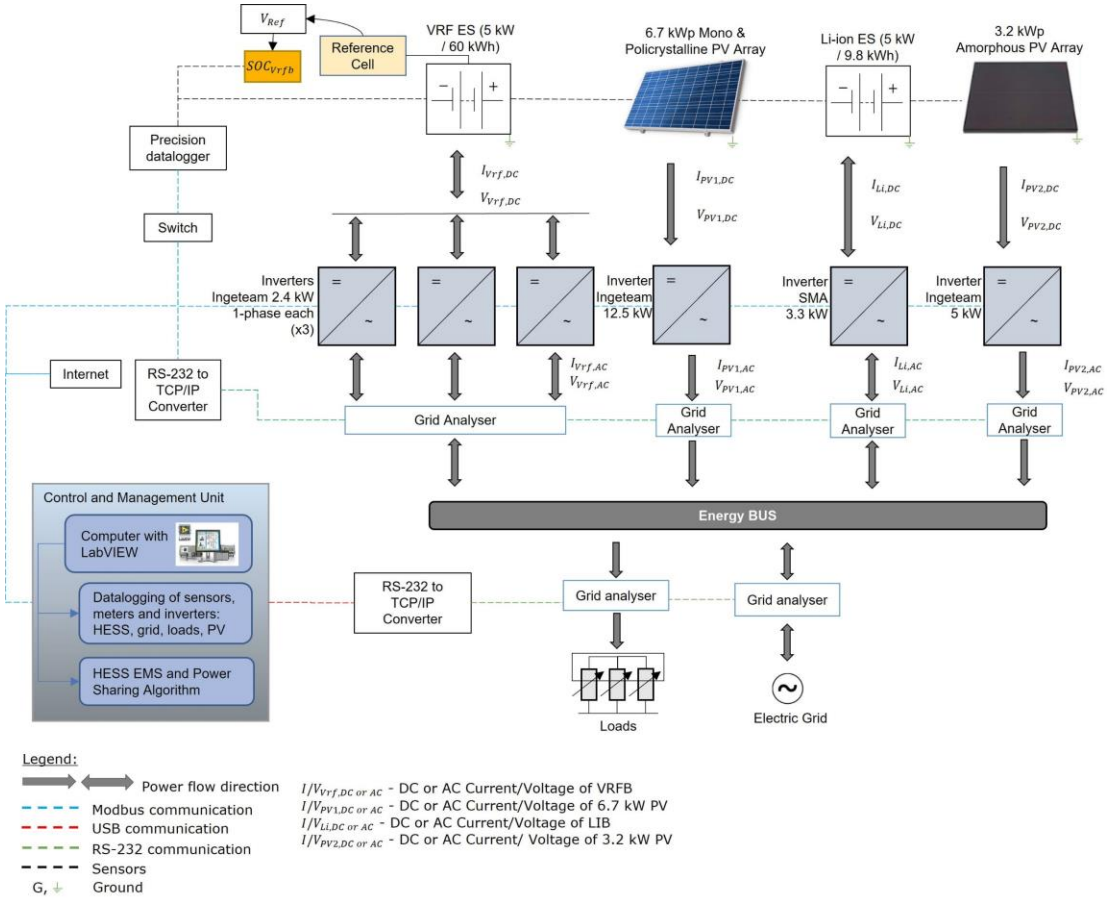


Figure 2 – HESS microgrid architecture.

### 3.2. PV installations and consumption inputs

The PV generation profile results from 2019 data treatment of the two existing PV systems. The data acquisition of both PV systems is made at rates of 1s and 2s. The data sets were treated separately, averaged to a 1-min period and later used as input for the modelling. 1-minute data averages were chosen to shorten the simulation running time whilst still taking into account PV generation fluctuations.

The consumption profile used is a 15-minute average of the data made available by the Portuguese DSO company E-REDES, for 2019, for each Portuguese energy consumption sector for the normal low voltage (NLV) buildings sector [46]. The consumption load profile data was processed to correspond to the PV generation 1-minute time resolution. Figure 3 shows one-week examples of PV generation and consumption profiles for (a) winter and (b) summer.

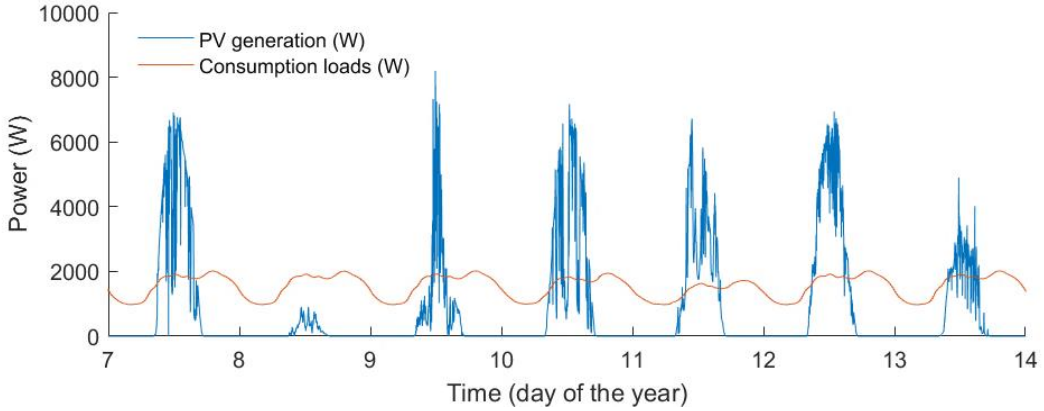


(a)

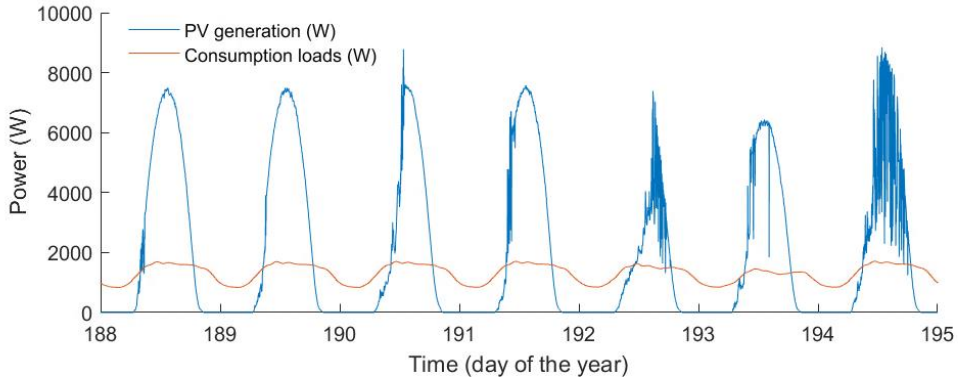


(b)

Figure 3 - PV generation and consumption data used as input, with one-week examples for (a) of winter and (b) summer. The PV generation profile is a result of the 1-minute data treatment of the two PV systems (3.2 and 6.7 kWp) and the consumption profile obtained.

### 3.2.1. PV degradation

The degradation performance of PV installations is a worldwide research topic to assess lifetime of PV systems better and provide information to the manufacturers to work on improving its modules lifetime. Generally, the modules with no relevant defects over their lifetime are in agreeance with the manufacturer's warranty not degrading more than 20% of their initial power in the first 25 years of operation (-0.8%/year). In ordinary situations, the degradation value is even lower. A study of 110MW of PV installations, in 25 installations over Europe with installations operation data records up to 30 years, showed PV modules degradation ranging from -0.1%/year and -0.75%/year, respectively, from different manufacturers [47].

In the context of this work, a PV module annual efficiency degradation of -0.45%/year was considered as reasonable and was applied to the input PV data along the simulation timeframe.

### 3.2.2. Consumption profile increase

Future energy consumption projections for 2030 and 2040 were presented in a study developed by the International Energy Agency (IEA) [48], where three main scenarios were shown, regarding the "stated policies", the "sustainable development", and the "current policies" for the years 2030 and 2040, to be compared with actual data of the 2000 and 2018 years. The global electricity demand by scenario for the building sector is shown in Figure 4 [48].

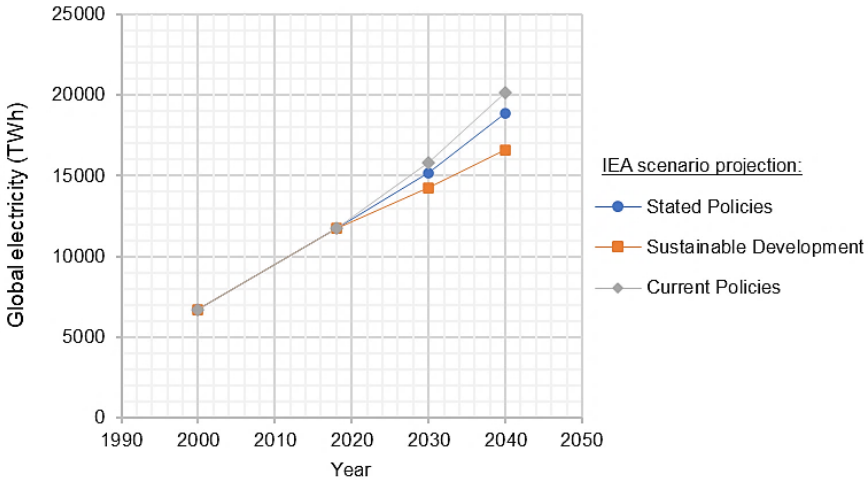


Figure 4 - Global electricity demand for the building sector, in TWh [48].

Considering the proposed IEA future energy demand scenarios for 2030 and 2040 observed in Figure 5, and the lack of detail on how these projections could impact each building profile (in an undifferentiated way, e.g., services, residential), a 2 %/year increase was considered in the consumption profile mentioned in Section 3.2, to scale-up future electric consumption and complement the analysis of this work. Besides the associated uncertainty in IEA projections, the inclusion of this energy demand projected increase rate can lead to a better approximation of future electricity energy consumption in buildings.

## 3.3. Battery models

The description of each BESS operation is obtained through its simulation model. The batteries' physical constraints must be included in the model as boundaries, such as the maximum allowable power and capacity, SOC and depth of discharge (DOD) limits, efficiencies and lifetime. Other constraints are related to the model's initial definitions and are battery-related as well (e.g., initial SOC).

The replacement of the battery at a specified capacity should be defined at the beginning of the project. In this work, the authors considered the battery replacement in the 15$^{th}$ year, the final year of the analysis period.

### 3.3.1. VRFB modelling

One of the modelling approaches used to describe the multiphysics of the VRFB is the nonlinear Nernst-Plank equation which is included in an equivalent circuit that describes the significant reaction occurring in the real-time operation of VRFB with reduced complexity and satisfying results. The VRFB was firstly fully experimentally characterised, and the model was validated with an energy management strategy developed in [49]. The model includes thermal effects, transients, dynamic SOC and auxiliary power consumption.

In this work, the available defined SOC ranges from 5 to 95 %, with the EMS initiation at 50% SOC. The available charge and discharge power range is from -5000 to 5000 W and considers a power-SOC relation. The battery is operated at 20-35°C, and the energy capacity degradation is 0 %/year [39] [50].

Regarding the previously calculated efficiency of the VRFB-connected power electronics, its inclusion is made, and the inverters' standby mode is considered to be 30 W.

### 3.3.2. LIB modelling and lifetime

The authors used real-time battery operation and data acquisition to develop a LIB model for the referred battery based on the equivalent electrical model and the modified Shepperd model [51]. This model did not consider battery ageing since it was based on data obtained at certain current (power) levels.

LIB ageing strongly depends on operation conditions: temperature, SOC, total energy throughput (electrochemical operating windows), and charge and discharge operating rates. Consensus exists on the lack of a universal lithium-ion lifetime model, although calendar life and the number of cycles are recognised as fade mechanisms [52]. The charge and discharge cycles' patterns and the operating conditions can further decrease lifetime. The battery energy capacity reduction due to calendar and charge-discharge cycles and lifetime fade determines the replacement of battery systems, impacting the overall investment plan. The voltage curve is dependent on the battery SOC, the operating current, resistance, and energy capacity. The internal resistance increases with

the calendar time, causing a decrease in the usable voltage range. The operation of the battery at higher currents implies a higher speed voltage decrease, reducing the use of the battery bulk capacity. The thermal behaviour of the model is generally obtained using a heat transfer with the environment to represent the instantaneous thermal effects (energy losses), affecting the battery energy capacity and the internal resistance.

In this work, the LIB model is based on the combination of the model developed in [51] and the lifetime prediction model developed by the National Renewable Energy Laboratory (NREL), for the NMC LIB technology, included in their System Advisor Model (SAM) software. SAM is dedicated to commercial battery systems suited for real-time battery control algorithms [52]. The energy capacity loss is described in calendar time or in cycle number, and in this work, the authors follow the calendar time approach. To describe the voltage reduction with calendar time, a constant internal resistance is attributed to represent the impact on voltage.

The NREL lithium-ion ageing model uses Eq. (1) and (2) to determine the adequate battery energy capacity (%) [52],

$$q = q0 - kcal \times \sqrt{t} \quad (1)$$

Where $q0$ is given as 1.02 fraction, $t$ is the day, and the stress factor, $kcal$, is given in the following Eq. (2),

$$kcal = a \times e^{b\left(\frac{1}{T} - \frac{1}{296}\right)} \times e^{c\left(\frac{SOC}{T} - \frac{1}{296}\right)} \quad (2)$$

Where the coefficient $a$ is 0.00266 in unit of $1/\sqrt{day}$, $b$ is -7280 K, $c$ is 930 K, and T is the temperature in K.

Regarding battery voltage, the internal cell resistance considered is 0.001155 **Ω** (extracted value from SAM). Concerning the battery's thermal behaviour, the effective capacity varies with the ambient temperature, being 100 % at 23 °C, which is considered to be a reasonable value given the controlled environment provided by the air conditioning unit.

The LIB operating SOC range is 10-90%, and the SOC of 50% was chosen for its initial state. The inverter connected to the LIB has a nominal power capacity of 3.3 kW, which is assumed as the maximum power capacity retrieved from the battery. In that sense, the inverter limits for charge and discharge power range are from -3300 to 3300 W. For the standby mode of the LIB inverter, a value of 5 W is used.

### 3.4. Energy Management Strategies and HESS Power Sharing/Allocation Scenarios

The energy management strategy baseline is the self-consumption maximisation strategy, considering the following premise: the energy fluxes priorities are the same for the different scenarios. Here, the PV generation is primarily self-consumed. The BESS only charge with the surplus PV-generated energy and discharges to supply consumption loads, while the grid is seen as the last resource to exchange energy with the building grid. The subjacent EMS prioritises the PV generated energy for direct self-consumption and, if not possible, the exceeding generated energy is sent to charge the batteries; otherwise, it is sent to the grid. From the prosumer perspective, the priority levels are the consumption of PV generated energy and then from the battery. If neither of those possibilities is available, the energy is consumed from the grid. A simple description of the algorithm architecture is presented in Figure 5.

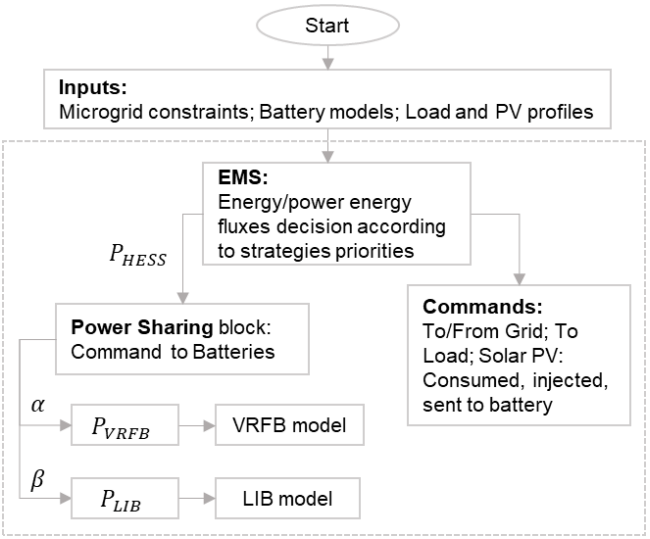


Figure 5 - EMS and power allocation strategy for the HESS case study.

To properly analyse the EMS and power allocation control, which defines the operation algorithms of the HESS, five scenarios have been built, including the previously referred inputs. Scenarios 1, 2 and 3 obey a HESS power allocation method, consisting in a power filter applied to the overall HESS power command, expressed in equation Eq. (3):

$$P_{HESS} = \alpha P_{VRFB} + \beta P_{LIB} \quad (3)$$

Where $\alpha$ and $\beta$ are constants that establish a percentage of the total battery power command, $P_{HESS}$. The $P_{VRFB}$ and $P_{LIB}$ are the VRFB and the LIB power commands, respectively. In the following, the five scenarios are described.

- *Scenario 1:* Consists in the roughest HESS power command allocation. The power allocation among the HESS is defined as constant percentage values of the total power command. The battery with the greater energy capacity will be attributed with the highest percentage of the overall battery command, and in this case, the vanadium redox flow battery. In that sense, and considering Eq. (3), it includes a constant value of $\alpha = 0.75$ and of $\beta = 0.25$ for LIB in their defined SOC range.

- *Scenario 2:* Aims at using the energy capacity of the LIB in a controlled way to increase its lifetime (relying on the LIB P(SOC) relationship to avoid extreme levels of power and SOC). The LIB P(SOC) relation is detailed in Figure 6 (a) and (b). In this case, the VRFB sustains the baseload of the consumption profile.

  The variable $\beta$ is dynamic, and as such, at each step is updated, as well as the LIB power command. The constant $\alpha$ is obtained by $\beta - 1$ through the subtraction of one unit. Scenario 2 is based on the P(SOC) relation defined for the LIB, based on the obtained experimental data. This definition is explained through Figure 6.

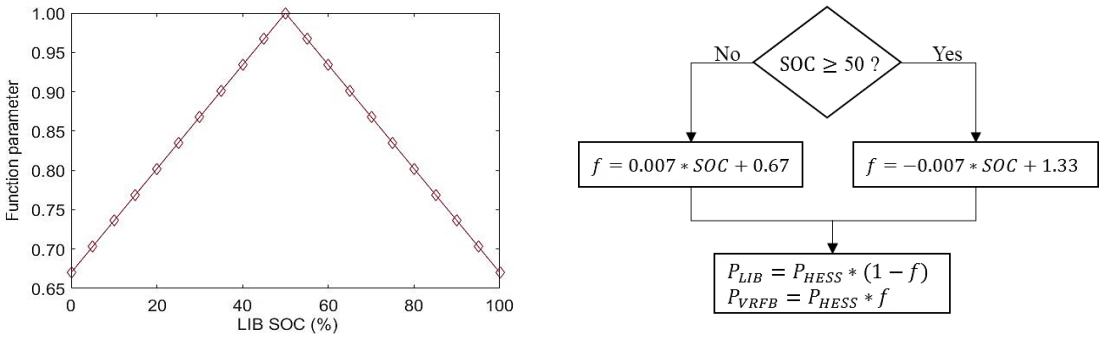


(a) (b)

Figure 6 - Details of Scenario 2 of LIB operation based on (a) the function with the (b) P(SOC) equations flux gram detailed, where $f$ is the intermediate calculus power command.

- *Scenario 3:* This scenario aims to be an algorithm capable of operating both batteries, including the execution of distinct EMS independently. LIB executes a peak-shaving approach, with its operation among a power range above the -1000 W and below the 1000 W, while VRFB power command fulfils, within its possibilities, the rest of the needed energy/power.

- *Scenario 4:* Given the seasonal PV variation and consumption profiles, this scenario intends to analyse the impact of not choosing the maximum possible SOC operation range of the batteries. The impact is evaluated by observing three indicators: SCR, LCOE and OBU (defined further ahead).

Different battery SOCs ranges are investigated, considering two cases: summer and winter. In the first, the SOC range is made variable in summer and constant in winter; in the second, the opposite is studied. Additionally, a third case presents the optimum configuration for each indicator.

Scenario 4 arose in the context of the noticeable effects in the results of Scenarios 1-3, given that the batteries SOC lay in extreme limits during winter and summer. In the winter, it lays at lower SOC values ; therefore, less available discharge capacity exists during this period. In the summer, it lays at higher values and therefore, less available charge energy capacity exists. Scenario 4 aims to reduce those effects, and it analyses the impact of not choosing the maximum possible SOC operation range of the BESS. For that, the SOC ranges for both battery technologies were combined and simulated, as expressed in Table 2.

Table 2 - LIB and VRFB SOC range definition studied on the base of Scenario 4.

| | |
|---|---|
| LIB Minimum SOC value | 10, 20, 30 or 40 |
| LIB Maximum SOC value | 50, 60, 70, 80 or 90 |
| VRFB Minimum SOC value | 5, 15, 25, 35 or 45 |
| VRFB Maximum SOC value | 55, 65, 75, 85 or 95 |

To avoid deceptive results, a lower DOD limit is needed for the values referred in Table 2. DODs lower than 40 % were not considered output results since an investment in those would not be justified (for example, 40-50% SOC range).

- *Scenario 5:* This scenario provides baseline scenarios, with a single battery case for VRFB and a single battery case for LIB, i.e., the use of one battery to execute the EMS of self-consumption maximisation.

The batteries SOC range are defined in Section 3.3, except for Scenario 4, due to the seasonal SOC range variation.

### 3.5. Evaluation indicators

An appropriate evaluation can be obtained through the determination of performance indicators related to investment and energetic perspectives.

As the most relevant economic indicators, the analysis relies on the determination of the following indicators: the Net Present Value (NPV), expressed in €; the Levelized Cost of Energy (LCOE), expressed in €/kWh and is based on the calculation of the Total Life-Cycle Cost (TLCC) and in the Present Value of the Operation and Maintenance Cost (PVOM); the Internal Rate of Return (IRR) expressed in %; and on the Simple Payback (SPB), expressed in years. The indicators are calculated based on the equations expressed in [53], explained in detail in previous works of the authors, as in [54].

The chosen energy indicators are determined for one full year, and the presented result is the average of the obtained annual values. The analysis comprises an energetic evaluation with the following indicators: self-consumption ratio (SCR), self-sufficiency ratio (SSR), grid-relief factor (GRF), battery use (OBU), energy from the grid (EG), from grid use (FGU), to grid use (TGU), from battery use (FBU) to battery use (TBU). These energy performance indicators are already detailed in previous authors' works, as in [55] or some in [56].

### 3.6. Economic analysis and tariffs details, and related inputs

The economic analysis considers the effectively consumed solar PV energy, the discharged energy from the battery or batteries (depending on the scenario), and the energy sent to the grid. The expenses considered are concerning to the energy that is received from the grid.

The economic inputs which compose the different scenarios are detailed in this section. Table 3 presents the overall economic inputs and tariff details used.

Some expenses presented in Table 3 are eliminated for Scenario 5, given the single ESS instead of the HESS. In the case of Scenario 5-LIB, the following costs are considered null: VRFB, VRFB inverters and OPEX related to VRFB. Regarding Scenario 5-VRFB, the LIB and its inverter costs are considered null. The remaining costs are not altered, except for the cost of cabling, installation, PV structure and related, which are reduced by one-third of the presented value in Table 3, to better to fit the scope of the single ESS analysis.

Table 3 - Economic input expenses for modelling tool.

| Equipment/component | Value (with VAT) |
|---|---|
| Module price (€/Wp) | 0.35 * |
| Total PV installed power modules (Wp) | 9750 (30 modules of 325 W each) |
| Discount rate** (%) | 10 [11] |
| Inflation rate (%) | 7.2 [57] [11] (average) |
| Annual Energy increase rate (%) | 5.6 [57] (average) |
| 6.7 kWp BAPV inverter (€) | 2432 [58] |
| 3.2 kWp fixed-mounted PV inverter (€) | 1483 [59] |
| Lithium-ion battery (€) | 4527 [60] |
| Lithium-ion battery inverter (€) | 2125 [61] with VAT and delivery to Europe |
| VRFB (€) | 48080 (2404 €/kW + 601 €/kW; € ≅ USD) [62] |
| VRFB inverters (€) | 3×1159 [63] |
| Cabling, installation, PV structure and related (€) | 2850 * |
| Overall system operation & maintenance (OPEX) (€/year) | 500 *** |
| Daily contracted power tariff (€/day) | 0.2796 [64] |
| High/ low tariff (€/kWh) (bi-hourly) | 0.2116/ 0.1145 [64] |

* Company quote from 2020; ** Depends on expectation; *** VRFB tank inert gas (highly pure argon).

Inflation and energy rates were extracted from PORDATA website, which presents the updated and yearly values of Portuguese statistics. The used values correspond to the 2022 year. The discount rate consulted to be in the range of the published works [11] [65].

Benefiting from the bi-hourly tariff, the considered energy value cost (€/kWh) depends on the consumption period. A contracted power of up to 6.9kVA and 100 kWh/month of energy consumption was considered [64].

## 4. Results

This section addresses the main outputs of the study, considering the developed simulation tool used to evaluate the LIB+VRFB HESS configurations and the single ESS scenarios detailed in Section 3.4. Following the proposed methodology, the HESS and single ESS scenarios 1-5 were built to answer the research questions enunciated in Section 1.

Scenario 1 is the first approach to HESS operation and is considered a direct method that makes a soft approach to power distribution, considering only the energy capacity of the batteries. Scenario 2 presents an approach to better control the LIB operating conditions and prevent operation in limit boundaries through obeying the P(SOC) real-time relation (SOC measurement dependent). Scenario 3 considers the use of LIB to fulfil the values within the range of -1000W to 1000W, identified as a similar approach to peak-shaving using an ESS. Scenario 4 evaluates the seasonal variation of the SOC range of the batteries. With scenario 4, it is possible to vary the batteries' SOC range to favour the result based on the seasonality of PV generation and consumption profiles. Scenario 5 is used as the baseline, with configurations for the single BESS.

The five scenarios will be evaluated through KPIs in the techno-economic assessment.

### 4.1. Scenarios 1, 2, 3 and 5

The results of the different Scenarios defined in Section 3.4., excluding Scenario 4, are presented through the KPIs obtained in Figure 7, below. The ideal best value of each energy indicator is represented with an orange line to improve the readability of Figure 7. The best value is attributed from the point of view of the prosumer, previously detailed in Section 3.4. The prosumer prioritises the PV self-consumption and aims to reduce the use of the batteries and the grid, simultaneously reducing the use of the batteries and the grid.

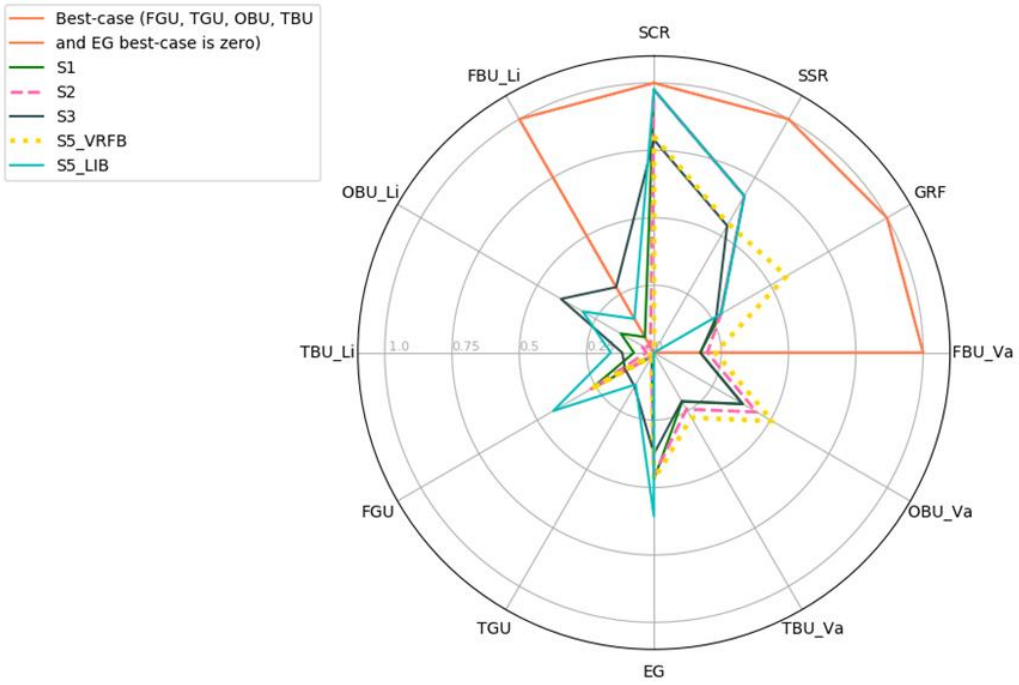


Figure 7 - Battery-related energy KPIs for Scenario 1, 2, 3 and 5. EMS-related energy KPIs for Scenario 1, 2, 3 and 5. The "_Va" corresponds to the VRFB and "_Li" to the LIB output values. Each scenario is represented as "S".

The economic indicators were calculated for Scenarios 1, 2, 3 and 5. The economic KPIs NPV, LCOE, IRR and SPB are presented in Table 4 for each case.

Table 4 - Economic KPIs of Scenarios 1, 2, 3 and 5.

| **Configuration** | **HESS** | | | **VRFB single** | **LIB single** |
|---|---|---|---|---|---|
| **Scenario/Economical parameter** | **Scenario 1** | **Scenario 2** | **Scenario 3** | **Scenario 5** | |
| Total investment (€) | 68403 | 68403 | 68403 | 59851 | 14946 |
| NPV (€) | -4140 | -3821 | 1251 | 4768 | 24764 |
| LCOE (€/kWh) | 0.46 | 0.46 | 0.35 | 0.42 | 0.28 |
| IRR (%) | -3.01 | -3.00 | 3.00 | 2.00 | 31.0 |
| SPB (years) | 9.69 | 9.62 | 8.21 | 8.69 | 4.10 |

### 4.2. Scenario 4 results

The SOC ranges defined in Table 2 are tested, for the EMS and power allocation of Scenario 1, given the simplicity of the approach and overall worst performance. To evaluate this scenario, three main KPIs are observed: the priority of the EMS is to maximise self-consumption ratio, and, in this case, SCR proves its relevance; the second priority is to minimise the battery utilisation, which can be validated with the OBU indicator; and, finally, the third priority is to observe the LCOE indicator, to address the financial return better. The winter and summer cases are compared with the baseline of all year variable SOC range (corresponding to Scenario 1 simulated by SOC combinations in Table 3).

As previously outlined, Scenario 4 results are based on data profiles and conditions defined along with the methodology and, for this reason, are valid only within the defined conditions. Table 5 presents the three best cases results of this optimisation, considering the output of the previously mentioned evaluating indicators.

Table 5 - Scenario 4 output results. SCR obtained value is the priority of the overall Scenario, LCOE and OBU are the second priorities. Uc means "use-case".

| KPI | Uc1 – Variable throughout all year | | Uc2 – Winter variable, summer fixed | | Uc3 – Winter fixed, summer variable | |
|---|---|---|---|---|---|---|
| | Best value | SOC range | Best value | SOC range | Best value | SOC range |
| SCR | 0.848 | VRFB decisive: [5, 95] | 0.848 | VRFB decisive: [5, 95]; [15, 95]; [25, 95]; [35, 95] | 0.848 | VRFB decisive: [5, 65]; [5, 75]; [5, 85]; [5, 95]; |
| LCOE (€/kWh) | 0.797 | LIB determinant: [10, 90] | 0.797 | VRFB: [5, 95]. LIB: [10, 60]; [10, 70]; [10, 80]; [10, 90] | 0.797 | LIB decisive: [10, 90] |
| OBU | LIB decisive: 0.110 | VRFB: [5, 95] LIB: [40, 80] | LIB decisive: 0.143 | LIB decisive: [40, 80] | LIB decisive: 0.135 | LIB decisive: [40, 80] |

### 4.3. Scenario 4 economic and energy results

Figure 7 shows that neither of the proposed scenarios corresponds to an optimum for all the calculated energy KPIs compared with the defined ideal best values. Scenarios 1, 2 and 5-VRFB present similar SCR, SSR, GRF, EG and FGU indicators. The highest VRFB energy exchange is obtained in Scenario 5 (OBU_Va), and for LIB in Scenario 3 (OBU_Li).

In Scenario 1 the VRFB is the primary energy exchanger (OBU, FBU and TBU). Table 4 shows that this configuration is the least attractive approach of all scenarios, considering the obtained economic KPIs of NPV, IRR and SPB.

In Scenario 2, the VRFB is a promising candidate to operate with LIB, given the different energy capacities and theoretical 100% DOD. From the energetic KPIs in Figure 7, the LIB use is highlighted as being the lowest compared to other scenarios. The economic KPIs results present a slightly better output, although close to scenario 1.

In Scenario 3, the LIB and VRFB batteries' energetic use are closer. Figure 7 shows the generally lower SCR, SSR, FGU, GRF than Scenarios 1, 2 and 5-VRFB, but higher in the ones associated with the LIB use (OBU_Li, FBU_Li, TBU_Li). Economically, Scenario 3 presents better financial results than the studied HESS approaches for all the KPIs studied. It also presents the second-lowest LCOE and second-lowest SPB and the second-highest IRR. Scenario 3 indicates that the HESS LIB+VRFB configuration with the suited EMS and power allocation method can improve the competitiveness for the VRFB single case, and although the highest investment, the batteries are better energetically managed.

In Scenario 4, with the help of Table 5, the priority is achieved with the best SCR maintained as 0.848 for the three cases. The second priority can be the LCOE (lowest cost) or the OBU (lowest battery energy exchange). Regarding Uc1 (variable all year), the lowest LCOE of 0.797 €/kWh corresponds to a VRFB SOC range of 5-95 % and 10-90 % for LIB. The lowest use of the batteries presents 11 % for LIB, maintaining the SCR, as the VRFB with 5-95 % and LIB with 40-80 %. Regarding Uc2 (winter variable, summer fixed), the best SCR can be achieved with the operation of VRFB with a maximum value of 95% but a lower value from 5-35 %. The lowest LCOE is achieved through a VRFB operating range from 5-95%, although LIB should be operated until the minimum SOC of 10 %, though the highest limit can be variable (60-90%). The lowest OBU is about 14 %, and the LIB range should stay at 40-80 %. Concerning Uc3 (winter fixed, summer variable), the lowest SOC could remain at 5 %, and the highest range is from 65-95 %. The OBU result is similar to the previously discussed case, and the lowest LCOE is achieved at a 10-90 % LIB range.

The increase of the lower limits and the decrease of higher limits of SOC range can benefit the battery's lifetime and simultaneously maintain or improve (not worsen) the KPIs (depending on the goal). This is the case of the 1-3 and 5 scenarios, where more than one SOC range offers a satisfactory (energy and economical) result and favours the operation far from the maximum boundaries.

In Scenario 5, VRFB single case presents the most similar energy KPIs to Scenario 1 and 2, although battery-related KPIs (with the indexing batteries names) are distinct. In terms of economic indicators, this scenario is not the best nor the worst. LIB single case presents itself in the middle of the energy indicators, except the case of FGU and EG, meaning the highest dependence from the grid. Through the observation of Table 4, this configuration presents the lowest investment, LCOE and SPB, and the highest NPV and IRR.

Generally, considering the methodology followed and defined inputs, the HESS system is only competitive when Scenario 3 is compared to Scenario 5-VRFB. Considering the current costs, none of the HESS configurations studied compete with Scenario 5-LIB. Despite this result, it must be considered that the lifetime of lithium batteries depends on the type of technology and its operation and use over the lifetime and that this work carried out its analysis for fifteen years. In case the lithium battery has to be replaced before the considered timeframe (another option for the replacement factor could be, for example, in the case of its energy capacity being less than 50% of the initial nominal energy capacity), the economic analysis must be updated, which will weigh on the indicators. This issue does not arise with the VRFB, whose lifetime is above the considered period.

Although the battery system cost decrease is expected, investing in HESS should be weighted for each application. Applications that find HESS investment competitive could rely on the determined energetic KPIs, which could compensate the investment (costs difference in using a single battery or a HESS). Those applications are related to enhancing the energy management strategy applied to the system, which depends on the goal of the application or service it aims to provide.

## 5. Conclusion

Current literature presents a lack of EMSs and power allocation that better concerns the economic and energy perspectives of HESS configurations, especially the LIB and VRFB for the building sector. The configuration LIB and VRFB (3.3 kW/ 9.8kWh and 5kW/ 60 kWh, respectively) set a favourable collaborative performance, given the complementary differences, allowing different combinations of power allocation and EMSs, answering to different problems, or improving case scenarios.

In this work, the EMSs of ESS and power allocation techniques of HESS are clarified with the proposal of five case scenarios, three of which are HESS approaches. The

evaluation is done by calculating KPIs of single-ESS, and relevant analysis is addressed. Through the studied scenarios, one can conclude that the competitiveness of the ESS-single cases is possible with HESS, depending on the goal. It is possible to state that the VRFB-single case is improved by adding a LIB (HESS), Scenario 3. The seasonality factor, addressed in Scenario 4, could be a relevant approach in some geographical areas (e.g., Portugal), depending on the consumption and PV generation profiles and the exigency that the designed EMS makes of the battery use.

In general, the best LCOE results obtained (Table 4) show that these technologies still need improvement to reach grid parity. Additional cashflows of adding battery storage to a project are not quantifiable in the present analysis, as is the case of matters of security of supply frequency balancing issues, among others, considered crucial in the technology use and suitability.

When managing the HESS, the renewable energy sources' generation and consumption profiles significantly impact the project output and are highly dependent on the desired goal. The initial investment costs (CAPEX) of a battery system are relevant in the project analysis, and their costs are expected to be reduced in the following years due to the increasing adoption of VRE and massive application. The management of the overall electric system will include HESS management, sometimes with distinct EMSs competing for goals and different energy storage characteristics.

## 6. Future research work

The results obtained are based on a developed in-house tool that allows the overall microgrid assessment based on variation inputs. The analysis will improve results accuracy if the characterisation of the systems is improved, overall tool optimisation additions are achieved, and recent analysis costs are made. In this work, the representation of LIB lifetime is based on existing experience in literature, and a complete approach could be developed and tested in the future for further use.

Concerning Scenario 3, the LIB SOC measurement in real-time operation of LIB is needed. The investigation is on course to obtain more accurate methods of determining SOC. Without accurate SOC measurement, Scenario 3 results are affected. Despite the conditions of the Scenario 4 approach, each project should further assess the seasonality factor, depending on the geography and year. Other approaches to deal with seasons could be investigated, for example, for the consumption patterns within daily periods. Beyond the energy and economical approach followed in this work, the real-time

implementation still needs to be addressed to complement the simulation and collect data using the microgrid of the University of Évora.

To better evaluate the benefits of investments in HESS, the simulated and other promising energy management controls should be achieved with the exploitation of each of these studied scenarios to reach the grid parity of HESS.

## Acknowledgements

The authors would like to thank Dr. Afonso Cavaco for reviewing this work. This work was co-funded in the COMPETE 2020 (Operational Program Competitiveness and Internationalisation) through the ICT project HyBRIDSTORAGE with reference POCI-01-0247-FEDER-048270. It was also supported by INIESC – Infraestrutura Nacional de Investigação em Energia Solar de Concentração -, FCT / PO Alentejo / PO Lisboa, Candidatura: 22113 – INIESC AAC 01/SAICT/2016 (2017-2021). The authors acknowledge the support of the ICT – Institute of Earth Sciences. This work was also supported by the PhD. scholarship (author Ana Foles) of FCT – Fundação para a Ciência e Tecnologia –, Portugal, with the reference SFRH/BD/147087/2019.

## References

[1] IEA, "Energy Storage," 2021. [Online]. Available: https://www.iea.org/fuels-and-technologies/energy-storage. [Accessed: 07-Jan-2022].

[2] European Commission, "The EU Clean Energy Package," 2019.

[3] B. Zakeri and S. Syri, "Electrical energy storage systems: A comparative life cycle cost analysis," *Renew. Sustain. Energy Rev.*, vol. 42, pp. 569–596, 2015.

[4] J. Liu, C. Hu, A. Kimber, and Z. Wang, "Uses, Cost-Benefit Analysis, and Markets of Energy Storage Systems for Electric Grid Applications," *J. Energy Storage*, vol. 32, no. February, p. 101731, 2020.

[5] G. Castagneto Gissey, P. E. Dodds, and J. Radcliffe, "Market and regulatory barriers to electrical energy storage innovation," *Renew. Sustain. Energy Rev.*, vol. 82, pp. 781–790, Feb. 2018.

[6] G. Fong, R. Moreira, and G. Strbac, "Economic analysis of energy storage business models," in *2017 IEEE Manchester PowerTech, Powertech 2017*, 2017.

[7] A. Z. AL Shaqsi, K. Sopian, and A. Al-Hinai, "Review of energy storage services, applications, limitations, and benefits," *Energy Reports*, vol. 6, pp. 288–306, 2020.

[8] S. Hajiaghasi, A. Salemnia, and M. Hamzeh, "Hybrid energy storage system for microgrids applications: A review," *J. Energy Storage*, vol. 21, no. December 2018, pp. 543–570, 2019.

[9] T. S. Babu, K. R. Vasudevan, V. K. Ramachandaramurthy, S. B. Sani, S. Chemud, and R. M. Lajim, "A Comprehensive Review of Hybrid Energy Storage Systems: Converter Topologies, Control Strategies and Future Prospects," in *IEEE Access*, 2020, vol. 8, pp. 148702–148721.

[10] J. Faria, J. Pombo, M. do Rosário Calado, and S. Mariano, "Power management control strategy based on artificial neural networks for standalone PV applications with a hybrid energy storage system," *Energies*, vol. 12, no. 5, 2019.

[11] B. K. Das, R. Hassan, M. S. Islam, and M. Rezaei, "Influence of energy management strategies and storage devices on the techno-enviro-economic optimisation of hybrid energy systems: A case study in Western Australia," *J. Energy Storage*, vol. 51, no. January, p. 104239, 2022.

[12] A. Prasanthi, H. Shareef, M. Asna, A. Asrul Ibrahim, and R. Errouissi, "Optimisation of hybrid energy systems and adaptive energy management for hybrid electric vehicles," *Energy Convers. Manag.*, vol. 243, no. March, p. 114357, 2021.

[13] F. Pilati, G. Lelli, A. Regattieri, and M. Gamberi, "Intelligent management of hybrid energy systems for techno-economic performances maximisation," *Energy Convers. Manag.*, vol. 224, no. August, p. 113329, 2020.

[14] G. Aghajani and N. Ghadimi, "Multi-objective energy management in a micro-grid," *Energy Reports*, vol. 4, pp. 218–225, 2018.

[15] J. C. Hernández, F. Sanchez-Sutil, and F. J. Muñoz-Rodríguez, "Design criteria for the optimal sizing of a hybrid energy storage system in PV household-prosumers to maximise self-consumption and self-sufficiency," *Energy*, vol. 186, 2019.

[16] M. Gomez-Gonzalez, J. C. Hernandez, D. Vera, and F. Jurado, "Optimal sizing and power schedule in PV household-prosumers for improving PV self-consumption and providing frequency containment reserve," *Energy*, vol. 191, p.

116554, 2020.

[17] Y. Zhang, Z. Yan, C. C. Zhou, T. Z. Wu, and Y. Y. Wang, "Capacity allocation of HESS in micro-grid based on ABC algorithm," *Int. J. Low-Carbon Technol.*, vol. 15, no. 4, pp. 496–505, 2020.

[18] W. Zhuang, J. Ye, Z. Song, G. Yin, and G. Li, "Comparison of semi-active hybrid battery system configurations for electric taxis application," *Appl. Energy*, vol. 259, p. 114171, 2020.

[19] B. Bendjedia, N. Rizoug, M. Boukhnifer, and L. Degaa, "Energy management strategies for a fuel-cell/battery hybrid power system," in *Institution of Mechanical Engineers. Part I: Journal of Systems and Control Engineering*, 2020.

[20] D. Aloisio *et al.*, "Modeling, realisation and test on field of a fuel cell - Na/NiCl2 battery hybrid system as a base transceiver station power supply," *Instrum. Mes. Metrol.*, vol. 17, no. 3, pp. 423–442, 2018.

[21] G. N. Prodromidis and F. A. Coutelieris, "Simulations of economical and technical feasibility of battery and flywheel hybrid energy storage systems in autonomous projects," *Renew. Energy*, vol. 39, no. 1, pp. 149–153, 2012.

[22] S. Resch and M. Luther, "Reduction of Battery-Aging of a Hybrid Lithium-Ion and Vanadium-Redox-Flow Storage System in a Microgrid Application," in *2020 2nd IEEE International Conference on Industrial Electronics for Sustainable Energy Systems, IESES 2020*, 2020, pp. 80–85.

[23] A. H. Fathima and K. Palanisamy, "Integration and energy management of a hybrid Li-VRB battery for renewable applications," *Renew. Energy Focus*, vol. 30, no. September, pp. 13–20, 2019.

[24] European Commission, "Hybrid Battery energy stoRage system for advanced grid and beHInd-de-meter Segments," 2021. [Online]. Available: https://cordis.europa.eu/project/id/963652.

[25] K. Smith, "Poland's largest hybrid battery energy storage system commences full-scale technology demonstration," *Hitachi*, 2020. [Online]. Available: https://www.hitachi.eu/en/poland-largest-hybrid-battery-energy-storage-system.

[26] A. Colthorpe, "Duke's long and short duration ultracapacitor-battery project goes live," *Energy Storage News*, 2019. [Online]. Available: https://www.energy-storage.news/news/dukes-ultracapacitor-battery-system-trialling-multiple-

services-up-and-runn.

[27] Ralph Diermann, “European scientists want to develop hybrid vanadium redox flow battery with supercapacitor,” *pv magazine,* 2021. [Online]. Available: https://www.pv-magazine.com/2021/01/22/european-scientists-want-to-develop-hybrid-vanadium-redox-flow-battery-with-supercapacitor/.

[28] Hybrid Energy Storage Solutions Ltd., “Hybrid Energy Storage Solutions Ltd.,” 2021. [Online]. Available: https://hesstec.net.

[29] L. Stoker, “‘World first’ grid-scale lithium-vanadium hybrid project will be in the UK,” *Energy Storage News,* 2019. [Online]. Available: https://www.energy-storage.news/news/world-first-grid-scale-lithium-vanadium-hybrid-project-will-be-in-the-uk.

[30] European Association for Storage of Energy, “Large-Scale Lithium-ion and NAS® Hybrid Battery System Demonstration Project Launched in Niedersachsen,” 2018. [Online]. Available: https://ease-storage.eu/news/ngk-launches-a-large-scale-lithium-ion-and-nas-hybrid-battery-system-demonstration-project/.

[31] Invinity Energy Systems, “Australia’s largest commercial energy storage system launches at Monash University,” 2019. [Online]. Available: https://invinity.com/austrialias_largest_energy_storage_system/.

[32] 2021 Consortium for Battery Innovation, “Batteries in action: hybrid energy storage project,” 2021. [Online]. Available: https://batteryinnovation.org/batteries-in-action-hybrid-energy-storage-project/.

[33] Asseco CEIT, “Hydealist project hybrid energy system for AGV in logistics,” 2021. [Online]. Available: https://www.asseco-ceit.com/sk/vyskum-a-vyvoj/projekt-hydealist-hybridny-energeticky-system-pre-agv-v-logistike/.

[34] UK Research and Innovation, “Hybrid Battery Optimisation,” 2019. [Online]. Available: https://gtr.ukri.org/projects?ref=105298.

[35] X. Luo, J. Wang, M. Dooner, and J. Clarke, “Overview of current development in electrical energy storage technologies and the application potential in power system operation,” *Appl. Energy,* vol. 137, pp. 511–536, 2015.

[36] E. López, L. Fialho, L. V. Vásquez, A. Foles, J. S. Cuesta, and M. C. Pereira, “Testing and evaluation of batteries for commercial and residential applications in AGERAR project,” in *Mission 10 000: BATTERIES*, 2019.

[37] G. L. Kyriakopoulos and G. Arabatzis, "Electrical energy storage systems in electricity generation: Energy policies, innovative technologies, and regulatory regimes," *Renew. Sustain. Energy Rev.*, vol. 56, pp. 1044–1067, 2016.

[38] EPRI, "Vanadium Redox Flow Batteries: An In-Depth Analysis," Palo Alto, CA, 2007.

[39] Á. Cunha, J. Martins, N. Rodrigues, and F. P. Brito, "Vanadium redox flow batteries: a technology review," *Int. J. Energy Res.*, 2014.

[40] D. Parra *et al.*, "An interdisciplinary review of energy storage for communities: Challenges and perspectives," *Renew. Sustain. Energy Rev.*, vol. 79, no. May 2016, pp. 730–749, 2017.

[41] R. Amirante, E. Cassone, E. Distaso, and P. Tamburrano, "Overview on recent developments in energy storage: Mechanical, electrochemical and hydrogen technologies," *Energy Convers. Manag.*, vol. 132, pp. 372–387, 2017.

[42] A. R. Dehghani-Sanij, E. Tharumalingam, M. B. Dusseault, and R. Fraser, "Study of energy storage systems and environmental challenges of batteries," *Renew. Sustain. Energy Rev.*, vol. 104, no. January, pp. 192–208, 2019.

[43] redT energy, "redT energy storage." [Online]. Available: https://redtenergy.com.

[44] LG Chem, "Residential Energy Storage Unit for Photovoltaic Systems," Seoul, Korea, 2016.

[45] National Instruments, "LabVIEW." [Online]. Available: https://www.ni.com/pt-pt/support/downloads/software-products/download.labview.html#443274.

[46] E-REDES and Q-metrics, "Update of consumption, production and of self-consumption for the year 2019," 2019. [Online]. Available: https://www.e-redes.pt/sites/eredes/files/2019-03/DocMetodologico_Perfis2019_20190111v2.pdf.

[47] L. Fialho, F. Martinez-Moreno, and N. Tyutyundzhiev, "Envelhecimento e reparação de Instalações Fotovoltaicas (Parte 1)," *O Instalador*, vol. 297, p. 92, 2021.

[48] IEA, "World Energy Outlook 2019," 2019.

[49] A. Foles, L. Fialho, M. Collares-Pereira, and P. Horta, "Vanadium Redox Flow Battery Modelling and PV Self-Consumption Management Strategy Optimization," in *EU PVSEC 2020 - 37th European Photovoltaic Solar Energy*

*Conference and Exhibition*, 2020.

[50] M. Guarnieri, P. Mattavelli, G. Petrone, and G. Spagnuolo, "Vanadium Redox Flow Batteries," *IEEE Ind. Electron. Mag.*, no. december, pp. 20–31, 2016.

[51] A. Foles, L. Fialho, M. Collares-Pereira, and P. Horta, "Validation of a Lithium-ion Commercial Battery Pack Model using Experimental Data for Stationary Energy Management Application," *Open Res. Eur.*, 2021.

[52] NREL, "Battery Lifespan," *Transportation and Mobility Research*. [Online]. Available: https://www.nrel.gov/transportation/battery-lifespan.html. [Accessed: 02-Jul-2021].

[53] W. Short, D. J. Packey, and T. Holt, *A Manual for the Economic Evaluation of Energy Efficiency and Renewable Energy Technologies*. 1995.

[54] A. Foles, L. Fialho, and M. Collares-Pereira, "Techno-economic evaluation of the Portuguese PV and energy storage residential applications," *Sustain. Energy Technol. Assessments*, vol. 39, no. March, p. 100686, 2020.

[55] A. Foles, L. Fialho, M. Collares-Pereira, and P. Horta, "An approach to implement photovoltaic self-consumption and ramp-rate control algorithm with a vanadium redox flow battery day-to-day forecast charging," *Sustain. Energy, Grids Networks*, vol. 30, p. 100626, 2022.

[56] A. Foles, L. Fialho, and M. Collares-Pereira, "Microgrid Energy Management Control with a Vanadium Redox Flow and a Lithium-Ion Hybrid Battery System for PV Integration," in *38th European Photovoltaic Solar Energy Conference and Exhibition*, 2021, pp. 1464–1469.

[57] PORDATA, "Inflation Rate (Growth Rate - Consumer Price Index)." [Online]. Available: https://www.pordata.pt/en/Portugal/Inflation+Rate+(Growth+Rate+++Consumer+Price+Index)+total+and+individual+consumption+by+purpose-2315. [Accessed: 14-Dec-2021].

[58] Techno Sun, "Ingecon Sun 3 Play 20kW TL, INGETEAM." [Online]. Available: https://b2b.technosun.com/shop/product/gri173-ingecon-sun-3-play-20kw-tl-m-ingeteam-7282?category=1639#attr=.

[59] Suministros Orduna, "Catálogo Suministros Fotovoltaicos." [Online]. Available: https://www.suministrosorduna.com/pt-pt/catalogo/.

[60] EUROPE - SOLAR STORE.COM, "LG Chem RESU 10 - 48V lithium-ion

storage battery." [Online]. Available: https://www.europe-solarstore.com/lg-chem-resu-10-48v-lithium-ion-storage-battery.html.

[61] EUROPE - SOLAR STORE.COM, "SMA Sunny Island 4.4M." [Online]. Available: https://www.europe-solarstore.com/solar-inverters/sma/sunny-island/sma-sunny-island-4-4m.html.

[62] K. Mongird, V. Viswanathan, J. Alam, C. Vartanian, V. Sprenkle, and R. Baxter, "2020 Grid Energy Storage Technology Cost and Performance Assessment," 2020.

[63] Suministros del Sol, "Ingecon Sun 1Play 5TL M Ingeteam Inverter." [Online]. Available: https://suministrosdelsol.com/en/ingeteam-inverters/276-ingecon-sun-lite-5tl-inverter.html. [Accessed: 11-Jan-2022].

[64] ERSE - Entidade Reguladora dos Serviços Energéticos, "Tarifas e Preços para a Energia Elétrica e Outros Serviços em 2020," 2020.

[65] T. Steckel, A. Kendall, and H. Ambrose, "Applying levelized cost of storage methodology to utility-scale second-life lithium-ion battery energy storage systems," *Appl. Energy*, vol. 300, no. July, p. 117309, 2021.

## 4.5. Thesis contributions to the modelling tool and real-scale prototype for the HyBRIDSTORAGE project

### 4.5.1. Introduction of tool concepts

The HyBRIDSTORAGE project [1] – Hybrid Energy Battery Systems – 48270, POCI-01-0247-FEDER-048270/Portugal 2020, aims at developing a sizing and energy management simulation tool to improve the technical, energetic, and economic performances of hybrid battery systems. The development of this tool promotes the implementation and further commercialisation of such systems, highlighting their potential role of active participation in the management of efficient and smart grids. The tool includes the simulation of the performance of the system, considering the final application and client requirements. With the building of a HESS demonstrator, the project allows the implementation of real-time application algorithms for their operation, ensuring autonomous and efficient battery control and management (and RES when applicable).

The main objectives of this project are summarised in the following bullet points:

- Development of a digital tool for hybrid battery systems design that includes their performance results, with or without the inclusion of solar PV installations. An in-depth literature review is made to disclose the most relevant technical-scientific and economic performance indicators that should evaluate the HESS and identify the market limitations of their implementation.
- Investigation and development of suited control and management for the HESS operation, ensuring the technical-economic-energetic intended optimisation. In this context, the value-stacking multiparameter optimisation algorithms are intended to be further addressed in developing control algorithms.
- Validation of the studied HESS solutions in operational scenarios. The battery solutions that fit better for the required application are installed, and the developed control is implemented in real-time. The HESS solution is monitored, and the operational data is acquired to calculate the technical-economic-energetic performance parameters.

The sizing and control tool simulates the HESS performance and aims to optimise the operation of different EES technologies. It allows studying these systems in different

contexts, such as in grid-connected with the permission and without the permission of inject the power to the grid, and with or without the inclusion of solar PV generation. The optimisation minimises the cost of the system along its lifetime, updated to the initial investment moment (NPV). The tool provides a range of optimisation objectives defined by the user, including multiobjective optimisation, simultaneously improving economic, technical or energy indicators. The user can select the optimal solution, considering other non-simulation factors, e.g., client expectations, portability of the system, specific variables minimisation (weight, volume, among others) or specific technical restrictions of the existing installation and local characteristics. A schematic of the HESS tool functioning is presented in Figure 49, as well as the HESS energy flows.

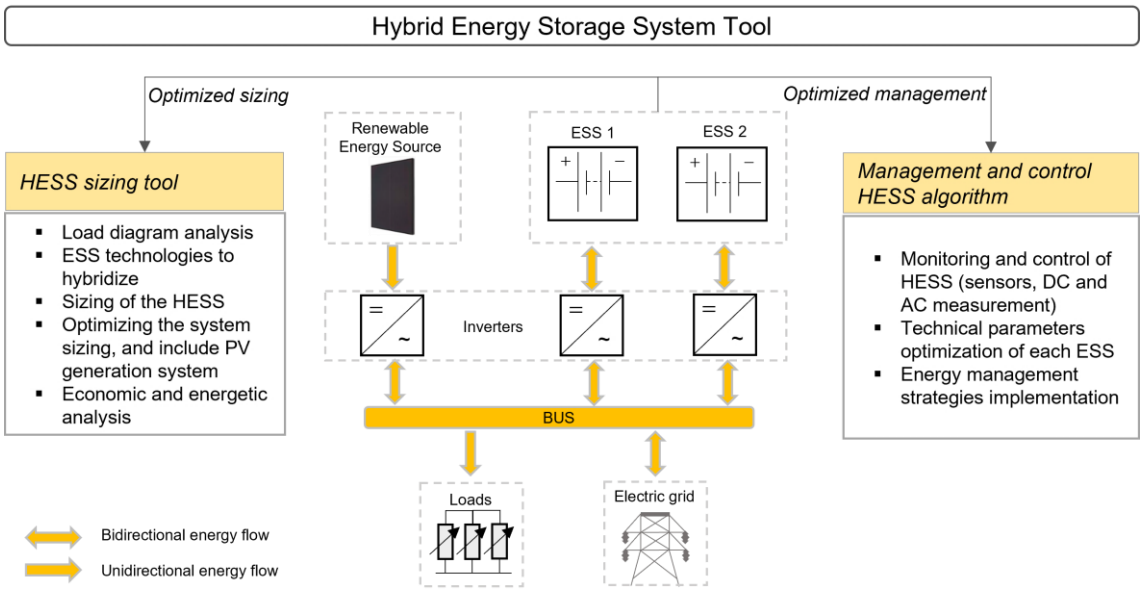


Figure 49. HESS tool general functioning and its integration with the remaining elements: RES, inverters, loads and grid.

The development of this tool follows the main steps: determination of objectives, identification of risks and possible solutions, testing and further development, next iteration planning and evaluation of the final product by the client.

### 4.5.2. Tool operating details

The simulation tool is built with a modular block programming approach. The main program comprises different submodules, and its re-utilisation and modification are developed to simplify the programmed occurring processes. The modularity allows the

gradual addition of new modules with different components and more accessible information updates, implying the longer lifetime of the overall tool. This programming approach increases the efficiency of the tool within the technical and regulatory context.

The programming language is defined within the project, preferably in an open-source language. The minimum application timeframe will suit a range of 1 minute to 1 hour. The user should be able to promptly implement new iterations to its structure, including the addition of other EESs technologies (models), new relevant evaluation parameters, different power allocation algorithms and EMSs and different ways of optimisation sizing and control restrictions. Additionally, the final solution must be a customised tool based on EES performance and validated models.

The HESS developing tool accounts for the input data from the client, the simulation, and the results of this assessment. Figure 50 presents the HESS sizing and control, and the operation tool included inputs, such as consumption profile, models of the batteries or electric grid details, and the outputs results, such as the economic and energetic evaluation.

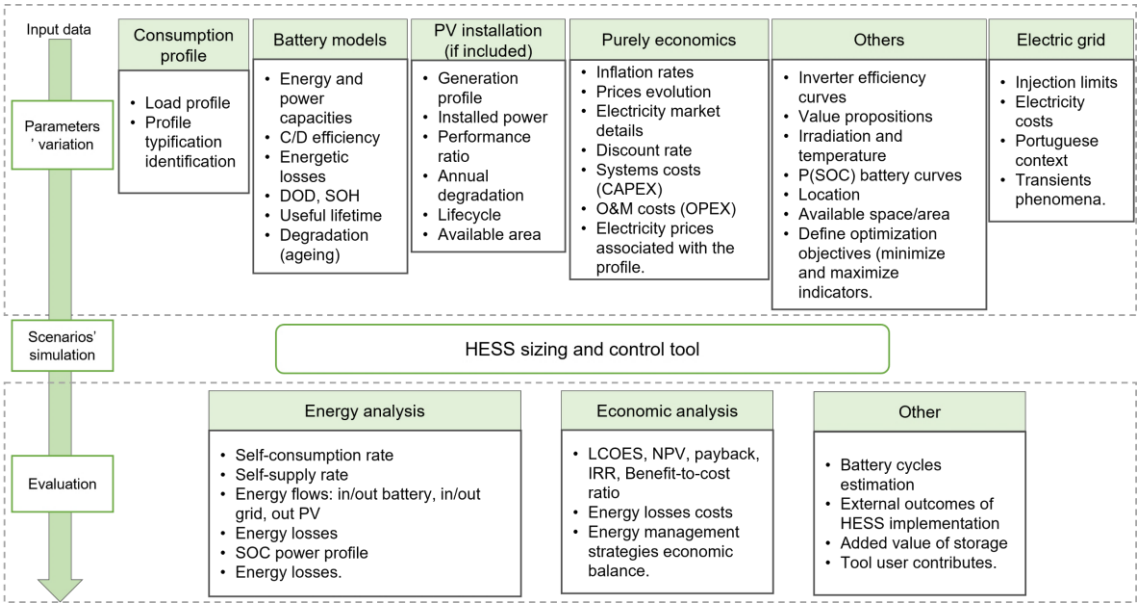


Figure 50. Relevant inputs and outputs of the HESS sizing and control and operation tool.

The simulation tool must obey the following premises:

- Allow a smooth adaptation of any battery technology type.
- Have a functional and friendly Human-Machine Interface.

- Correspond to smart energy management characteristics, contributing to the centralised management of the energy flow within the application.
- Obey the principles of the EMSs: peak-shaving, energy arbitrage, self-consumption maximisation, energy control and quality, among other relevant ones.
- Allow the creation of *value stacking* algorithms, considering simultaneous operation modes, improving the EES competitiveness and maximising the operating time. *Value stacking* is an approach that enhances the resiliency of the tool (not only dependent on market variations).
- Allow efficient programming.
- Optimise the identified and defined key parameters.

Within the operation processes of the tool, a relevant module contains the algorithms that compose the management of the HESSs. These algorithms are the energy and power allocation methods used to operate each EES unit and the EMS applied in the studied context. In a more finalised stage, this model should provide key relevant EMSs and power allocation (well-defined) scenarios that the client must use to assess HESS competitiveness for its context.

### 4.5.3. Validation with the demonstrator

The building of a HESS demonstrator will allow the validation of the simulation tool and its improvement. The demonstrator should allow the execution of the algorithms in real-time operation; the real-time operation should be consulted and could be adapted within the real-time execution of the algorithm and should be able to receive correct information from the external environment (measurements of the: SOC, voltage, current, temperature, EES dynamic internal electrochemistry data, operation alarms, among others). The previously described characteristics are the basis of the designed algorithms and are included in the control and management operation, presented in the following flowchart of Figure 51.

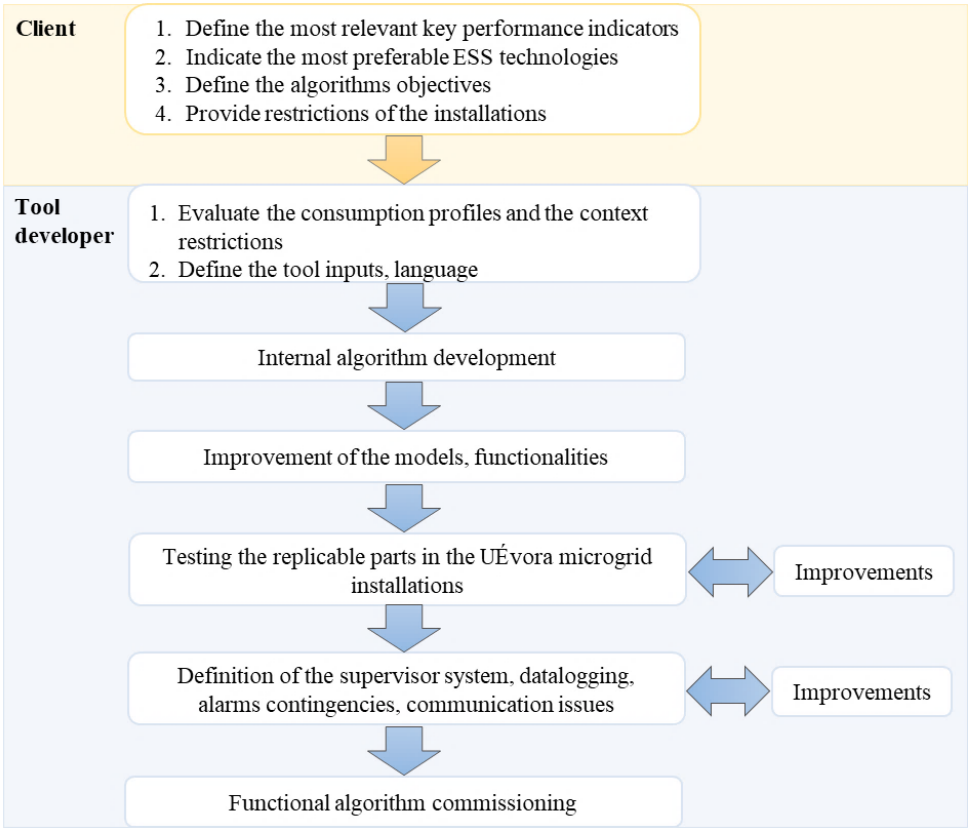


Figure 51. Simplified scheme of the HESS control and management algorithms.

The internal algorithm validation is achieved through the measured obtained data upon implementation. In that case, the algorithm should be easily implemented with communication language protocols suited to other existing equipment, such as those allowed by LabVIEW. The program interface of the implementation phase should have a simple, efficient, and interactive presentation. It should graphically allow the visualisation of the real-time operation data, including the report of alarms and automatic responses, e.g., on-stop or standby, ensuring safe operation. The datalogging should be performed in a database structure (e.g. .txt or .csv), be smoothly updatable by the tool developer and be scalable and replicable to the addition and interaction of other EES technologies.

### 4.5.4. Expected outcomes

The HyBRIDSTORAGE project [1] aims to develop innovative solutions to support the sizing, implementation, and operation of HESS, implying the development of a modelling tool with HESS operation algorithms (energy/ power allocation strategies).

This fact allowed the identification of a battery sector gap, allowing the improvement, adaptation and optimisation of the HESS interaction options from a technical, economic, and energetic evaluation perspective. The project promotes the smart control and management of EES, contributing to higher stability and uninterruptible security of energy supply, minimising costs, and improving the technical quality of the solution.

The tool is expected to solve a current need for HESS sizing and control in the design phase of the project. The sizing and control solutions have a higher potential for development due to the inexistence of these types of tools in the market or their existence at low development stages. In this case, the aim is to allow it to detailly size individual EES and multi-EESs to a project and of different technologies (with different performances and suitability). The tool is aimed to be developed in open-sourced software with low operation costs, ensuring an evolutive programming process to the addition of new EES technologies and allowing the economic and energy optimisation of the overall system and consequently the O&M costs reduction, according to its lifetime. The results are expected to be easily validated, replicable, and adaptable to other EES technologies and sizes, presenting accurate results. The EMSs algorithms ensure the competitiveness of the proposed HESS solutions.

The HESS assessment is achieved through economic key performance indicators, such as the NPV, LCOE, IRR, CAPEX, and payback, ensuring an upgraded analysis of the state of the art. The technical indicators are, for example, lifetime, efficiency, time of response, operating windows, and operational flexibility, among others. The improvement of these indicators is achieved through the joint operation of the EESs and their implemented energy management strategy, which should include a value-stacking methodology.

The client will be able to work with a robust tool for the commercialisation of innovative HESS solutions. The remote control of the HESS should be implemented to facilitate user interaction with the ongoing operation and allow the tool developer to check the obtained parameters. The layer of security is considered through protected access accounts.

The global battery market is increasing due to the RES penetration, the growth of the EV market, and some government initiatives from countries that support both of these integrations [2]. These factors are supported by the expected improvement of battery performance and prediction models, battery operation management with smart systems, and optimisation of economic parameters.

This hybrid battery system development ensures the selection of each EES strength to improve the hybrid competitiveness, foster the RES integration, enhance energy efficiency optimisation, electricity supply reliability and energy security and access. In countries where the RES is increasing, such as Spain or Italy, this tool could offer an opportunity to improve the grid interface with the HESS. In countries where the electric grid is unstable, such as Puerto Rico Island, this tool could increase the power quality of the grid.

As a recent field, HESSs demonstrators are found in reports and research papers. Its integration with the grid and RES and overall EMSs operation is currently an object of research. In the case of the HyBRIDSTORAGE project [1], the HESS pilot demonstrator will demonstrate the operational aspects of the overall set and validate the simulation tool.

### 4.5.5. References

[1] capWatt, “Projecto HyBRIDSTORAGE - Hybrid Energy Battery Systems.” [Online]. Available: https://capwatt.com/pt/apoios/hybridstorage.

[2] IEA, “Energy Storage,” 2021. [Online]. Available: https://www.iea.org/fuels-and-technologies/energy-storage. [Accessed: 07-Jan-2022].

# CHAPTER 5

# Conclusion

In order to address the first question of this thesis, on the framework of the current Portuguese market and its potential application for PV and battery setup, a detailed study of these configurations (in this case, using lithium-ion technology) was developed and applied to the Portuguese residential framework. The main outcomes allowed to conclude that the PV+battery configuration for the residential sector was not profitable in the studied context due mainly to the high upfront cost of the batteries, although pointing benefits of battery inclusion in that scenario. The current downward trend in battery costs can point to a change in these results; however, considering the economic assumptions taken, it currently points to a non-interesting application considering the Portuguese residential solar self-consumption maximisation.

In order to improve the state of the art regarding battery modelling and simulation, the technical and energy performance parameters of several different battery technologies were determined: lithium-ion, vanadium redox flow and second-life lithium-ion. Carrying out the tests using the LabVIEW environment allowed the collection of relevant data from emerging technologies, identifying the technical KPIs of each of these technologies. The experimentally collected data served as input parameters of performance models of a lithium-ion and vanadium redox flow battery, validating them. These validated models enabled their general integration into larger simulation models of the microgrid (to include loads and solar generation), allowing the study and optimisation of economic evaluation parameters, such as LCOE, or energetic evaluation parameters, such as the total energy exchanged with the battery throughout the testing period. As presented in the papers composing this thesis, different models were published with experimental validation of their parameters.

The effort allocated along this thesis timeframe was also devoted to the procurement, engineering and commissioning of several real-scale electrochemical storage technologies and their integration into the existing network and control, as described in

Chapter 2. This led to the deepening of knowledge and experience with regard to the design and monitoring of a microgrid, the commissioning of these innovative systems and the development of good practices of operation and maintenance.

This research differs from previous studies in identifying BESS performance parameters (KPIs) and their contribution to energy management evaluation. Unlike previous approaches focused on simulation-only or evaluation through a single dimension, this work combines the different value dimensions of the ESS technologies: economic, technical, and energetic, to accurately characterise the role of a battery in the assessment of concrete projects or scenarios. Additionally, this thesis is focused on documenting the practical testing and modelling of such battery systems, providing inputs to the current state of the art of emerging electrochemical storage technologies.

Evaluating energy management strategies is crucial for battery integration in a project. The recognition of this relevance allowed the study and development of energy management strategies in this thesis. One of them resulted in a publication for the full-scale implementation of a strategy devoted to PV power ramp rate control. The study allowed the identification of solutions to maximise self-consumption and perform ramp rate control with simultaneous competing objectives, solve a problem foreseen by the significant penetration of solar PV in the grid, and make the best possible use of the battery for this purpose using a Portuguese daily solar resource forecast.

Different technologies of batteries can present complementary technical KPIs, whose realisation opened a path for studying the operation and control of HESS. This hybridised solution could gather an overall improvement of system dynamics, whose objective is to improve overall strategy KPIs. In a second investigation, different approaches to managing this hybrid battery system were developed to study the performance potential of the hybridisation of lithium and vanadium-based batteries. The chosen method to manage this hybridised system highly influences the joint performance of the batteries. The work developed with single and hybrid battery systems allowed the continuous development of a tool that simulates energy management strategies and supports the building of real-scale demonstrators, including optimising their control operation in real-time.

The continuous penetration of VREs and their impact on the power system urges for flexible, reliable, and resilient networks, where BESS and smart energy management could help in the achievement of this goal. BESS may act as an electricity cost reduction element in the power sector, deferring investments or eliminating the need for

other costlier dispatchable technologies while enabling the broad penetration of non-dispatchable VRE sources. In this sense, VREs become an asset of the energy system enhanced by battery energy storage.

To comply with the guidelines established by the European Commission, the substitution of fossil-fuelled sources by renewable energy urges energy storage solutions, which rely on battery technologies for the sectors of buildings and mobility. The present status of this sector faces obstacles regarding the optimal integration of storage technologies in the power generation system. This thesis allowed the study and identification of new opportunities for solar PV+battery or hybrid battery systems solutions, expecting to further contribute to pursuing a fully integrated and decarbonised energy system.

# CHAPTER 6

# Future Research Lines

---

For distributed applications, the benefits of applying BESSs have been an object of assessment in recent research studies, e.g., [1] or [2]. It contributes to the developing markets for capacity, flexibility, and ancillary services, enhancing the benefits of digital and innovative electric systems or services. These features contribute to the solar plus storage market development, framed by the Portuguese Decree-Law 15/2022 [3]. In this sense, the research and development path on battery energy storage presents opportunities, already identified during the period of this thesis, to explore new energy services, such as peer-to-peer trading, the optimised integration in upcoming energy communities or isolated grids, or topics regarding the vehicle to grid capabilities (EVs acting as grid-connected BESS).

However, the future competitiveness of a BESS is also related to an array of technical and non-technical issues, such as:

- Regulatory simplification for grid connection, based on the new energy services
- Reliance provision with demonstrator pilots over longer periods, bringing higher degrees of confidence to users, companies and investors.
- Recognition of ancillary services as competitive and fair, and close to the demand
- Enable revenue stacking as an ability to optimise the assets (set of options)
- Recognition of the BESS as a core part of the energy transition to a flexible and reliable grid with dispatchable renewable energy
- Allow market flexibility, i.e., not constraining the market participants.

In order to improve BESS integration, control, efficiency, safety and cost, it is necessary to continue improving the battery electrical performance modelling, providing reliable and validated simulation systems for short- and long-term timeframes, and enabling the simulation of more complex architectures such as hybrid battery systems. The

simulation framework should also evolve to encompass different management strategies: individual and collective self-consumption schemes, car charging management, power management assets, load flexibility, etc.

Three main existent projects in the Renewable Energies Chair contributed to the developed work of the present thesis, enabling the addition of systems to the experimental grid at the University of Évora. Those projects were AGERAR [4], adding a lithium-ion battery and nickel-sodium chloride battery; POCITYF [5], which allowed to integrate second life lithium-ion battery prototypes (for isolated and residential applications) and a SmartLamPost (EV charger); and SOLAR TECH [6], where a hybrid supercapacitor, a second-life lithium-ion battery and a new PV system were acquired. The experimental grid is currently a flexible infrastructure with increasing complexity, providing support to ongoing R&D tasks and a valuable hands-on experience for the team.

In addition to the BESS, power electronics and precision monitoring equipment were critical elements in the research development phases. This equipment will allow to pursue new research lines, perform rehearsals, and fast prototyping with an ever-growing collaboration network with an innovation ecosystem composed of other institutions, researchers, companies, end-users and investors.

Within those elements, developing a lithium-ion lifetime model using the second-life lithium-ion experimental information is an emerging research line aligned with the European Commission guidelines on battery projects. Other emerging topic focus on the integration, operation, characterisation, and investigation of EMS approaches using the supercapacitor's recent acquisition. Within the EMS approach, a compelling investigation relies on the operation and testing of the supercapacitor to control PV or load power ramps in real time, stabilise the grid and operate in conjunction with the other energy storage technologies.

The integrated novel workstation performs the experimental grid control, currently using LabVIEW software at this development stage. The existing software already has an extensive customised library with capabilities for tasks of control, communication, alarm, datalogging and data processing, and it should be built upon to further extend it. This grid controller aggregates the control of the different grid assets, providing flexibility in developing new scientific and diagnostic tools for future grid control and monitoring. An interesting new research topic addresses the development of a low-cost

controller capable of executing the existing programming and EMSs, exploiting the current results and reaching a suitable TRL to take it to the next level: the market.

Hybrid battery storage systems present themselves as a potential future research topic, with the study of new control strategies highlighting the competitiveness of merging different technologies. The final product should achieve improved efficiency, longer lifetime, lower costs, and better economic performance results. Further research will also include transdisciplinary questions, such as load or generation forecast, the gamification of energy communities and their energy behaviour, addressing social challenges, but always targeting our greatest challenge: the decarbonisation of our lifestyle.

## 6.1. References

[1] J. Liu, C. Hu, A. Kimber, and Z. Wang, "Uses, Cost-Benefit Analysis, and Markets of Energy Storage Systems for Electric Grid Applications," *J. Energy Storage*, vol. 32, no. February, p. 101731, 2020.

[2] A. Z. AL Shaqsi, K. Sopian, and A. Al-Hinai, "Review of energy storage services, applications, limitations, and benefits," *Energy Reports*, vol. 6, pp. 288–306, 2020.

[3] República Portuguesa, *Decreto-Lei n.º 15/2022 | DRE*. Portugal, 2022, pp. 3–185.

[4] Interreg España-Portugal, "AGERAR - Almacenamiento Y Gestión De Energías Renovables En Aplicaciones Comerciales Y Residenciales." [Online]. Available: https://www.poctep.eu/es/2014-2020/almacenamiento-y-gestión-de-energías-renovables-en-aplicaciones-comerciales-y.

[5] Pocityf, "Leading the smart evolution of historical cities," 2022. [Online]. Available: https://pocityf.eu.

[6] University of Évora, "SOLAR TECH - Transferência de Tecnologia e Conhecimento em Energia Solar e Armazenamento de Energia." [Online]. Available: https://www.uevora.pt/investigar/projetos?id=4195.

# Annex

- Scientific poster presented at Conference "EUPVSEC", 2021

UNIVERSITY OF ÉVORA | RENEWABLE ENERGIES CHAIR_10 YEARS | POCITYF

## Microgrid energy management control with a Vanadium Redox Flow and a Lithium-ion hybrid battery systems for PV integration


Ana Foles[a,b,1], Luís Fialho[a,b], Manuel Collares-Pereira[a,b]

[a]Renewable Energies Chair, University of Évora. Pólo da Mitra da Universidade de Évora, Edifício Ário Lobo de Azevedo, 7000-083 Nossa Senhora da Tourega, Portugal

[b]Institute of Earth Sciences, University of Évora, Rua Romão Ramalho, 7000-671, Évora, Portugal

[1]anafoles@uevora.pt



### Abstract

Hybrid energy storage systems combine multiple energy storage technologies, to improve the overall storage's performance and lifetime, compared to a single storage unit. This work proposes an online power/energy management control of a hybrid energy storage system, with a simulation tool developed by the authors. The hybridized system is composed by two PV installations (3.6 kWp and 6.7 kWp), a vanadium redox flow battery (VRFB) (5 kW /60 kWh) and a lithium-ion battery (LIB) (3.3 kW /9.8 kWh). The simulation architecture is done using MATLAB, where three hypothetical operation scenarios are simulated, with the aim of optimize the energy usage according to its technical characteristics, current operation state and the PV generation, for a one-year period. The system's overall performance is evaluated through three technical key-performance indicators. The combination of different energy storage technologies is a feasible solution which depends on the application goals and on the assuring of the accuracy and reliability of the system and its control strategy.


### Methodology

**Microgrid installation**

- ✓ PV installations (3.6 kWp and 6.7 kWp) + datalogging
- ✓ Communication established to the batteries' inverters
- ✓ Precision monitoring equipment (energy, power, temperature, etc.)

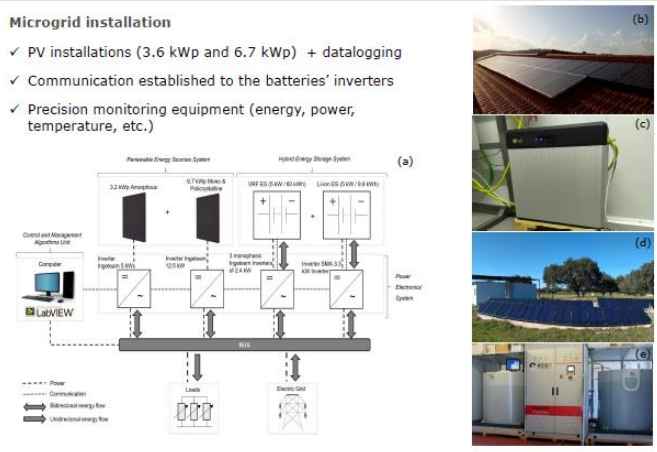


**Figure 1:** (a) Scheme of the hybrid battery energy storage and solar photovoltaic installation energy fluxes; (b) Solar PV installation 6.7 kWp; (c) LIB LG Chem Resu 10, 3.3kW/ 9.8kWh; (d) Solar PV installation 3.6 kWp; (e) REDT VRFB 5kW/60 kWh.

**Hybrid Batteries Power-Sharing Simulation**

- ✓ Software simulation tool validated with a real-scale microgrid
- ✓ Flexible arquitecture to simulate Energy Management Strategies (EMS)
- ✓ Lithium-Ion Battery (3.3 kW/9.8 kWh) validated Model
- ✓ Vanadium Redox Flow Battery (5.0 kW/ 60 kWh) validated Model

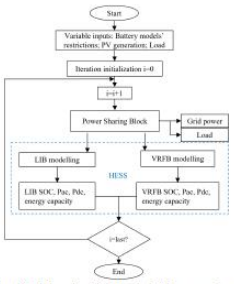


**Figure 2:** Simplified flowchart for the hybrid energy storage system simulation, implemented in MatLab.

### Results

| Scenario I | Scenario II | Scenario III |
|---|---|---|
| The power sharing is distributed with a fixed power value for each of the batteries. In this scenario, 75% of the total energy is attributed to the VRFB, and the rest is attributed to the LIB. | Scenario I but without fixed power allocation ratios. HESS is operated depending on the LIB state of charge. It obeys to a power-SOC relation, and the remaining power is requested/retrieved from VRFB. Soc(LIB)<=50: p=0.0067*Soc(LIB)+0.1667 Soc(LIB)>50: p=-0.0050*Soc(LIB)+1.300 | Dynamic variability power command for LIB and fixed value for VRFB. It is the realization of two services for each battery (similar as if LIB executes a peak shaving strategy). |

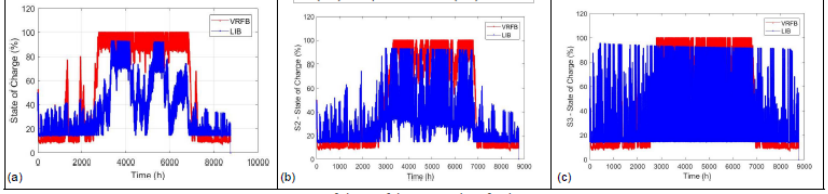


**Figure 3:** State of charge of the VRFB and LIB for the 3 Strategies

**Table I:** Results of the technical performance indicators: SCR, GRF and BU for the 3 simulated scenarios.

| Scenario | SCR | GRF | BU LIB | BU VRFB |
|---|---|---|---|---|
| I | 0.53 | 0.35 | 0.55 | 0.67 |
| II | 0.53 | 0.27 | 0.63 | 0.64 |
| III | 0.53 | 0.36 | 0.54 | 0.64 |

Legend:
**SCR** – Self-consumption ratio (Share of the PV generation consumed by the installation from the total of the PV energy generation);
**GRF** – Grid relief factor (Measure of the total grid use in the overall load consumption needs);
**BU** – Battery use (Share of energy of the power battery command in the overall energy consumption).

### Conclusions

- ➢ Scenario I is a rough approach as HESS power sharing method.
- ➢ Scenario II improves the systems dynamic, as lowering the time spent in high or low states of charge and power levels.
- ➢ Scenario III offer the efficient realization of different tasks.
- ➢ SCR is maintained in the three scenarios, the GRF is the smallest for Scenario II given the better batteries exploitation. VRFB executes the baseload in all the scenarios, shown by its BU indicator. The LIB BU indicator presents a higher use in Scenario 2 even though the LIB operation is controlled by the SOC-power profile.
- ➢ A robust cost analysis is a future prospective of the present work.


### Acknowledgements

The authors would like to thank the support of this work, developed under the European POCITYF project, financed by 2020 Horizon under grant agreement no. 864400. This work was also supported by the PhD. Scholarship (author Ana Foles) of FCT – Fundação para a Ciência e Tecnologia –, Portugal, with the reference SFRH/BD/147087/2019.


### References


[1] IRENA, *Innovation landscape for a renewable-powered future: Solutions to integrate variable renewables*. 2019.
[2] A. Z. AL Shaqsi, K. Sopian, and A. Al-Hinai, "Review of energy storage services, applications, limitations, and benefits," *Energy Reports*, vol. 6, pp. 288–306, 2020.
[3] D. EDP and Q-metrics, "Update of consumption, production and of self-consumption for the year 2019," p. 29, 2019.
[4] A. Foles, L. Fialho, M. Collares-Pereira, P. Horta. "Vanadium Redox Flow Battery Modelling and PV Self-Consumption Management Strategy Optimization," 2020.

- Scientific poster presented at Conference “Mission: 10000 Batteries”, 2019

MISSION 10.000: Batteries

# Testing and evaluation of batteries for commercial and residential applications in AGERAR project

E. López González[1*], L. Fialho[2], L. Vargas Vázquez[1], A. Foles[2], J. Sáenz Cuesta[1], M. Collares Pereira[2]

[1] Instituto Nacional de Técnica Aeroespacial (INTA), Área de Energías Renovables-CEDEA, Ctra. S.Juan-Matalascañas, km.34, 21130, Mazagón (Huelva), Spain

[2] Universidade de Évora, Cátedra Energias Renováveis, Casa Cordovil, Rua D. Augusto Eduardo Nunes n.7, 7000-651 Évora, Portugal

(*) lopezge@inta.es

## Introduction

The AGERAR project (Storage and management of renewable energies in commercial and residential applications) aims to evaluate technical solutions to promote energy efficiency and sustainability criteria in commercial and residential micro grids. One of the main activities of the project focuses on the test, evaluation and comparison of different battery technologies, suitable for commercial and residential applications, from cells and modules to complete systems. This technological validation will provide reliable information to main stakeholders, based on experimental data, about the real performance and potential benefits of these technologies, in terms of efficiency, lifetime, costs, and safety, among others.

The University of Évora (UÉvora) and the Spanish National Institute for Aerospace Technology (INTA) have been testing and evaluating several technologies of batteries: UÉvora is focused on commercial Li-ion based systems and Vanadium Redox Flow Batteries (VRFB), while INTA is testing Li ion cells and packs with lithium titanium oxide (LTO) anode, as well as Aluminum ion secondary battery cells.

## Testing and evaluation of batteries for commercial and residential applications

UÉvora has designed and developed a specific VRFB three-phase microgrid to rehearse and characterize PV + storage systems and study its integration into the grid/building in real scale. A similar experimental facility has been designed to rehearse and characterize PV + Li-ion based storage systems.

The tests performed at INTA on cells and packs involve the use of a battery test station, with 4 high voltage channels (up to 400 A in the range 0 - 60V), and 4 low voltage channels (up to 10 A in the range 0 - 5V).

VRFB manufacturer technical specifications

| | Units | Value/Range |
|---|---|---|
| Total Energy Capacity | kWh | 60 |
| Number of cells in the Stack | | 40 |
| Standard Maximum Power | kW | 5.0 |
| Operating voltage range | V | Up to 65 |
| Volume | $m^3$ | 1.8×2 (tanks) |
| Maximum current | A | 200 secondary fuse |
| Lifetime | | +10,000 deep charge/discharge cycles |

Li-ion battery manufacturer technical specifications

| | Units | Value/Range |
|---|---|---|
| Total Energy Capacity | kWh | 9.8 (25ºC, 100% SOC) |
| Usable Energy Capacity | kWh | 8.8 |
| Battery Nominal Capacity | Ah | 189 |
| Volume | $m^3$ | 0.05 |
| Weight | Kg | 75 |
| Voltage Range | VDC | 42.0-58.8 |
| Nominal Voltage | VDC | 51.8 |
| Max. Current | A | 119 A at 42 V |
| Nominal / Max. Power | kW | 3.3 / 5.0 |
| Peak Power | kW | 7.0 kW for 3 sec. |
| Peak Current | A | 166.7 A for 3 sec. |
| Lifetime (80% DOD, 25ºC) / (90% DOD, 25ºC) | | 10000 / 6000 |
| Battery Pack Round-Trip Efficiency | % | >95% (under specific conditions) |

LTO pack technical specifications

| AGERAR Pack (13S1P) | Units | Value/Range |
|---|---|---|
| Nominal voltage | V | 48.1 |
| Max. voltage | V | 54.6 |
| Min. voltage | V | 35.1 |
| Max. current: | | |
| Charge cont. | A | 138.0 (3C) @23±3°C |
| Discharge cont. | A | 552 (12C) @23±3°C |
| Discharge peak | A | 690 (15C) <10sec , > SOC 50% |
| Nominal Energy Capacity | kWh | 2.2 |
| Volume | $m^3$ | 0.0083 |
| Weight | kg | 15.47 |
| Cycle life to 80% of remaining capacity | | ≥5000 (1C/1C), 80% DOD or 3.4~4.1V (@23±3°C) |

Al-ion cells technical specifications

| Manufacturer | Albufera Energy Storage | |
|---|---|---|
| | Units | Value/Range |
| Nominal voltage | V | 1.7 |
| Max. voltage | V | 2.3 |
| Min. voltage | V | 1.0 |
| Capacity | mAh | 25 |
| Current: | | |
| Charge cont. | mA | 25 (1C) @23±2°C |
| Discharge cont. | mA | 2.5 (C/10) @23±2°C |
| Discharge peak | mA | 25 (1C) @23±2°C |
| Charging temperature range | ºC | 0-50 |
| Discharging temperature range | ºC | 0-60 |

VRFB control unit and electrolyte tanks



VRFB stack

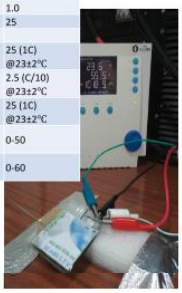

## Results and Discussion

The Vanadium Redox Flow Battery (VRFB) has been tested at UÉvora in 6 consecutive full charge-discharge cycles, using the range from 5% up to 90% of state of charge.

| | Results |
|---|---|
| Total Capacity (Charge Capacity) (kWh) | 86.3 ± 2.30 |
| Max. Useful Capacity (Discharge Capacity) (kWh) | 66.5 ± 4.26 |
| Energy Density (per unity of mass) (Wh/kg) | 18.5 ± 4.26 |
| Energy Density (per unity of volume) (Wh/L) | 17.5 ± 4.26 |
| Fastest/Slowest Charge | 51h41min. / 70h10min. |
| Fastest/Slowest Discharge | 26h54min. / 109h7min. |
| Charge and Discharge Efficiency (complete cycles) (%) | 77.1 ± 3.36 |
| Max. Charge and Discharge Power (kW) | 7.20 |
| Response Time | Seconds (s) |
| Typical discharge time | Hours (h) |

VRFB performance results under the operated conditions

The lithium-ion battery of UÉvora has been rehearsed at constant power rates, from a range of 20% to 90% of state of charge, corresponding to a period of 27 complete cycles.

| | Results |
|---|---|
| Total Capacity (Charge Capacity) (kWh) | 6.46 ± 0.482 |
| Max. Useful Capacity (Discharge Capacity) (kWh) | 5.45 ± 0.373 |
| Energy Density (per unity of mass) (Wh/kg) | 72.73 ± 4.967 |
| Energy Density (per unity of volume) (Wh/L) | 109.11 ± 7.450 |
| Fastest/Slowest Charge | 2h04min / 10h46min |
| Fastest/Slowest Discharge | 1h33min / 3h48min |
| Charge and Discharge Efficiency (complete cycles) (%) | 84.6 ± 0.075 |
| Max. Charge and Discharge Power (kW) | 3.30 |
| Response Time | Seconds (s) |
| Typical discharge time | Hours (h) |

LG Li-ion battery performance results under the operated conditions

The LTO based Li-ion pack has been tested at INTA for more than 2000 hours, in successive cycles with different load profiles, obtained from real data and simulations, for winter and summer seasons in the South of Spain and Portugal. Periodically, the cells have been individually characterized, without significant changes in their performance, in comparison with the initial reference tests

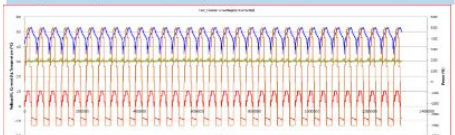

Li-ion pack test: voltage, current, power and temperature curves corresponding to 30 daily cycles, summer Spain profile, climatic chamber at 30 ºC and 60 % RH

| AGERAR Pack (13S1P) | Units | Value/Range |
|---|---|---|
| Usable energy capacity | kWh | 2.1 |
| Nominal / Max. Power cont. | kW | 2.2 (1C) / 19.4 (12C) @23±3°C |
| Measured specific energy | Wh/kg | 136 |
| Measured energy density | Wh/l | 253 |
| Battery Pack Round-Trip Efficiency | % | ≥ 97 |

LTO based Li-ion battery performance results under the operated conditions

Al ion cells have been successfully tested in more than 10 charge/discharge cycles, at different currents, achieving the performance criteria defined for these tests.

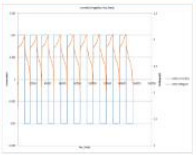

Al-ion cell test: voltage and current curves corresponding to 9 charge / discharge cycles

## Conclusions

- Preliminary conclusions demonstrate the technical feasibility of LTO based Li-ion and VRF batteries for the commercial and residential applications considered in the AGERAR project.
- In addition to the suitability of the batteries, there are other critical components to consider in the design, development and installation of battery energy storage systems suitable for these applications, in particular the battery monitoring and management system (with cell balancing capabilities) and the power conditioning system.
- The measured technical parameters of the characterization made proved to be non-negligible in the development of these technologies and will allow the development of improved energy management strategies with optimization on the systems' performance, benefiting the end user and the overall economic results of these energy storage solutions.
- VRF and Li-Ion batteries were performed according to the manufacturers' specifications, although the VRFB even surpassed some of the values announced in its specifications sheet. It should be pointed out that this specific battery was installed in UÉvora as a prototype, with the aim of being tested in the referred microgrid facility at different operating conditions and giving feedback to the manufacturer, over the operation period.
- LTO batteries show a good behavior at different operating conditions, without significant loss of performance after more than 2000 hours of operation.
- Regarding Al ion batteries, the technology is very promising, mainly regarding cost and environmental issues, but it is currently at TRL 3-4, and an important effort is still necessary to implement it in commercial and residential applications.

**Acknowledgements**
**The project AGERAR (Ref. 0076_AGERAR_6_E) is co-financed by the European Regional Development Fund (ERDF), within the INTERREG VA Spain-Portugal cooperation programme (POCTEP).**

More information at http://institucional.us.es/agerar/